

**ANGIOTENSIN II INDUCED PREMATURE SENESCENCE OF HUMAN
VASCULAR SMOOTH MUSCLE CELLS**

**Thesis submitted for the degree of
Doctor of Philosophy
at the University of Leicester**

**By
Yogita Mistry BSc (Hons)**

**Department of Cardiovascular Sciences
University of Leicester
2009**

Abstract

Senescence is a state of irreversible growth arrest in cells with potentially tumourigenic changes such as irreparable DNA damage. However, senescent cells accumulate with age, altering tissue structure and function and have been observed in atherosclerotic plaques and at sites predisposed to atheroma in man. Recent studies show that long term inhibition of the renin-angiotensin system attenuates the effects of ageing in rodent cardiovascular tissue. Therefore, this thesis investigated whether angiotensin II accelerates senescence of human vascular smooth muscle cells (hVSMC) *in vitro* and whether the mechanism involves reactive oxygen species, DNA damage, telomere attrition and cell cycle regulatory proteins. Since mitochondria are integral to theories of cellular ageing, the effect of angiotensin II on mitochondrial biogenesis and function were studied.

Angiotensin II exposure enhanced superoxide generation via NADPH oxidase in hVSMC, although inhibitors identified the mitochondrial respiratory chain as a contributing source. Angiotensin II induced DNA strand breaks in the Comet assay and accelerated telomere attrition. Senescence associated- β -galactosidase activity was induced by angiotensin II after exposure for 30 days, but also after just 24 hours and after successive short treatments over three days. These effects were attenuated by an angiotensin II type-1 receptor antagonist and antioxidants. Simultaneously, increased expression of p21 and p53 were observed. Angiotensin II induced alterations in mitochondria. A rapid increase in mtDNA content, gene transcript levels involved in initiating mtDNA transcription and replication and ATP levels in hVSMC, suggested mitochondrial biogenesis occurs in response to stress. These data suggest that angiotensin II induces both accelerated replicative senescence (telomere-dependent) and stress-induced premature senescence (telomere-independent) of hVSMC, dependent upon the treatment regime used. These findings explain the anti-ageing effects of life-long angiotensin II blockade in rodents, and may provide a mechanism for accelerated vascular ageing and cardiovascular disease progression in the ageing human population.

For Mum and Dad

x



Acknowledgements

I would like to thank Dr Karl E. Herbert and Professor Bryan Williams for their support, guidance and enthusiasm throughout this entire project.

A special thanks to Dr R. A. Hastings and Dr T. Poolman for their assistance with experimental techniques and equipment, and to all my fellow colleagues in the Department of Cardiovascular Sciences.

Finally, a huge thank you to my family and friends for their support and encouragement.

Contents

	Page
Abstract	II
Dedication	III
Acknowledgements	IV
Contents	V
Index of Figures	VII
Index of Tables	IX
Abbreviations	X
CHAPTER ONE: Introduction	Page
1.1 Vascular Ageing	2
1.2 Cellular Senescence	3
1.3 Vascular Cell Senescence, Ageing and CVD	11
1.4 Angiotensin II	17
1.5 ROS Initiated Responses in the Vasculature	25
1.6 Mitochondria, Oxidative Stress and Ageing	35
1.7 Hypothesis and Aims	41
CHAPTER TWO: Materials and Methods	Page
2.1 Materials	43
2.2 Equipment	55
2.3 Methods	59
CHAPTER THREE: Establishing a human vascular smooth muscle cell model to study the ageing effects of Angiotensin II	Page
3.1 Background	85
3.2 Aims	89
3.3 Experimental Approach	90
3.4 Results	93
3.5 Discussion	103
CHAPTER FOUR: Effect of Angiotensin II on senescence in cultures of human vascular smooth muscle cells	Page
4.1 Background	112
4.2 Aims	118
4.3 Experimental Approach	119
4.4 Results	123
4.5 Discussion	137

CHAPTER FIVE: The induction of stress-induced premature senescence with acute angiotensin II exposure	Page
5.1 Background	152
5.2 Aims	158
5.3 Experimental Approach	159
5.4 Results	165
5.5 Discussion	186
CHAPTER SIX: Mitochondrial alterations and angiotensin II-induced premature senescence	Page
6.1 Background	199
6.2 Aims	205
6.3 Experimental Approach	206
6.4 Results	210
6.5 Discussion	224
CHAPTER SEVEN: General Discussion and Future work	Page
7.1 General discussion	235
7.2 Future work	242
APPENDICES	Page
Appendix I: Inhibition of Ang II induced DNA damage by E3174	244
Appendix II: Raw data and calculations for the relative quantification of mitochondrial biogenesis gene expressions	245
Appendix III: PCR product sequencing data of mitochondrial biogenesis genes	247
Appendix IV: Communications arising from this thesis	249
REFERENCES	250

Index of Figures

	Page
1.1 Oncogenic Ras-induced tumour formation and senescent signalling mechanism	8
1.2 Human cell senescent signalling pathways in response to the various stress signals	10
1.3 Formation of the Angiotensin hormones of the RAS	18
1.4 Diverse Ang II signalling responses in VSMC	19
1.5 Redox-dependent signalling via vascular NAD(P)H oxidase	29
1.6 Ras and Akt induced ROS-mediated cellular senescence	34
1.7 Diagrammatic representation of the mitochondrion and mtRC complex	36
1.8 PGC1 α signalling in mitochondrial biogenesis	37
3.1 Modulation of the cell cycle in response to Ang II stimulation	87
3.2 hVSMC exhibit typical 'hill-and-valley' growth characteristics	94
3.3 Characterization of hVSMC by immunofluorescence staining of α -smooth muscle actin	95
3.4 hVSMC exhibit SM-MHC protein expression	96
3.5 Ang II receptor subtype protein expression in hVSMC	97
3.6 Successive Ang II treatment stimulates cell proliferation	99
3.7 hVSMC proliferation and cytotoxicity determined by MTT activity	100
4.1 Ang II causes telomere attrition in hVSMC	123
4.2 Telomerase levels in hVSMC	125
4.3 DNA damage in hVSMC measured using the Comet assay	126
4.4 Late passage hVSMC (passage 21) exhibit enlarged and irregular-shaped cell morphology associated with cellular senescence	128
4.5 Optimisation for the detection of SA- β -gal activity in hVSMC	129
4.6A Ang II accelerates senescence in hVSMC	132
4.6B Dose-response of Ang II treated SA- β -gal positive cells	133
4.7 Caspase-3/7 activity in hVSMC	134
4.8 Nuclei staining of hVSMC with Hoechst 33258 to determine apoptosis	136
5.1 Common intracellular signalling mechanism activated by SIPS and replicative senescence	155
5.2 Effect of repeated t-BHP stresses on SA- β -gal activity in hVSMC	167
5.3 A single Ang II exposure induces premature senescence in hVSMC	168
5.4 Ang II-induced premature senescence is mediated via AT ₁ R activation and ROS generation	169
5.5 Effect of repeated Ang II stresses on SA- β -gal activity in hVSMC	171
5.6 H ₂ O ₂ and Ang II stimulate intracellular ROS generation in hVSMC	173
5.7 Lucigenin-derived chemiluminescent detection of O ₂ ⁻ generation in hVSMC lysates	174
5.8 NADPH oxidase activity is the major source of O ₂ ⁻ production in untreated hVSMC	176
5.9 Ang II induces NADPH-mediated O ₂ ⁻ generation in hVSMC	177
5.10 Differences in protein loading detected with α -tubulin for Western blot analysis	179
5.11 Western analyses of p21 and p53 protein expression levels in hVSMC treated with acute Ang II	180

5.12	hASMC-hTERT exhibit many typical characteristics of SMC <i>in vitro</i>	182
5.13	A single Ang II exposure induces premature senescence in hASMC-hTERT	184
5.14	Successive Ang II exposure had no effect on the replicative senescence and proliferation in hASMC-hTERT	185
6.1	Proposed mechanisms of mitochondrial dysfunction in response to cardiovascular risk factors that may trigger cell senescence or contribute to ageing and CVD development	201
6.2	Effect of mitochondrial inhibitors and antioxidants on Ang II-induced premature senescence of hVSMC	211
6.3	Ang II induces NADPH-mediated mitochondrial O ₂ ^{·-} generation in hVSMC	213
6.4	Detection of mitochondrial O ₂ ^{·-} with MitoSOX™ red in live hVSMC	215
6.5	Ang II increases mtDNA content of hVSMC following a single exposure	216
6.6	Successive Ang II exposure stimulates increased mtDNA content in hVSMC	218
6.7	Effect of short Ang II exposure on the mRNA expression of genes involved with mitochondrial biogenesis	219
6.8	ATP production in hVSMC	221
6.9	Effect of repeated Ang II stresses on the ATP content of hVSMC	223
7.1	Proposed mechanisms of Ang II-mediated SIPS	239
4.3C	Ang II induces DNA damage in hVSMC via the AT ₁ R	244

Index of Tables

		Page
1.1	Typical features of cellular senescence	4
1.2	Characteristics and responses mediated by angiotensin receptor subtypes	20
1.3	Properties of ROS and RNS generated in the vasculature	26
1.4	Physiological and pathological consequences of ROS in VSMC	31
2.1	Reagents and materials used for immunofluorescence cell staining of α -smooth muscle actin	45
2.2	Senescent cell staining kit reagents	46
2.3	Reagents and materials utilized to stain whole cell DNA with Hoechst 33258	47
2.4	Stimulators and inhibitors of cellular ROS	48
2.5	Primary and secondary antibodies used for Western blotting	50
2.6	Restriction enzymes used for Southern blotting	51
2.7	All reagents and materials of the TeloTAGGG Telomerase PCR ELISA kit	52
2.8	Primer sets used to amplify specific nDNA and mtDNA sequences	53
2.9	Primers sequences used to amplify human mitochondrial biogenesis genes and endogenous control	54
2.10	Final concentrations of ROS inhibitors	68
2.11	Final concentrations of ROS stimulators	68
2.12	Blocking solutions and conditions for incubation prior to specific primary antibody labelling	74
2.13	Primary and secondary antibody dilutions and conditions for the proteins of interest	74
2.14	Primary and secondary antibody dilutions and conditions for the labelling of equal protein loading	75
3.1	Trypan blue exclusion of hVSMC exposed to Ang II	98
3.2	Trypan blue exclusion of hVSMC exposed to E3174	102
4.1	Evidence of human vascular ageing and senescence in cardiovascular pathologies/ risk factors	116
5.1	Common characteristics determined in both replicative senescent and SIPS human fibroblasts (<i>in vitro</i>)	154
5.2	Trypan blue exclusion of hVSMC exposed to t-BHP	166
5.3	Inhibition of acute Ang II stimulated $O_2^{\cdot-}$ via antagonists of AT ₁ R, NAD(P)H oxidase and ROS, in hVSMC lysates	178
6.1	Alterations in mtDNA content of hVSMC following acute Ang II exposure	217

List of Abbreviations

AAA	Abdominal aortic aneurysms
ABB	Alkaline blotting buffer
ACE	Angiotensin converting enzyme
<i>Ace</i> ^{-/-}	ACE-deficient
ADMA	Asymmetrical dimethylarginine
ADP	Adenosine diphosphate
ADP-CR	Adenosine diphosphate-converting reagent
<i>Agt</i> ^{-/-}	Angiotensinogen-deficient
Akt/PKB	Akt kinase/Protein kinase B
ALU	Arbitrary light units
AMPK	AMP-activated protein kinase
Ang I	Angiotensin I
Ang II	Angiotensin II
Ang IV	Angiotensin IV
Anti-DIG-POD	Anti-digoxigenin peroxidase
Apocynin	4-hydroxy-3-methoxyacetophenon
APS	Ammonium persulfate
ARB	Ang II receptor blocker
ATM	Ataxia telangiectasia mutated
ATP	Adenosine triphosphate
ATR	Ataxia telangiectasia and Rad-3-related
AT ₁ R	Angiotensin II type-1 receptor
AT _{1A} R	Angiotensin II type-1A receptor
AT _{1B} R	Angiotensin II type-1B receptor
AT ₂ R	Angiotensin II type-2 receptor
AT ₃ R	Angiotensin II type-3 receptor
AT ₄ R	Angiotensin II type-4 receptor
AU	Arbitrary units
AUC	Area under the curve
BSA	Bovine serum albumin
BSA/TBST	BSA in TBS with tween-20
C	Cytochrome c
Ca ²⁺	Calcium ions
CAGE	Chymostatin-sensitive Ang II-generating enzyme
CaMKIV	Ca ²⁺ /calmodulin-dependent protein kinase IV
cAMP	Cyclic adenosine monophosphate
CCCP	Carbonyl cyanide 3-chlorophenylhydrazone
CDKI	Cyclin dependent kinase inhibitor
cDNA	Complementary DNA
<i>c-fos</i>	Proto-oncogene proteins
CKD	Chronic kidney disease
cGMP	Cyclic guanosine monophosphate
CM-H ₂ DCFDA	5-(and-6)-chloromethyl-2',7'-dichloro-dihydrofluorescein diacetate, acetyl ester
CO ₂	Carbon dioxide
COX-2	Cyclooxygenase-2
CPD	Cumulative population doubling

Angiotensin II induced premature senescence

CREB	cAMP response element binding protein
cSrc	Non-receptor protein-tyrosine kinase
Ct	Cycle threshold
CuZnSOD	Copper-zinc SOD
CVD	Cardiovascular disease
DEPC	Diethyl pyrocarbonate
DCFDA	Dichlorodihydrofluorescein diacetate
DMEM	Dulbecco's modified eagle's medium
DMSO	Dimethyl sulphoxide
DNA	Deoxyribonucleic acid
DNA-PK	DNA-activated protein kinase
DNA pol	DNA polymerase
DPBS	Dulbecco's phosphate buffered saline
DPI	Diphenylene iodonium
DSB	Double-strand breaks
DTT	Dithiothreitol
e ⁻	Free electron
E3174	EXP 3174 (active metabolite of Losartan)
EC	Endothelial cell
ECL	Enhanced chemiluminescence
ECM	Extracellular matrix
ecSOD	Extracellular SOD
EDTA	Diaminoethanetetra-acetic acid
EGF	Epidermal growth factor
EGTA	Ethylene glycol-bis(β-aminoethyl ether)-N,N,N',N'-tetraacetic acid
EMEM	Earle's minimum essential medium
eNOS	Endothelial nitric oxide synthase
EPC	Endothelial progenitor cell
ERK	Extracellular signal-regulated kinase
ERRα	Estrogen-related receptor α
ET-1	Endothelin-1
EtOH	Ethanol
FAD ⁺	Flavin adenine dinucleotide
FADH ₂	Flavin adenine dinucleotide dehydrogenase
FCS	Foetal calf serum
Fe ²⁺ / Fe ³⁺	Iron ions
FITC	Fluorescein isothiocyanate
Gab1	Growth factor receptor-bound protein-2-associated binder-1
GPx	Glutathione peroxidase
Grb2	Growth factor receptor-bound protein-2
Grb10	Growth factor receptor bound protein-10
GSH	Glutathione
GSSG	Oxidised glutathione
G ₀ -phase	Non-dividing dormant state
G ₁ -phase	Preparing for proliferation
H ⁺	Hydrogen proton
hASMC-hTERT	Human aortic smooth muscle cells transfected with human telomerase
HBSS	Hank's balanced salt solution

Angiotensin II induced premature senescence

HCl	Hydrochloric acid
5-HD	5-hydroxydecanoic acid
HDF	Human dermal fibroblasts
Hdm2	Human double minute proteins
HMW	High molecular weight
H ₂ O	Water
H ₂ O ₂	Hydrogen peroxide
HOCl	Hypochlorous acid
H ₃ PO ₄	Orthophosphoric acid
HPRT1	Hypoxanthine phosphoribosyltransferase 1
HRP	Horseradish peroxidase
hTERT	Human telomerase catalytic subunit
hUVEC	Human umbilical vein endothelial cell
hVSMC	Human vascular smooth muscle cell
Hypertrophy	Increase in cell size without change in DNA content
Hyperplasia	Increase in cell number
IGF-1	Insulin-like growth factor-1
IGFBP-3	Insulin-like growth factor-binding protein-3
IGFBP-5	Insulin-like growth factor-binding protein-5
IGT	Impaired glucose tolerance
IMS	Industrial methylated spirit
iNOS	Inducible nitric oxide synthase
IP ₃	Inositol triphosphate
IPAH	Idiopathic pulmonary arterial hypertension
K ⁺	Potassium ions
KCl	Potassium chloride
KH ₂ PO ₄	Potassium phosphate
KOH	Potassium hydroxide
LCLA	Lucigenin chemiluminescence assay
LDL	Low-density-lipoproteins
LMP	Low melting point
Lucigenin	Bis-N-methylacridinium nitrate
MAPK	Mitogen-activated protein kinase
MEF2	Myocyte enhancer factor 2
MEK	Mitogen-activated extracellular signal-regulated kinase
MI	Myocardial infarction
Milk/TBST	Milk in TBS with tween-20
mitoK _{ATP}	Mitochondrial ATP-sensitive potassium channel
MitoSOX TM	MitoSOX TM red mitochondrial superoxide indicator
Mito-TEMPO	(2-(2,2,6,6-tetramethylpiperidin-1-oxyl-4-ylamino)-2-oxoethyl) – triphenylphosphonium chloride
MMP	Matrix metalloproteinase
MMP-1	Matrix metalloproteinase-1
MnSOD	Manganese SOD
M-phase	Mitosis
MPO	Myeloperoxidase
mtDNA	Mitochondrial DNA
mtRC	Mitochondrial respiratory chain
mRNA	Messenger RNA
MTT	3-(4,5-dimethyl-thiazol-2-yl)-2,5-diphenyl tetrazolium bromide

Angiotensin II induced premature senescence

mtTFA	Mitochondrial transcription factor A
Na ⁺	Sodium ions
NAC	N-acetyl-L-cysteine
NaCl	Sodium chloride
NADH	Nicotinamide adenine dinucleotide
NAD(P)H	Nicotinamide adenine dinucleotide (phosphate) (reduced form)
NaF	Sodium fluoride
Na ₂ HPO ₄	Disodium hydrogen orthophosphate
NaOH	Sodium hydroxide
nDNA	Nuclear DNA
NEAA	Non-essential amino acids
NEB	New England Biolabs
NMP	Normal melting point
NMR	Nucleotide monitoring reagent
nNOS	Neuronal nitric oxide synthase
·NO	Nitric oxide
NOS	Nitric oxide synthase
Nox	Gp91phox homologs
NP-40	Nonidet-P40
NRF1	Nuclear respiratory factor 1
NRF2	Nuclear respiratory factor 2
NRR	Nucleotide releasing reagent
O ₂	Oxygen
O ₂ ^{·-}	Superoxide
·OH	Hydroxyl radical
O/N	Overnight
ONOO ⁻	Peroxynitrite
8-oxo-G	Oxidative modifications of guanine residues in DNA
PAGE	Polyacrylamide gel electrophoresis
PAI-1	Plasminogen activator inhibitor-1
PARP-1	Poly-(ADP)-ribose polymerase-1
PBMC	Peripheral blood mononuclear cells
PBS	Phosphate buffered saline
PD	Population doublings
PDGF	Platelet derived growth factor
PGC1 α	Peroxisome proliferator-activated receptor γ coactivator-1 α
Phox	<u>Phagocyte oxidase</u>
Pi	Inorganic phosphate
PI3K	Phosphatidylinositol-3-kinase
PKA	Protein kinase A
PLA ₂	Phospholipase A ₂
PLC	Phospholipase C
PLC-8	Phospholipase C-8
PLD	Phospholipase D
PML	Promyelocytic leukaemia
PNK	T4 Polynucleotide kinase
POLG	Mitochondrial DNA polymerase γ enzyme
Pot-1	Telomeres-1
PPAR α	Peroxisome proliferator activated receptor α
PPAR δ	Peroxisome proliferator activated receptor δ

Angiotensin II induced premature senescence

PR-	Without phenol red
pRb	Hypophosphorylated retinoblastoma protein
PyK2	Proline-rich tyrosine kinase 2
RAS	Renin-angiotensin system
Rb	Retinoblastoma protein
RIPA	Radio immuno precipitation assay
RIRR	ROS-induced ROS release
RLU	Relative light units
RLU/sec	Relative light units per second
RNA	Ribonucleic acid
RNS	Reactive nitrogen species
ROS	Reactive oxygen species
6-ROX	Reference dye
RPA	Replication protein A
RT	Room temperature
RT-PCR	Real-time polymerase chain reaction
SA- β -gal	Senescence-associated β -galactosidase
SAHF	Senescence-associated heterochromatin foci
SDS	Sodium dodecylsulfate
Seladin-1	FAD-oxidoreductase
Shc	Adaptor protein
SHP2	Tyrosine phosphatase containing Src 2 homology
SHR	Spontaneously hypertensive rat
SHRSP	Spontaneously hypertensive rats stroke-prone
SH-SH	Disulphide bonds
SIPS	Stress induced premature senescence
siRNA	Small interference RNA
SM22	Calcium-binding protein
SMC	Smooth muscle cell
SM-MHC	Smooth muscle-myosin heavy chain
SOD	Superoxide dismutase
S-phase	DNA synthesis
SSB	Single-strand breaks
STASIS	Stress aberrant signalling-inducing senescence
STAT	Signal transducers and activators of transcription proteins
tDNA	Telomere DNA
t-BHP	<i>Tert</i> -butylhydroperoxide
TBS	Tris buffered saline
TBST	Tris buffered saline with Tween-20
TE	Tris-EDTA
TEMED	N,N,N',N'-tetramethylethylenediamine
TERT	Catalytic subunit of telomerase reverse transcriptase
TGF- β	Transforming growth factor- β
Tiron	4,5-dihydroxy-1,3-benzene disulfonic acid
TNF α	Tumour necrosis factor- α
TRAP	Telomeric repeat amplification protocol
TRBF1	Telomere repeat binding factor 1
TRBF2	Telomere repeat binding factor 2
TRF	Terminal restriction fragment
Tris	Tris(hydroxymethyl)-methylamine

Angiotensin II induced premature senescence

Triton X-100	t-Octylphenoxypolyethoxyethanol
Trx	Thioredoxin
TrxR	Thioredoxin reductase
TTFA	Thenoyltrifluoroacetone
Tween-20	Polyoxyethylene sorbitan monolaurate
U	Ubiquinol
UP H ₂ O	Ultrapure water
UV	Ultra violet
VEGF	Vascular endothelial growth factor
Vitamin C	L-ascorbic acid
Vitamin E	α -tocopherol
VSMC	Vascular smooth muscle cell
WBC	White blood cell
Xanthine	2,6-dihydroxypurine
XO	Xanthine oxidase
XRCC1	X-ray cross-complementing factor 1
$\Delta\Psi_M$	Mitochondrial membrane potential

CHAPTER ONE

Introduction

Chapter 1.0: Introduction

1.1 Vascular Ageing

Age is an important risk factor for cardiovascular diseases (CVD). In the Western world, CVD are the leading cause of morbidity and mortality due in part to an ageing population.

Age-related changes in blood vessels include increased wall thickness, stiffness (arteriosclerosis), blood and pulse pressure and endothelial cell (EC) dysfunction (Lakatta and Levy, 2003). These structural and functional changes are accelerated in the occurrence of age-associated CVD (Najjar *et al.*, 2005). Cellular senescence has a critical role in vascular pathophysiology, as alterations in the functional behaviour of senescent vascular cells are consistent with changes identified in vascular diseases, such as atherosclerosis (Bennett *et al.*, 1998; Minamino *et al.*, 2002). Vascular ageing can therefore be defined as the progressive phenotypic changes that arise within the vasculature with advancing age that ultimately lead to deterioration or loss in normal vascular function, which may ultimately result in death.

Angiotensin II (Ang II) is a major effector component of the renin-angiotensin system (RAS). Hemodynamic stress and sympathetic activity contribute to the increase in Ang II with age, which governs the adaptive responses to age-related vascular changes in order to maintain function (Najjar *et al.*, 2005). The RAS is also associated with increased oxidative stress and inflammation, which are also observed in several CVD. Various cardiovascular risk factors may predispose to oxidative stress. The latter is often considered a major contributor of vascular ageing (Matthews *et al.*, 2006; Minamino *et al.*, 2003).

Many age-associated vascular changes at the cellular and physiological level can be considered as risk factors themselves in the development of CVD. The association between cellular senescence, vascular ageing and CVD is highly suggestive of a causal link between the processes, although a direct link has not been determined as yet.

1.2 Cellular Senescence

1.2.1 Characteristics of cellular senescence

Cellular senescence is an important cell cycle regulatory mechanism that halts normal cell division in response to various intrinsic and extrinsic stress signals, which may be potentially oncogenic (Campisi, 2001; Itahana *et al.*, 2001). It is also initiated when a critical level of damage occurs, restricting further cell division (Campisi, 2001; Ben-Porath and Weinberg, 2005).

Senescent cells present a G₁ deoxyribonucleic acid (DNA) content and are unable to enter the S-phase; they remain viable, metabolically active but unable to divide. Altered gene and protein expression compared to that of normal proliferating cells (Neumeister *et al.*, 2002) tends to be cell-type specific, and possesses a distinctive altered morphology (Goldstein, 1990). In addition to these changes, they generally display acquired resistance to cell death (apoptosis) (Wang, 1995).

Common morphological, biochemical and nuclear characteristics have been observed in various types of cell undergoing senescence. Many of these are often used as biomarkers to identify senescent cells *in vitro* and *in vivo* (Burrig, 1991; Dimri *et al.*, 1995; Minamino *et al.*, 2002; Matthews *et al.*, 2006). **Table 1.1** displays these classical features of cellular senescence.

Many propose cell senescence to contribute to organismal ageing, where the gradual accumulation of senescent cells with age may cause alterations in tissue structure and function (Campisi, 2001; Campisi, 2005) initiating the development of age-related pathologies, e.g. atherosclerosis, osteoarthritis (Campisi, 2001). For example, senescent chondrocytes have been shown to accumulate with age in articular cartilage, increasing the risk of osteoarthritis (Martin *et al.*, 2004).

Table 1.1 Typical features of cellular senescence

<i>Senescent features</i>
<i>Morphological alteration</i>
<ul style="list-style-type: none"> ↑ cell size flattened cells (loss of typical cell shape) vacuolisation (↑ vacuole-rich cytoplasm) ↑ granularity ↑ polyploidy (multiple copies of entire genome in a cell)
<i>Biochemical change</i>
<ul style="list-style-type: none"> ↑ perinuclear activity of senescence-associated beta-galactosidase (SA-β-gal) (↑ cell lysosomal content) overexpression of cell cycle regulatory proteins: p16^{INK4a}; p21^{CIP1}; p53 underphosphorylated retinoblastoma protein (Rb) ↑ reactive oxygen species (ROS) production overexpression of oncogenes: e.g. Ras; promyelocytic leukaemia (PML)
<i>Nuclear alteration</i>
<ul style="list-style-type: none"> ↓ telomeric DNA DNA damage (phosphorylated histone γH2AX) chromatin condensation senescence-associated heterochromatin foci (SAHF)

These are the major cellular features that occur as a consequence of senescence. Several of these characteristics are often used as biomarkers to identify senescent cells *in vitro*. (Reviewed by Neumeister *et al.*, 2002; Ben-Porath and Weinberg, 2005; Campisi, 2005; McCrann *et al.*, 2008)

1.2.2 Categories of cellular senescence

1.2.2.1 Replicative senescence

In non-transformed cells, the progressive loss in proliferative capacity due to many rounds of cell division eventually results in a state of permanent cell growth arrest, which is termed ‘replicative senescence’ (Ben-Porath and Weinberg, 2005). Hayflick and colleagues first described this concept of senescence; they observed a limited proliferating lifespan of normal human cells *in vitro* (Hayflick and Moorhead, 1961). The limited number of cell divisions is considered a ‘biological clock’, eventually triggering cell-signalling pathways to cease cell division. Since this form of senescence is due to loss of telomere function, it is also known as ‘telomere-dependent senescence’.

1.2.2.2 Stress-induced premature senescence (SIPS)

The long-term exposure to subcytotoxic stresses in proliferating cells leads to the premature induction of senescence, which is also termed ‘stress-induced premature senescence’ (SIPS) (Toussaint *et al.*, 2002) or stress aberrant signalling-inducing senescence (STASIS). This rapid stimulation of senescence is elicited by various extrinsic stresses such as exposure to agents inducing oxidative stress (H_2O_2 (de Magalhães *et al.*, 2004), t-BHP (Dumont *et al.*, 2001), ethanol (Dumont *et al.*, 2002) and ultra violet (UV) radiation (Debacq-Chainiaux *et al.*, 2005)), inadequate nutrients for cell growth and cell-cell contact (Ramirez *et al.*, 2001). These effects are independent of telomere dysfunction and may also be defined as ‘telomere-independent senescence’.

Both of the main forms of senescence can be induced by a DNA damage-response and activate p53. They exhibit the typical cellular features described in **table 1.1** (apart from telomere changes). The only apparent difference therefore, is that replicative senescence is programmed at a specific time in the lifespan of a cell when telomeres become critically short, whereas SIPS is not programmed but results from the response to a given acute stress, e.g. when DNA is damaged beyond repair (Suzuki and Boothman, 2008).

Senescence can be induced in response to a range of cell stress-related stimuli. Telomere attrition or dysfunction is an important trigger, as the main function of telomeres is believed to be the maintenance of integrity of sub-telomeric DNA encoding genes. Other well-characterised initiators are irreparable DNA damage, enhanced oxidative stress, oncogene activation, improper growth conditions (Ben-Porath and Weinberg, 2005; Campisi, 2005) and epigenetic changes to chromatin structure (Neumeister *et al.*, 2002). These main triggers of senescence are discussed below in section **1.2.3**.

1.2.3 Initiators of senescence

1.2.3.1 Telomere uncapping and/or dysfunction

Telomere shortening is regarded as a major trigger of replicative senescence (Itahana *et al.*, 2001; Ben-Porath and Weinberg, 2005). Telomeres are termed ‘replicometers’, that count numbers of cell divisions due to a gradual shortening of the average length of

telomeres (Harley *et al.*, 1990; von Zglinicki, 2001; Neumeister *et al.*, 2002). Telomeres are chromosomal protective cap structures, consisting of long ‘TTAGGG’ DNA repeat sequences (in man) that gradually shorten with each cell division. Human cells senesce when telomeres (often expressed as the Terminal Restriction Fragment (TRF) length) reach a critical length of 4-7kb, reduced from 15-20kb in the germ line (Harley *et al.*, 1990). In fact, it is likely that a single critically shortened telomere is sufficient to induce growth arrest. It is thought that critically shortened telomeres or an altered telomere structure due to loss of telomere-binding proteins, can no longer protect genes encoding DNA sequences. This signals the activation of senescence within the cell (Masutomi *et al.*, 2003; Stewart *et al.*, 2003). The shortening of telomeres is additionally affected by the presence of telomerase, a ribonucleoprotein involved in synthesizing telomeric DNA repeats, thereby maintaining telomere length (Harley *et al.*, 1990). The general tenet is that most somatic cells contain very low levels of telomeres, hence the limited potential for proliferation.

Exactly how truncated telomeres signal a cell to undergo senescence is not clear, but ‘telomere uncapping’ is thought to be one such mechanism (Blackburn, 2001). The end of each telomere has an extended guanine-rich 3’ nucleotide overhang, which is intercalated into the double-stranded telomere DNA forming a telomeric ‘t-loop’ (Stewart *et al.*, 2003), which acts as a protective cap structure. Opening of this loop would leave the single-stranded overhang exposed to DNA damage (von Zglinicki, 2001), thereby triggering senescence. This has been determined in senescent cells where loss of single-stranded telomere DNA results in a telomeric overhang (Stewart *et al.*, 2003). Uncapped telomeres may be identified as a DNA double-strand break (DSB), also initiating a DNA damage response. Common DNA damage foci have been detected in telomeres of senescent cells, and contain proteins such as γ -H2AX, 53BP1, MDC1 and NBS1 (d’Adda di Fagagna *et al.*, 2003; Herbig *et al.*, 2004), which further emphasises signalling of the DNA-damage response pathway via telomere attrition.

1.2.3.2 DNA damage

Exposure to radiation and DNA-damaging agents (e.g. ROS) can cause direct damage to DNA and trigger cells to undergo senescence (Wahl and Carr, 2001). Persistent damage to DNA can induce SIPS or accelerate telomere erosion (von Zglinicki, 2002; d’Adda di Fagagna *et al.*, 2003) thereby inducing replicative senescence.

ROS-induced DNA damage can cause oxidation of histones (DNA protecting proteins), DNA base oxidation, single-strand breaks (SSB) and DSB, that can cause cells to undergo premature growth arrest (Campisi, 2001). This response of the cell to DNA damage is dependent upon the harmful agent and dosage administered, by either inducing senescence as a result of minor damage or apoptosis due to significant damage (Ben-Porath and Weinberg, 2005). Cell cycle arrest is further determined by the severity of DNA damage where it can be transient to allow for DNA repair or permanent as a result of irreparable damage (Bertram and Hass, 2008).

Extensive work has shown DNA damage to activate the tumour suppressor protein, p53. The initial DNA-damage signals a cascade of protein kinase activity, including of ataxia telangiectasia mutated (ATM), ataxia telangiectasia and Rad-3-related (ATR) and DNA-activated protein kinase (DNA-PK). Histone H2AX molecules situated close to the site of DNA damage are phosphorylated and stimulate p53 (Shiloh, 2003; von Zglinicki *et al.*, 2005).

Multiple forms of DNA damage maybe one of the potential causes of the different forms of senescence that are instigated by telomere dysfunction and oncogene activation (d'Adda di Fagagna *et al.*, 2003; Di Micco *et al.*, 2006).

1.2.3.3 Oxidative stress

ROS act as secondary messengers in the cell-signalling senescence pathways. However, enhanced ROS can lead to a state of oxidative stress (imbalance between ROS and antioxidants in cells and tissues) and participate in senescence by causing damage to biomolecules, for example, by oxidizing DNA, lipids and proteins (Chen *et al.*, 1998). Substantial ROS-induced damage to genomic DNA accelerates senescence via the DNA-damage response pathway (Bertram and Hass, 2008).

ROS are regarded as major mediators of SIPS. For example, sublethal H₂O₂ and *tert*-butylhydroperoxide (t-BHP) exposures induced premature senescence of human fibroblasts (Chen *et al.*, 1998; Dumont *et al.*, 2001). Moreover, when grown under ambient oxygen (O₂) conditions of ~20%, these cells underwent early senescence compared with those grown in just 2 to 3% O₂ (Chen *et al.*, 1995).

1.2.3.4 Oncogene activation

Oncogenic activation is an intrinsic stress that can cause rapid cell senescence to suppress tumour formation. Overexpression of Ras or Raf oncogenes can trigger healthy cells to undergo early senescence (Serrano *et al.*, 1997). Ras/Raf signalling initiates senescence through the mitogen-activated protein kinase (MAPK) pathway, which is mainly coordinated via p16^{INK4a} induction (Campisi, 2005), but also via p53 (Serrano *et al.*, 1997). Activated oncogenes endorse cells to initially undergo uncontrollable proliferation. This stress response then triggers cells to enter senescence, to prevent tumour transformation (Ferbeyre *et al.*, 2002), as illustrated in **figure 1.1**.

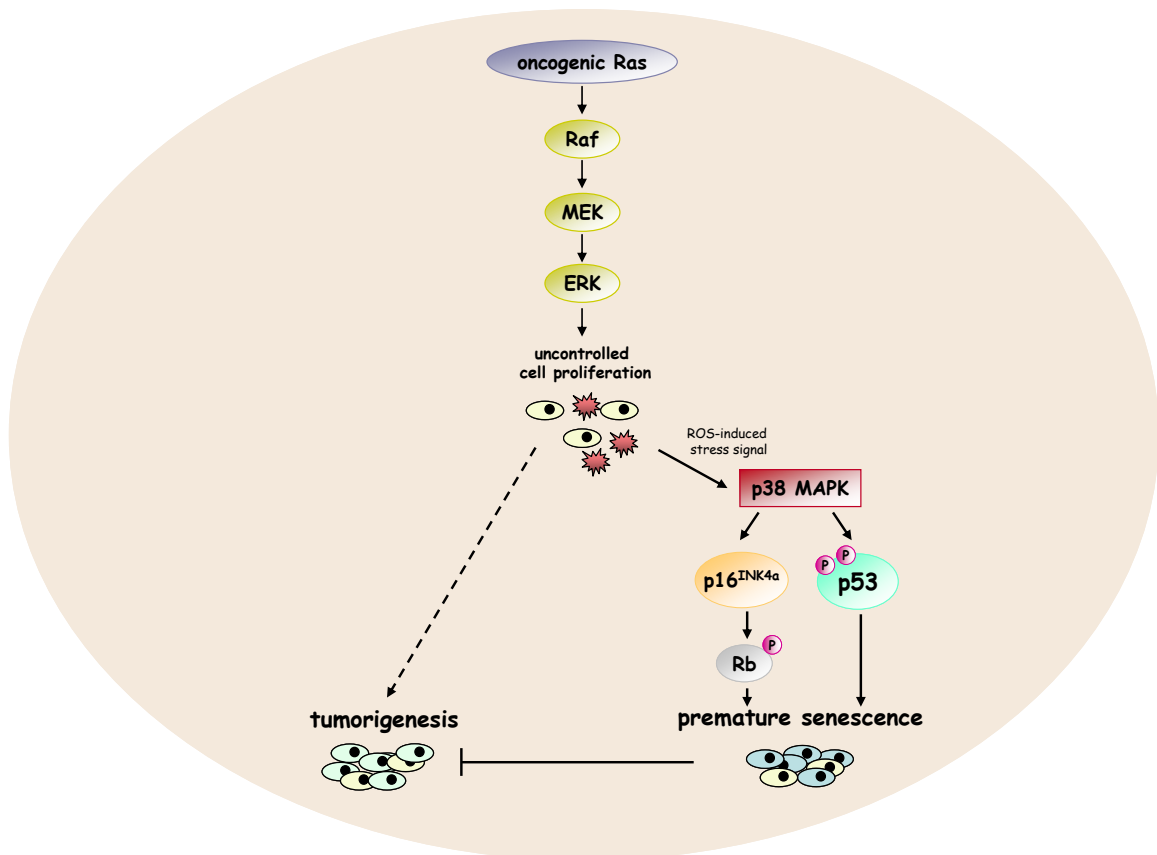


Figure 1.1 Oncogenic Ras-induced tumour formation and senescent signalling mechanism. Overexpression of various oncogenes including Ras, activate the Raf-MEK-ERK-MAPK pathway resulting in tumorigenesis. ROS generated via the initial uncontrollable cell proliferation can act as a stress signal and activate p38 MAPK and thereby trigger cells to undergo rapid growth arrest, to prevent tumour formation. In human cells, Ras predominantly triggers senescence via overexpression of p16^{INK4a} although this mechanism can also be initiated by p53 expression (Serrano *et al.*, 1997). ERK, extracellular signal-regulated kinase; MEK, mitogen-activated extracellular signal-regulated kinase. (Adapted from Bringold and Serrano, 2000; Han and Sun, 2007)

Constitutive activation of oncogenes has been shown to induce premature senescence. This has been observed with overexpression of Ras in vascular smooth muscle cells (VSMC), which then exhibit a senescent phenotype resembling that detected in atherosclerosis (Minamino *et al.*, 2003). Oncogenic Raf has also been shown to initiate rapid senescence in human lung fibroblasts (Zhu *et al.*, 1998).

1.2.3.5 Inadequate growth conditions

A deficiency in cell nutrients and growth promoting factors, as well as improper cell-cell and cell-matrix contacts are additional extrinsic stresses that can promote premature growth arrest of cells *in vitro* (Ben-Porath and Weinberg, 2005). Early loss of cell growth has also been demonstrated when human fibroblasts have been grown in media containing 0.25% (v/v) serum and when human keratinocytes were not cultured on feeder layers (Ramirez *et al.*, 2001), which shows that improper cell contacts leads to the rapid onset of senescence. The activation of p16^{INK4a} has strongly been implicated in response to these stresses, since the induction of premature senescence is independent of telomere attrition (Rheinwald *et al.*, 2002).

1.2.3.6 Multiple stresses

The various triggers of cellular senescence previously discussed are not exclusively independent, as cells can be exposed to more than any one of these stresses simultaneously. It has been proposed that numerous stresses exerted in a population of cells can induce an accumulative growth arrest (Ben-Porath and Weinberg, 2005). Additionally, extrinsic stresses such as oxidative stress, DNA damage and oncogene overexpression can affect intrinsic stresses. For example, enhanced ROS can cause damage to DNA and accelerate telomere erosion (von Zglinicki *et al.*, 1995), but is also thought to be involved in oncogenic Ras mediated senescence (Lee *et al.*, 1999). The diversity of stresses that signal a cell to undergo senescence is both varied and complex, essentially allowing the mechanism of senescence to be induced in response to altered or damaged cell function.

1.2.4 Diverse cell senescence signalling pathways

The tumour suppressor proteins p53 and pRb play a major role in the senescence induction, by mediating cascade signalling pathways. These pathways can be triggered independently or interact to promote growth arrest (Campisi, 2001; Ben-Porath and

Weinberg, 2005) depending upon the stress signal incurred, as shown in **figure 1.2**. Both replicative senescence and SIPS can be mediated by the core p53 and pRb cell signalling pathways to induce growth arrest.

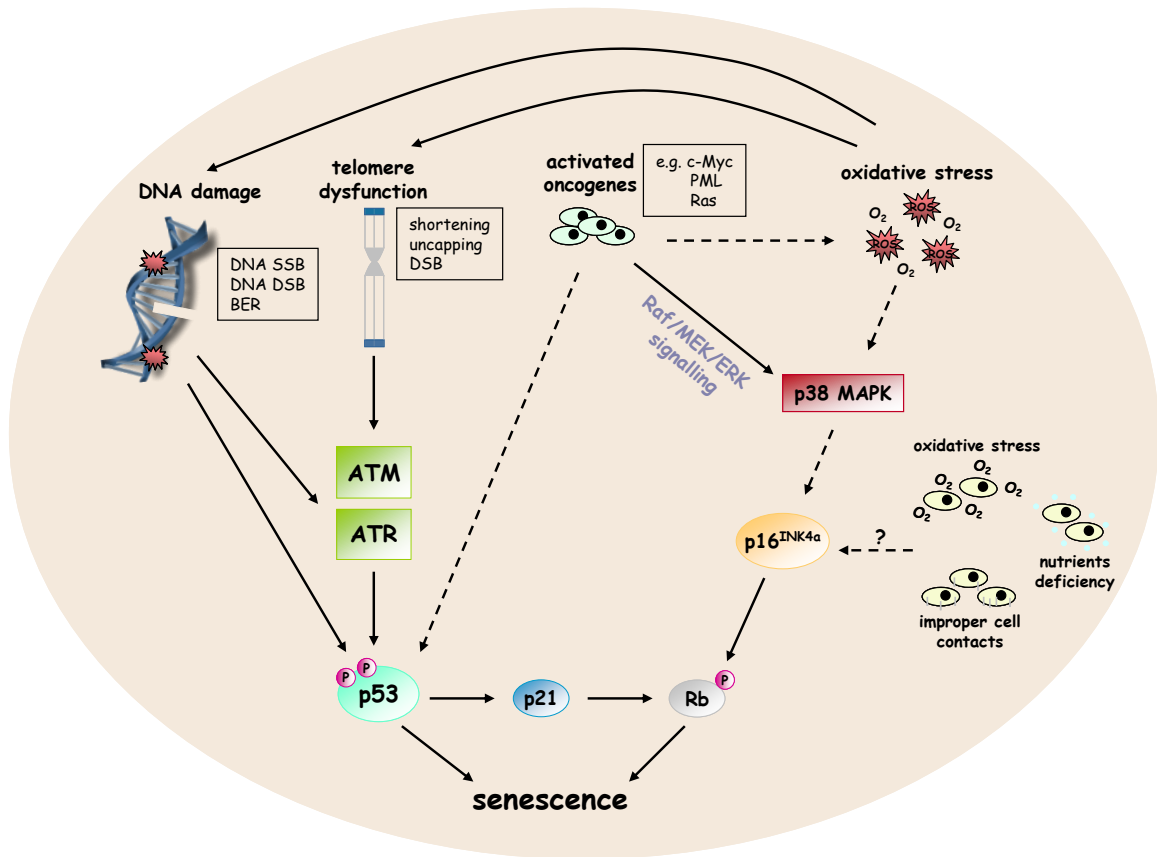


Figure 1.2 Human cell signalling senescence pathways in response to the various stress signals. Schematic representation shows the overlap in signalling senescence triggered by the diverse stimuli. Telomere dysfunction and DNA damage activate ATM/ATR kinases and stabilize p53. Oxidative stress and overexpressed oncogenes tend to mediate effects through p38 activation and p16^{INK4a} expression (Ben-Porath and Weinberg, 2005), although oncogenic Ras can induce p53 in response to elevated ROS production (Campisi, 2005). Inadequate cell growth conditions and insufficient cell contacts can trigger rapid senescence via p16^{INK4a} (Rheinwald *et al.*, 2002). These mechanisms have been mainly determined from human fibroblast studies. (*Adapted from Ben-Porath and Weinberg, 2005; Han and Sun 2007*)

1.2.5 Hayflick mosaic

In vivo, the proliferative potential of cells/tissues is never entirely lost since the renewal of cells by stem cells allows for senescent cells to be replaced by “young” ones. Therefore, the ‘Hayflick mosaic’ has been described as the small number of cells in the tissues of aged people that are likely to be senescent which interfere with the overall homeostasis of tissues or organs that may contribute to ageing (Shay and Wright, 2000).

1.3 Vascular Cell Senescence, Ageing and CVD

1.3.1 Vascular cell senescence

Many age-related changes in vascular structure and function are suggested to contribute to the increased risk of CVD development in the elderly. Major changes include a decrease in blood vessel compliance and increase in inflammation (Najjar *et al.*, 2005). Alterations at the cellular level have also been extensively investigated in relation to ageing and disease progression. Many typical senescent characteristics are detected in aged vascular cells; this coincides with alterations determined in atherosclerosis (Minamino *et al.*, 2002; Gorenne *et al.*, 2006; Matthews *et al.*, 2006) which strongly suggests that cellular senescence has a major role in vascular pathology.

Dysfunctional, senescent vascular cells are considered to alter the overall tissue or organ function (Campisi, 2005) and thereby contribute to the development of many age-related CVD, e.g. atherosclerosis, ischemic heart disease and myocardial infarction (Minamino *et al.*, 2004; Erusalimsky and Kurz, 2005). The incidence of CVD increases with age, as tissue function is thought to decline due to the gradual loss in cell renewal capacity and/or repair.

1.3.2 Vascular cell senescence in vitro

EC and VSMC undergo senescence *in vivo* and *in vitro* (Minamino *et al.*, 2004). EC have a critical role within the vasculature, maintaining vascular tone. A vast accumulation of senescent EC is considered to have an extreme effect on vascular integrity, function and homeostasis (Foreman and Tang, 2003). Senescent EC display a reduction in nitric oxide ($\cdot\text{NO}$), $\cdot\text{NO}$ synthase activity (Minamino *et al.*, 2002) and prostacyclin production that causes impairment of the vasodilatory function of the vessel. In addition to these changes, these cells also display upregulation of adhesion molecules, proinflammatory cytokines and plasminogen activator inhibitor-1 (PAI-1) (Erusalimsky and Kurz, 2005).

VSMC have a major structural role within blood vessels and are primarily involved with vasoconstriction. Senescent VSMC display decreased elastase production which contributes to arterial stiffness; and a diminished response to $\cdot\text{NO}$ and β -adrenoceptor stimulation with advancing age (Crass *et al.*, 1992).

1.3.3 Progeroid syndromes

Progeroid syndromes are characterised by accelerated ageing and shortened lifespan. Analysis of these conditions has advanced our understanding of accelerated cell senescence and human ageing.

Fibroblasts isolated from people with Werner and Hutchinson-Gilford Syndrome displayed premature replicative senescence *in vitro*, reducing the cumulative cell population doubling to 70% compared with fibroblasts from healthy people (Faragher *et al.*, 1993; Chang, 2005). Both these progeroid conditions are associated with the early development of atherosclerosis. In particular, Werner Syndrome is a result of a genetic mutation in the RecQ helicase, which functions to maintain genomic stability (Gray *et al.*, 1998). Murine models of the condition have exhibited similar cell ageing characteristics to that observed in humans with Werner Syndrome, with rapid telomere loss having a major role in the pathology (Chang *et al.*, 2004). Another suggestion is that increased DNA mutations and damage may lead to genomic instability and cellular abnormalities which trigger the early onset of vascular cell senescence, and maybe the underlying causes of accelerated atherosclerosis and premature ageing in these conditions (Capell *et al.*, 2007). However, atherosclerosis has not been observed in other progeria syndromes that are associated with shortened telomeres, such as Ataxia Telangiectasia and Dyskeratosis Congenita (Erusalimsky and Kurz, 2005), suggesting not all age-related disorders develop via a telomere-dependent mechanism.

1.3.4 Evidence for the role of vascular cell senescence in CVD

1.3.4.1 Replicative vascular cell senescence

A number of EC and VSMC within atherosclerotic lesions exhibit morphological features characteristic of cell senescence. Senescent EC found on the surface of atherosclerotic plaques appear as large giant-like cells, showing irregularities in patterning positions (Burrig, 1991) and also appear flattened (Minamino *et al.*, 2002). Similar observations of senescent VSMC in the intima of atherosclerotic lesions and in

aortic aneurysms probably result from substantial cell replication (Minamino *et al.*, 2003; Liao *et al.*, 2000).

SA- β -gal activity is a commonly used cytochemical biomarker of cellular senescence and is shown to correlate with cellular ageing. Cultivated cells approaching growth arrest express increased β -galactosidase activity at pH 6.0 (Dimri *et al.*, 1995), commonly measured as a blue cytochemical staining of the cytoplasm. Vascular cells staining positive for SA- β -gal have been detected in atherosclerotic plaques of human coronary arteries isolated from ischemic heart disease patients (Minamino *et al.*, 2002) and in VSMC derived from plaques compared to those from normal arteries (Gorenne *et al.*, 2006). Additionally, other senescent markers have been detected in VSMC derived from advanced plaques; these include increased expression of cyclin dependent kinase inhibitors (CDKI) p16^{INK4a} and p21, shortened telomeres and extensive oxidative DNA damage (Matthews *et al.*, 2006). These are all hallmarks of cell ageing.

Accumulating evidence has shown telomere shortening to result in unprotected chromosome ends, thereby playing a prominent role in triggering cell senescence (Neumeister *et al.*, 2002; Minamino *et al.*, 2004). Telomere shortening has been observed in cultured human EC and VSMC following extensive cell division (Chang and Harley, 1995; Minamino *et al.*, 2001). This loss of telomeres has been determined in different vascular cell types. It has been correlated with increasing age and progressive atherosclerotic grades in abdominal aortas (Okuda *et al.*, 2000). Telomere attrition in coronary EC may contribute to dysfunction that could enhance the development of coronary artery disease (Ogami *et al.*, 2004).

Moreover, shortening of telomeres in white blood cells (WBC) has been detected in numerous conditions that associate with the risk for CVD, such as diabetes, hypertension, impaired glucose tolerance, life stress, obesity, and smoking (Jeanclos *et al.*, 1998; Benetos *et al.*, 2001; Adaikalakoteswari *et al.*, 2007; Epel *et al.*, 2004; Valdes *et al.*, 2005). This further emphasises that loss of telomeres is associated with dysfunctional cells, which is a well-known characteristic of cells undergoing replicative senescence.

It still remains unclear as to whether senescence arises from or is a consequence of telomere attrition or dysfunction (Minamino *et al.*, 2004). Changes in TRF length indicate a link between CVD and accelerated vascular ageing. For example, telomere DNA length, assessed by the Southern Blotting technique was shorter in cultured EC isolated from iliac arteries, compared to iliac veins (Chang and Harley, 1995). It was suggested that this may be due to iliac arteries being exposed to higher hemodynamic stress *in vivo* and greater cell turnover from disturbed blood flow. The rate of telomere loss also increased with an increase in donor age (Chang and Harley, 1995).

Significantly shorter mean TRF lengths of white cells were observed in subjects at risk of premature myocardial infarction (MI), compared to controls (Brouillette *et al.*, 2003). An increase of 2.8 to 3.2-fold was found in subjects at-risk of MI and displaying shorter than average telomeres, independent of other risk factors. This study showed a potential link between biological ageing and the development of coronary artery disease, and contributed to our understanding of the variations in biological ageing (telomere DNA length) and disease onset (Brouillette *et al.*, 2003; 2007). The mean telomere lengths in blood of healthy people, 60 years and over were analysed by quantitative polymerase chain-reaction (qPCR) and Southern blotting. Those with shorter telomere lengths, showed a 3.2-fold increase in mortality rate from heart disease, and an 8.5-fold increase from infectious diseases (Cawthon *et al.*, 2003).

A possible X-linked mechanism of inheritance for telomere length was proposed following a family-based cohort of the Flemish Study, which observed environmental, genetic and health aspects. A high agreement of TRF lengths was seen between mothers and offspring and between fathers and daughters only, suggesting that genetic predisposition to age-related diseases could be related to shortened telomeres that are inherited in an X-linked manner (Nawrot *et al.*, 2004).

1.3.4.2 SIPS of vascular cells

The accumulation of ROS-induced cellular damage is implicated in the induction of premature senescence and may favour the onset of CVD. Premature vascular cell senescence has been detected following vascular injury and during disease development. For example, the repeated balloon catheter denudations of rabbit carotid arteries caused increased SA- β -gal activity in the injured arteries (Fenton *et al.*, 2001).

It was proposed that the stress incurred by denudations and enhanced proliferation of vascular cells may have led to the onset of premature senescence.

VSMC from the fibrous caps of human atheromas exhibited increased SA- β -gal activity *in vitro*. This coincided with p16^{INK4a} and p21 CDKI expression and telomere loss, but also presented increased oxidative DNA damage. This was mimicked by oxidant exposure to VSMC *in vitro* (Matthews *et al.*, 2006) suggesting a mechanism for the induction of premature senescence *in vivo*.

Increased levels of the senescent biomarker apolipoprotein J have been determined in serum of type II diabetic patients with developing coronary heart disease (Trouwakos *et al.*, 2002). This protein has been associated with both replicative senescence and SIPS, but in this instance the elevated levels corresponded to early cellular changes that resembled those observed in various CVD.

A subpopulation of peripheral-blood mononuclear cells (PBMC) taken from people with chronic kidney disease (CKD) revealed accelerated telomere attrition, increased p53 expression and overexpression of proinflammatory cytokines (Ramirez *et al.*, 2005). Shortened telomeres correlated with the increased C-reactive protein levels indicating inflammation as a possible cause. The acute senescence of these cells was considered to arise from repeated cellular activation (Ramirez *et al.*, 2005).

Taken together the evidence indicates that premature senescence within the vasculature may have a significant role in vascular ageing and in the initiation of vascular pathologies.

1.3.5 Telomere-dependent and -independent vascular cell senescence

As previously described, cell senescence is commonly categorized as either replicative or SIPS (section 1.2.2), which is mainly based upon the length of time taken to detect substantial senescence and the type of stress induced. Senescence can also be classified as being telomere-dependent or telomere-independent, although this definition only accounts for loss in telomeres and discounts other triggers that maybe involved in the senescence mechanism. The induction of senescence is complex and can be initiated by various stresses (discussed in 1.2.3.6).

Several CVD strongly associated with senescence cannot be grouped under this classification, since many of these diseases present at late-age, e.g. atherosclerosis. The evidence of shortened telomeres in this disease with advancing age would suggest this to be a telomere-dependent mechanism of senescence. However, in addition to this, the expression of other biomarkers of senescence indicate early growth arrest of cells, e.g. dual staining of VSMC with p16^{INK4a} and SA-β-gal expression and increased oxidative DNA damage (Matthews *et al.*, 2006), which suggests also a telomere-independent mechanism. From this, it might be suggested that atherosclerosis involves either one or the other senescent mechanism; but is more accurately an amalgamation of telomere-dependent and –independent senescence mechanisms.

1.4 Angiotensin II

1.4.1 Synthesis of Ang II

Ang II is a multifunctional octapeptide hormone that has a major effector role in the RAS, cardiovascular homeostasis (Taubman, 2003) and in adaptive responses to ageing within the vasculature and disease (Duprez, 2006). Ang II is synthesized mainly via the renal RAS (plasma) and locally via tissue RAS. The renal-derived renin cleaves hepatic-derived angiotensinogen to form angiotensin I (Ang I) which is then converted to Ang II (Phillips *et al.*, 1993), as shown in **figure 1.3**. Additionally outlined are the alternative pathways that can also convert Ang I to Ang II, via enzymes (e.g. tonin and cathepsin), which may have a significant role in the development of disease states. Almost all components of the RAS are present in tissues to enable local Ang II synthesis. This is the case within the vasculature, except that renin is absent (Touyz and Schiffrin, 2000). Local Ang II formation is regulated by the uptake of renal-derived renin from the circulation and angiotensin-converting enzyme (ACE) in vascular cells.

1.4.2 Function of Ang II and signalling mechanisms

Ang II primarily functions as a vasoconstrictor by inducing contraction of blood vessels to ensure ample blood flow. It is therefore essential in the structural and functional integrity of vessels. Ang II also has a role in modulating blood pressure, contributing to the regulation of sodium and water homeostasis, central nervous system mechanisms (e.g. thirst), and maintaining vascular tone (Touyz and Schiffrin, 2000).

Ang II induces pleiotropic actions in the vasculature. Short-term rapid effects of Ang II lead to contraction, whereas longer-term effects regulate vasomotor tone, induce cell growth, migration and differentiation, apoptosis and extracellular matrix (ECM) deposition (Touyz and Schiffrin, 2000). However, it can also act as a ‘proinflammatory’ mediator by stimulating the production of ROS, inflammatory cytokines and adhesion molecules via the expression of transcription factors. This can result in inflammation, EC dysfunction and vascular remodelling (Touyz, 2005) which are commonly observed in CVD such as atherosclerosis, MI, vascular remodelling and cardiac hypertrophy (Weiss *et al.*, 2001; Touyz *et al.*, 2003).

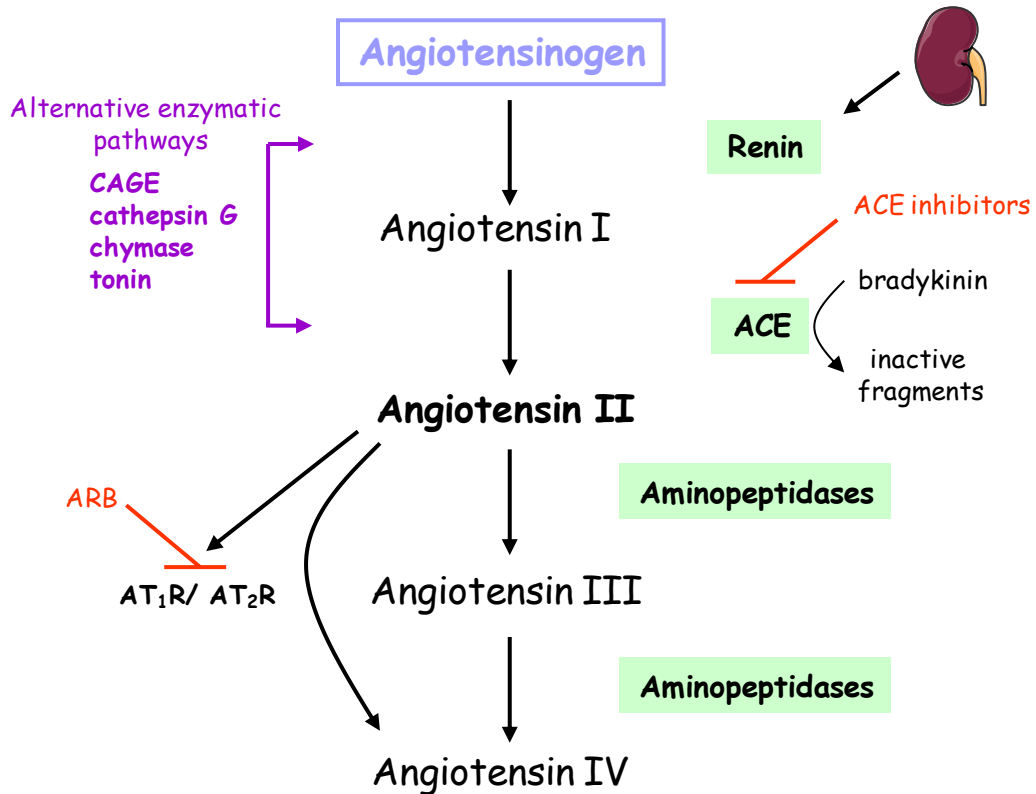


Figure 1.3 Formation of angiotensin hormones of the RAS. The angiotensinogen precursor is converted to angiotensin I by renin, and then further hydrolysed to Ang II via ACE. Ang II can alternatively be generated by other enzymes from its precursors; these include chymase, cathepsin G, chymostatin-sensitive Ang II-generating enzyme (CAGE) and tonin (Urata *et al.*, 1996). This may contribute to increased Ang II levels observed in disease. The expression of bradykinin inhibits the effect of ACE thereby preventing the formation of Ang II, and can also bind to Ang II receptors modifying their expression (Watanabe *et al.*, 2005). Synthetic ACE inhibitors also prevent ACE from converting Ang I to Ang II. Local Ang II formation in vascular tissue occurs via the same mechanism since all components of the RAS are present in tissue except renal-derived renin, which is absorbed from circulating plasma. The Ang II secreted binds to Ang II receptors on nearby cells, inducing an intracellular response. Eventually, aminopeptidases degrade Ang II to angiotensin III and IV (Touyz and Schiffrin, 2000). Red lines indicate inhibitors of Ang II formation and activation, which include ACE inhibitors and Ang II receptor blockers (ARB).

Complex Ang II-signalling pathways initiate these intracellular responses via the activation of phospholipase C (PLC), tyrosine kinases, MAPK, matrix metalloproteinases (MMP) and growth factors, as summarised in **figure 1.4**. Ang II can also elicit an effect via NAD(P)H oxidase activation by stimulating ROS production (see section **1.5.4.1**).

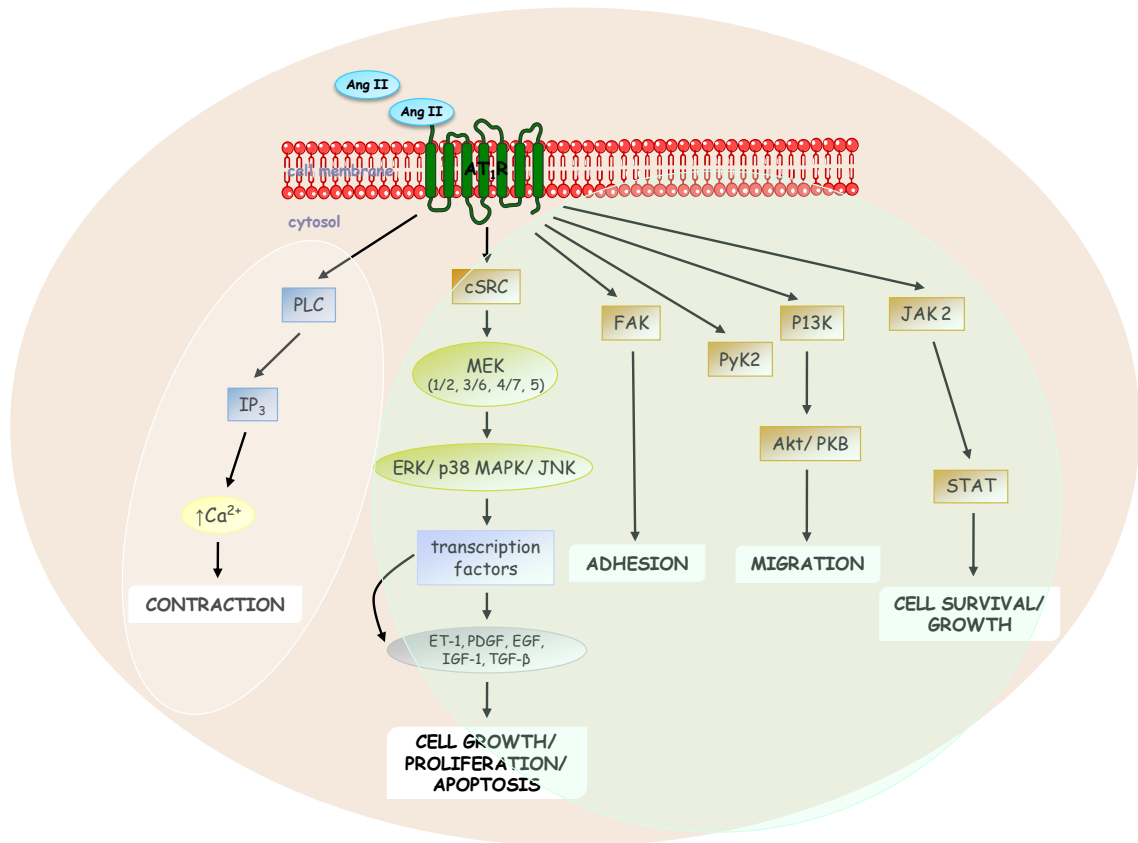


Figure 1.4 Diverse Ang II signalling responses in VSMC. Various cellular effects of Ang II are initiated by binding to Ang II type-1 receptors (AT₁R). This receptor activation leads to phosphorylation of tyrosine kinases (brown boxes) further initiating downstream signalling molecules. Activation of MEK/ MAPK cascades regulates cell growth, proliferation, apoptosis, migration and adhesion; which may occur several hours or days after signalling (circled light green). Additionally, Ang II can induce growth factor production influencing cellular growth. PLC – inositol triphosphate (IP₃) signalling causes the rapid release of calcium (Ca²⁺) ions initiating contraction which occurs within seconds (circled white). Akt/PKB, Akt kinase/protein kinase B; EGF, epidermal growth factor; ET-1, endothelin-1; FAK, focal adhesion kinase; IGF-1, insulin-like growth factor-1; JAK2, janus kinase 2; PI3K, phosphatidylinositol-3-kinase; PDGF, platelet-derived growth factor; Pyk2, proline-rich tyrosine kinase 2; cSrc, non-receptor protein-tyrosine kinase; STAT, signal transducers and activators of transcription proteins; TGF-β, transforming growth factor β. (*Adapted from Touyz and Schiffrin, 2000; Touyz, 2005*)

1.4.3 Ang II receptor subtypes

Ang II effects are mainly mediated by binding to G-protein coupled plasma membrane receptors, the so-called AT₁R and type-2 receptors (AT₂R). Additional receptors include Ang II type-3 and type-4 receptors (AT₃R and AT₄R) but these are not fully elucidated. Ang II does not directly bind to AT₄R. The degradation peptide angiotensin IV (Ang IV (Ang 3-8)) mediates its effects via this receptor. The characteristics and physiological responses mediated via AT₁R, AT₂R and AT₄R are summarised in **table 1.2**.

Table 1.2 Characteristics and responses mediated by angiotensin receptor subtypes

<i>Characteristics</i>	<i>Receptor subtypes</i>		
	<i>AT₁R</i>	<i>AT₂R</i>	<i>AT₄R</i>
Structure	359 amino acids, 7 transmembrane domains (human) (AT _{1A} R + AT _{1B} R – rat)	363 amino acids, 7 transmembrane domains (human and rat)	dimer connected by disulfide bonds
Molecular mass	41- 42 kDa	40- 41 kDa	α -50 kDa; β -140 kDa
Affinity	Ang II> Ang III> Ang I	Ang III> Ang II> Ang I	Ang IV> LVV-hemorphin-7
Location	adrenal glands, brain, heart, kidneys, liver and highly expressed in VSMC	adrenal glands, brain, ↑foetal tissue, heart, kidneys, myometrium, ovaries	adrenal glands, bladder, brain, colon, EC, heart, kidneys, spinal cord
Antagonists	Candesartan, Irbesartan, Losartan (active metabolite E3174), Valsartan	CG-42112, PD123177, PD123319	divalinal-Ang IV
Receptor coupled to Signal transduction pathways	G-protein ↓adenylate cyclase, ↑Ca ²⁺ , IP ₃ , PLA ₂ , PLC, PLD, MAPK/JAK/STAT pathways	G-protein ↓guanylate cyclase, ↑cGMP, K ⁺ , ·NO, PLA ₂ , prostaglandins	tyrosine kinase Gab1, Grb2, Grb10, PI3K, PLC-8, SHP2, Shc
Physiological effects	↑blood pressure, Na ⁺ /H ₂ O reabsorption, ↑contractility, aldosterone secretion, vascular cell growth, vasoconstriction	↑blood pressure, PAI-1 expression, anti-proliferation, apoptosis, vasodilation	↑blood flow, ·NO release, PAI-1 expression, kidney natriuresis, vasorelaxation
Pathological effects	hypertension, coagulation, inflammation, promotes cell growth	↓blood pressure, vascular injury, inhibits VSMC growth	ischemia injury, seizures, ↑renal blood flow

Summarises the main receptor activated responses mediated in the cardiovascular system. Specific Ang II-signalling transduction pathways are initiated upon activation of a specific receptor subtype. E3174, EXP3174; Gab1, Grb2-associated binder-1; Grb-2, -10, growth factor receptor-bound protein-2, -10; K⁺, potassium ions; PL-A₂, -C, -C8, -D, phospholipase A₂, C, C8, D; Shc, adaptor protein; SHP2, tyrosine phosphatase containing Src homology 2 domains; ↑increased effect; ↓decreased effect. (*Adapted from Wright and Harding, 1997; de Gasparo et al., 2000; Mehta and Griendling, 2007*)

1.4.4 Inhibitors of Ang II

Major clinical studies have shown blocking of the RAS can protect against adverse cardiovascular effects and minimise the risk of mortality (Dahlöf *et al.*, 2002; McMurray *et al.*, 2003; Aguilar *et al.*, 2004). Hypertension is one of the main contributing risk factors in the development of CVD, which is mediated by high circulating levels of Ang II. Since Ang II mediates its effects mainly via the AT₁R, many pharmacological agents have been developed to inhibit Ang II and target this receptor, therefore aiming to reduce blood pressure and prevent the onset of disease. There are two main classes of pharmacological inhibitors, ACE inhibitors and ARB (Ruilope *et al.*, 2005).

1.4.4.1 ACE inhibitors

ACE inhibitors competitively inhibit ACE, which prevents the conversion of Ang I to Ang II and results in reduced levels of plasma and tissue-generated Ang II. These inhibitors are not specific and do not completely inhibit Ang II production since it can be generated via non-ACE pathways (**figure 1.3**). ACE inhibitors were the first developed pharmacological agents that blocked the RAS by interfering with Ang II formation.

There are various ACE inhibitors, which include Captopril, Enalapril, Ramipril and Perindopril (Wong *et al.*, 2004). The accumulation of plasma bradykinin as a result of blocking the conversion to Ang II, led to many side effects with these agents, such as dry cough, hypotension, decline in renal function and angio-oedema (Burnier and Brunner, 2000). This led to the development of new ACE inhibitors with a carboxyl or phosphoryl group attached, which minimised these side-effects and additionally improved binding efficiency to ACE and tissue absorption.

These agents are effective in lowering blood pressure, in inducing regression of left ventricular hypertrophy and in improving endothelial function. They are relatively successful in treating hypertension and congestive heart failure (Dinh *et al.*, 2001). For those intolerant to ACE inhibitors, alternative antagonists of the RAS are used, such as ARB.

1.4.4.2 ARB

ARB do not reduce Ang II formation but block the action of Ang II at the AT₁R site (**figure 1.3**). Irrespective of how Ang II is synthesized these inhibitors antagonize AT₁R-mediated effects enabling the circulating high levels of Ang II to bind to AT₂R, which also contributes to the beneficial anti-hypertensive effects of ARB (Ruilope *et al.*, 2005). ARB commonly used in the treatment of hypertension are Losartan, Candesartan, Valsartan and Ibersartan (Burnier and Brunner, 2000). Losartan is a biphenyl-tetrazole 'sartan' agent that is metabolized in the liver and generates an active carboxylic acid derivative, EXP 3174 (E3174). This major metabolite is highly potent and has a high binding affinity for AT₁R with no affinity for AT₂R. It is a non-competitive antagonist in the presence of Ang II and has a plasma half-life of 6 to 9 hours *in vivo* (Triggle, 1995). Binding studies in Ang II treated rat VSMC revealed inhibition with E3174 with an IC₅₀ = 1.1×10^{-9} mol/L, which is 40 times more potent than Losartan (Wong *et al.*, 1990). E3174 is marketed as Losartan, which has to be metabolized to generate active E3174 (Burnier and Brunner, 2000). When intravenously administered, E3174 is effective at reducing blood pressure (Wong *et al.*, 1990). *In vitro* studies comparing E3174 with various other biphenyl-tetrazole sartans showed Candesartan to have a higher potency due to its binding affinity which resulted in a long-lasting inhibition (Vanderheyden *et al.*, 1999). ARB are generally better tolerated than ACE inhibitors, and are also effective in lowering blood pressure and improving arterial compliance (Shargorodsky *et al.*, 2002) and endothelial function in hypertensive patients. In addition, ARB can also minimise inflammation as determined in patients with atherosclerosis (Navalkar *et al.*, 2001). These responses have led to a reduced risk of mortality.

1.4.5 Ang II inhibition and cardiovascular ageing

ACE inhibitors and ARB have been observed to prevent many age-related alterations in structure and function of the vasculature. Treatment with the ARB, Candesartan, reduced ECM components within rodent and human vessels; these are a contributing element in vascular remodelling (Intengan and Schiffrin, 2000) which is a characteristic of vascular ageing.

Chronic treatment of Wistar rats with Enalapril or Losartan (6 or 18 months) prevented many age-related cardiovascular changes, such as left ventricular hypertrophy, aortic

stiffness and improved endothelial function and increased NOS activity, even in normally ageing rats (Gonzalez-Bosc *et al.*, 2001). Both of these inhibitors also attenuated changes in kidney mitochondria from ageing rats, by preventing a decline in the energy production capacity and preventing an increase in mitochondrial-derived ROS (de Cavanagh *et al.*, 2003), both of which are associated with ageing. It has therefore been proposed that long-term blockade of Ang II may delay the development of various age-related changes in the cardiovascular system (Ferder *et al.*, 2002).

1.4.6 Genetic manipulation of Ang II in experimental models

Inhibiting the effects of Ang II by treatment with ACE inhibitors and ARB results in beneficial effects on the vasculature and delays the onset of various CVD. However, the effects of Ang II are not entirely eliminated since it can mediate effects via AT₂R activation and can be synthesized via alternate pathways (**figure 1.3**). Therefore, a better understanding of the physiological (and pathological) mechanisms of Ang II via specific modes of activation has been gained from gene targeted experiments in animal models. One of the first targeted knockouts was of the early precursor of Ang II – angiotensinogen (*Agt*^{-/-}), which resulted in mice with exceptionally low blood pressure, significant renal defects and hypertrophy of renal blood vessels which caused death before weaning (Tanimoto *et al.*, 1994). Similar observations were determined in renin-deficient mice (Yanai *et al.*, 2000) and ACE knockout mice (*Ace*^{-/-}) (Krege *et al.*, 1995) although the latter survived for up to 12 months and also revealed impaired male fertility (Esther *et al.*, 1996). Knockout of these key RAS components, therefore, identified a role for Ang II in regulating blood pressure, maintaining vascular and renal structure and in survival.

Knockout models of Ang II receptor subtypes were expected to specifically clarify the effects mediated by Ang II upon receptor activation. Mice have two AT₁R subtypes (AT_{1A}R and AT_{1B}R) and experiments were performed by knockout of each individual subtype. AT_{1A}R knockout mice displayed low blood pressure and following Ang II infusion only a small rise in blood pressure was detected over a prolonged period of time, compared to wild-type mice where a rapid increase was observed after 20 seconds (Ito *et al.*, 1995). Treatment of this model with Losartan caused a further decline in blood pressure similar to levels detected in *Agt*^{-/-} and *Ace*^{-/-} models, suggesting blood pressure is regulated via AT_{1B}R (Oliverio *et al.*, 1997). The same effect was

observed in double knockout models of the AT₁R subtypes, where ACE inhibition caused a rise in blood pressure, indicating a response via AT₂R (Oliverio *et al.*, 1998). AT₂R-null mice displayed slightly higher blood pressure than wild-type mice, which was further elevated and sustained following Ang II infusion over 7 days. This identified AT₂R activation to have a counteractive role in regulating blood pressure (Siragy *et al.*, 1999).

The importance of Ang II in vascular ageing and CVD has also been studied using gene targeted models. The overexpression of ACE in healthy rat carotid arteries caused increased vessel wall thickness which is indicative of hypertrophy (Morishita *et al.*, 1994) which suggested Ang II has a promoting role in vascular remodelling. AT₁A_R knockout and wild-type mice transplanted with bone marrow cells which express AT₁A_R, reduced the progression of Ang II-induced atherosclerosis and aneurysms formation, whereas expression of these receptors in vascular tissue are involved in the Ang II promotion of these inflammatory diseases (Cassis *et al.*, 2007). This identified Ang II to have a role in the initiation and regression of disease.

The ApoE and AT₂R double-knockout mice displayed exaggerated atherosclerotic changes compared to the ApoE knockout model, which suggested AT₂R stimulation to have a role in preventing the development of atherosclerosis (Iwai *et al.*, 2005).

1.5 ROS Initiated Responses in the Vasculature

1.5.1 Role of ROS in the vasculature

ROS are the universal products of oxidative cellular metabolism (Loscalzo, 2003). They are molecules or ions formed by the incomplete, one-electron reduction of O₂, forming oxygen radicals and some non-radical derivatives of oxygen. ROS have the potential to damage bio-molecules by oxidizing lipids, proteins and DNA, and also act as important mediators in various cell signalling pathways and thereby regulate cell function by initiating alterations in gene transcription, protein synthesis and enzyme activity (Touyz and Schiffrin, 2004).

ROS have a major physiological role in the cardiovascular system, by functioning as secondary messengers in a controlled manner in signal transduction pathways, which maintain cardiac and vascular integrity. Some vasoactive agents such as Ang II and growth factors such as vascular endothelial growth factor (VEGF) can generate ROS in vascular cells. Uncontrolled levels of ROS leading to a state of oxidative stress, have been implicated in the initiation and progression of CVD such as hypertension, type II diabetes, atherosclerosis, ischemic heart disease and chronic heart failure (Landmesser and Harrison, 2001).

At the cellular level, Ang II mediates some of its effects by ROS production and signalling. Ang II also effectively activates NAD(P)H oxidase which further augments intracellular ROS generation in vascular cells, which can lead to oxidative stress and potentially initiate and/or contribute to pathophysiological states within the cardiovascular system.

1.5.2 ROS and reactive nitrogen species (RNS)

The various ROS generated within all vascular cells include superoxide (O₂^{•-}), H₂O₂, hydroxyl radicals (•OH), •NO and peroxynitrite (ONOO⁻) (Touyz and Schiffrin, 2004). The latter two are conventionally termed as RNS. The formation of these ROS/RNS species, their properties and specific cellular scavengers are summarized in **table 1.3**.

Table 1.3 Properties of ROS and RNS generated in the vasculature

<i>Species</i>	<i>Formation</i>	<i>Cellular properties</i>	<i>Endogenous ROS scavengers</i>
$O_2^{\cdot-}$	$2 O_2 \xrightarrow{e^-} 2 O_2^{\cdot-}$ [univalent reduction of O_2 in the presence of a e^-]	Highly reactive; Unstable Short-lived (seconds) Hydrophilic; membrane impermeable Possible uptake - anion channels (Han <i>et al.</i> , 2003)	SOD [CuZnSOD; ecSOD; MnSOD] (Fridovich, 1997)
H_2O_2	$2 O_2^{\cdot-} \xrightarrow{SOD} H_2O_2$ [spontaneous or SOD catalysed]	Reactive; Stable Half-life $>O_2^{\cdot-}$ Lipophilic; membrane permeable	Catalase Glutathione peroxidase (Schafer and Buettner, 2001) Thioredoxin
$\cdot OH$	$H_2O_2 \xrightarrow{Fe^{2+}} \cdot OH + Fe^{3+}$ (metal-catalysed Haber-Weiss/ Fenton reaction)	Highly reactive Localized damage at site of generation	Any nearby molecule
$\cdot NO$	$L\text{-Arginine} \xrightarrow{(NOS)} L\text{-Citruilline} + \cdot NO$	Reactive; Stable gas Short-lived (seconds) Lipophilic; membrane permeable Diffusion	ADMA (Vallance and Leiper, 2004) Hemoglobin
$ONOO^-$	$O_2^{\cdot-} + \cdot NO \rightarrow ONOO^-$	Highly reactive Short-lived (seconds)	Uric acid

Initial $O_2^{\cdot-}$ generation can form H_2O_2 or generate $ONOO^-$ in the presence of $\cdot NO$. H_2O_2 can be further reduced by metal ions to form $\cdot OH$. ADMA, asymmetrical dimethylarginine; CuZnSOD, copper-zinc SOD; e^- , free electron; ecSOD, extracellular SOD; Fe^{2+} and Fe^{3+} , iron ions; MnSOD, manganese SOD; NOS, nitric oxide synthase; SOD, superoxide dismutase.

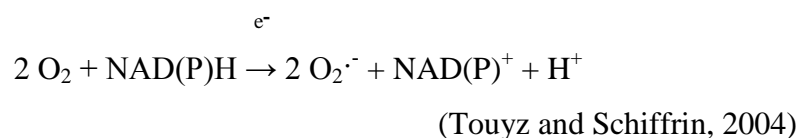
1.5.3 Vascular enzymatic sources of ROS

All vascular cells within vessel walls are reported to produce ROS, including EC, VSMC and adventitial fibroblasts. The quantity of ROS they generate is dependent upon the effects of diverse stimuli. ROS generation is initiated by multiple enzymatic systems, but is mainly generated via the activation of membrane-bound nicotinamide adenine dinucleotide phosphate (reduced form; NAD(P)H) oxidase. Other ROS generating systems include xanthine oxidase (XO), NOS, mitochondrial respiratory chain (mtRC) enzymes, cytochrome P-450, and phagocytic myeloperoxidase (MPO) (Touyz and Schiffrin, 2004). The magnitude of ROS derived from these sources is dependent upon the type of cell and quantity of enzymes present within these cells. These sources of ROS are discussed below in relation to VSMC.

1.5.4 Molecular sources of ROS

1.5.4.1 NAD(P)H oxidase

NAD(P)H oxidase is reported to be the main source of $O_2^{\cdot-}$ in VSMC (Griendling *et al.*, 1994; Touyz and Schiffrin, 2001). This preassembled multimeric enzyme complex (Lassègue and Clempus, 2003) is constitutively functional and produces low but sustained levels of intracellular $O_2^{\cdot-}$. This is consistent with a role in signalling cascades and differs from phagocytic NAD(P)H oxidase which is only active upon stimulation and generates high bursts of $O_2^{\cdot-}$ (Babior *et al.*, 2002). Vascular NAD(P)H oxidase comprises of specific subunits, which include gp91phox (phagocyte oxidase) (Nox2), p22phox, p40phox, p47phox and p67phox (Lassègue and Clempus, 2003). Different homologs of Nox2 are now recognized and include Nox1, Nox4 and Nox5, which have different functional roles in vascular cells. Nox1 is expressed in rat VSMC (Touyz *et al.*, 2002) whereas Nox4 is abundantly expressed in all vascular cells. Increased Nox5 expression has been detected in the vasculature of coronary artery disease patients (Guzik *et al.*, 2008). The combined functional effect of these subunits drives the generation of $O_2^{\cdot-}$. NAD(P)H activation causes the production of $O_2^{\cdot-}$ by donating one e^- to molecular O_2 :



NAD(P)H oxidase activity is regulated by various stimulatory factors, such as vasoactive agents (e.g. Ang II, ET-1), growth factors (e.g. VEGF and thrombin), cytokines (e.g. tumour necrosis factor- α ; TNF α) (Lassègue and Clempus, 2003), metabolic factors (e.g. glucose and insulin) (Inoguchi *et al.*, 2000) and physical factors (e.g. shear stress, stretch, and strain) (Lassègue and Clempus, 2003).

Ang II is a potent stimulator of NAD(P)H activity by signalling via AT₁R. This causes the increased expression and/or activation of NAD(P)H subunits (Griendling *et al.*, 1994; Touyz *et al.*, 2002) resulting in sustained O₂⁻ generation, which is followed by increased intracellular H₂O₂ production. ROS affect signal transduction pathways and induce many processes, e.g. induction of hypertrophy and thereby contributes to hypertension (Griendling *et al.*, 1994; Zafari *et al.*, 1998). Therefore elevated O₂⁻ via this source can lead to oxidative stress and contribute to the development of CVD, as shown in **figure 1.5**.

DNA damage induced by oxidative stress has been detected in VSMC in human atherosclerotic plaques (Matthews *et al.*, 2006). Exogenous Ang II exposure causes elevated O₂⁻ and H₂O₂ production in VSMC, leading to increased cell proliferation and hypertrophy (Griendling *et al.*, 1994; Zafari *et al.*, 1998). These changes are associated with hypertension and remodelling *in vivo*.

1.5.4.2 XO

Xanthine oxidoreductase is a ubiquitous metalloflavoprotein with two interchangeable forms, xanthine dehydrogenase (reducer) and XO (oxidizer), which metabolize hypoxanthine, xanthine and NADH/O₂ substrates to generate O₂⁻ and H₂O₂. Elevated O₂⁻ production by XO activity in VSMC results in hypertrophy, which suggests this enzyme maybe involved in mediating vascular remodelling effects (Matesanz *et al.*, 2007). Enhanced activity has also been determined in conditions of ischemia/reperfusion injury, hypercholesterolemia, and a role in EC dysfunction has been suggested (Landmesser *et al.*, 2002; Spiekermann *et al.*, 2003).

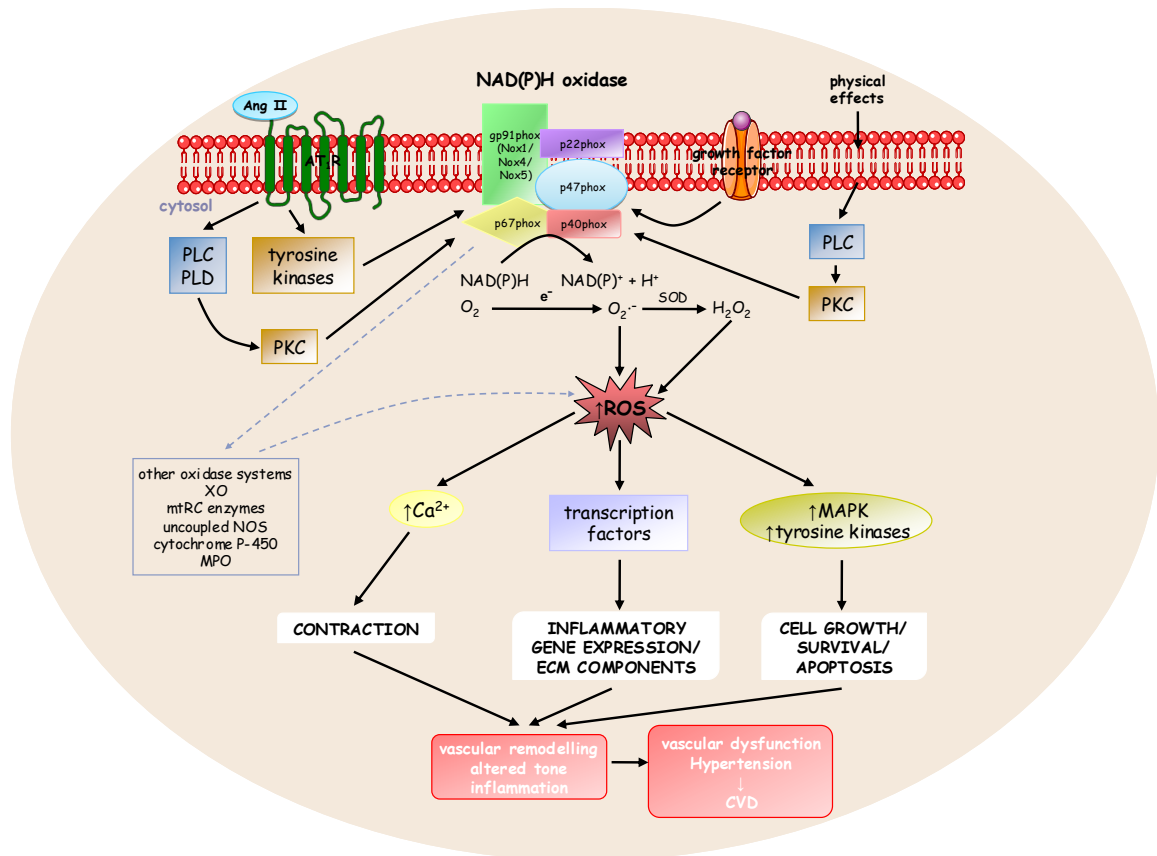


Figure 1.5 Redox-dependent signalling via vascular NAD(P)H oxidase. Intracellular $O_2^{\cdot-}$ generation is slow and sustained in VSMC. Growth factors, vasoactive agents (Ang II) and physical stress initiate various signalling pathways that stimulate ROS generation via NAD(P)H oxidase. Intracellular ROS influence downstream signalling mechanisms, which if uncontrolled, can lead to significant alterations in the vasculature and contribute to the development of CVD. (Adapted from Touyz and Schiffrin, 2004; Touyz, 2005).

1.5.4.3 Uncoupled NOS

There are three isoforms of NOS namely endothelial NOS (eNOS), inducible NOS (iNOS) and neuronal NOS (nNOS). NOS are oxidoreductases, transferring electrons from the reductase domain to the oxidase domain. They oxidize the amino acid L-arginine to generate $\cdot\text{NO}$, which has a favourable effect in the vasculature by regulating blood pressure and vessel tone. A deficiency in the NOS essential cofactor tetrahydrobiopterin or substrate L-arginine, can cause uncoupling of NOS, causing $O_2^{\cdot-}$ generation by NOS (Vasquez-Vivar *et al.*, 2003). In hypertension, NAD(P)H oxidase-derived $O_2^{\cdot-}$ is highly elevated, causing uncoupling of NOS (Landmesser *et al.*, 2003). A similar mechanism is also implicated in atherosclerosis, diabetes and hypercholesterolemia.

1.5.4.4 mtRC complexes

The mtRC complexes are regarded as the main source of cellular ROS generation. During aerobic metabolism these mtRC enzymes undergo oxidation and reduction reactions, harnessing energy in the form of phosphate bonds of ATP and resulting in the leakage of e^- and in $O_2^{\cdot-}$ generation to a small extent. Complexes I and III are responsible for the majority of $O_2^{\cdot-}$ formation (Lenaz, 1998). Although Ang II primarily stimulates ROS generation via NAD(P)H oxidase, ROS mediated via this enzyme can potentially enhance further ROS generation via mitochondria. For example, it has been demonstrated Ang II induces mitochondrial ROS via enhanced NAD(P)H oxidase-derived ROS during ischemia/reperfusion injury in rat VSMC (Kimura *et al.*, 2005b).

1.5.4.5 Phagocytic MPO

MPO is a heme enzyme that metabolizes H_2O_2 to form mainly hypochlorous acid (HOCl). MPO is mainly associated with inflammatory diseases, and has been identified as a source of ROS generation in atherosclerotic lesions (Winterbourn *et al.*, 2000).

1.5.5 Physiological and pathological consequences of ROS

ROS are important in regulating vascular function via redox-signalling processes. As such they are involved in growth, apoptosis, migration, matrix regulation and inflammatory gene expression. When excessive oxidants overwhelm the capacity of endogenous antioxidants it causes an imbalance in the redox state, causing 'oxidative stress' (Taniyama and Griendling, 2003) which is believed to significantly contribute to the development and progression of age-associated vascular diseases (Touyz and Schiffrin, 2004). However, ROS can induce either physiological or pathological effects depending upon the type and concentration of species generated, as detailed in **table 1.4**.

1.5.6 Antioxidant defence in the vasculature

The normal redox state within vascular cells is maintained by balancing ROS production with the action of cellular antioxidants. These antioxidants tightly regulate oxidants by inhibiting oxidation reactions. There are both enzymatic and non-enzymatic antioxidant systems. The enzyme systems include SOD, catalase, glutathione peroxidase (GPx) and thioredoxin reductase (TrxR), and non-enzymatic systems include uric acid and vitamins C and E.

Table 1.4 Physiological and pathological consequences of ROS in VSMC

<i>ROS/RNS</i>	<i>ROS/RNS induced vascular responses</i>	
	<i>Physiological</i>	<i>Pathological</i>
$O_2^{\cdot-}$	Vasoconstriction	↑Inflammatory genes - atherosclerosis Hypertension (Fortuño <i>et al.</i> , 2004)
H_2O_2	Regulates VSMC growth Proliferation Vasoconstriction Vasodilation (Miura <i>et al.</i> , 2003)	↑Hypertrophy - vascular remodelling, hypertension (Zhang <i>et al.</i> , 2005)
$\cdot OH$	Apoptosis	Reperfusion injury (Negishi <i>et al.</i> , 2001) Inflammation - atherosclerosis
$\cdot NO$	Inhibits VSMC proliferation, adhesion molecules and tissue factor expression ↓Blood pressure Vasodilation Haemostasis Promotes angiogenesis Apoptosis Platelet function (Naseem, 2005)	↑ → Apoptosis - atherosclerosis ↓ → EC dysfunction - vascular remodelling, hypertension, atherosclerosis
$ONOO^-$	↓Endothelial-dependent vasodilation	Primary inducer of vascular lesions e.g. atherosclerosis (Beckmann <i>et al.</i> , 1994; Patel <i>et al.</i> , 2000) Hypertension Ischemia/reperfusion injury Lipid peroxidation - cellular damage

Table summarises the diverse cellular functions initiated by specific ROS/RNS induced in a physiological response or that initiates or contributes to a pathological state in blood vessels.

1.5.6.1 SOD

SOD are the main enzyme scavenger of $O_2^{\cdot-}$ and consist of a metal-containing active centre. The three isoenzymes of SOD are cytosolic CuZnSOD, ecSOD and the mitochondrial, MnSOD. ecSOD is secreted by VSMC, regulating the oxidant levels in the vascular interstitium (Wassmann *et al.*, 2004) and is reduced in advanced atherosclerotic lesions (Luoma *et al.*, 1998) suggesting that extracellular ROS production maybe elevated in this situation.

1.5.6.2 Catalase

Catalase is located in the cytosol and within peroxisomes. It scavenges H_2O_2 and thereby indirectly removes $O_2^{\cdot-}$ from cells. During chronic oxidative stress, catalase rapidly metabolizes H_2O_2 to protect the cell from damage (Wassmann *et al.*, 2004). For example, ROS generation, induced in VSMC by exogenous Ang II, was reduced by the overexpression of catalase (Zafari *et al.*, 1998)

1.5.6.3 Other enzymatic antioxidants

GPx

GPx is a selenoprotein with different isoforms located in the cytosol and mitochondria of cells. GPx use reduced glutathione (GSH) as a substrate to reduce H_2O_2 and lipid hydroperoxides to form H_2O , lipid alcohols and oxidized GSH (GSSG). Under normal cellular conditions GSSG is maintained at less than 1% of the total GSH, and during chronic oxidative stress it is greatly increased (Dickinson and Forman, 2002). GPx is important in maintaining cardiovascular function, as the overexpression of GPx in murine models prevented cardiac remodelling and heart failure (Shiomi *et al.*, 2004).

TrxR

TrxR are a family of thiol-containing antioxidant enzymes that also contain selenium within an active site. TrxR act together with thioredoxin (Trx) and NADPH to form an oxidoreductase system (Yamawaki *et al.*, 2003). The redox-active centre of Trx, -Cys-Gly-Pro-Cys-, undergoes reversible oxidation/reduction at the two cysteines. The Trx/TrxR system metabolises oxidized thiols on proteins by re-forming reduced thiol groups (Wassmann *et al.*, 2004). Oxidation of NADPH then restores the reduced Trx. Upregulation of this antioxidant has been observed in the development of

atherosclerosis and is possibly involved in the defence against CVD (Furman *et al.*, 2004).

1.5.6.4. Non-enzymatic antioxidants

Vitamin C and E

Vitamin C (L-ascorbic acid) and vitamin E (α -tocopherol) are mainly acquired through diet and supplements. They scavenge ROS, for example, they prevent low-density-lipoprotein (LDL) oxidation which is associated with EC dysfunction and is implicated in atherosclerosis (Villacorta *et al.*, 2007). Studies of both vitamins taken in combination have shown lower oxidative stress levels, and improved endothelial-dependent vasodilation and a decline in blood pressure in hypertension. For example, adult spontaneously hypertensive rats stroke-prone (SHRSP) treated with both vitamins for 6 weeks, displayed reduced vascular NAD(P)H oxidase and increased SOD activity, displaying a reduction in oxidative stress with improved vascular structure and function (Chen *et al.*, 2001b).

1.5.7 ROS induced cellular senescence

Intracellular ROS act as signalling molecules in pathways determining cell fate, where high-levels tend to favour apoptosis and lower levels tend to trigger cellular senescence. As previous described, various extrinsic and intrinsic factors trigger the onset of senescence. Many of these factors commonly elevate intracellular ROS, which maybe the initiator for signalling growth arrest. This concept is further supported by the observation that exogenous ROS (e.g. H₂O₂, t-BHP) cause SIPS of cells *in vitro* (Dumont *et al.*, 2001; Matthews *et al.*, 2006). Activity of the oncogene Ras has been shown to induce senescence by enhancing ROS generation in further downstream signalling pathways (Colavitti and Finkel, 2005).

Rodent primary cell cultures incubated with H₂O₂ or with overexpressed Ras (did not induce cell proliferation) showed increased p53 and p16^{INK4a} levels thereby triggering rapid cell senescence (Serrano *et al.*, 1997). Activated Akt protein in EC have also been shown to accelerate growth arrest, via ROS generation (Miyachi *et al.*, 2004). The two proposed signal transduction pathways that can initiate senescence via ROS production are by activated Ras and Akt proteins, as shown in **figure 1.6**.

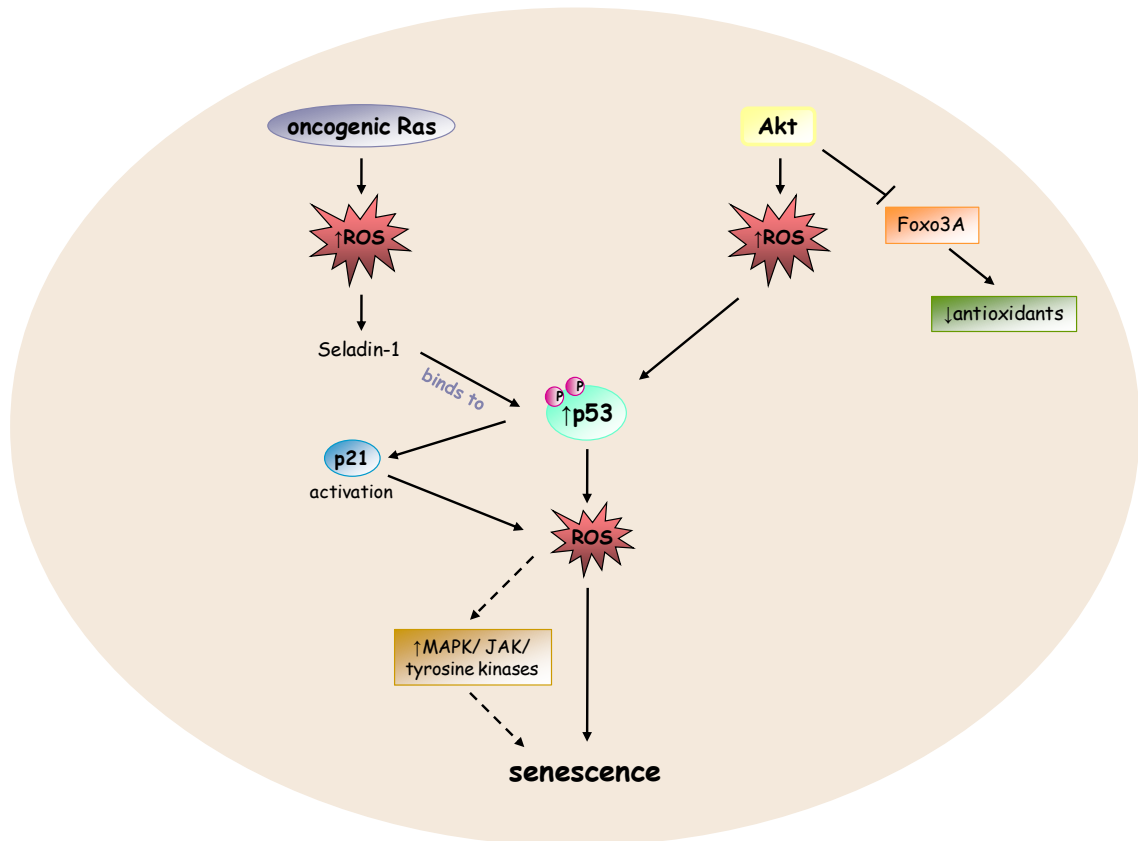


Figure 1.6 Ras and Akt induced ROS-mediated cellular senescence. Activated Ras causes an increase in ROS, which activates FAD-oxidoreductase (Seladin-1), which then binds directly to p53, initiating senescence. The other pathway is through forced expression of Akt kinase, as seen in EC. Activation of Akt inhibits transcription factor Foxo3A, causing a reduction in antioxidant defences (e.g. MnSOD) leading to increased ROS, which in-turn increases p53 activity (*Adapted from Colavitti and Finkel, 2005*)

Evidence for oxidative stress in CVD such as atherosclerosis, type II diabetes and hypertension (Touyz and Schiffrin, 2001; Sampson *et al.*, 2002; Matthews *et al.*, 2006) provides a potential mechanism for the induction of vascular cell senescence *in vivo* (Kunieda *et al.*, 2006).

1.6 Mitochondria, Oxidative Stress and Ageing

1.6.1 Mitochondria

1.6.1.1 Mitochondrial structure and function

Mitochondria are subcellular organelles with several known functions. The primary function is to mediate aerobic respiration to conserve cellular energy in the form of adenosine triphosphate (ATP). This is synthesized via the Krebs cycle and oxidative phosphorylation systems, as described in **figure 1.7**. ATP is then utilized via metabolic pathways. Mitochondria additionally have a role in pyruvate and β -fatty acid oxidation, nitrogen metabolism, heme and iron-sulphur biosynthesis, Ca^{2+} homeostasis and apoptosis.

The number of mitochondria present in cells varies between different types of cells and due to extracellular stimuli depending upon the required cellular energy. Thus, the number of mitochondria can be increased by mitochondrial biogenesis.

1.6.1.2 Mitochondrial biogenesis

The biogenesis process refers to the control of mitochondrial replication, involving the generation of its components, the import of components from the cytoplasm and the complex cross-talk signalling between the nucleus and mitochondria. Mitochondria are not newly synthesized, but are postulated to arise from the extended growth of pre-existing mitochondria by fission. Signalling by nuclear coactivators, such as peroxisome proliferator-activated receptor γ coactivator-1 α (PGC1 α) and nuclear transcription factors control the expression of the numerous nuclear genes involved in mitochondrial replication (Scarpulla, 2008) (**figure 1.8**).

Under physiological states, mitochondrial biogenesis is modulated through the expression of regulatory transcription factors depending upon energy requirements and hormonal responses. Alterations have been detected in response to cold temperatures (Ricquier and Bouillaud, 2000), caloric restriction (Civitarese *et al.*, 2007) and intense physical exercise (Wright *et al.*, 2007).

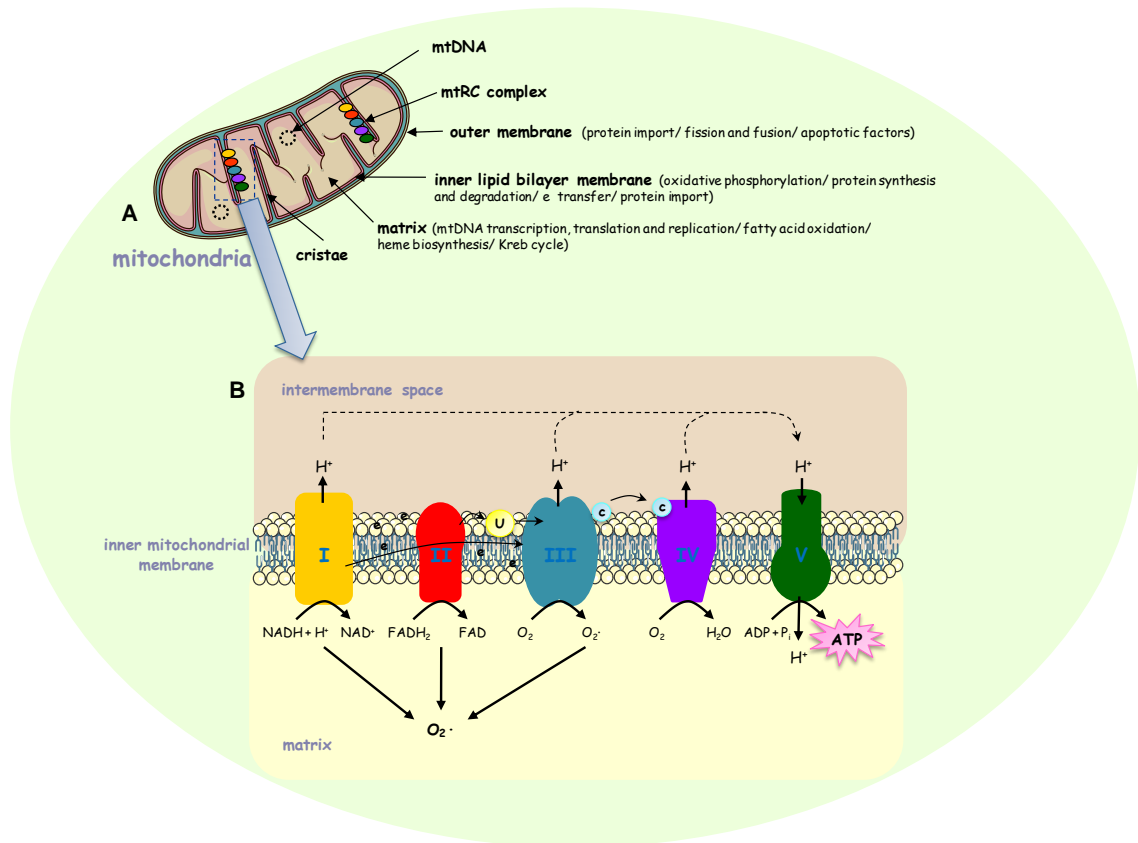


Figure 1.7 Diagrammatic representation of the mitochondrion and mtRC complex. **A**, Cross-section of a mitochondrion. The double-membrane bound organelle contains its own unique genome, mitochondrial DNA (mtDNA). The mtRC complexes are bound in the inner membrane. Different functions of the mitochondria are conducted in the different compartments. **B**, mtRC complexes involved in oxidative phosphorylation and ATP synthesis. A membrane potential generated in the inner membrane leads the oxidation of NADH to NAD⁺, this initiates an electron flow through complex II, which oxidizes flavin adenine dinucleotide dehydrogenase (FADH₂) to flavin adenine dinucleotide (FAD⁺), then through complex III via ubiquinol (U). The electrons are then transferred by cytochrome c (C) to complex IV, where O₂ is reduced to H₂O. The harnessed electro-chemical gradient from the electron flow and proton (H⁺) transfer from the complexes into the intermembrane space are utilized by complex V to drive the production of ATP (Hatefi, 1985). ROS is simultaneously produced by this process, as O₂⁻ is generated via complexes I and III (Li *et al.*, 1999), and upon the activation of complex II. Complex I, NADH dehydrogenase; II, succinate/ubiquinone oxidoreductase; III, ubiquinol/cytochrome oxidoreductase; IV, cytochrome c oxidase; V, ATP synthase; ADP, adenosine diphosphate; Pi, inorganic phosphate. (Adapted from Ryan and Hoogenraad, 2007)

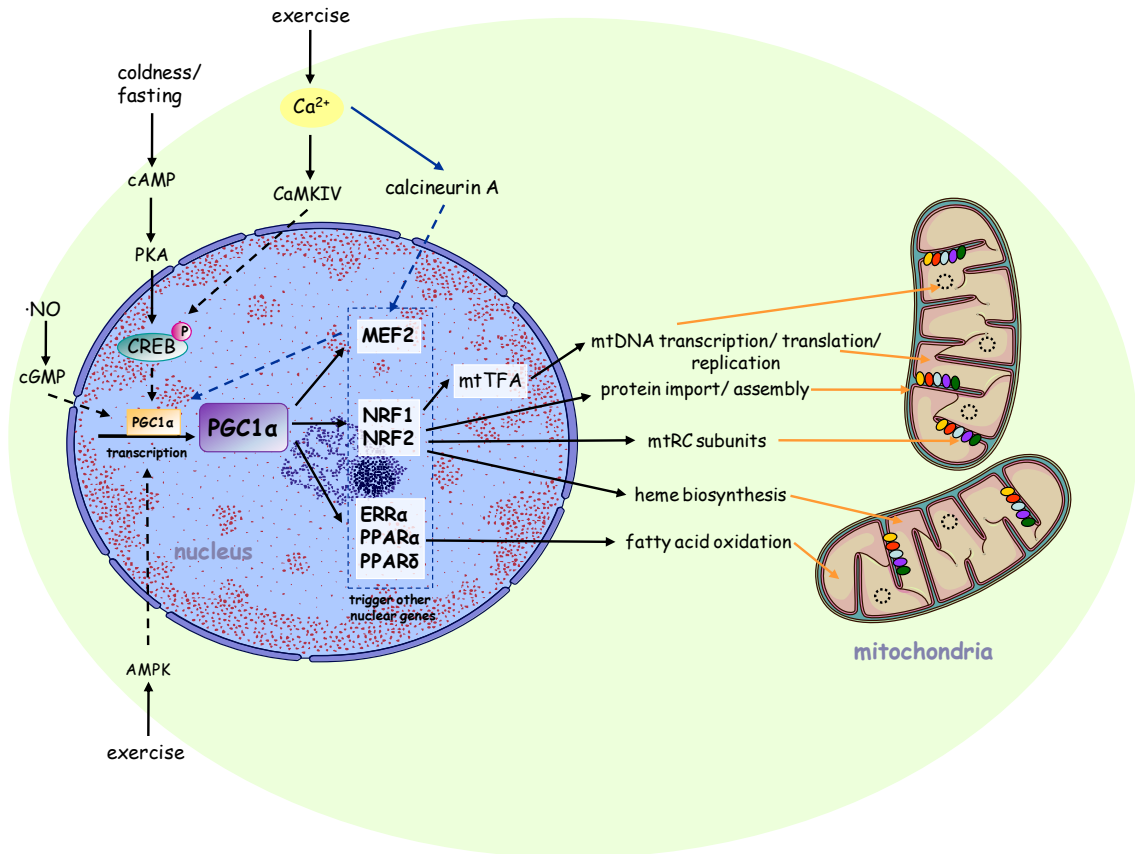


Figure 1.8 PGC1 α signalling in mitochondrial biogenesis. Many internal and external cell stimuli initiate the transcription of PGC1 α in the nucleus, as well as signalling via myocyte enhancer factor 2 (MEF2) and cAMP response element binding (CREB) protein activation. PGC1 α coactivates the expression of various nuclear transcription factors (nuclear respiratory factor 1 (NRF1), 2 (NRF2), estrogen-related receptor α (ERR α), peroxisome proliferator activated receptor α and δ (PPAR α and δ)) which in turn governs the expression of nuclear genes that signal specific alterations in mitochondria, mediating biogenesis. This highly complex process involves coordinated nuclear-mitochondrial communications in response to numerous stimuli. AMPK, AMP-activated protein kinase; CaMKIV, Ca²⁺/calmodulin-dependent protein kinase IV; cAMP, cyclic adenosine monophosphate; cGMP, cyclic guanosine monophosphate; mtTFA, mitochondrial transcription factor A; PKA, protein kinase A. (Adapted from Scarpulla, 2008)

Under pathological states, an increase in mitochondria occurs as a compensatory response due to the presence of damaged or impaired mitochondria. This is often observed in conditions of oxidative stress (Lee *et al.*, 2000; Rasbach and Schnellmann, 2007) and related disease conditions such as insulin resistance (Patti *et al.*, 2003) and Alzheimer's (de la Monte *et al.*, 2000). Mitochondrial biogenesis is therefore considered a cell survival response by meeting energy demands and/or primary response to mitochondrial injury.

Although the mechanism of mitochondrial biogenesis has not been fully elucidated, experimental evidence strongly indicates that ·NO signalling maybe involved. Exogenous ·NO promoted PGC1 α , NRF1 and mitochondrial transcription factor A (mtTFA) expression in various cell lines, consistent with increased ATP generation (Nisoli *et al.*, 2004). ·NO signalling in this process is mediated by the cGMP pathway, activating soluble guanylate cyclase which directly increases PGC1 α and the other related genes, resulting in increased functional mitochondria. Ca²⁺-dependent signalling enzymes have also been implicated in this process, as the constitutive expression of CaMKIV in mice results in elevated mitochondria (Wu *et al.*, 2002) and this pathway is also sensitive to ATP levels within the cell.

Alterations in mitochondrial biogenesis have been characterised in CVD, for example reduced mitochondrial components and function were detected in lung EC taken from patients with idiopathic pulmonary arterial hypertension (IPAH) (Xu *et al.*, 2007). This was hypothesised to be due to the low levels of ·NO associated with the disorder, as ·NO is involved in the biogenesis process. Moreover, in rodent models of heart failure down-regulation of genes associated with mitochondrial bioenergetics and biogenesis were observed (Garnier *et al.*, 2003) presumably since the heart requires high levels of ATP. These studies demonstrate that defects in aspects of the mitochondrial biogenesis process can contribute to/cause CVD.

1.6.2 Mitochondrial theory of ageing

The accumulation of free radicals was first linked to ageing by Denham Harman in 1956. He proposed the “Free Radical Theory of Ageing”. The “Mitochondrial Theory of Ageing” developed from this theory where deleterious formation of ROS in cells was generated via the respiratory process, that is, via mitochondria (Harman, 1972). Mitochondria are the main generators of cellular ROS, derived as a by-product of the production of ATP. The increased generation of cellular ROS with ageing causes accumulated oxidative damage and organelle dysfunction, which gives rise to the mitochondrial theory of ageing.

The increase in ROS-induced damage to mitochondrial components such as mtDNA and respiratory chain complexes increases with age, most likely due to close proximity of these biomolecules to the site of ROS generation and due to limited repair

mechanisms. These damaged components are considered to further increase ROS generation due to disruption of proper mtRC function. Moreover, increased mtDNA mutations in murine models with defective mitochondrial DNA polymerase, result in premature ageing phenotypes and shortened lifespan (Trifunovic *et al.*, 2004).

ROS are continuously generated within cells yet it is still not clear exactly how they cause or contribute to the development of ageing. ROS can trigger cellular senescence and can cause mitochondrial dysfunction. Both of these effects accumulate with age. This has identified a possible relationship between mitochondria and senescence which is yet to be fully determined.

1.6.3 Mitochondrial dysfunction in CVD

Extensive oxidative stress can induce damage to mtRC enzymes, mtDNA, lipids, and proteins, impairing their function and initiating further ROS formation. Damage or alterations to mitochondria are hypothesized to contribute to ageing and CVD development.

Defective mitochondrial components resulting in dysfunctional mitochondria have been determined in several CVD associated with oxidative stress. The myocardium is associated with high levels of mitochondria to sustain its function, and much lower levels of ATP were detected in the failing human myocardium, due to mtRC impairment (Beer *et al.*, 2002). A similar effect was detected in EC taken from people with IPAH, accompanied by reduced mitochondria and mtDNA due to a decline in mitochondrial biogenesis (Xu *et al.*, 2007). The elevated ROS produced during ischemia/reperfusion elicits numerous damaging effects in mitochondria, such as oxidized proteins, mitochondrial swelling, mtRC impairment and enhanced mitochondrial membrane permeability (Khaliulin *et al.*, 2004). Moreover, accumulating evidence of damaged mtDNA in vascular cells has been implicated in development of atherosclerosis (Ballinger *et al.*, 2002).

1.6.4 Mitochondria, senescence and ageing

At present, there is no direct connection linking mitochondria and senescence. However, there is substantial evidence to suggest senescence may be induced due to the substantial ROS generated by mitochondria. Oxidative damage can result in

dysfunctional mitochondria giving rise to even more ROS production, which is proposed to contribute to telomere shortening consequently accelerating the onset of replicative senescence. This was supported by a recent study showing enhanced mitochondrial $O_2^{\cdot-}$ and mtDNA damage in human fibroblasts with increasing replicative age (Passos *et al.*, 2007), indicating mitochondrial ROS may have a role in telomere-dependent senescence.

mtDNA damage and mutations in mitochondria have been observed in senescent cells. For example, mitochondria isolated from donors between 20 weeks to 103 years of age were introduced into human mtDNA-less cells. They showed decreased growth and respiratory rate, indicating that mitochondria may have a role in triggering senescence (Laderman *et al.*, 1996). In-depth analysis of senescent fibroblasts grown *in vitro*, showed the accumulation of oxidized proteins and lipofuscin in mitochondria; these are indicators of oxidative stress (Sitte *et al.*, 2001; Passos and von Zglinicki, 2005). These observations suggest that defective mitochondria are likely to be involved or contribute to the induction of cellular senescence.

The extreme murine model of the homozygous knock-in expression of the proof-reading deficient catalytic subunit of mtDNA polymerase γ enzyme (POLG), exhibited numerous mtDNA mutations and deletions accompanied by many physical age-related phenotypes (Trifunovic *et al.*, 2004). Although this model is consistent with the notion that cumulative mtDNA mutations arise with age, many of these phenotypes have not been observed in diseases manifesting from single mtDNA mutations. Another model has demonstrated the strong link between ageing and the effect on mitochondria. The prolonged lifespan of rodents following treatment with chronic ARB and ACE inhibitors revealed protection against ageing effects in various tissues (de Cavanagh, *et al.*, 2003). The prevention of age-related dysfunction was associated with prevention of age-induced mitochondrial changes further strengthening the link between mitochondrial function and senescence. The ultrastructure of renal mitochondria is affected by the RAS and a role for impairment in mitochondria and the development of age-related CVD has been suggested (de Cavanagh, *et al.*, 2008a).

1.7 Hypothesis and Aims

Vascular cell senescence and telomere attrition have been associated with CVD development and ageing. The pleiotropic effects of Ang II may be mediated via ROS production, initiate numerous cell signalling pathways which play a major role in vascular physiological and pathological outcomes in the cardiovascular system. This project aimed to investigate the hypothesis that Ang II promotes senescence of VSMC via ROS production.

Investigating the mechanism(s) through which Ang II initiates senescence at the cellular level could help to determine whether it plays a role in the accumulation of senescent cells in blood vessels and subsequently in vascular ageing and development of disease. This may also suggest mechanisms for current therapies and ways in which novel therapies might be applied.

The experimental aims were:

- To establish a hVSMC culture model to analyse alterations in molecular and cellular function following Ang II exposure
- To investigate the induction of hVSMC senescence by Ang II exposure
- To determine the extent to which Ang II stimulates intracellular ROS production in hVSMC, and the source of ROS
- To investigate the effect of Ang II on cell cycle regulatory proteins and the relationship to the induction of senescence
- To establish whether telomere attrition has a significant role in Ang II mediated senescence
- Since mitochondrial function is implicated in ageing this thesis also aimed to assess the affects of Ang II on mitochondria, mitochondrial biogenesis, mitochondrial ROS and ATP

CHAPTER TWO
Materials and Methods

Chapter 2.0: Materials and Methods

2.1 Materials

2.1.1 Cell culture and treatment reagents

2.1.1.1 Cell lines and primary cells

Human vascular smooth muscle cells (hVSMC) were isolated from human saphenous vein explants, taken from varicose vein surgery.

Human dermal fibroblast (HDF) cells were isolated from human skin biopsies of the buttock region, by Paulene Quinn, Department of Cardiovascular Sciences, University of Leicester, UK.

Hep G2 cells were originally isolated from a human liver biopsy taken from a male patient (15-years old) with hepatocellular carcinoma. These cells were purchased as an established cell line from ATCC (<http://www.lgcstandards-atcc.org/>).

Human aortic smooth muscle cells (17-year old donor) transfected with the human catalytic subunit of telomerase (hASMC-hTERT) were a kind gift from Professor Laura Niklason, Department of Anaesthesia and Biomedical Engineering, Yale University, Conn, USA.

HeLa cells were originally derived in 1951 from cervical cancer cells taken from the patient Henrietta Lacks. These cells were purchased as an established cell line from ATCC (<http://www.lgcstandards-atcc.org/>).

2.1.1.2 Cell culture consumables

Nunclon cell culture flasks (T25, T75 and T175cm²), clear multi-well plates (6, 12, 24 and 96-well) and flat bottom polystyrene white 96-well microplates were purchased from NuncTM, Fisher Scientific UK Ltd, Loughborough, Leicestershire, UK. Serological pipettes (5, 10 and 25ml) and 15ml plastic centrifuge tubes were from Corning Life Sciences, Fisher Scientific UK Ltd.

Cell scrapers were from Techno Plastic Products, AG, Trasadingen, Switzerland. Sterile plastic syringes (10 and 20ml) were obtained from BD Plastipak™, Becton Dickinson UK Ltd, Oxford, UK and Acrodisc® sterile syringe filters (0.45µm) from Pall Corporation, Ann Arbor, MI, USA.

2.1.1.3 Cell culture media

Basal media

The basal medium RPMI 1640 with L-glutamine, phenol red and without phenol red indicator were purchased from Lonza, Wokingham, Berkshire, UK. Dulbecco's Modified Eagle's Medium (DMEM) with high glucose (containing 4500mg/L glucose, 110mg/L sodium pyruvate and 4mmol/L L-glutamine) and Earle's Minimum Essential Medium (EMEM) (without L-glutamine) were from Gibco, Invitrogen UK Ltd, Paisley, Scotland, UK.

Cell media additives and supplements

Foetal calf serum (FCS) (Batch number: 4647HI) was purchased from BioSera Ltd, UK. Additional reagents and media additives that were purchased from Lonza were 200mmol/L L-glutamine, 5000units/5000µg penicillin-streptomycin solution, 10× trypsin-diaminoethanetetra-acetic acid (EDTA) solution (5mg/ml porcine trypsin and 2mg/ml EDTA), 1mol/L HEPES buffer and Dulbecco's phosphate buffered saline (DPBS) without Ca²⁺ and Mg²⁺; pH 7.4, and SmGM®-2 singlequotes® (consisting of insulin, hFGF-B, and hEGF). MEM non-essential amino acid (NEAA) solution (100×) was from Sigma-Aldrich, Poole, UK. Human smooth muscle cell growth supplement (20×) was obtained from TCS CellWorks, Botolph Claydon, Buckingham, UK and 50mg/ml hygromycin B in DPBS was from Invitrogen UK Ltd.

2.1.1.4 Cell treatment reagents

Synthetic human angiotensin II (Ang II) acetate salt, *tert*-butylhydroperoxide (T-HYDRO® solution, 70% (w/v) in water) (t-BHP), hydrogen peroxide (H₂O₂) solution (30% (w/v), catalase (H₂O₂ scavenger) (from bovine liver; 1,824 units per mg), 4-hydroxy-3-methoxyacetophenon (apocynin), 5-hydroxydecanoic acid sodium salt (5-HD), dimethyl sulphoxide (DMSO), N-acetyl-L-cysteine (NAC), rotenone and superoxide dismutase (SOD) (from bovine liver) were purchased from Sigma-Aldrich. Thenoyltrifluoroacetone (TTFA) was from Fisher Scientific UK Ltd. E3174, the AT₁R

antagonist and active metabolite of the drug Losartan, was a kind gift from Merck & Co, Inc., Rahway, New Jersey, USA. Ethanol (absolute) (EtOH) was from VWR International (BDH) Ltd and (2-(2,2,6,6-tetramethylpiperidin-1-oxyl-4-ylamino)-2-oxoethyl)-triphenylphosphonium chloride, monohydrate (mito-TEMPO) was purchased from ALEXIS® Biochemicals, Axxora (UK) Ltd, Bingham, Nottingham, UK.

2.1.1.5 Markers of cell viability

Trypan blue solution (contained 0.81% sodium chloride (NaCl), 0.06% potassium phosphate and 0.4% (^{w/v}) bromophenol blue) and 3-(4,5-dimethyl-thiazol-2-yl)-2,5-diphenyl tetrazolium bromide (MTT) were purchased from Sigma-Aldrich. Isopropanol (also known as propan-2-ol) and clear 96-well microplates were obtained from Fisher Scientific UK Ltd. The ApoGlow® adenylate nucleotide ratio assay kit was purchased from Lonza, Wokingham, Berkshire, UK.

2.1.2 Cell imaging

2.1.2.1 Immunofluorescence

All antibodies, reagents and materials used for immunofluorescence cell staining, are listed in **table 2.1**.

Antibody	Supplier
Anti- α -smooth muscle actin (clone 1A4)	Sigma-Aldrich
Goat anti-mouse IgG (Fc specific)	Sigma-Aldrich
fluorescein isothiocyanate (FITC) conjugate	
Reagent	
Bovine serum albumin (fraction V) (BSA)	Sigma-Aldrich
Clear nail varnish	The Boots Company PLC, UK
DPBS	Lonza
Industrial methylated spirit (IMS)	Genta Medical, York, UK
Paraformaldehyde	BDH Ltd, Poole, UK
Tris(hydroxymethyl)-methylamine (Tris)	Fisher Scientific UK Ltd
t-Octylphenoxypolyethoxyethanol (Triton X-100)	Sigma-Aldrich
Ultrapure water (UP H ₂ O)	Laboratory grade
VectorShield mounting medium for fluorescence	Vector Laboratories, Inc., Burlingame, CA
Material	
Glass microscope slides	BDH Ltd
Circular glass coverslips (22mm diameter)	BDH Ltd
Sterile Petri-dishes (60mm diameter)	Nunc TM , Fisher Scientific UK Ltd

Table 2.1 Reagents and materials used for immunofluorescence cell staining of α -smooth muscle actin.

2.1.2.2 Senescence associated β -galactosidase (SA- β -Gal) staining

The senescent cell staining kit was purchased from Sigma-Aldrich. Reagents within the kit are all detailed in **table 2.2**.

Reagent	Reagent components
10 \times Fixation buffer	20% Formaldehyde 2% Glutaraldehyde 70.4mmol/L Na ₂ HPO ₄ 14.7mmol/L KH ₂ PO ₄ 1.37mol/L NaCl 26.8mmol/L KCl
10 \times Phosphate-buffered saline (PBS)	-
Reagent B	400mmol/L Potassium ferricyanide
Reagent C	400mmol/L Potassium ferrocyanide
10 \times Staining solution	-
40mg/ml X-gal solution	-

Table 2.2 Senescent cell staining kit reagents.

Additional reagents and materials that were used, but not included in the kit were: glycerol which was obtained from Sigma-Aldrich; laboratory standard UP H₂O was used to dilute some reagents of the kit; sterile plastic syringes (10 and 20ml) were from BD PlastipakTM, Becton Dickinson UK Ltd; acrodisc[®] sterile filters (0.2 μ m) were from Pall Corporation; parafilm was obtained from Brand GMBH & Co, Germany.

2.1.3 Measurement of apoptosis

2.1.3.1 Caspase-3/7 activity assay

The Caspase-Glo[®] 3/7 assay (containing caspase-glo[®] 3/7 buffer and caspase-glo[®] substrate (lyophilized)) was purchased from Promega, Chilworth Science Park, Southampton, UK. Acetate plate sealers (8.3 \times 13.3cm) were from Dynex Technologies Ltd, Worthing, West Sussex, UK and IMS was from Genta Medical.

2.1.3.2 Hoechst 33258 staining

All reagents and materials used for staining and visualising fragmented DNA in whole cells are listed in **table 2.3**.

Reagent/ Material	Supplier
Absolute methanol	Fisher Scientific UK Ltd
Clear nail varnish	The Boots Company PLC
DPBS	Lonza
Glycerol	Sigma-Aldrich
Hoechst 33258, pentahydrate (bis-benzimide) 10mg/ml solution in water	Molecular Probes, Inc., Invitrogen UK Ltd
Micro-oil immersion oil	BDH Ltd
Circular glass coverslips	BDH Ltd
Glass microscope slides	BDH Ltd

Table 2.3 Reagents and materials utilized to stain whole cell DNA with Hoechst 33258.

2.1.4 Reactive oxygen species (ROS) measurements

2.1.4.1 Fluorescent-based measurement of ROS formation

The fluoroprobe 5-(and-6)-chloromethyl-2',7'-dichlorodihydrofluorescein diacetate, acetyl ester (CM-H₂DCFDA) was purchased from Molecular Probes, Inc., Invitrogen UK Ltd. Hank's balanced salt solution (HBSS) (with Ca²⁺ and Mg²⁺) was from Gibco, Invitrogen UK Ltd, DPBS was from Lonza and DMSO was from Sigma-Aldrich.

2.1.4.2 Lucigenin chemiluminescence assay (LCLA)

Bis-N-methylacridinium nitrate (lucigenin), DMSO, ethylene glycol-bis/ β -aminoethyl ether)-N,N,N',N'-tetraacetic acid (EGTA), KH₂PO₄ and protease inhibitor cocktail for mammalian tissue (containing the inhibitors: 104mmol/L AEBSF, 0.08mmol/L aprotinin, 4mmol/L bestatin, 1.4mmol/L E-64, 2mmol/L leupeptin and 1.5mmol/L pepstatin A) were purchased from Sigma-Aldrich. Potassium hydroxide (KOH) and sucrose were from Fisons Plc, Loughborough, Leicestershire, UK. Hydrochloric acid (10.2mol/L) (HCl) was from Fisher Scientific UK Ltd and EtOH (absolute) was from VWR International (BDH) Ltd, UK. All stimulators and inhibitors of ROS are listed in **table 2.4**.

Flat bottom polystyrene white 96-well microplates were from Fisher Scientific UK Ltd and black 1.5ml eppendorfs were from MP Biomedical, Cambridge, UK.

Stimulator	Supplier
Antimycin A (from <i>Streptomyces</i> species)	Sigma-Aldrich
β -nicotinamide adenine dinucleotide (NADH) (disodium salt, reduced form)	Sigma-Aldrich
β -nicotinamide adenine dinucleotide phosphate (NADPH) (tetrasodium salt, reduced form)	Sigma-Aldrich
2,6-dihydroxypurine (xanthine)	Sigma-Aldrich
Succinate (disodium salt)	Sigma-Aldrich
Inhibitor	
Antimycin A (from <i>Streptomyces</i> species)	Sigma-Aldrich
Carbonyl cyanide 3-chlorophenylhydrazone (CCCP)	Sigma-Aldrich
4,5-dihydroxy-1,3-benzene disulfonic acid (tiron) (disodium salt, hydrate)	Sigma-Aldrich
Diphenylene iodonium (DPI) (DPI chloride)	Sigma-Aldrich
5-HD	Sigma-Aldrich
Indomethacin	Sigma-Aldrich
NAC	Sigma-Aldrich
Rotenone	Sigma-Aldrich
TTFA	Fisher Scientific UK Ltd

Table 2.4 Stimulators and inhibitors of cellular ROS.

2.1.4.3 Fluorescent-based measurement of mitochondrial $O_2^{\cdot-}$

The fluoroprobe MitoSOXTM red mitochondrial $O_2^{\cdot-}$ indicator (MitoSOXTM) was purchased from Molecular Probes, Inc., Invitrogen UK Ltd. DMSO was from Sigma-Aldrich and HBSS (with Ca^{2+} and Mg^{2+}) was from Gibco, Invitrogen UK Ltd.

2.1.5 Extraction and quantitation methods

2.1.5.1 DNA extraction and quantitation

The QIAamp® DNA blood mini kit was purchased from QIAGEN. EtOH (VWR International (BDH) Ltd) was additionally required to dilute buffers AW1 and AW2 from the kit, before usage. DPBS was purchased from Lonza. Quantitation of DNA was determined by the fluorescence-based Quant-iTTM PicoGreen® dsDNA assay kit, purchased from Molecular Probes, Inc., Invitrogen UK Ltd. The clear 96-well microplates were from NuncTM, Fisher Scientific UK Ltd.

2.1.5.2 Ribonucleic acid (RNA) extraction and quantitation

The High Pure RNA Isolation kit was purchased from Roche Applied Science. EtOH (VWR International (BDH) Ltd) was required to prepare Wash Buffers I and II from the kit and DPBS was from Lonza. Total RNA was quantified using the fluorescent Quant-iT™ RNA assay kit and Qubit™ assay tubes (0.5ml) from Molecular Probes, Inc., Invitrogen UK Ltd. Filter pipette tips (for P2-P200 pipettes) were from Rainin Instruments, Anachem Ltd.

2.1.5.3 RNA quality and PCR primer quantitation

TE buffer, pH 7.4 (DNase and RNase free) was from Fluka and Riedel-de Haën, Gillingham, UK.

2.1.5.4 Protein extraction and quantitation

The lysis buffer used to extract whole cell protein from cultured cells consisted of β-mercaptoethanol, magnesium acetate, and protease inhibitor cocktail (for mammalian tissue), which were obtained from Sigma-Aldrich. EDTA, HCl, KCl, and tris were from Fisher Scientific UK Ltd.

Membrane-bound proteins were extracted from cells using radio immuno precipitation assay (RIPA) buffer which consisted of nonidet-P40 (NP-40), protease inhibitor cocktail, sodium deoxycholate, SDS, and sodium fluoride (NaF), which were all purchased from Sigma-Aldrich. EDTA, HCl, NaCl, and tris were from Fisher Scientific UK Ltd.

Protein quantitation using the Bio Rad protein assay dye reagent concentrate was from Bio Rad Laboratories Ltd. BSA was from Sigma-Aldrich and clear 96-well microplates were from Nunc™, Fisher Scientific UK Ltd.

2.1.6 Molecular biology techniques

2.1.6.1 Western blotting

The Western blotting reagents purchased from Bio Rad Laboratories Ltd were 30% (^{w/v}) acrylamide/bis solution (29:1) and precision plus protein standards, all blue. Ammonium persulfate (APS), HCl, methanol, KCl, NaCl, NaOH, 5% (^{w/v}) trichloroacetic acid and tris were from Fisher scientific UK ltd. BSA,

β -mercaptoethanol, bromophenol blue, DMSO, dithiothreitol (DTT), glycerol, glycine (electrophoresis grade), 30% (^w/_v) H₂O₂, isopropanol, luminol, N, N, N', N'-tetramethyl-ethylenediamine (TEMED) (electrophoresis reagent), p-coumaric acid, polyoxyethylene sorbitan monolaurate (tween-20), ponceau S and sodium dodecylsulfate (SDS) were obtained from Sigma-Aldrich. DPBS was from Lonza, IMS was from Genta Medical and non-fat Marvel milk powder was from Premier International Foods (UK) Ltd, Lincolnshire, UK. RestoreTM Western Blot Stripping Buffer was purchased from Perbio Science UK Ltd, Cramlington, Northumberland, UK. The antibodies used in Western blotting are listed in **table 2.5**.

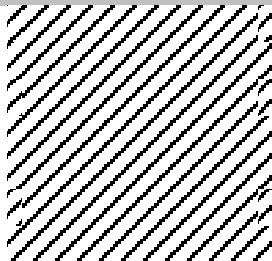
Primary antibody	Antibody class	Supplier
Anti-AT ₁ R [TONI-1] (mouse)	Monoclonal	Abcam plc, Milton road, Cambridge, UK
Anti-AT ₂ R (C-18) (goat)	Polyclonal	Santa Cruz Biotechnology, Inc., Santa Cruz, California, USA.
Anti- α -tubulin (clone DM1A; mouse)	Monoclonal	Sigma-Aldrich
Anti- β -actin (clone AC-15; mouse ascites fluid)	Monoclonal	Sigma-Aldrich
Anti-myosin (smooth) (clone HSM-V; mouse ascites fluid)	Monoclonal	Sigma-Aldrich
Anti-p16 (C-20) (rabbit)	Polyclonal	Santa Cruz Biotechnology, Inc.
Anti-p21 (F-5) (mouse)	Monoclonal	Santa Cruz Biotechnology, Inc.
Anti-p53 (DO-1) (mouse)	Monoclonal	Santa Cruz Biotechnology, Inc.
Anti-telomerase (rabbit)	Polyclonal	Abcam plc
Secondary antibody		
Donkey-anti-goat IgG – H & L horseradish peroxidase (HRP)		Abcam plc
Goat-anti-rabbit IgG – peroxidase conjugate (whole molecule)		Sigma-Aldrich
Rabbit-anti-mouse IgG – H & L HRP		Abcam plc

Table 2.5 Primary and secondary antibodies used for Western blotting. All primary antibodies were directed against human proteins.

SaranTM film wrap was purchased from Fisher Scientific UK Ltd. Whatman filter paper was from Whatman International Ltd, Maidstone, UK. Hybond ECL nitrocellulose membrane (20×20cm) and Hyperfilm ECL (5×7 inches) were obtained from Amersham Biosciences UK Ltd, Little Chalfont, Buckinghamshire, UK.

2.1.6.2 Southern blotting

The restriction enzymes used for Southern blotting are detailed in **table 2.6**.

Restriction enzyme	Recognition site	Supplier
<i>Hinf</i> I	5' ... G [↓] A N T C ... 3'	New England Biolabs (NEB) UK
	3' ... C T N A [↑] G ... 5'	Ltd, Hitchin, Hertfordshire, UK
<i>Rsa</i> I	5' ... G T [↓] A C ... 3'	New England Biolabs (NEB) UK
	3' ... C A [↑] T G ... 5'	Ltd

Table 2.6 Restriction enzymes used for Southern blotting.

NEBuffer 2, T4 polynucleotide kinase (PNK) and 10× PNK buffer were also obtained from New England Biolabs (NEB) UK Ltd. BSA, 2,7-diamino-10-ethyl-9-phenyl-phenanthridinium bromide (ethidium bromide), SDS, and sodium citrate were purchased from Sigma-Aldrich. EDTA, glacial acetic acid, HCl, NaCl, NaOH and tris were from Fisher Scientific UK Ltd. Disodium hydrogen orthophosphate (Na₂HPO₄) and orthophosphoric acid (H₃PO₄) were purchased from Fisons Plc. Agarose (electrophoresis grade), BlueJuiceTM gel loading buffer (containing: 65% (^{w/v}) sucrose, 10mmol/L tris-HCl, pH7.5, 10mmol/L EDTA, and 0.3% (^{w/v}) bromophenol blue), 1kb DNA ladder and high molecular weight (HMW) DNA markers were from Invitrogen UK Ltd.

The oligonucleotide complementary to the telomere sequence (TTAGGG)₄ was synthesized by Invitrogen UK Ltd. The $\gamma^{32}\text{P}$ -ATP (9.25MBq) and $\gamma^{32}\text{P}$ -CTP (9.25MBq) were obtained from Amersham Biosciences UK Ltd. The QIAQUICK nucleotide removal kit was purchased from QIAGEN, Crawley, West Sussex, UK, and the RediprimeTM II kit was from Amersham Biosciences UK Ltd.

Whatman filter paper was from Whatman International Ltd. KODAK scientific imaging film and quickdraw blotting sheets were from Sigma-Aldrich. HybondTM-XL nylon membrane for nucleic acid transfer was from Amersham Biosciences UK Ltd. Paper towels were from Kimberley-Clarke Europe Ltd, Reigate, Surrey, UK and SaranTM film wrap was from Fisher Scientific UK Ltd.

2.1.6.3 DNA Damage Measurements - Comet assay (single cell gel electrophoresis)

HBSS (without Ca²⁺ and Mg²⁺) was purchased from Gibco, Invitrogen UK Ltd. EDTA, HCl, NaCl, tris, and NaOH were all from Fisher Scientific UK Ltd. DMSO and triton X-100 were purchased from Sigma-Aldrich. Low melting point (LMP) agarose and normal melting point (NMP) agarose were obtained from Invitrogen UK Ltd. DPBS was purchased from Lonza, IMS was from Genta Medical, EtOH was from VWR International (BDH) Ltd, and SYBR green 1 stain was from Molecular Probes, Inc., Invitrogen UK Ltd.

Glass microscope slides were from BDH Ltd and square glass coverslips (18×18mm) were from Menzel-Glazer; Bios Europe Ltd, Skelmersdale, Lancashire, UK.

2.1.6.4 Detection of telomerase activity

The TeloTAGGG telomerase PCR ELISA kit was purchased from Roche Applied Science, Roche Diagnostics Ltd, Burgess Hill, UK. The reagents and materials included in the kit are listed in **table 2.7**.

Reagents	Materials
Lysis buffer	96-well microplate (precoated with streptavidin and post-coated with blocking reagent)
2× Reaction buffer	Self-adhesive cover foils
Denaturation reagent	
Hybridization buffer	
10× Washing buffer	
120mU Anti-DIG-POD (Anti-digoxigenin peroxidase)	
Conjugate dilution buffer	
TMB substrate (containing POD substrate 3,3',5'5'-tetramethyl benzidine)	
Stop reagent	
Positive cell extract (telomerase expressing human kidney cells) (293 cells)	

Table 2.7 All Reagents and materials of the TeloTAGGG Telomerase PCR ELISA kit

Diethyl pyrocarbonate (DEPC) and mineral oil were purchased from Sigma-Aldrich. DPBS was from Lonza and filter pipette tips (DNase and RNase free) were from Rainin Instruments, Anachem Ltd.

2.1.6.5 Complementary DNA (cDNA) synthesis

Reverse transcription of RNA using DyNAmo™ cDNA synthesis kit was purchased from New England Biolabs (NEB) UK Ltd, nuclease-free water was from Qiagen and filter pipette tips were from Rainin Instruments, Anachem Ltd.

2.1.6.6 Polymerase chain reaction (PCR)

Quantitative PCR (qPCR)

The PCR primers used to amplify specific nuclear DNA (nDNA) (encodes the acidic ribosomal phosphoprotein PO gene) and mitochondrial DNA (mtDNA) (partially encodes NADH dehydrogenase subunit 6, glutamic acid transfer RNA, and partially cytochrome b genes) sequences are listed in **table 2.8**. These primers were manufactured by Invitrogen UK Ltd.

Accession No.	Primer	Primer sequence	Length (bp)
nDNA (NM_001002)	36B4d (sense)	5' CCCATTCTATCATCAACGGGTACAA 3'	75
	36B4u (antisense)	5' CAGCAAGTGGGAAGGTGTAATCC 3'	
mtDNA (J01415)	mt14620 (sense)	5' CCCCACAAACCCATTACTAAACCCA 3'	222
	mt14841 (antisense)	5' TTTCATCATGCGGAGATGTTGGATGG 3'	

Table 2.8 Primer sets used to amplify specific nDNA and mtDNA sequences.

MX4000® 8-tube strips (0.2ml volume capacity), 8-cap strips and Brilliant® SYBR® green QPCR core reagent kits [comprising of SureStart® Taq DNA polymerase (5U/μl; 500U), 10× core PCR buffer, 50mmol/L magnesium chloride, 20mmol/L dNTP mix (5mmol/L each of dATP, dCTP, dGTP, and dTTP), 100% DMSO, 50% glycerol, 10,000× SYBR® green 1 solution and 1mmol/L 6-ROX (reference dye)] were purchased from Stratagene, Amsterdam, Netherlands. Water for molecular biology work (DNase and RNase-free) was obtained from Sigma-Aldrich. EDTA, HCl and tris were from Fisher Scientific UK Ltd and TE buffer, pH 7.4 (DNase and RNase free) was from Fluka and Riedel-de Haën.

Reference DNA was extracted from a mixture of whole blood, comprising of four different blood samples, these were diluted to generate standards of known concentrations for both quantitative PCR.

Real-Time PCR (RT-PCR)

Published PCR primer sequences used to amplify the human mitochondrial biogenesis genes, PGC1 α and mtTFA were taken from Norrbom *et al.*, 2004 and Civitarese *et al.*, 2007 respectively, and primers for the endogenous control gene, hypoxanthine phosphoribosyltransferase 1 (HPRT1) was designed by Dr Tiago Duarte, Department of Cancer Studies and Molecular Medicine, University of Leicester. All PCR primer sequences are listed in **table 2.9** and were manufactured by Fisher Scientific UK Ltd.

Gene	Accession No.	Primer sequence	Length (bp)
PGC1 α	NM_013261	5' CCAAACCAACAACCTTTATCTCTTCC 3' 5' CACTTAAAGGTGCGTTCAATAGTC 3'	101
mtTFA	NM_003201	5' CCCAGATGCAAAAACACTACAGAACTAA 3' 5' TCCGCCCTATAAGCATCTTGA 3'	102
HPRT1	L29382	5' GCAGACTTTGCTTTCCTTGGTCAG 3' 5' GTCTGGCTTATATCCAACACTTCGTG 3'	103

Table 2.9 Primer sequences used to amplify human mitochondrial biogenesis genes and endogenous control

The SYBR® Green JumpStart™ Taq ReadyMix™ was from Sigma-Aldrich. MicroAmp™ fast reaction 8-strip tubes and 8-strip caps were purchased from Applied Biosystems, Warrington, UK. Filter pipette tips were from Rainin Instruments, Anachem Ltd.

2.1.6.7 BigDye DNA sequencing

The MinElute® PCR purification kit used to purify PCR products was obtained from Qiagen. EtOH was from VWR International (BDH) Ltd and TE buffer, pH 7.4 was from Fluka and Riedel-de Haën. Purified products were quantified using the Quant-iT™ PicoGreen® dsDNA assay kit, purchased from Molecular Probes, Inc., Invitrogen UK Ltd. Clear 96-well microplates were from Nunc™, Fisher Scientific UK Ltd.

2.1.6.8 Agarose gel electrophoresis

Agarose (electrophoresis grade), BlueJuice™ gel loading buffer and HMW DNA markers were purchased from Invitrogen UK Ltd. Hyperladder V (DNA bands between 25bp and 500bp) was from Bionline, Humber Road, London, UK. EDTA, glacial acetic acid and tris were from Fisher Scientific UK Ltd, and ethidium bromide was from Sigma-Aldrich.

2.2 Equipment

2.2.1 Cell culture and treatment

Equipment	Source
Centaur centrifuge and CO ₂ incubator	Sanyo E & E Europe BV, Loughborough, Leicestershire, UK
Class II microbiological safety cabinet	Walkers Safety Cabinets Ltd, Glossop, Derbyshire, UK
EDP3 electronic LTS multichannel pipette (20-200µl)	Mettler-Toledo Ltd, Beaumont Leys, Leicester, UK
EG & G Berthold LB96V Luminometer and WinGlow software (version 1.24)	Berthold Technologies, Redbourn, UK
Haemocytometer (cell counting chamber slide)	Weber Scientific International Ltd, UK
Kinematica (plate shaker)	Philip Harris Scientific, Shenstone, Staffordshire, UK
Multichannel pipette (25 - 200µl)	Anachem Ltd, Luton, Bedfordshire, UK
Nikon inverted trinocular phase contrast microscope (Model TMS-F)	Nikon UK Ltd, Kingston Upon Thames, Surrey, UK
Ultra absorbance microplate reader	Bio-Tek Instruments, Inc.
Waterbath	Grant Instruments (Cambridge) Ltd, Barrington, Cambridge, UK

2.2.2 Cell imaging

Equipment	Source
Class II microbiological safety cabinet	Walkers Safety Cabinets Ltd
Fumehood	Morgan and Grundy Ltd, Uxbridge, Middlesex, UK
Hybaid (Maxi 14) hybridisation oven	Thermo Scientific, ABgene products, Epsom, UK
Incubator (no CO ₂)	Sanyo E & E Europe BV
Nikon Eclipse E400 fluorescent microscope and Nikon inverted trinocular phase contrast microscope (Model TMS-F)	Nikon UK Ltd

2.2.3 Apoptosis detection

Equipment	Source
EG & G Berthold LB96V Luminometer and WinGlow software (version 1.24)	Berthold Technologies
Hamamatsu Orca AG camera system	Hamamatsu Photonics UK Ltd, Welwyn Garden City, Hertfordshire, UK
Kinematica (Platform shaker)	Philip Harris Scientific
Multichannel pipette (25 - 200µl)	Anachem Ltd
Nikon Eclipse TE2000E inverted microscope	Nikon UK Ltd
Sutter DG4 fast fluorescence illumination system	Prior Scientific Instruments Ltd, Fulbourn, Cambridge, UK.
Volocity Acquisition software	Improvision, Viscount Centre II, University of Warwick Science Park, Coventry, UK

2.2.4 Reactive oxygen species (ROS) detection

Equipment	Source
Cary Eclipse Fluorescence Spectrophotometer with plate-reader attachment and Cary Eclipse software	Varian Ltd, Yarnton, Oxford, UK
CO ₂ incubator, Micro Centaur microfuge and Soniprep 150 sonicator	Sanyo E & E Europe BV
Cytofluor® series 4000 Multi-well plate reader and Cytofluor® software	Perseptive Biosystems, MA, USA
EG & G Berthold LB96V Luminometer and WinGlow software (version 1.24)	Berthold Technologies

2.2.5 Western blotting

Equipment	Source
Heating Block	Teche (Cambridge) Ltd, Duxford, Cambridge, UK
Hybridisation oven and shaker	Stuart Scientific, UK
Hypercassette	Amersham GE Healthcare UK Ltd, Chalfont, Buckinghamshire, UK
Kinematica (Platform shaker)	Philip Harris Scientific
Power pack, Western blot gel casting, electrophoresis and protein transfer equipment	Bio Rad Laboratories Ltd, Hemel Hempstead, Hertfordshire, UK
Spiramax (Rotational mixer)	Denley, Sussex, UK
X-ray film processor (Curix 60)	AGFA Geraert Ltd, Brentford, Middlesex, UK

2.2.6 Southern blotting

Equipment	Source
Hybaid cylinder tubes and nylon mesh	Thermo Scientific
Large electrophoresis tanks, large gel trays (20.3×19.4cm) and gel combs (23 wells)	Designed by University of Leicester Workshop, UK
Power pack	Bio Rad Laboratories Ltd
Radiation Geiger counter	Mini-Instruments Ltd, Essex, UK
Telometric version 1.2 software	Bioinformatics Facility, Fox Chase Cancer Center, Philadelphia, USA
Waterbath (37°C and 56°C)	Grant Instruments (Cambridge) Ltd
X-ray film processor (Curix 60)	AGFA Geraert Ltd

2.2.7 Molecular biology techniques

Equipment	Source
AlphaImager™ 1220 Documentation and Analysis System	Alpha Innotech Ltd, Cannock, UK
Chromas (version 1.45) software	http://www.technelysium.com.au/chromas.html
Cytofluor® series 4000 multi-well plate reader and Cytofluor® software	Perseptive Biosystems
Dark incubation trays, medium tanks, gel trays (23.5 × 14cm) and gel combs (14 wells)	University of Leicester Workshop
DNA thermal cycler 480	Perkin-Elmer LAS (UK) Ltd, UK
Horizontal (Maxi) gel electrophoresis tank	Fisher Scientific UK Ltd
Hybaid PCR Sprint thermal cycler	Mandel Scientific Company Inc., Ontario, Canada
Hybridisation oven and shaker	Stuart Scientific, UK
Komet (4.0) single cell analysis software	Kinetic Imaging Ltd, Liverpool, UK
MicroAmp™ fast 48-well tray, StepOne™ Real-time PCR machine and software	Applied Biosystems
Micro Centaur microfuge	Sanyo E & E Europe BV
Micropestles (1.5 – 2.0ml), slide scorer, mini microcentrifuge and Wilson staining jars	Fisher Scientific UK Ltd
Multichannel pipette (25-200µl)	Anachem Ltd
MX4000™ multiplex quantitative PCR machine and Tube-strip picofuge	Stratagene, Amsterdam, Netherlands
NCBI Basic Local Alignment Search Tool (BLAST) software	http://www.ncbi.nlm.nih.gov/BLAST/
Nikon Eclipse E400 fluorescent microscope	Nikon UK Ltd
Power pack	Bio Rad Laboratories Ltd
Qubit™ fluorometer	Invitrogen UK Ltd
Ultra absorbance plate reader	Bio-Tek Instruments, Inc
UV-visible spectrophotometer (UV-1601)	Shimadzu UK, Milton Keynes, UK

2.3 Methods

2.3.1 Cell culture and treatments

2.3.1.1 Cell culture

Originally, hVSMC were derived by primary culture of human saphenous vein explants as previously described (O'Callaghan and Williams, 2000). Cells used in this project were obtained from stocks stored in liquid nitrogen. hVSMC were cultured in RPMI 1640 media containing 10% (v/v) FCS with the additional supplements; 2.5% (v/v) human smooth muscle cell growth supplement, 100µg/ml L-glutamine, 100µg/ml penicillin/streptomycin, and 20mmol/L HEPES buffer. Only early passage hVSMC (passages 2 to 9) were studied.

Prior to Ang II exposure, 90% confluent cells were rendered quiescent in media containing 0.5% (v/v) FCS (media consisted of all additional supplements, excluding human smooth muscle cell growth supplement) for 24 hours before experimentation. The limited presence of growth factors (from FCS) prevented down-regulation of AT₁R gene expression (Nickenig and Murphy, 1994) and synchronized cells into the G₀-phase of the cell cycle.

HDF were from frozen stocks obtained by primary culture of human skin taken from the buttock region. Cells were cultured in DMEM with high glucose containing 10% (v/v) FCS, 100µg/ml L-glutamine and 100µg/ml penicillin/streptomycin. Cells were studied between passages 7 to 12 and rendered quiescent in media containing 1% (v/v) FCS for 24 hours.

Hep G2 cells were cultured in DMEM with high glucose containing 10% (v/v) FCS, 100µg/ml L-glutamine and 100µg/ml penicillin/streptomycin.

hASMC-hTERT was a kind gift from Professor Laura Niklason (Yale University, USA). These cells were originally isolated from a 17-year old donor before transfection with hTERT. They were cultured in DMEM with high glucose containing 20% (v/v) FCS, 100µg/ml penicillin/streptomycin, SmGM®-2 singlequotes® (insulin, hFGF-B, and

hEGF) and 60µg/ml hygromycin B. Cells were rendered quiescent in media containing 1% (v/v) FCS with no singlequot supplements, for 24 hours.

HeLa cells were cultured in EMEM (without L-glutamine) containing 10% (v/v) FCS, 100µg/ml L-glutamine and 1% (v/v) NEAA.

All cells were incubated at 37°C in Sanyo incubators with 5% (v/v) carbon dioxide (CO₂).

All cell types were sub-cultured by trypsinization. Cells were incubated with 2 to 3ml of pre-warmed 2× trypsin-EDTA solution (stock solution diluted with DPBS) for 5 minutes at 37°C, to detach them from the surfaces of culture vessels. The effect of trypsin-EDTA was neutralized with cell media and the cell suspensions were centrifuged at 180g for 5 minutes. Cells were resuspended in fresh media and divided into sterile flasks or multi-well plates.

2.3.1.2 Cumulative population doublings (CPD)

hVSMC cultured for SA-β-gal staining in 6-well/12-well plates were seeded at a density of 5×10⁴/1×10⁴ cells per well. Cells were seeded at 4×10⁵ cells/T75cm² flask for determining mtDNA content of cells by qPCR. At each passage, cells were counted using a haemocytometer and population doublings (PD) were calculated using the following formula:

$$PD = (\log_{10}Y - \log_{10}Z) / \log_{10}(2)$$

(**Y** indicates the number of cells harvested; **Z** indicates the number of cells seeded). CPD was calculated as the sum of all PD with every successive passage.

2.3.1.3 Cell treatments

Ang II was dissolved in UP H₂O and sterilised by filtration (0.2µm) immediately before cell treatment. Cells were rendered quiescent by serum deprivation as described in **2.3.1.1**, before relatively short incubation periods with Ang II (1 to 24 hours). Successive Ang II treatment over long periods was conducted in medium containing 10% (v/v) FCS, where cells were treated on alternate days and also sub-cultured once confluence was reached. Working concentrations of H₂O₂ and t-BHP were made up in UP H₂O and filter sterilised before treating cells for 1 to 24 hours.

AT₁R inhibitors, ROS scavengers and mitochondrial complex inhibitors were filter sterilised prior to pre-treatment of cells for 1 to 4 hours, followed by Ang II exposure. Apocynin, rotenone and TTFA were dissolved in DMSO. 5-HD was dissolved in EtOH. Catalase and E3174 were dissolved in DPBS, whereas NAC and mito-TEMPO were made up in UP H₂O. All of the cell treatments were conducted at 37°C with 5% CO₂.

2.3.1.4 SIPS induction

Cells were seeded at a density of 2×10^4 cells per well in 6-well plates. After 48 hours, cells were rendered quiescent for 24 hours as described in **2.3.1.1**, and then incubated with Ang II for 2 hours. Ang II was removed afterwards by changing the culture medium (containing 0.5% (v/v) FCS) to allow for cells to recover for 24 hours prior to subsequent exposures. Treatment with 40µmol/L t-BHP was conducted in the same manner using media containing 10% (v/v) FCS.

2.3.1.5 Cell viability measurements

Trypan blue exclusion method

Trypan blue is a polar dye only absorbed by cells with ruptured cell membranes. Dead cells appear blue stained and viable cells appear clear or translucent. Cells were resuspended in a known volume of media, and a small portion was then further diluted 1:1 with 0.4% (w/v) trypan blue solution. Cells were left to stand for 2 minutes to allow the dye to penetrate dead cells, before counting the number of blue and clear cells using a haemocytometer. Cells were counted in four 1.0mm² regions and the mean values were used to calculate the percentage of viable cells using the equation below:

$$\% \text{ Viability} = \frac{\text{Number of live cells}}{\text{Number of live} + \text{Number of dead cells}} \times 100$$

MTT colorimetric assay

Cell proliferation and viability were detected using the quantitative colorimetric MTT assay developed by Mossman, which was then later refined to improve sensitivity and reliability (Denizot and Lang, 1986). The assay is based on the reduction of the tetrazolium salt, MTT, by the mitochondrial enzyme succinate dehydrogenase in viable cells, to form a blue formazan product (Mosmann, 1983). The amount of formazan produced is proportional to the number of viable cells present.

Cells were seeded into clear 96-well microplates at a density of 1×10^3 cells per well and grown to confluence. Treatment was performed in complete media without phenol red (PR⁻) indicator. After treatment, the cell media was discarded from all wells using a multichannel pipette and the microplate was inverted and blotted on tissue paper several times to remove any residual media. MTT solution (1mg/ml) was made in RPMI 1640 PR⁻ basal media, filter sterilised and 100µl was added per well. The microplate was incubated at 37°C in the dark (covered with foil) for 4 hours to allow for MTT reduction. MTT solution was then discarded, and the microplate was inverted and blotted to remove any remaining MTT solution. The visible blue formazan product was solubilised by the addition of 100µl of isopropanol per well and slow agitation on a plate shaker for 5 minutes at room temperature (RT). Absorbance was measured at 562nm and 690nm (reference) wavelengths using the Ultra absorbance microplate reader.

ApoGlow® adenylate nucleotide ratio assay

Metabolically viable cells have maintained levels of adenosine triphosphate (ATP) which gradually degrade upon the onset of apoptosis, where an increase in adenosine diphosphate (ADP) levels is observed. In necrosis, ATP levels rapidly drop and coincide with increased ADP levels.

The ApoGlow® assay primarily allows for the distinction between apoptosis, necrosis and proliferation of cells *in vitro*. However, ATP production is strongly associated with mitochondria and was used to assess mitochondrial function. The reaction utilizes luciferase to generate light from the reaction of ATP and luciferin. The light intensity generated correlates with ATP concentration and ADP is then determined from the conversion of ATP by luciferase. Cells were seeded into white 96-well microplates (7×10^3 cells per well in 100µl of media) for 24 hours prior to treatment in 10% (v/v) FCS containing media. All microplates and prepared reagents were equilibrated to RT for 30 to 45 minutes prior to the end of treatment.

An electronic multichannel pipette was used to add all reagents to the wells. Five minutes after the addition of the nucleotide releasing reagent (NRR) (100µl per well), 20µl per well of the nucleotide monitoring reagent (NMR) (1:10 dilution in tris-acetate buffer) was added and a 1 second integrated reading expressed as arbitrary light units

(ALU) (*Reading A*) was taken in the luminometer (temperature controlled at 22°C), to measure ATP levels. The ATP signal was then allowed to decay to a steady-state for 10 minutes prior to *Reading B*. Finally, ADP was converted to ATP by the addition of ADP converting reagent (ADP-CR) (20µl per well) and *Reading C* was taken after a 5-minute incubation period. The ADP:ATP ratio was calculated as described (Bradbury *et al.*, 2000) using the equation below:

$$\frac{\text{Reading C} - \text{Reading B}}{\text{Reading A}}$$

Relative ATP was calculated from the initial reading of wells; *Reading A* - *Reading B*. But ATP was also expressed as ALU/µg protein.

2.3.2 Cell imaging

2.3.2.1 Microscopy images

Light microscopy images were taken of hVSMC grown in T75cm² Nunc™ flasks, in media containing 10% (v/v) FCS. Phase contract microphotographs were taken at ×40 and ×100 magnifications, using a colour camera attached to a Nikon inverted trinocular phase contrast light microscope.

2.3.2.2 Immunofluorescence

Cells were seeded on sterile, round, glass coverslips (immersed in 70% IMS then air-dried for 30 minutes to sterilize) in 6-well plates at 2×10⁴ cells per well, grown to near confluence (80%) in media containing 10% (v/v) FCS and then rendered quiescent for 7 days (as described in section 2.3.1.1). Cells were fixed in 4% (w/v) paraformaldehyde in DPBS for 20 minutes at 4°C, followed by 3 washes for 2 minutes each with tris buffered-saline (TBS) (24.8mmol/L tris; 137mmol/L NaCl; 2.7mmol/L KCl, pH7.4), permeabilized (0.5% (v/v) triton X-100 in TBS) for 10 minutes, and washed 3 times in washing buffer (0.1% (v/v) triton X-100 in TBS) for 5 minutes each. Cells were blocked (0.1% (v/v) triton X-100; 2% (w/v) BSA in TBS) for 10 minutes at RT, then incubated with the anti-α-smooth muscle actin antibody (1:600) in blocking buffer at 37°C for 1 hour in the dark. After washing, the cells were incubated with anti-mouse IgG FITC conjugate secondary antibody (1:400) for 1 hour at 37°C in the dark. Excess unbound secondary antibody was removed by washing with a final rinse in

UP H₂O. Coverslips were mounted on microscope slides with VectorShield mounting medium for fluorescence, and sealed with clear nail varnish.

Fluorescent images were taken under a FITC filter (excitation: 485nm; emission: 530nm wavelengths) at ×400 magnification, using a Nikon Eclipse E400 fluorescent microscope.

2.3.2.3 SA-β-gal assay

Expression of the β-galactosidase enzyme at pH 6.0 is a widely used biomarker for cellular senescence *in vivo* and *in vitro*. The cytochemical staining for SA-β-gal activity was measured in cultured cells using the commercially available ‘Senescent Cells Staining Kit’, as described by (Dimri *et al.*, 1995). Cells were grown to confluence in 6 or 12-well plates and treated with Ang II as described in **2.3.1.3** or **2.3.1.4**.

After treatment, cells were trypsinized, counted using a haemocytometer and re-seeded at $5 \times 10^4 / 1 \times 10^4$ cells in 6/12-well plates. This allowed for a sufficient number of cells to adhere over 24 hours. Cells were rinsed twice with PBS, fixed in fixation buffer (2% formaldehyde; 0.2% glutaraldehyde; 7.04mmol/L Na₂HPO₄; 1.47mmol/L KH₂PO₄; 137mmol/L NaCl; 2.68mmol/L KCl) for 6 to 7 minutes at RT. After washing 3 times with PBS, the fixed cells were incubated with fresh, sterile SA-β-gal staining mixture (1mg/ml X-gal solution; 1× staining mixture; 5mmol/L reagent B; 5mmol/L reagent C, pH 6.0) at 37°C in a Sanyo incubator (without CO₂) for 24 hours. To prevent cells from drying out parafilm was used to seal edges of the multi-well plates during the staining period. Senescent cells specifically stain at pH 6.0 therefore cells were not incubated in a CO₂-rich environment, since this may alter the pH of the solution.

Blue stained, senescent cells were visualized using a Nikon inverted trinocular phase contrast light microscope and counted manually from 5 fields of view selected at random from each well. After the staining period, the SA-β-gal staining solution was removed and cells were overlaid with 1ml of 70% (v/v) glycerol per well for long-term storage at 4°C. Images were taken at ×100 magnification using a Nikon inverted trinocular phase contrast light microscope.

2.3.3 Apoptosis measurements

2.3.3.1 Caspase-3/7 activity

Caspase-3 and -7 are cysteine aspartic acid-specific proteases involved in the execution of apoptosis. Caspases are activated through intrinsic and extrinsic signalling pathways. Extracellular signalling initiates the extrinsic pathway where activation of the death-receptor initiates caspase-8 which is cleaved and activates caspase-3. The intrinsic pathway is mediated by the release of cytochrome c from mitochondria, which initiates caspase-9 then activates caspase-3. Caspase-3 cleaves downstream cellular targets resulting in apoptosis (Li *et al.*, 2007b).

Following cell lysis, the Caspase-Glo® 3/7 DEVD substrate reagent is cleaved generating a luminescent signal from luciferase. The luminescence produced is proportional to the quantity of caspase-3/7 activity. hVSMC were seeded at 3×10^3 cells per well in white 96-well microplates (100µl media per well) and grown to confluence. This was assessed by viewing cells simultaneously and identically seeded in clear 96-well microplates. After cell treatment, the microplate was equilibrated to RT for 30 minutes prior to the end of the incubation period.

All the caspase-Glo® 3/7 reagents were thawed and equilibrated to RT for 30 to 45 minutes. Caspase-Glo® 3/7 buffer was poured in the caspase-Glo® 3/7 substrate bottle and the contents were mixed by inverting and swirling, then left to equilibrate for a further 10 minutes. The reagent was added to the microplate (100µl per well) and agitated at medium speed on a platform shaker for 30 seconds at RT to aid cell lysis. Luminescence was measured 1 to 2 hours after the addition of the reagent (Relative light units per second (RLU/sec) in the luminometer, maintained at 22 to 24°C. The background measurement of cell culture medium alone was subtracted from the measurements of treated cells.

2.3.3.2 Detection of DNA fragmentation using Hoechst 33258 staining

Hoechst 33258 is a cell-permeable blue fluorescent DNA-binding dye. The changes in nuclear morphology can be used to analyse apoptosis. Apoptotic cells have brightly blue fluorescent nuclei. The nuclear material may be irregular-shaped, condensed or fragmented to form apoptotic bodies. In contrast, the nuclei of viable cells display uniform blue staining and a regular ovoid appearance.

Cells were cultured to near confluence on sterilized, glass coverslips in 6-well plates. After treatment, cells were rinsed twice with warmed DPBS then fixed in 500 μ l absolute ice-cold methanol for 2 to 3 minutes at RT. After washing twice with DPBS the fixed cells were incubated with fresh Hoechst 33258 solution (2.5 μ g/ ml) prepared in DPBS, for 15 minutes at RT with protection from light (covered with foil). Cells were then rinsed 4 times with DPBS to sufficiently remove any excess Hoechst dye. Each coverslip was mounted onto a microscope slide using 25 μ l 1:1 (v/v) DPBS/glycerol solution and sealed with clear nail varnish.

Cell nuclei were visualized under a DAPI filter (excitation: 340-380nm; emission: 435-485nm) using a Nikon Eclipse TE2000E inverted microscope with a Sutter DG4 fast fluorescence illumination system, and Hamamatsu Orca AG Camera System. Four random fields of view were scored for each slide and the percentage of apoptotic cells was calculated. A drop of immersion oil was placed onto the coverslips prior to capturing images at \times 400 magnifications, using the Volocity Acquisition software.

2.3.4 ROS measurements

2.3.4.1 Measurement of ROS in intact cells

ROS generation induced by cell treatment was measured with the fluorescent probe CM-H₂DCFDA, a chloromethyl derivative of dichlorodihydrofluorescein diacetate (DCFDA), which exhibits better retention in viable cells than DCFDA. Cells were grown to confluence in 96-well microplates for 2 days. Fresh media was added to the wells and then CM-H₂DCFDA (10 μ mol/L in DMSO) was added. Cultures were incubated in the dark at 37°C for 30 minutes to allow for sufficient cellular uptake of the probe, then rinsed twice with pre-warmed HBSS before treatment. Finally, 100 μ l of HBSS was added to each well and fluorescence was measured using the Cytofluor multi-well fluorescence plate reader (excitation; 485 \pm 20nm; emission: 530 \pm 20nm).

2.3.4.2 Measurement of NAD(P)H oxidase activity

NAD(P)H oxidase activity was measured as described by Griendling *et al* (1994) with some modifications. NAD(P)H oxidase is a known major source of O₂⁻ production in VSMC. hVSMC were grown in T175cm² flasks to extract sufficient quantities of protein for measuring O₂⁻ production. Quiescent hVSMC were treated with Ang II for various periods of time (1 to 24 hours), and experiments involving pre-incubation with

E3174 prior to Ang II exposure were as described in **2.3.1.3**. Cells were rinsed with DPBS, trypsinized, and centrifuged at 180g for 5 minutes at RT. Cells were washed twice with ice-cold DPBS, transferred to chilled eppendorfs and centrifuged at 9300g for 5 minutes at 4°C. Waste supernatant was discarded and the cell pellets were resuspended in 300µl of ice-cold lysis buffer (20mmol/L KH₂PO₄, 1mmol/L EGTA, pH 7.4, 10% (v/v) protease inhibitor cocktail). Each cell lysate was then sonicated 3 times with 10 second bursts at 30% power and cooled on ice for 30 seconds between each sonication. Lysates were centrifuged at 800g for 10 minutes at 4°C to remove unbroken cells and debris, and then transferred to chilled eppendorfs. The protein content was determined using the Bradford protein assay (**2.3.5.7**).

The lucigenin chemiluminescence assay (LCLA) was used to measure NAD(P)H oxidase activity in protein extracts. The luminometer was switched on and allowed 10 to 15 minutes to warm up to 37°C (preset temperature). A white, 96-well microplate was placed in the luminometer and 100µg of cell lysate were added into the selected wells. All reaction components combined in each well were made up to a final volume of 200µl. Ice-cold assay buffer (50mmol/L KH₂PO₄, 1mmol/L EGTA, 150mmol/L sucrose, pH 7.4) was added. A final concentration of 10µmol/L lucigenin was added which specifically detects O₂^{·-} and is not involved with redox cycling (Skatchkov *et al.*, 1999) and the ROS and oxidase inhibitors used in experiments were added as 1:200 dilutions. The final concentrations of all inhibitors are detailed in **table 2.10**. The plate was then left in the luminometer at 37°C for 5 minutes prior to the addition of NADPH. NADPH and the other ROS stimulators investigated are listed in **table 2.11**.

Chemiluminescence was measured every 40 seconds for 40 minutes in the luminometer. The total quantity of O₂^{·-} generated over that time was calculated for the area under the kinetic curve using the trapezoidal rule (Le Floch *et al.*, 1990), for each reaction.

ROS inhibitor	Target of ROS inhibition (oxidase enzyme/ ROS)	Final concentration ($\mu\text{mol/L}$)
Antimycin A	Mitochondrial complex III	10
CCCP	Mitochondrial complex IV and uncoupler of mtRC	10
DPI	Flavoprotein	50
5-HD	Mitochondrial ATP-sensitive potassium (mitoK _{ATP}) channels	100
Indomethacin	Cyclooxygenase	20
NAC	Free radical scavenger and increases GSH	10,000
Rotenone	Mitochondrial complex I	10
Tiron	Nonenzymatic O ₂ ^{•-} scavenger	10,000
TTFA	Mitochondrial complex II	10

Table 2.10 Final concentrations of ROS inhibitors.

ROS stimulator	Target of ROS production (oxidase enzyme)	Final concentration ($\mu\text{mol/L}$)
Antimycin A	Mitochondrial complex III (inhibitor) (added in conjunction with succinate)	30
NADH	NAD(P)H oxidase	400
NADPH	NAD(P)H oxidase	400
Succinate	Mitochondrial complex II	5000
Xanthine	Xanthine oxidase	1000

Table 2.11 Final concentrations of ROS stimulators.

2.3.4.3 Measurement of mitochondrial O₂^{•-}

Mitochondrial O₂^{•-} production induced by cell treatment was measured with the fluorescent probe MitoSOXTM, a fluorogenic dye that is highly selective in detecting O₂^{•-} in mitochondria of live cells. The reagent is selectively targeted to the mitochondria where it is oxidized by O₂^{•-} and exhibits red fluorescence. Cells were grown to confluence in 6-well plates for 48 hours in media containing 10% (v/v) FCS. Following treatment, cells were rinsed twice with pre-warmed HBSS (containing Ca²⁺ and Mg²⁺). A 5mmol/L stock solution of MitoSOXTM was prepared with DMSO then diluted to a working concentration of 5 $\mu\text{mol/L}$ with HBSS. The MitoSOXTM working concentration (500 μl) was added to each well, and the plate was incubated in the dark at 37°C for 10 minutes, to allow for the fluoroprobe to be taken up by cells and oxidized. Cells were then rinsed with HBSS (3 \times). Finally, 500 μl of HBSS was added to each well and fluorescence was measured using the Cary Eclipse Fluorescence Spectrophotometer plate reader (excitation: 510nm; emission: 580nm). Fluorescent measurements were recorded in the advanced readings set-up in the Cary Eclipse software, and calculated relative to untreated cells loaded with the probe.

2.3.5 Extraction and quantitation methods

2.3.5.1 DNA extraction

The QIAamp® DNA blood mini kit was used to extract DNA from cells. Each cell pellet was resuspended in 200µl DPBS and QIAGEN protease (20µl) and Buffer AL (200µl) were added with mixing by pulse vortexing for 15 seconds. Cell lysates were incubated at 56°C for 10 minutes, briefly centrifuged in a microcentrifuge, EtOH (200µl) was then added and pulse vortexed again. Lysates were briefly centrifuged again then transferred to QIAamp spin columns (with collection tubes) and centrifuged at 11,000g for 1 minute. The columns were placed in clean 2ml collection tubes and 500µl Buffer AW1 was added. Following centrifugation at 11,000g for 1 minute, columns were placed in clean collection tubes. Buffer AW2 (500µl) was added to the column, centrifuged at 11,000g for 3 minutes, then placed into clean 1.5ml eppendorfs and centrifuged again to ensure the complete removal of wash buffer. Buffer AE (55µl) was added to the column and incubated for 5 minutes at RT prior to centrifuging at 11,000g for 1 minute, to elute the DNA.

2.3.5.2 DNA quantitation

The Quant-iT™ PicoGreen® dsDNA assay kit was used to quantify the extracted DNA from cells. The PicoGreen reagent is a sensitive fluorescent nucleic acid stain for double-stranded DNA (dsDNA). A range of λDNA concentrations was generated in TE buffer to create a standard curve (50, 25, 10, 2 and 0 ng). These were diluted 2-fold with PicoGreen solution (diluted 200-fold in TE buffer for a working concentration). DNA samples were diluted 1:50 with TE buffer, and 10µl of each were added to 90µl TE buffer in a 96-well microplate. PicoGreen solution (100µl) was added to each well and the fluorescence was read in the Cytofluor multi-well plate reader (excitation: 485nm; emission: 530nm). The concentration of DNA within samples was determined against the fluorescence values obtained from the standard curve.

2.3.5.3 RNA extraction

The High Pure RNA Isolation kit was used to extract total RNA from cultured cells. The incorporated DNase treatment step purified isolated RNA from residual genomic DNA. Each cell pellet was resuspended in 200µl DPBS then 400µl of lysis buffer was added and mixed by vortexing for 15 seconds. Lysates were transferred to high pure filter tubes (with collection tubes) and centrifuged at 8000g for 1 minute. The

flow-through was discarded and filters were re-inserted in collection tubes. In sterile eppendorfs, 90µl of DNase incubation buffer was added to 10µl DNase 1 for each sample, mixed, then pipetted onto each filter and incubated for 15 minutes at RT. Wash buffer I (500µl) was added to each filter then centrifuged at 8000g for 1 minute. The flow-through was discarded and the same wash was performed using wash buffer II, then again using 200µl of wash buffer II, centrifuging at 11,000g for 2 minutes to ensure the removal of residual wash buffer. Filter tubes were inserted into sterile 1.5ml eppendorfs and 35µl of elution buffer was added to each filter and centrifuged at 8000g for 1 minute to elute the purified RNA.

2.3.5.4 Total RNA quantitation

Purified total RNA was quantified using the Quant-iT™ RNA assay kit. The Quant-iT™ RNA reagent is an ultrasensitive fluorescent nucleic acid stain for RNA and was diluted 200-fold in Quant-iT™ RNA buffer for a working concentration. Each Quant-iT™ RNA standard (#1 and #2) (10µl) was added to 190µl of the working concentration in Qubit™ assay tubes, and 1µl of each RNA sample (diluted 1:30) was added to 199µl of the working concentration. All tubes were mixed by vortexing (3 seconds) then incubated for 3 minutes at RT. The fluorescent readings of RNA standards #1 and #2 were consecutively read, followed by each RNA sample in the Qubit™ fluorometer. RNA sample concentrations were given in ng/ml units, relative to the 2 standard values. The original concentration of RNA samples was calculated by accounting for the dilution of samples.

2.3.5.5 RNA quality and PCR primer quantitation by UV spectrophotometry

Total RNA samples were diluted 1:200, and PCR primers were reconstituted with 100µl TE buffer, pH 7.4. PCR primers and diluted RNA samples were diluted 1:100 with TE buffer, pH 7.4 and UV readings were taken at 230, 260 and 280nm. The ratio of A_{260}/A_{280} was used to determine the quality of RNA with respect to protein and A_{260}/A_{230} with respect to phenol and guanidine contaminants. Readings at 260nm were used to quantify and determine the concentration of PCR primers.

One absorbance unit at 260nm of single-stranded DNA equates to 33µg/ml of DNA. Pure RNA is acceptable between the ranges of 1.7-2.1 of the A_{260}/A_{280} ratio.

2.3.5.6 Protein extraction

Protein was extracted from whole cells (10^6 cells) by adding 20 μ l of chilled cell lysis buffer (3mmol/L β -mercaptoethanol; 3mmol/L EDTA; 50mmol/L KCl; 5mmol/L magnesium acetate; 10% (v/v) protease inhibitor cocktail; 50mmol/L tris-HCl, pH 7.4).

Membrane-bound proteins were extracted from cells (3×10^6 cells) by adding 80 μ l of RIPA buffer (2mmol/L EDTA; 150mmol/L NaCl; 10mmol/L NaF; 1% (v/v) NP-40; 10% (v/v) protease inhibitor cocktail; 0.1% (w/v) SDS; 0.5% (w/v) sodium deoxycholate (initially made as a 10% (w/v) stock solution); 50mmol/L tris-HCL, pH 7.5). Cells were resuspended by vortexing then homogenized using micropestles (25 strokes per cell sample), on ice. Cell lysates were then incubated on ice for 1 hour then centrifuged at 9300g for 10 minutes at 4°C. The supernatants were transferred to sterile chilled eppendorfs and stored at -80°C.

2.3.5.7 Protein quantitation

Proteins were quantified using a modified method, originally described by Bradford (1976). A 1mg/ml BSA stock solution was used to generate a protein standard curve of the following concentrations in cell lysis buffer (used for protein extraction): 0.5; 0.4; 0.3; 0.2; 0.1mg/ml BSA. Protein extract samples were diluted 1:25 with cell lysis buffer. Each BSA standard and diluted protein extract were transferred to a 96-well microplate, in triplicate (10 μ l). The Bio Rad protein assay dye reagent was diluted to 20% (v/v) in UP H₂O and 200 μ l was added to each well. The microplate was incubated at RT for 10 minutes then read in the absorbance plate reader at 595nm. Protein concentrations were calculated against the BSA standard curve.

2.3.6 Molecular biology methods

2.3.6.1 Western blotting

SDS-polyacrylamide gel electrophoresis (PAGE)

All glass plates (spacer plates and short plates), casting frames and well combs were cleaned with IMS. One spacer plate and short plate were assembled together in a casting frame and secured in a casting stand for each polyacrylamide gel made. Firstly, the resolving gel (2 gels) (375mmol/L tris-HCl pH8.8; 350 μ mol/L SDS; 220 μ mol/L APS; 0.002% (v/v) TEMED) was prepared containing 12% (w/v) acrylamide/bis solution 29:1, which allowed the distinction between different sized proteins. APS solution was added

to the gel mix lastly to initiate polymerization and 7ml of the resolving gel was then added using a pipette between each short and spacer plate. The gels were overlaid with 1ml isopropanol and left to set at RT for 40 minutes. Once the gels had set the isopropanol layer was poured away and 4ml of the stacking gel (124mmol/L tris-HCl pH 6.8; 4% (v/v) acrylamide/bis solution 29:1; 347 μ mol/L SDS; 218 μ mol/L APS; 0.001% (v/v) TEMED) was added on top of each resolving gel, filling the remaining space between both plates. A 10-well comb was slotted into each stacking gel, and the gel left to set at RT for 40 minutes.

Once the stacking gels had set, the gel casts were released from the casting stands then the casting frames and well combs were removed. Two gel casts were assembled into each electrophoresis tank with the short plates facing each other. The tank was filled with 1L of SDS-PAGE running buffer (192mmol/L glycine; 3mmol/L SDS; 25mmol/L tris) and used to wash the wells out using a pipette. Equal concentrations of protein lysate for each sample (20 μ g/40 μ g) (determined by Bradford protein assay, section 2.3.5.7) were added to equal amounts of 2 \times loading buffer (70 μ mol/L bromophenol blue; 20mmol/L DTT; 10% (v/v) glycerol; 62.5mmol/L tris-HCl pH 6.8) and heated at 95°C for 5 minutes. Protein lysates assessed under non-reduced conditions (when labelled for AT₁R, AT₂R or telomerase) were added to equal amounts of 2 \times loading buffer containing no DTT and were not heated prior to loading in wells. The precision plus protein standards were loaded into the first wells (6 μ l) and the protein lysates were loaded in the subsequent wells. The proteins were separated by electrophoresis at 120V for 70 minutes.

Protein transfer

Transfer buffer (24.8mmol/L tris; 192mmol/L glycine; 10% (v/v) methanol) was prepared during the electrophoresis stage. Whatman filter paper (4 sheets) and nitrocellulose membrane were cut to the size of short plates for each gel. The nitrocellulose membrane was soaked in UP H₂O for 2 minutes then transfer buffer for 5 minutes, and filter papers were only soaked in transfer buffer for 5 minutes. Transfer sponges (2) were soaked in a trans-blot tank filled with transfer buffer.

The electrophoresis tank was disassembled and the glass plates were pulled apart gently. The stacking gel was cut away using a scalpel and the remaining gel was rinsed in transfer buffer. On the black surface of each transfer cassette the following were stacked in order: 1 transfer sponge; 2 filter papers; 1 gel; 1 nitrocellulose membrane; 2 filter papers and 1 transfer sponge. Trapped air bubbles were rolled out before closing the cassette as these could affect protein transfer, then the cassette was slotted into the clamp within the tank (black surface of the cassettes were placed facing the black side of the clamp). Electrophoresis was then carried out at 60V for 1 hour at RT (or 30V O/N).

Immunoblotting

The trans-blot tank was disassembled, gels and filter papers were discarded and membranes were placed in a small tray containing UP H₂O and washed for 2 to 3 minutes at RT. All washes and antibody incubations were performed on a platform shaker and rotational mixer.

Membranes were then incubated with Ponceau S stain (6.5mmol/L Ponceau S, 5% (^{w/v}) trichloroacetic acid) for 5 minutes at RT to verify protein transfer. This staining solution was poured back into its bottle (re-usable) and the membranes were washed several times with UP H₂O. The stained protein bands remaining were removed by brief washing with 0.1mol/L NaOH for 30 seconds, followed by several washes in UP H₂O. Membranes were blocked with non-fat marvel milk powder in TBS with tween-20 (TBST) (TBS; 0.001% (^{v/v}) tween-20) (milk/TBST) or BSA in TBST (BSA/TBST) under different incubation conditions, as optimized by preliminary experiments, detailed in **table 2.12**. After the appropriate blocking period, the membranes were rinsed with TBST twice for 15 minutes each; then incubated with specific primary antibodies, listed in **table 2.13**.

Primary antibody	Blocking solution	Incubation conditions
Anti-AT ₁ R [TONI-1] Anti-AT ₂ R	5% (w/v) BSA/TBST	O/N at 4°C
Anti- α -tubulin	5% (w/v) BSA/TBST (anti-AT ₁ R) 5% (w/v) milk/TBST (anti-myosin) 10% (w/v) milk/TBST (anti-p16; p21; p53 and telomerase)	1 hour at RT
Anti- β -actin	5% (w/v) BSA/TBST (anti-AT ₂ R)	1 hour at RT
Anti-p16 Anti-p21 Anti-p53	10% (w/v) milk/TBST	1 hour at RT
Anti-myosin (smooth)	5% (w/v) milk/TBST	O/N at 4°C
Anti-telomerase		1 hour at RT

Table 2.12 Blocking solutions and conditions for incubation prior to specific primary antibody labelling. Different blocking solutions were used when confirming equal protein loading using either anti- α -tubulin or β -actin, which were dependent upon the primary antibody originally labelled for (detailed in brackets).

Primary antibody	Dilution (μ l)	Incubation conditions
Anti-AT ₁ R [TONI-1]	1:200	O/N at 4°C
Anti-AT ₂ R	1:400	O/N at 4°C
Anti-myosin (smooth)	1:2000	O/N at 4°C
Anti-p16	1:200	O/N at 4°C
Anti-p21	1:200	1 hour at RT
Anti-p53	1:400	O/N at 4°C
Anti-telomerase	1:200	O/N at 4°C
Secondary antibody		
Donkey-anti-goat IgG – H & L HRP	1:10,000 (anti-AT ₂ R)	1 hour at RT
Goat-anti-rabbit IgG–peroxidase conjugate (whole molecule)	1:5000 (anti-p16 and telomerase)	1 hour at RT
Rabbit-anti-mouse IgG–H & L HRP	1:5000 (anti-p21 and p53) 1:10,000 (anti-AT ₁ R, myosin and telomerase)	1 hour at RT

Table 2.13 Primary and secondary antibody dilutions and conditions for the proteins of interest. In all cases, antibodies were diluted in the respective blocking solutions as detailed in **table 2.12**. The specific secondary antibody dilutions used for primary antibodies are listed in brackets.

Membranes were then rinsed again with TBST twice for 15 minutes, followed by incubation with the appropriate secondary antibody (**table 2.14**), and afterwards rinsed several times with TBST to ensure the sufficient removal of excess antibody.

Primary antibody	Dilutions (μl)	Incubation conditions
Anti- α -tubulin	1:10,000	15 minutes at RT
Anti- β -actin	1:20,000	O/N at 4°C
Secondary antibody		
Rabbit-anti-mouse IgG –H & L HRP	1:10,000	1 hour at RT

Table 2.14 Primary and secondary antibody dilutions and conditions for the labelling of equal protein loading. β -actin expression was only determined for membranes previously labelled for AT₂R, whereas α -tubulin expression was determined for all other previously labelled proteins of interest.

Enhanced chemiluminescence (ECL) detection and densitometric analysis

Washed membranes were laid onto Saran wrap and 1ml of the ECL solution (100mmol/L tris-HCl, pH 8.5, 197 μ mol/L p-coumaric acid (made in DMSO), 1.2mmol/L luminol (made in DMSO), 0.009% (^{w/v}) H₂O₂) was transferred over each membrane using a pipette, then incubated for 1 minute at RT. Membranes were then quickly placed onto a clean Saran wrap and sealed in hypercassettes. Under red light, films were exposed for 30 seconds to 1 minute, and then developed in the X-ray film processor. Band intensities on films were quantified by densitometry using the AlphaImager documentation and analysis system.

Western blot membrane stripping

Membranes relabelled with different proteins of interest, were incubated in 15ml of RestoreTM Western Blot Stripping Buffer for 15 minutes at RT with agitation, to remove the primary and secondary bound antibodies. After numerous washes with TBST at RT, the membranes were then incubated with the relevant blocking solution for the protein of interest (**table 2.12**), then subsequently labelled with primary and secondary antibodies (**tables 2.13 and 2.14**).

2.3.6.2 Southern blotting

Gel electrophoresis and blotting

The Southern blotting technique was described by Southern (1975) to identify and locate the presence of a specific DNA sequence in a DNA sample by using a complementary piece of DNA, known as a probe.

DNA was extracted and quantified as described in **2.3.5.1** and **2.3.5.2**. DNA (2µg per sample) was cut into fragments by digesting with restriction enzymes *HinfI* and *RsaI* (20 Units *HinfI*; 20 Units *RsaI*; in NEBuffer 2 (containing; 25mmol/L NaCl; 5mmol/L tris-HCl; 5mmol/L MgCl₂ and 500µmol/L DTT)) at 37°C for 4 hours. These restriction enzymes were used as they cut at frequent sites along the DNA and therefore minimize the size of the sub-telomeric region.

The DNA fragments for each sample were separated onto a large agarose gel (0.5% (^{w/v}) agarose, 250ml of 1× TAE buffer (40mmol/L tris; 1mmol/L EDTA; 0.1% (^{v/v}) glacial acetic acid) and 0.02µg/ml ethidium bromide solution) and electrophoresis was performed in running buffer (2750ml of 1× TAE, 0.018mg/L of ethidium bromide solution). HMW and 1kb DNA ladders were combined (250ng each) and loaded in every fourth or fifth well along the gel. BlueJuice™ gel loading buffer (2µl) was added to each digested DNA sample (2µg) and this mixture was loaded into individual wells. Electrophoresis was carried out for 880V hours O/N at RT (or until 1.6kb DNA ladder marker had migrated off the gel). The gel was visualized using the AlphaImager gel documentation system to ensure the DNA marker bands had sufficiently separated.

The wells were cut off the top of the gel then placed in depurinating solution (1.2% (^{v/v}) HCl in 1L) for 10 minutes at RT on a platform shaker at slow speed, then agitated in 750ml of alkaline blotting buffer (ABB) (400mmol/L NaOH; 1mol/L NaCl) twice, for 15 to 20 minutes each. During these incubations filter papers (2×), a wick and a nylon membrane were cut and pre-soaked in ABB.

The Southern blot was assembled in the following order on a plate resting over a tray containing 1.5L ABB: a wick (either edges dipped in ABB, 1 gel, 1 nylon membrane, 2 sheets of filter paper, quickdraw blotting sheets (~10), stack of paper towels and a

weight on the top. This was left O/N to allow DNA transfer to the membrane by capillary action.

The blot was disassembled and the membrane was placed between 2 sheets of filter paper and baked at 80°C for 2 hours to fix the DNA. The blot was briefly rinsed in UP H₂O then stored at 4°C until hybridisation. The blotted gel was stained with ethidium bromide in UP H₂O and visualized to ensure absence of DNA bands.

Hybridisation and probing the blot

Each blot and a nylon mesh were placed in a Hybaid cylinder tube with 18ml hybridisation buffer (500mmol/L NaH₂PO₄; 1mmol/L EDTA; 243mmol/L SDS; 151mmol/L BSA; 0.4% (v/v) H₃PO₄, pH 7.2) and incubated at 50°C for 30 minutes (pre-hybridisation). The telomere probe was ³²P labelled by adding 2µl PNK, 5pmol/L (TTAGGG)₄ oligonucleotide, 5µl 10× PNK buffer and 5µl γ³²P-ATP to an eppendorf with incubation at 37°C for 30 minutes.

The probe was heated at 80°C for 10 minutes to stop the reaction, prior to purification using the QIAquick nucleotide removal kit to remove any unincorporated nucleotides (according to the manufacturer's protocol). The DNA ladders were dCTP labelled by denaturing 15ng HMW and 5ng 1kb DNA ladders in 45µl TE buffer (10mmol/L tris-HCl, 1mmol/L EDTA, pH 7.5) at 100°C for 5 minutes. This was chilled on ice for 5 minutes before adding to a Rediprime reaction tube. The γ³²P-CTP (5µl) was added to the DNA markers, mixed, incubated at 37°C for 10 minutes then stopped with 5µl of 200mmol/L EDTA. These probed DNA markers were then purified using the QIAquick nucleotide removal kit.

The hybridisation buffer in the Hybaid cylinder tube was then replaced with the purified telomere (200µl) and DNA marker probes (5µl) in 10ml of hybridisation buffer, and left to hybridise the blot at 50°C O/N. Blots were briefly washed to remove excess labelling with 2× SSC (150mmol/L NaCl; 15mmol/L sodium citrate)/0.1% (w/v) SDS at RT with slow agitation, followed by two more washes in 1× SSC/0.1% (w/v) SDS.

Blots were covered in Saran wrap and exposed to Kodak scientific imaging film at -80°C O/N. The AlphaImager documentation system and Telometric 1.2 software were

used to measure terminal restriction fragment (TRF) lengths of telomere DNA. The mean TRF length was calculated using the following equation where OD_i is the optical density of the telomere smear at a given position on the gel and MW_i is the molecular weight at that position:

$$\Sigma (OD_i) / \Sigma (OD_i / MW_i)$$

2.3.6.3 Comet assay

The Comet assay was carried out according to the method developed by Singh *et al* (1988) with slight modifications. The assay was conducted in minimal light to prevent any DNA damage by photosensitisation, until the neutralisation stage. Treated cells, grown in 6-well plates, were placed on ice, the media was discarded and cells were rinsed once with DPBS. Chilled mincing solution (0.8× HBSS, 10% (v/v) DMSO, 20mmol/L EDTA, pH 7.5) (60µl) was added to each well and the cells were scraped from the plate and transferred to chilled eppendorfs on ice. For each sample, 10µl cell suspension were mixed with 120µl 0.6% (w/v) LMP agarose then 60µl of each cell mix were laid onto agarose pre-coated microscope slides (1% (w/v) NMP agarose). Slides were left on ice to set for 5 to 10 minutes before adding a final layer of 0.6% (w/v) LMP agarose and square coverslip on top, then left to set on ice.

Coverslips were removed and slides were then placed vertically in Wilson jars and immersed in chilled lysis buffer (2.5mol/L NaCl; 100mmol/L EDTA; 10mmol/L tris pH 10.0; 1% (v/v) triton X-100) at 4°C O/N. Slides were removed and excess buffer was wiped off, then slides were washed with TE buffer (3×) and left for 10 minutes, then placed in a horizontal gel electrophoresis tank containing chilled electrophoresis buffer (300mmol/L NaOH; 1mmol/L EDTA; pH ≥13) and incubated for 30 minutes to allow DNA unwinding. Electrophoresis was then carried out at 25V (~300mA) for 20 minutes at 4°C. Slides were washed with neutralisation buffer (0.4mol/L tris-HCl pH 7.5) (3× for 5 minutes each) then fixed in EtOH for 5 minutes and eventually air-dried at RT.

SYBR Green 1 stain (60µl) was added to the slides and overlaid with coverslips, and cells were visualised under a FITC filter (excitation 485nm; emission 530nm) using a Nikon Eclipse fluorescent microscope. DNA damage was scored using the Komet analysis software, where 50 cells were counted per slide. The mean percent tail DNA

(% tail DNA) measurement defined as the intensity of the comet tail in relation to the head was used as a measure of DNA damage.

2.3.6.4 Telomerase activity detection

Telomerase activity was measured using the TeloTAGGG Telomerase PCR ELISA kit. This photometric enzyme immunoassay amplifies telomerase-mediated elongation products by telomeric repeat amplification protocol (TRAP) reactions, and detects them by ELISA.

Preparation of cell extracts

Trypsinized cells were resuspended in media and 2×10^5 cells per sample were transferred to sterile eppendorf tubes. Cells were centrifuged at 3200g for 10 minutes at 4°C to pellet, then washed in DPBS and centrifuged again. Cell samples were kept on ice and resuspended in 200µl lysis buffer by retropipetting (3×), then incubated on ice for a further 30 minutes. Lysates were centrifuged at 11,000g for 20 minutes at 4°C to pellet cell debris and 175µl of the supernatant was transferred to sterile eppendorfs. The positive control cell extract was prepared by incubating 5×10^3 '293' cells with 1µl DNase-free RNase (DEPC treated H₂O) for 20 minutes at 37°C. The negative control cell extract was prepared by heating the '293' cell extract for 10 minutes at 85°C.

TRAP

All PCR reactions (including controls) were set up on ice containing the following: 2µl cell extract (equivalent to 2×10^3 cells); 25µl reaction mixture, made up to a volume of 50µl with UP H₂O and overlaid with 50µl mineral oil. Reactions were conducted in a DNA thermal cycler under the following conditions: 25°C for 30 minutes; 94°C for 5 minutes; 30 cycles of 94°C (30 seconds), 50°C (30 seconds) and 72°C (90 seconds); 72°C for 10 minutes. The amplified products were placed on ice after completion of the TRAP.

Hybridization and ELISA

In sterile eppendorf tubes, 5µl of each amplified product were added to 20µl of denaturation reagent and incubated at 25°C for 10 minutes. Hybridization buffer was then added and mixed by vortexing. The mixture (100µl) was transferred to each well of the precoated MP modules (fixed in a 96-well microplate) and covered with a

self-adhesive seal to prevent evaporation. The MP modules were incubated in a 37°C Hybaid oven on a medium speed platform shaker for 2 hours. The hybridization solution from every well was then discarded, wells were rinsed 3 times with 1× washing buffer (250µl volumes) for 30 seconds each, then 100µl of the anti-DIG-POD working solution (10mU/ml) (anti-DIG POD stock solution diluted with conjugate dilution buffer) was added per well. The plate was re-sealed and incubated at 25°C with medium speed agitation for 30 minutes. The anti-DIG POD solution was discarded from each well, and rinsed 5 times with 1× washing buffer, then 100µl of RT TMB substrate solution was added. The plate was sealed again and incubated at 25°C with agitation for 20 minutes, for colour development. Finally the stop reagent (100µl) was added to the wells to stop colour formation. Absorbance was then read at 450nm and 690nm (reference) wavelengths.

2.3.6.5 cDNA synthesis

The DyNAmo™ cDNA Synthesis kit was used to generate cDNA as follows: to 1µg of total RNA for each sample, 10µl of 2× RT buffer, 300ng/µl of random hexamer primers, 2µl of M-MuLV RNase H⁺ reverse transcriptase enzyme were added with RNase-free water to a final volume of 20µl. All reverse transcription reaction was performed in the hybaid PCR sprint thermal cycler at 25°C for 10 minutes, 37°C for 30 minutes, then 85°C for 5 minutes. Samples were then stored at -20°C until used for PCR amplification.

2.3.6.6 qPCR

PCR reactions were set up under a cell culture hood using filter pipette tips, autoclaved eppendorfs and sterile vials to prevent DNA contamination from other sources.

The Brilliant® SYBR® Green qPCR Core Reagent kit was used to quantify amplification of nDNA and mtDNA gene transcripts by PCR. This fluorescent-based PCR technique involves the SYBR Green dye, which fluoresces when bound to dsDNA and monitors the accumulation of PCR products in real-time. The fluorescence signal from each PCR is displayed as an amplification plot, reflecting change in fluorescence during cycling. Quantification of each PCR product is based upon cycle threshold (Ct), which is inversely proportional to log of the initial copy number. The number of cycles for each reaction to reach an arbitrary threshold fluorescence signal is considered the quantity of PCR product generated.

For the nDNA PCR, a standard curve of reference DNA comprising of 3.125 to 50ng was performed by 2-fold serial dilution in TE buffer, pH 7.4; and these were given arbitrary values of 1 to 16 in the MX4000TM software. Reactions were set up for diluted DNA samples (3ng/ μ l) are follows: 15ng template DNA; 1 \times core PCR buffer; 2mmol/L MgCl₂; 200 μ mol/L each dNTPs; 100nmol/L 36B4D primer; 100nmol/L 36B4U primer; 8% (v/v) glycerol; 3% (v/v) DMSO; 0.5 \times SYBR green; 30nmol/L 6-ROX dye; 1.25 units SureStart *Taq* DNA polymerase in a 25 μ l reaction. PCR were run in a MX4000TM multiplex quantitative PCR instrument with the following thermal profile: 95°C for 10 minutes; 40 cycles of 95°C (30 seconds), 60°C (60 seconds) and 72°C (60 seconds).

For the mtDNA PCR, a standard curve of reference DNA was comprised of 62.5 to 1ng by 2-fold serial dilution (arbitrary values of 1 to 16 in the MX4000TM software) and experimental DNA samples were diluted to 50pg/ μ l. PCR reactions were performed with the same reagent concentrations and thermal profile as detailed for nDNA, except with 250pg template DNA, 100nmol/L mt14620 primer and 100nmol/L mt14841 primer. mtDNA content was calculated from the initial template quantity values, as a ratio of the mtDNA against the nDNA PCR product values.

2.3.6.7 RT-PCR

RT-PCR of mitochondrial biogenesis gene transcripts PGC1 α and mtTFA, and the endogenous control gene, HPRT1, were performed on the StepOneTM PCR machine using SYBR® Green JumpStartTM *Taq* ReadyMix. Standard amplification curves were generated for each target and endogenous control gene of a 10-fold dilution of cDNA (1, 0.1, 0.01 and 0.001 dilutions corresponding to 50, 5, 0.5 and 0.05ng of total RNA, respectively (PGC1 α : 100, 10, 1, 0.1ng of total RNA)) to determine equal linearity between the Ct and log of input RNA and efficiency of the PCR (where slope of the standard curve ranged between -3.8 and -3.4).

Gene transcript levels for each target gene were individually determined for each sample. cDNA solutions were diluted 1:3 with TE buffer, pH 7.4 (1 μ l = 16.7ng of total RNA) and added to 100nmol/L of primers (HPRT1 and mtTFA), 12.5 μ l of ReadyMix and 1 \times ROX dye. PCR was performed as follows: 95°C for 4 minutes, 50 cycles of 95°C (30 seconds), 55 (HPRT1), 60 (mtTFA) or 62°C (PGC1 α) (1 minute), and 72°C (30 seconds). Following these cycles, a dissociation curve was generated of an increase in

temperature from 55 to 95°C for 30 seconds (sufficient PGC1 α gene expression required 2 μ l of cDNA (33ng of total RNA) and 200nmol/L of primers). All reactions were run in triplicate. No-template controls were included in every PCR. Amplification was not detected in reverse transcription minus controls for every sample, indicating no residual genomic DNA present in the extracted RNA.

The Ct values of each target gene for treated samples were normalized against untreated samples using the Pfaffl mathematical method (Pfaffl, 2001), then corrected for changes in the endogenous control gene (HPRT1). This method calculates the ratio of relative gene expression from real-time PCR efficiencies determined from the standard curve, and enables quantification of small changes in gene expression.

Gene amplification of DNA and cDNA samples were measured by SYBR green fluorescence (excitation: 492nm; emission: 520nm) and normalised against the reference ROX dye (excitation 585nm; emission: 610nm), to account for fluorescent variations between wells of the same replicate. The dissociation curve was used to determine true amplification of the product, where melting of products resulted in a drop in fluorescence. This temperature corresponded to the desired amplicon.

2.3.6.8 BigDye DNA sequencing

PCR products were purified using the MinElute® PCR Purification kit. Buffer PBI (100 μ l) was added to 20 μ l of a PCR product, mixed, then applied to a MinElute column and centrifuged at 11,000g for 1 minute. The flow-through was discarded and 750 μ l Buffer PE was added to the column and centrifuged again at 11,000g for 1 minute. The column was additionally centrifuged (11,000g) for 1 minute to ensure the removal of residual buffer. Buffer EB (10 μ l) was added onto the centre of the column, placed into a sterile 1.5ml eppendorf, incubated for 1 minute at RT, and then centrifuged at 11,000g for 1 minute to recover the purified PCR product.

The purified PCR product was quantified using the Quant-iT™ PicoGreen® dsDNA assay kit (2.3.5.2). Each sample was diluted to 10ng in 8 μ l of TE buffer, pH 7.4 and PCR primers were diluted to 1pmol/ μ l (total 10 μ l) then underwent PCR, Big-Dye incorporation, purification and sequencing by PNAFL, Hodgkin Building, University of Leicester.

2.3.6.9 Agarose gel electrophoresis

Real-time PCR products were run on agarose gels to determine the size of the PCR product. A 2% (^{w/v}) agarose gel was made in 1× TAE buffer. BlueJuice™ gel loading buffer (4μl) was added to each PCR product sample (36μl) and the mixture loaded in each well. DNA ladder markers (HMW and Hyperladder V) were loaded into the outer 2 wells of the gel and electrophoresis was conducted for 1 hour at 70V. Images of the DNA bands were taken using the AlphaImager gel documentation system.

2.3.7 Data analysis and statistical testing

The relative quantification of mitochondrial biogenesis gene transcripts was calculated using the Pfaffl mathematical method. DNA sequencing data of PCR products was analysed using the Chromas (version 1.45) software.

Data was represented as mean and standard error of the mean (SEM). Comparisons between dose treatments or groups were by One-way ANOVA with a Dunnett's or Bonferroni multiple comparisons post-test, using the GraphPad Prism® 5 software. A p-value <0.05 was considered statistically significant.

CHAPTER THREE

Establishing a Human Vascular Smooth Muscle Cell Model to Study the Ageing Effects of Angiotensin II

Chapter 3.0: Establishing a human vascular smooth muscle cell model to study the ageing effects of Angiotensin II

3.1 Background

3.1.1 Functional and structural characteristics of VSMC in vitro and in vivo

VSMC are an important component of the vasculature, forming the medial layer of blood vessels. Together with matrix components their main function is contraction and relaxation which alters the luminal diameter of vessels in order to maintain blood pressure. They also exhibit a role in vascular growth, development, structural remodelling and repair of injury by increasing the rate of proliferation, migration and production of extracellular matrix (ECM) components (Owens *et al.*, 2004). The different functions of VSMC arise from their broad diversity in phenotype, ranging from contractile to synthetic. Different phenotypes of VSMC maybe observed within the same vessel and between different vessels (Frid *et al.*, 1997; Hao *et al.*, 2003). A specific phenotype is displayed in response to complex interactions of environmental stimuli, and changes in any one of these can cause a shift, known as ‘phenotypic modulation’ (Owens *et al.*, 2004).

Contractile smooth muscle cells (SMC) are elongated spindle-shaped cells containing a large proportion of contractile filaments within the cytoplasm (Chamley-Campbell *et al.*, 1979), whereas synthetic SMC have a cobblestone appearance (epithelioid), contain numerous organelles involved in protein synthesis and display higher proliferation and migratory rates than contractile SMC (Hao *et al.*, 2003). The proteins involved with SMC contraction are commonly used as markers to differentiate between phenotypes. However, no marker is specific for a particular phenotype, and variations in the level of expression of known markers are the most useful markers. The gradual decline in contractile protein markers (α -smooth muscle actin; desmin; smooth muscle-myosin heavy chain (SM-MHC); smoothelin A/B) that are highly expressed in contractile SMC, is characteristic of a more synthetic phenotype (Owen, *et al.*, 2004; Rensen, *et al.*, 2007). Heterogeneity in SMC morphology and phenotype has also been studied *in vivo*. The analysis of SMC isolated from bovine pulmonary arterial media illustrated four distinct subpopulations of SMC. The preluminal media was composed of small,

irregular-shaped cells expressing no contractile protein markers; the inner-middle media was composed of elongated spindle-shaped cells, circumferentially arranged and expressing the common contractile proteins; and the outer media was composed of large spindle-shaped cells oriented longitudinally, and thin spindle-shaped cells orientated circumferentially in compact clusters (Frid, *et al.*, 1997).

3.1.2 Circulating Ang II concentrations

Ang II is a multifunctional octapeptide hormone and is a dynamic component of the renin-angiotensin system (RAS), synthesized by plasma and local tissues (Levy, 2005). The effect of Ang II in tissues and cells varies. The interstitial fluid has higher levels of Ang II than in plasma, which has been studied by analysis with microdialysis probes implanted in the renal cortex of normal rats. The renal interstitial fluid Ang II concentrations were 3 to 5 pmol/ml and the corresponding plasma Ang II concentrations were <1 pmol/ml (Nishiyama *et al.*, 2002). Increased Ang II levels have been observed in Ang II-infused hypertensive models, where a sustained elevation of circulating Ang II leads to the accumulation of intrarenal Ang II (Von Thun *et al.*, 1994). Even though low Ang II concentrations are observed *in vivo* it is continuously synthesized, therefore to analyse Ang II effects *in vitro* much higher concentrations are generally used (up to micromolar concentrations), as it tends to be broken down rapidly. For example, Ang II treatment ranging between 10^{-8} and 10^{-6} mol/L stimulated a dose-dependent increase in cell number and migratory activity of human coronary artery SMC after 24 hours, whereas no differences were observed at lower concentrations (Kohno *et al.*, 2000).

3.1.3 Cellular responses mediated by Ang II in VSMC

The physiological effects mediated by Ang II are important in regulating VSMC function, such as modulating cell growth, apoptosis, influencing cell migration and ECM deposition, stimulating the generation of other vasoconstrictors and growth factors (Touyz and Schiffrin, 1999); as well as having a role in regulating blood pressure, plasma volume and activity of the sympathetic nervous system. Ang II affects VSMC growth by autocrine growth mechanisms, mainly initiated via the AT₁R. It stimulates proliferation (also known as hyperplasia; increase in cell number), hypertrophy (increase in cell size without change in DNA content) and displays anti-apoptotic effects (Berk, 2001). These effects occur at different stages of the cell cycle (**figure**

2.1). However, Ang II is also reported to promote apoptosis during disease progression (Taniyama and Griendling, 2003).

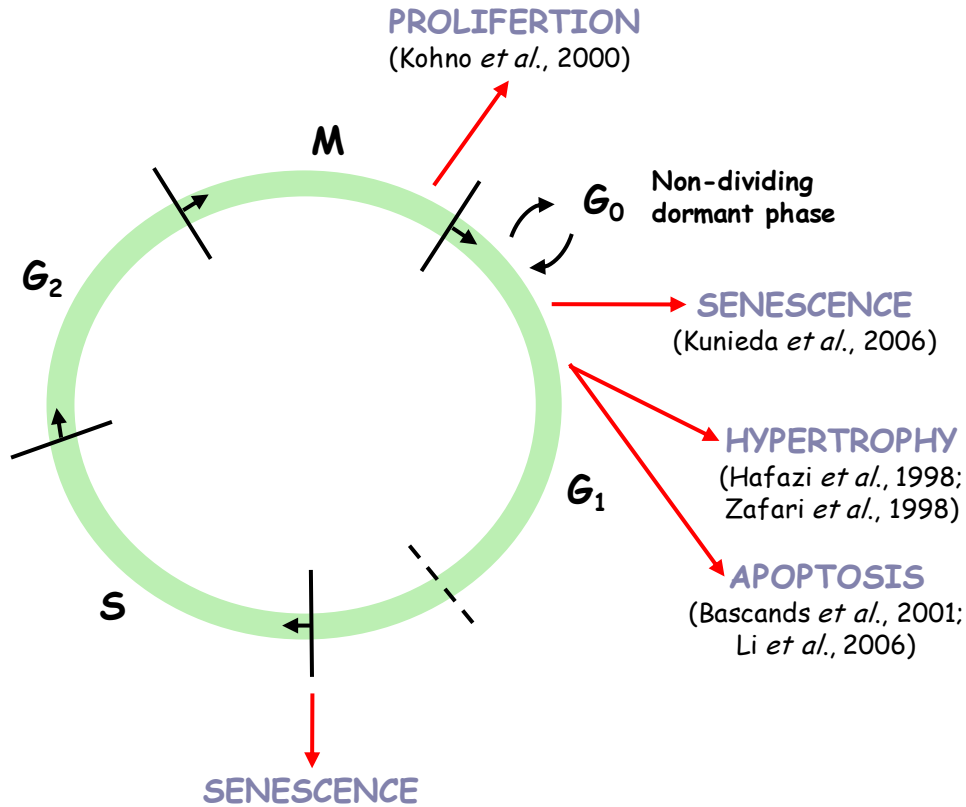


Figure 3.1 Modulation of the cell cycle in response to Ang II stimulation. Complete progression through the cell cycle results in cell proliferation. Inhibition of the G₁-phase by CDKI expression can lead to hypertrophy or induce apoptosis, depending upon the length and concentration of Ang II exposure. Halting the cell cycle phase at this stage or just after the S-phase can initiate senescence in cells.

The pleiotropic actions of Ang II are mediated via the activation of protein kinases, synthesis of growth factors, and stimulation of low level ROS generation.

The effects of Ang II are mediated by binding to the highly specific plasma membrane receptors, AT₁R and AT₂R. The AT₁R is extensively expressed in the vasculature, heart, adrenal glands, kidney and liver; whereas the AT₂R is mainly expressed in foetal tissue and rapidly declines after birth with a relatively low abundance expressed in adult tissues (characteristics of these receptors are fully summarized in **table 1.2**). Presence of the AT₁R has been extensively confirmed in SMC of human (Kohno, *et al.*, 2000), rodent (Lassègue *et al.*, 1995) and porcine (Itazaki *et al.*, 1993) origin. The AT₂R has only been highly detected in VSMC of atherosclerotic lesions (Sales *et al.*, 2005), those derived from the uterine artery (Sullivan *et al.*, 2005) and in the vascular wall of blood

vessels in human pituitary adenomas (Pawlikowski, 2006). Both receptors therefore play a vital role in modifying VSMC function and the activation and the up-regulation of these receptors is dependent upon different cell-signalling mechanisms. Ang II predominantly mediates its effects via the AT₁R, which is associated with growth, inflammation and vasoconstriction in vessels; whereas the AT₂R is associated with apoptosis, vascular injury and vasodilation (Touyz and Schiffrin, 2000). The expression of AT₁R has been shown in part, to regulate the effect of Ang II on target tissue. Increased Ang II exposure stimulated an increase in AT₁R activity in cells whereas chronic Ang II caused a down-regulation (Lassègue, *et al.*, 1995).

Pharmacological inhibitors of Ang II receptors such as angiotensin receptor blockers (ARB) have been used to prevent the effects mediated by Ang II *in vivo* and are therefore used in the treatment of hypertension, diabetes and various other CVD. Common examples include Losartan, Candesartan and Valsartan. E3174 is the active metabolite of Losartan which effectively blocks Ang II induced responses in VSMC, *in vitro* (Sachinidis, *et al.*, 1993). However, it has also been shown to be a competitive antagonist of the thromboxane A₂/prostaglandin endoperoxide receptor induced contractions in canine coronary arteries. This response has been proposed to contribute to the blood pressure lowering effects induced by Ang II receptor blockade (Li *et al.*, 1997).

3.2 Aims

- To investigate mechanisms of CVD development at the cellular and molecular level, *in vitro* studies are often performed by using cell culture systems/models to understand the effects of mediators and modifiers of these processes. The phenotypic changes of VSMC can be investigated in this way to model what may be happening *in vivo*. To confirm that VSMC isolated from adult saphenous vein explants were authentic SMC, characteristics of morphology, growth and contractile protein markers typical of SMC were investigated.
- To verify the presence of Ang II receptors in hVSMC, the protein expression of human AT₁R and AT₂R were determined via Western blotting analysis.
- To establish the effects of Ang II on VSMC growth. The rate of proliferation, viability and cytotoxicity were assessed by the measurement of population doublings (PD), trypan blue exclusion and mitochondrial activity over a range of Ang II concentrations. The effect of the AT₁R antagonist E3174 exposure on hVSMC was also assessed, to determine any cytotoxicity.

3.3 Experimental Approach

3.3.1 Cell culture

hVSMC were isolated from human saphenous vein explants, taken from varicose vein surgery. Cells were maintained in culture in media containing 10% (v/v) FCS and were rendered quiescent in media containing 0.5% (v/v) FCS, as described in section **2.3.1.1**. Cells were only used between passages 2 to 9.

HDF cells were isolated from human skin biopsies of the buttock region and established as a cell line by Paulene Quinn, Department of Cardiovascular Sciences, University of Leicester, UK. They were used to determine the expression of α -smooth muscle actin. Cells were maintained in culture as described in **2.3.1.1** and were not used beyond passage 12.

PD counts were performed to assess the proliferation of hVSMC. Cells were seeded at 1×10^4 cells per well in 6-well plates, until confluence was reached. Multiple Ang II exposures with 10^{-8} , 10^{-7} and 10^{-6} mol/L were conducted on alternate days and on the following days when cells were counted and re-plated. Single Ang II (10^{-8} mol/L) and E3174 (10^{-5} mol/L) treatments were conducted in cells rendered quiescent for 24 hours in media containing 0.5% (v/v) FCS, at 37°C. Cells were harvested by trypsinization, resuspended in 0.5ml of fresh media and counted using a haemocytometer. PD and CPD were calculated as described in section **2.3.1.2**.

3.3.2 Cellular viability

hVSMC viability was assessed using the trypan blue exclusion method as described in section **2.3.1.5**. Cells were seeded at 5×10^4 cells per well in clear 6-well plates and incubated at 37°C. Near confluent cells were treated for 24 hours at 37°C between 10^{-8} and 10^{-4} mol/L E3174, and cells were rendered quiescent prior to Ang II (10^{-9} to 10^{-5} mol/L) treatment. Following treatment, cells were trypsinized and resuspended in a known volume of media and an equal portion was then further diluted 1:1 with 0.4% (w/v) trypan blue solution. Transparent and blue-stained cells were counted for each of the different doses using a haemocytometer.

The MTT colorimetric assay was also used to evaluate cell viability and proliferation. hVSMC were seeded at 1×10^3 cells per well in clear 96-well microplates and grown to confluence for 3 to 4 days in media containing 10% (v/v) FCS. The media was changed to PR⁻ complete media 24 hours prior to treatment. H₂O₂ exposure over a range of concentrations was performed by a 2-fold serial dilution of a 2mmol/L stock solution, for 2 hours at 37°C. Cells were rendered quiescent then placed back into media containing 10% (v/v) FCS before exposure to Ang II. The range of Ang II concentrations was administered as a series of successive 1:10 dilutions using an initial stock concentration of 10^{-4} mol/L, and incubated for 24 hours at 37°C. The MTT assay was then conducted as described in section **2.3.1.5**.

3.3.3 Cell imaging

Cellular growth, appearance and structural morphology were determined visually by microscopy. Early passage hVSMC were grown to ~70% confluence in T75cm² NuncTM flasks. Phase contrast microphotographs were taken at $\times 40$ and $\times 100$ magnifications using a colour camera attached to a Nikon inverted trinocular phase contrast microscope (model TMS-F).

Expression of the contractile protein α -smooth muscle actin was assessed by immunofluorescence staining. hVSMC and HDF were seeded on sterile round glass coverslips (immersed in IMS then air-dried for 30 minutes to sterilize) at 2×10^4 cells per well in 6-well plates. Cells were grown to ~60% confluence in media containing 10% (v/v) FCS and then rendered quiescent for 7 days, as detailed in section **2.3.1.1**; this reduced the rate of cellular growth and function. Cells were then fixed and fluorescently labelled for α -smooth muscle actin as described in **2.3.2.2**. Fluorescent images were taken under a FITC filter at $\times 400$ magnification using a Nikon Eclipse E400 fluorescent microscope.

3.3.4 Western blotting

Protein expression in hVSMC and Hep G2 cells were determined by Western blotting (section **2.3.6.1**). The appropriate blocking solution, primary and secondary antibody dilutions for the specific labelling of proteins were performed as detailed in **table 2.12**, **2.13** and **2.14**.

3.3.4.1 Human smooth muscle myosin protein expression

To assess whether hVSMC exhibited a contractile phenotype characteristic of SMC, the protein expression of smooth muscle myosin was determined. RIPA buffer was used to extract membrane-bound proteins (section 2.3.5.6) from cells grown to confluence in media containing 10% (v/v) FCS and those rendered quiescent in media containing 0.5% (v/v) FCS. Protein samples (30µg protein per sample) were separated on 7% resolving gels under reduced and denaturing conditions. Membranes were blocked with 5% (w/v) milk/TBST overnight at 4°C before antibody labelling (**table 2.13**). Equal protein loading was confirmed by labelling for α -tubulin protein expression using 5% (w/v) milk/TBST blocking solution (**tables 2.12 and 2.14**).

3.3.4.2 Human Ang II receptor subtype protein expression

The human Ang II receptor subtype protein expression of AT₁R and AT₂R, were analysed in hVSMC and Hep G2 cells. RIPA buffer was used to extract membrane-bound proteins from hVSMC grown in media containing 10% (v/v) FCS and those rendered quiescent. Hep G2 cells were only grown in media containing 10% (v/v) FCS. Protein samples (20/40µg protein per sample for AT₁R/AT₂R respectively) were separated on 8% resolving gels under non-reduced and denaturing conditions. Membranes were blocked with 5% (w/v) BSA/TBST overnight at 4°C prior to antibody labelling (**table 2.13**). Equal protein loading was confirmed by labelling for α -tubulin protein expression for AT₁R labelled membranes, and β -actin for AT₂R labelled membranes using 5% (w/v) BSA/TBST as the blocking solution for both loading control antibodies (**tables 2.12 and 2.14**).

3.4 Results

3.4.1 Structural morphology of hVSMC

VSMC used in this study were obtained from adult human saphenous vein explants and were established as primary cell lines. To confirm these cells were SMC, characteristics of morphology, growth pattern and cytoskeletal protein expressions (α -smooth muscle actin and smooth muscle myosin) were investigated.

Confluent, early passage hVSMC appeared elongated, spindle-shaped and displayed the typical hill-and-valley growth arrangement described for SMC as indicated by the direction of arrows in **figure 3.2A** and **B**. Under higher magnification (**figure 3.2B**) these cells had visible granular perinuclear regions and an oval-shaped nucleus containing two or more smaller nucleoli.

hVSMC in culture were distinguished from other types of cell by labelling for the contractile protein marker α -smooth muscle actin, which selectively recognises the α -isoform of actin and does not react with EC and fibroblasts. Early passage hVSMC (passage 5) exhibited positive immunofluorescence staining of α -smooth muscle actin as shown in **figure 3.3A**. Cell staining was achieved by optimizing antibody dilutions and control treatments in both types of cells (anti- α -smooth muscle actin antibody only; FITC-labelled conjugate only; and neither antibody). None of these controls resulted in any positive staining.

The actin stained filament bundles were orientated in a bipolar manner from the nuclei, which is distinctive of spindle-shaped SMC (Nakamura *et al.*, 1998). No nuclear or cytoplasmic staining was observed between the filaments. HDF predominantly showed negative staining, but some positive staining was observed in a small number of cells (~20%; **figure 3.3B**). This suggested the presence of myofibroblasts, which share many typical characteristics of SMC, such as contractility, production of ECM components, and the expression of many common protein markers (i.e. α -smooth muscle actin, SM-MHC and calponin). The two cells can be distinguished by the quantity of protein marker expression, as SMC have much higher expression levels of α -smooth muscle actin than myofibroblasts (Owens *et al.*, 2004), as observed in **figure 3.3**.

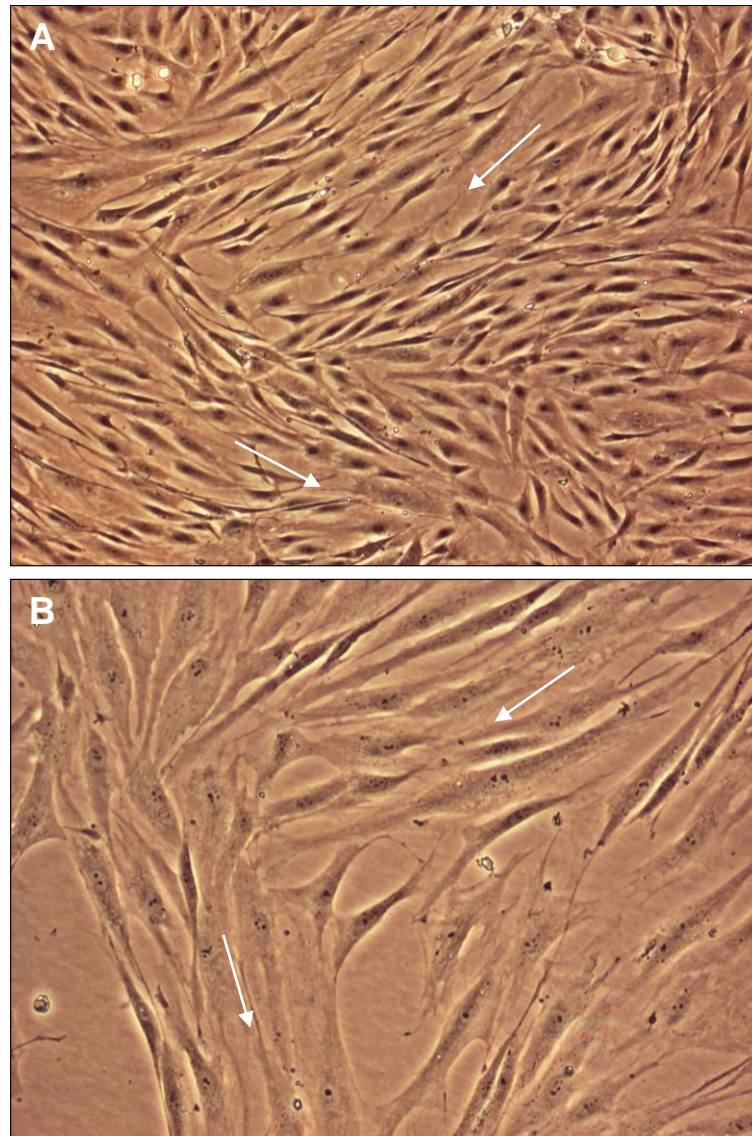


Figure 3.2 hVSMC exhibit typical 'hill-and-valley' growth characteristics. Phase contrast photomicrographs were taken of early passage hVSMC grown in media containing 10% (v/v) FCS. **A**, $\times 40$ magnification **B**, $\times 100$ magnification; arrows indicate the direction of cell growth.

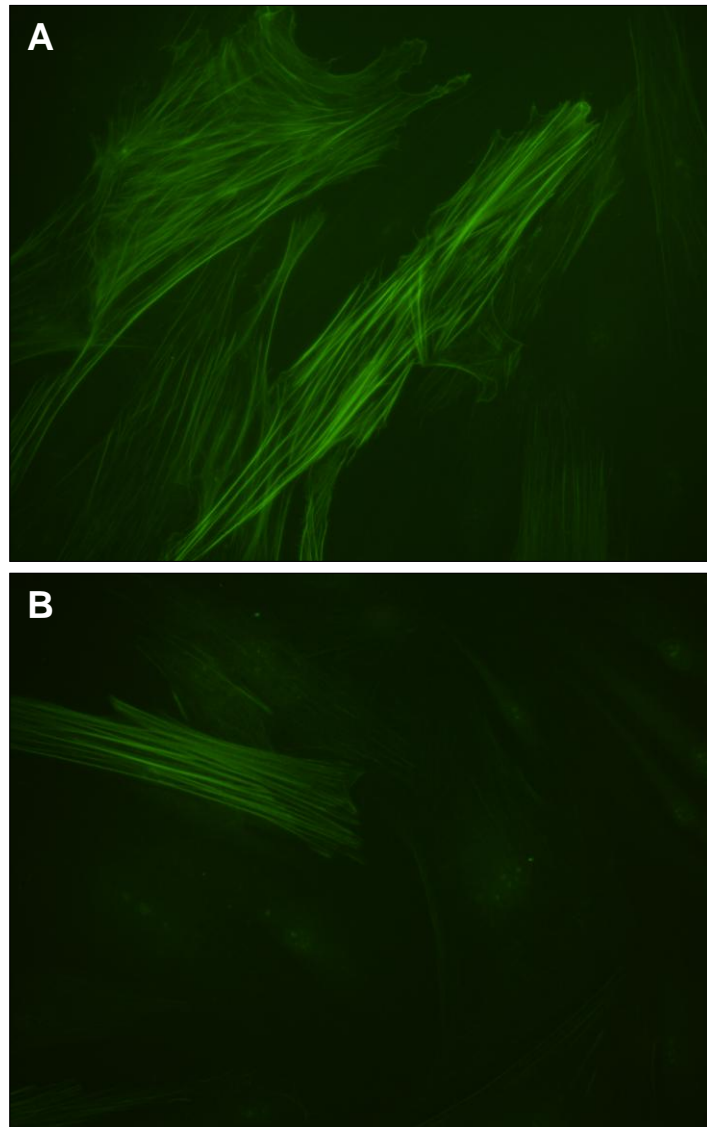


Figure 3.3 Characterization of hVSMC by immunofluorescence staining for α -smooth muscle actin. Sub-confluent cells were rendered quiescent for 7 days in media containing 0.5% (v/v) FCS (hVSMC) and 1% (v/v) FCS (HDF). Cells were labelled with anti- α -smooth muscle actin antibody (1:600) followed by a FITC conjugate (1:400) detection. **A**, hVSMC positively labelled for α -smooth muscle actin. **B**, Low levels observed in HDF. All images were taken at $\times 400$ magnification.

hVSMC in media containing 10% (v/v) FCS displayed low levels of α -smooth muscle actin (data not shown). Active proliferation has been suggested to cause a switch in actin expression (Gabbiani *et al.*, 1984). Thus cells were rendered quiescent to slow the rate of proliferation and allow for labelling of the α -isoform.

Consistent with the expression of α -smooth muscle actin, intense expression of SM-MHC was observed by Western blotting in proliferating cells but not in quiescent hVSMC (**figure 3.4**). This further indicated these cells exhibited a contractile phenotype. However, no detectable smooth muscle myosin light chains (15-26kDa) were observed within hVSMC.

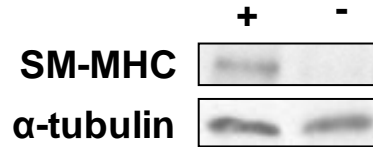


Figure 3.4 hVSMC exhibit SM-MHC protein expression. Cells grown in media containing 10% (v/v) FCS (+) and following quiescence in media containing 0.5% (v/v) FCS (-) for 24 hours. Cells were harvested in RIPA buffer. Western blot shows a clear distinct band corresponding to SM-MHC at \sim 200kDa, and α -tubulin (loading control) protein expression in 30 μ g protein lysate loaded per sample.

3.4.2 Assessment of Ang II receptor subtype expression

The expression of human AT₁R and AT₂R was determined in actively proliferating hVSMC and those rendered quiescent for 24 hours once confluence was reached. Quiescence was induced by serum deprivation, which is considered to arrest all cells in the G₀-phase of the cell cycle, due to the absence of growth stimulatory factors. This effect on cells is also reported to upregulate AT₁R (Nickenig and Murphy, 1994), and is important in measuring the specific affects induced by Ang II *in vitro*. Western blotting was performed using antibodies raised against these receptor subtype proteins to determine their expression in hVSMC, and to establish whether these cells would be likely to respond to Ang II. Equal quantity of protein loading was confirmed by uniform expression of α -tubulin. Hep G2 cells did not express the α -tubulin protein and therefore detection of β -actin was used to determine equal protein loading of samples.

All hVSMC grown in media containing 10% (v/v) FCS and those rendered quiescent for 24 hours (in media containing 0.5% (v/v) FCS) expressed different glycosylated forms of the AT₁R protein (**figure 3.5**). The most intense immunoreactive band was observed at 60kDa which corresponds to the mature glycosylated form of the receptor (Desarnaud, *et al.*, 1993). This showed the substantial presence of the fully native form of the AT₁R in the cell model, irrespective of the FCS content in media. Less intense bands were observed in quiescent cells at lower molecular masses of \sim 40 and 45kDa which corresponds to the presence of deglycosylated AT₁R. This maybe explained by the

slower protein turnover that occurs in the absence of growth and stimulatory factors from FCS (Barker, *et al.*, 1993). These protein bands were not expressed in the cells grown in media containing 10% (v/v) FCS.

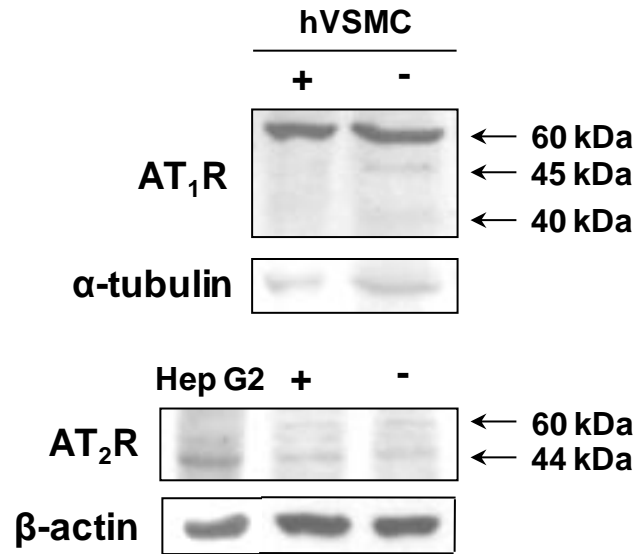


Figure 3.5 Ang II receptor subtype protein expression in hVSMC. Cells were grown in media containing 10% (v/v) FCS (+) and rendered quiescent in media containing 0.5% (v/v) FCS (-) for 24 hours. Cells were harvested in RIPA buffer. Western blots show human AT₁R and α-tubulin (loading control) protein expression in 20μg protein loaded per sample, whereas 40μg protein was loaded per sample to determine human AT₂R and β-actin (loading control) protein expression. Hep G2 cells were used as a positive control for AT₂R expression.

Low levels of AT₂R protein expression were detected in cells grown in media containing 10% (v/v) FCS and in reduced serum. The molecular weight of the glycosylated form of this receptor varies between cell types; therefore the expression of AT₂R was confirmed by using Hep G2 cells as a positive control. A single intense band at ~44kDa corresponded to the glycosylated native form of the AT₂R in Hep G2 cells, whereas much less intense bands at ~45 and 60kDa were observed in hVSMC; this did not differ according to the FCS content of cells. These data agree with literature suggesting adult human cells express relatively low levels of AT₂R (Matsubara *et al.*, 1998).

Although receptor expression was not quantitative, the predominant expression of AT₁R compared with AT₂R indicates that Ang II favours AT₁R activation. However, the expression of both subtypes may suggest the presence of AT₁R/AT₂R heterodimers within these cells.

3.4.3 Cell proliferation and viability following Ang II treatment

hVSMC growth and survival in the presence of Ang II was assessed over a range of concentrations in order to establish suitable Ang II concentrations that would not induce extensive cell death after single and multiple treatments. The trypan blue exclusion method was used to measure the viability of hVSMC following a single Ang II treatment.

A high percentage of cells excluding the trypan blue stain was maintained in untreated cells and even after exposure to Ang II for 24 hours (~80 to 90%), indicating no significant effect on hVSMC viability over a range of concentrations (**table 3.1**). However a decrease of 25 to 30% was observed with exposure to the highest Ang II concentration (10^{-5} mol/L) suggesting considerable cell damage or death. This concentration is very high and non-physiological, but indicates that high concentrations of Ang II could be cytotoxic.

Table 3.1 Trypan blue exclusion of hVSMC exposed to Ang II

<i>Ang II concentration (mol/L)</i>	<i>Trypan blue excluded cells (%)</i>
Control	90.8 ± 3.6
10^{-9}	85.7 ± 7.2
10^{-8}	81.8 ± 7.5
10^{-7}	84.8 ± 3.7
10^{-6}	90.4 ± 3.3
10^{-5}	63.5 ± 6.2*

Cells were rendered quiescent prior to treatment with a range of Ang II concentrations for 24 hours. Cells were harvested by trypsinization, resuspended in fresh media, diluted 1:1 with 0.4% trypan blue solution and counted using a haemocytometer. Values are mean±SEM; n=4 (10^{-5} mol/L; n=3) (*p<0.05 compared with control).

PD cell counts were performed to determine the effect of Ang II on the rate of hVSMC proliferation following multiple treatments over time. Ang II concentrations at both 10^{-8} and 10^{-7} mol/L induced a slight increase in the rate of hVSMC proliferation throughout the time period shown in **figure 3.6**, although this did not reach statistical significance in either case. The highest PD rate at each of the time points measured was observed with treatment at 10^{-8} mol/L. No significant difference was observed with 10^{-6} mol/L as the rate of proliferation was observed to be relatively similar to the untreated cells, which suggested a balance between cell death and proliferation.

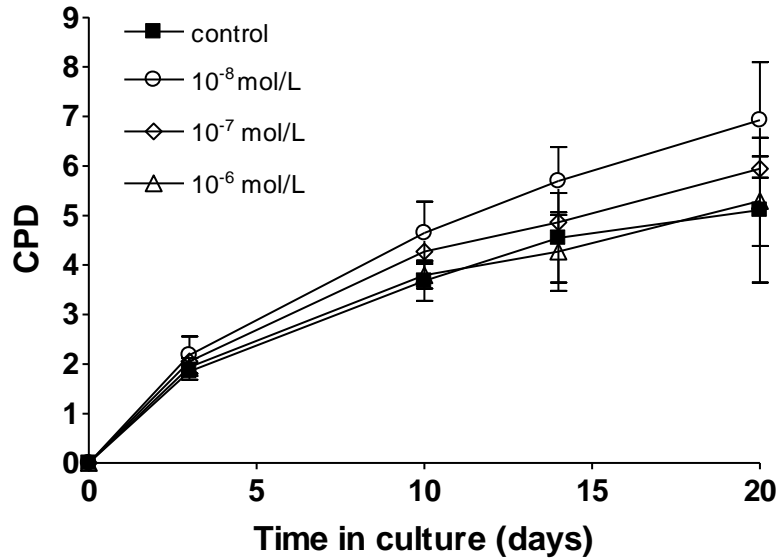


Figure 3.6 Successive Ang II treatment stimulates cell proliferation. Growth curves were determined by sub-culturing hVSMC treated with a range of Ang II concentrations at the indicated time points. Cells were treated in media containing 10% (v/v) FCS on alternate days and on the following days when cells were re-plated at 1×10^5 cells per well in 6-well plates. Cells were detached by trypsinization and counted using a haemocytometer. Values represent mean \pm SEM; $n=3$ (data did not reach statistical significance). CPD, cumulative population doubling.

A slight increase in PD after 24 hours was also observed in quiescent cells following single Ang II treatments of low concentration. Concentrations of 10^{-9} and 10^{-8} mol/L augmented the mean PD of hVSMC (1.27 ± 0.17 and 1.20 ± 0.12 respectively) compared with untreated cells (0.79 ± 0.15) (data did not reach statistical significance). Over 4 and 24 hours Ang II exposure, no substantial difference in protein content was detected (data not shown). This indicated that Ang II did not induce a strong hypertrophic response within these cells.

Both proliferation and viability were also investigated within the same set of hVSMC using the MTT assay, which is considered a measure of cellular function or activity. The MTT assay specifically measures mitochondrial succinate dehydrogenase (complex II) activity, whereby living cells convert MTT into a blue-coloured formazan product (Mosmann, 1983). The quantity of formazan product produced is an indication of cell proliferation, viability or cytotoxicity, or even mitochondrial function.

Sensitivity of the MTT assay can be affected by various parameters (Denizot and Lang, 1986) therefore preliminary experiments were conducted to establish a reliable method

for the measurement of MTT activity in hVSMC. Cells were cultured in RPMI 1640 PR⁻ media and treatment agents were diluted in the same basal media to avoid any interference with the spectral properties of the formazan product. Cell treatment was also performed in PR⁻ media containing 10% (v/v) FCS prior since no MTT activity was detected in quiescent cells.

MTT activity was only detected in the presence of cells (**figure 3.7A**) as no absorbance was detected from the clear plastic 96-well microplates (blank) or cell media alone. The positive control of a high concentration of H₂O₂ (1mmol/L) caused a significant reduction in MTT activity indicating cytotoxicity and/or mitochondrial damage.

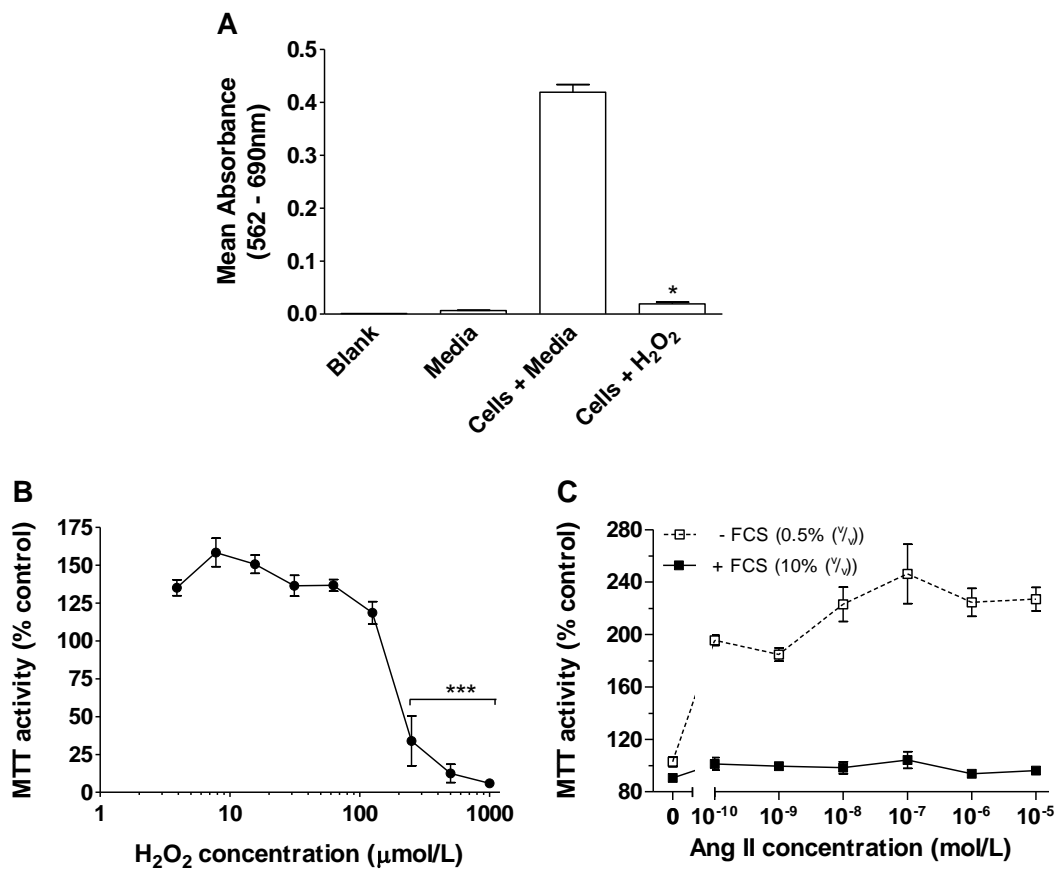


Figure 3.7 hVSMC proliferation and cytotoxicity determined by MTT activity. **A**, MTT activity was detected in proliferating hVSMC. H₂O₂ treatment (1mmol/L) for 2 hours induced cytotoxicity. Bars represent mean+SEM; n=8 (*p<0.05 compared with cells + media). **B**, Dose-dependent reduction in MTT activity following H₂O₂ treatment for 2 hours. A significant reduction was observed with concentrations $\geq 250\mu\text{mol/L}$. Values represent mean±SEM; n=7 to 8 (***p<0.001 compared with control (100%)). **C**, Ang II stimulated proliferation in hVSMC. Quiescent cells were placed in media containing 10% (v/v) FCS prior to exposure to a range of Ang II concentrations for 24 hours. Ang II stimulation of cells grown continually in media containing 10% (v/v) FCS did not change MTT activity. Values represent mean±SEM; - FCS: n=6 (p<0.01 for all doses compared with control); + FCS: n=8 (data did not reach statistical significance).

Cells treated over a range of H₂O₂ concentrations displayed changes in MTT activity, as a sigmoidal response was observed with increasing concentration. High concentrations of H₂O₂ ($\geq 250\mu\text{mol/L}$) caused a significant reduction in MTT activity indicating cytotoxicity and/or mitochondrial damage or dysfunction. Relatively low H₂O₂ concentrations of $<100\mu\text{mol/L}$ stimulated an increase in MTT activity relative to untreated cells (**figure 3.7B**), suggesting the stimulation of mitochondrial activity (and that cells remained viable when exposed to these concentrations).

Ang II has been shown to accelerate the rate of hVSMC proliferation (Touyz and Schiffrin, 2001; Wang *et al.*, 2005). Does it also upregulate or stimulate cellular metabolism, or is there any evidence of cell proliferation or cytotoxicity using the sensitive MTT method? FCS within cell media has numerous growth promoting factors which influence cellular mechanisms. MTT activity was therefore measured in Ang II treated cells in media containing 10% (v/v) FCS and those rendered quiescent (**figure 3.7C**). Quiescent cells placed back into media containing 10% (v/v) FCS prior to Ang II exposures, showed a significant concentration-dependent increase in MTT activity of between 2 to 2.5-fold compared to cells exposed to media containing 10% (v/v) FCS alone. The maximal response was observed with 10^{-7} mol/L. An overall minimal response was observed in cells within media containing 10% (v/v) FCS indicating no significant effect on MTT activity with Ang II exposure. No MTT activity was detected in cells exposed to Ang II after both serum deprivation and when treatment was conducted in media containing 0.5% (v/v) FCS (data not shown). These cells still remained adhered to the wells when viewed under a light microscope; however they were not undergoing proliferation as MTT activity was very low.

Cellular growth responses mediated by Ang II are primarily via AT₁R activity (Kohno *et al.*, 2000). A suitable concentration of the AT₁R antagonist E3174 was therefore investigated in order to study the effects of Ang II in the hVSMC model. The trypan blue exclusion method was used to assess any cytotoxic effects following just a single exposure of E3174. The effect on the rate of proliferation was determined by PD counts. Cells excluded trypan blue when exposed to a range of E3174 concentrations for 24 hours (**table 3.2**), indicating no detectable cytotoxic effect. A cellular viability of $\geq 95\%$ was observed over the whole range of concentrations and there was no difference compared with the untreated control cells. This indicated that a relatively high

concentration of E3174 could be used for up to a period of 24 hours without causing cytotoxicity in experiments or attempting to inhibit AT₁R of hVSMC.

As E3174 did not induce any loss in cell viability over the range of concentrations tested, treatment at a relatively high dose of 10⁻⁵ mol/L over a period of 24 hours was performed to establish whether there was any effect on PD. Quiescent cells treated with E3174 displayed a mean PD of 0.57 ±0.25 which was a 28% reduction when compared to untreated cells (0.79 ±0.28); of 3 replicates (data was not statistically significant).

Table 3.2 Trypan blue exclusion of hVSMC exposed to E3174

<i>E3174 concentration (mol/L)</i>	<i>Trypan blue excluded cells (%)</i>
Control	97.8 ± 0.7
10 ⁻⁸	96.7 ± 1.0
10 ⁻⁷	97.6 ± 0.9
10 ⁻⁶	97.5 ± 0.9
10 ⁻⁵	96.8 ± 0.6
10 ⁻⁴	95.0 ± 1.6

Confluent cells were exposed to a range of E3174 concentrations for 24 hours. Cells were then harvested by trypsinization, resuspended in fresh media, diluted 1:1 with 0.4% trypan blue solution and counted using a haemocytometer. Values are mean±SEM; n=5 (data did not reach statistical significance).

On treatment with Ang II for 24 hours at 10⁻⁸ mol/L, the population doubled (1.06 ±0.11). This was reduced slightly to 0.85 ±0.18 when pre-incubated with E3174 for 1 hour prior to Ang II (n=3; data was not statistically significant). This suggested that E3174 inhibited some of the Ang II induced proliferative response in hVSMC.

3.5 Discussion

The aim of the work described in this chapter was to establish a hVSMC model to assess the effects induced by the multifunctional vasoactive agent Ang II, upon cell cycle regulation (chapter 4.0 and 5.0) and mitochondria (chapter 6.0).

3.5.1 Morphological characteristics of hVSMC

SMC display a diverse array of phenotypes which enable blood vessels to attain flexibility in order to perform efficiently under physiological and pathological conditions. Phenotypes range from contractile to synthetic which determine the functions and characteristics expressed by the population of cells. The contractile phenotype is essential in maintaining vascular tone and stability, however in response to injury these cells can undergo proliferation, migration and induce ECM production, enabling them to adopt a different phenotype. The capability to undergo phenotypic modulation in response to changes in the local environment is an unusual property of SMC which is dependent upon the required function, and can therefore pose a problem when studied as a cellular model. In this chapter, morphology, proliferation and protein marker expression were assessed in the hVSMC model to establish the SMC phenotype prior to any treatment with Ang II.

All human saphenous vein derived SMC cultured between passages 2 to 9 were elongated and spindle-shaped in appearance; this was maintained after numerous sub-cultures. These SMC exhibited a typical hill-and-valley growth arrangement *in vitro* when near confluence was reached, which has also been described for other sources of human SMC (Touyz *et al.*, 2002) and those derived from other species (Christen, *et al.*, 1999; Frid, *et al.*, 1997; Nakamura *et al.*, 1998). The majority of these cells had oval-shaped nuclei containing small multiple nucleoli which has been previously described for spindle-shaped VSMC in culture (Chamley-Campbell *et al.*, 1979). The structural appearance was compared to HDF which had a similar elongated-shape but differed by the irregular growth pattern exhibited and overlapping displayed at confluence. HDF nuclei were much larger in size but also contained several prominent nucleoli.

Expression of contractile protein markers is commonly determined to confirm a more definitive SMC phenotype and was therefore used here. A high expression of α -smooth muscle actin after prolonged serum deprivation was observed in hVSMC, displaying the typical stress fiber-like organization. These were orientated parallel to the long axis of the cells which is typical of microfilaments involved in contractile functions; this identified the hVSMC to be of a contractile nature. Down-regulation in the expression of such protein markers has been observed in cultured VSMC switching towards a more synthetic phenotype (Christen *et al.*, 1999). Therefore the rate of hVSMC proliferation was reduced by serum deprivation to delay any phenotypic changes occurring prior to protein marker staining. This was compared with HDF which are also elongated and spindle-shaped in culture, and closely resemble hVSMC in morphology. Fibroblasts have been shown to be negative for α -smooth muscle actin staining (Nakamura *et al.*, 1998) and were used as a comparison. However, a low expression of ~20% of cells was observed in quiescent HDF which possibly suggested the presence of myofibroblasts within the culture. Myofibroblasts share similar characteristics to SMC in function and structure as well as protein marker expressions (Owens *et al.*, 2004). Nevertheless, the high levels of α -smooth muscle actin observed in hVSMC allowed them to be differentiated from HDF based on the quantitative difference in expression.

A high protein expression of SM-MHC was observed in early passage cells with no detection observed in quiescent cells. However, the expression of smooth muscle myosin light chain was not present in either proliferating or quiescent cells. This data together with α -smooth muscle actin staining reinforces that hVSMC express a contractile phenotype. The high expression levels of SM-MHC correlates to those observed in porcine VSMC (Christen *et al.*, 1999) and rat aorta-derived VSMC which were spindle-shaped compared to the levels expressed in epithelioidal-shaped cells (Bascands *et al.*, 2001).

The distinctive cell shape characteristics, growth arrangement and high expression of protein markers (α -smooth muscle actin and SM-MHC) in hVSMC strongly suggested the cellular model investigated to be predominantly of SMC expressing a contractile phenotype. This was maintained over the range of cell passages utilized for further experimentation. The contractile phenotype resembles one of the typical characteristics

exhibited by VSMC *in vivo*, which allowed for the responses of Ang II to be studied in the model that may reflect the response of cells in native tissue.

3.5.2 Ang II receptor subtype expression in hVSMC

The biological effects of Ang II are mediated by binding to specific membrane-bound Ang II receptors. The existence of human Ang II receptor subtypes was assessed by protein expression in order to verify whether Ang II might induce a response in the cell model. The presence of receptors was also used to further confirm the cell type to be that of SMC.

AT₁R and AT₂R expression have been previously determined in VSMC derived from rodent (Galindo *et al.*, 2005) porcine (Zahradka *et al.*, 1998) and human (Touyz *et al.*, 2001b) sources. The fully glycosylated form of the AT₁R at 60kDa was highly expressed in early passage hVSMC grown in media containing 10% (v/v) FCS and also those rendered quiescent for 24 hours. This data suggested that the cell model would respond to Ang II as the majority of physiological effects of Ang II are mediated by AT₁R, which is widely expressed in various cell types (Dinh *et al.*, 2001). The rate of cellular growth had no significant effect on the expression of the fully glycosylated receptor at the protein level, even though it had been suggested that growth factors (i.e. factors present in serum) substantially down-regulate AT₁R gene transcription and expression in cultured rat VSMC (Nickenig and Murphy, 1994). The inter-species differences have not been well studied in this respect.

Faint protein bands were visible at ~45 and ~40kDa in quiescent cells. These protein sizes may relate to the varying degrees of deglycosylation of the receptor molecule (Barker *et al.*, 1993) and therefore correspond to the immature forms of the AT₁R. By rendering cells quiescent, the rate of proliferation is reduced which in turn slows down the rate of protein turnover. This may explain the presence of these undeveloped forms of the receptor, although this still remains to be proven.

A much lower abundance of AT₂R expression was detected in hVSMC grown in media containing 10% (v/v) FCS and those rendered quiescent compared with AT₁R expression. This result was expected since these VSMC were derived from an adult source, and AT₂R are mainly expressed in foetal tissue where they play a vital role in

development (Dinh *et al.*, 2001). Even though the positive control (Hep G2) cells exhibited a high expression of the AT₂R protein at ~44kDa; faint bands were detected at ~45 and 60kDa in hVSMC. This demonstrated differences in AT₂R sizes and their deglycosylated forms within different human cells. Human myometrial tissue exclusively expresses AT₂R, where the native form has been detected at ~60 to 68kDa and the deglycosylated forms have been determined at ~36 and 46kDa (Servant *et al.*, 1994). Similar protein bands sizes have been determined more specifically in uterine artery VSMC derived from ewes (Sullivan *et al.*, 2005). These observations closely resemble the protein sizes of AT₂R in hVSMC described in this thesis.

Even though AT₁R is predominantly expressed in hVSMC, the coexpression of AT₂R (of low abundance) possibly suggests the presence of some AT₁R/AT₂R heterodimers. Moreover, it cannot be discounted that AT₂R expression within these cells may be because they are derived from diseased (varicose) veins, since the up-regulation of AT₂R has been associated with vascular remodelling, injury and disease development. Increased AT₂R expression was found following balloon injury in normal rat carotid arteries (Viswanathan and Saavedra, 1992).

The high expression of AT₁R and low levels of AT₂R observed in these cells in this thesis was similarly found in other hVSMC (Touyz *et al.*, 2001b) and rat aortic VSMC (Bascands *et al.*, 2001). This further suggests that the cells used were of VSMC origin.

3.5.3 Modulation of hVSMC growth following Ang II treatment

Ang II is well known for the induction of cellular growth involved in blood vessel development and cell growth in CVD (Touyz and Schiffrin, 2001; Touyz, 2005). Ang II can stimulate various cell signalling pathways and induces proliferation, hypertrophy, apoptosis and differentiation (Hafizi *et al.*, 1998; Bascands *et al.*, 2001; Berk, 2001; Kohno *et al.*, 2000). Differences in the resultant responses are dependent upon the type of cell, the presence of Ang II receptor subtypes and other growth-promoting factors and cytokines (Wolf and Wenzel, 2004). The growth effects induced following Ang II exposure were assessed in the hVSMC model by analysing the rate of proliferation and cell survival.

The trypan blue exclusion method used to determine cell viability showed no significant loss in hVSMC following single Ang II treatments over a range of concentrations; this suggested that Ang II did not induce a cytotoxic response. However, a ~30% reduction in viable cells was observed after exposure at 10^{-5} mol/L, suggesting cell death occurs in the presence of relatively high Ang II concentrations.

The PD assessed after successive Ang II exposures over 20 days in media containing 10% (v/v) FCS, were only slightly increased for the two lowest doses of Ang II (10^{-8} and 10^{-7} mol/L). The lowest doses appeared to induce a faster rate of proliferation which was maintained over the 20 days, suggesting no loss in cells following successive exposure. The highest concentration (10^{-6} mol/L) had no significant effect on the PD rate compared with untreated cells, which suggested a balance between cell proliferation and death, although this was not formally investigated.

To assess the growth effect mediated purely by Ang II alone, hVSMC were placed in media containing 0.5% (v/v) FCS, which contained sufficient FCS to maintain cell survival and prevent cell death. Since the population of cells as a whole would be in the same cell cycle phase (G_0/G_1), this allowed the effects of Ang II to be measured. FCS contains numerous growth promoting factors and its presence in media could therefore conceal the Ang II response being measured. The PD counts of quiescent cells following a single Ang II exposure showed a slight increase with low Ang II doses (10^{-9} and 10^{-8} mol/L). Similarly effects were observed after successive treatments.

hVSMC proliferation and viability in response to Ang II were also investigated using the MTT assay. Initial experiments showed the cell model to exhibit MTT activity. Cells submitted to oxidative stress with graded concentrations of H_2O_2 displayed measurable changes in MTT activity. The increased MTT activity levels at low concentrations indicated stimulation of mitochondrial activity and the dramatic decline observed with high concentrations indicated cell death. These experiments showed MTT activity to be present in hVSMC, and that changes in activity could be used to assess either cell stimulation or cell death induced by differing concentrations of Ang II.

A marked increase in MTT activity was observed following exposure to Ang II for 24 hours at all concentrations tested, after a 24 hour period of quiescence. The highest

activity was observed at 10^{-7} mol/L which indicated the greatest number of viable cells and increased PD. The same concentration-dependent response in MTT activity with Ang II treatment was observed in primary bovine VSMC, with a maximal 2.4-fold increase at 10^{-7} mol/L (Zhou *et al.*, 2006). This data closely resembled the results observed in this hVSMC model.

A significant increase in final cell number following 24 hours Ang II exposure at 10^{-7} mol/L was determined in early passage (passage 4 to 6) human coronary artery SMC (Kohno *et al.*, 2000). However, in contrast to these results no alteration in proliferation or viability was detected in quiescent human aortic VSMC treated with Ang II (10^{-7} mol/L) for 24 hours compared with untreated cells or in human coronary artery SMC. Instead an increase in hypertrophy was detected in response to Ang II (Li *et al.*, 2006a). Hypertrophic growth is defined by increased protein synthesis and cell size with no change in DNA synthesis; where cells remain in the G₁-phase of the cell cycle and do not progress through the S-phase (Wolf and Wenzel, 2004). This response was evaluated in hVSMC in this thesis (data not shown) and showed no substantial change in protein content following Ang II exposure, whereas an increase in proliferation was observed.

The growth response modulated by Ang II varies in SMC from different species and between those originating from different vessels, which may reflect the responses observed *in vivo*. It has also been proposed that heterogeneity exists in the VSMC phenotype expressed in arterial walls to perform specific functions (Frid *et al.*, 1997), and that phenotypes may respond differently to vasoactive stimuli. Therefore, it is not surprising that hVSMC from saphenous veins exhibited a proliferative response following Ang II treatment compared to a hypertrophic response induced in human coronary artery SMC (Kohno *et al.*, 2000) and aortic VSMC (Li *et al.*, 2006a). However, these forms of Ang II mediated growth may not be exclusive, as expansion of the cytoplasm in response to Ang II exposure has been described as a form of cell growth that causes an increase in cell surface area that is neither hypertrophy or proliferation (Kuma *et al.*, 2007). Other parameters may have also affected the Ang II-induced growth response such as cell culture conditions, confluence of cells prior to treatment and the period of quiescence and treatment.

No change in MTT activity was displayed following Ang II treatment in 10% (v/v) FCS containing media, compared with control cells. This was probably due to the presence of other stimulatory factors present in FCS, which are known to interfere with this assay (Denizot and Lang, 1986), and mask any effects induced. Even though this assay is regarded as an index of cell proliferation, it is specifically a measure of succinate dehydrogenase activity which is a component of the mtRC within mitochondria. It can therefore also be used to assess mitochondrial activity. However, other mitochondrial related cellular mechanisms and mitochondrial functions would need to be investigated further in order to fully describe this effect of Ang II on mitochondria (see chapter 6.0).

ARB are used for *in vitro* studies to assess the mechanism for the effects of Ang II at the cellular and molecular level. The active Losartan metabolite E3174, an AT₁R antagonist was assessed for its effect on hVSMC growth and survival. In agreement with other studies (Stanley *et al.*, 2000), E3174 at 10⁻⁵ mol/L did not significantly affect viability or PD of hVSMC in culture. The trend for a slight decrease in the PD of VSMC induced by Ang II in the presence of E3174 is supported by previous reports (Kohno *et al.*, 2000).

Conclusions

- Morphological studies showed early passage hVSMC isolated from adult saphenous veins to predominantly express α -smooth muscle actin and SM-MHC, strongly suggesting a contractile phenotype which is characteristic of VSMC *in vivo*.
- The mature, glycosylated form of the AT₁R subtype was highly expressed in proliferating hVSMC and those rendered quiescent.
- Low protein expression of the AT₂R subtype was detectable in lysates of hVSMC.
- Both single and multiple Ang II treatments increased the PD of hVSMC.
- No loss in cell viability was observed following single Ang II treatments, except at concentrations $\geq 10^{-5}$ mol/L.
- Mitochondrial complex II activity was stimulated following Ang II exposure in hVSMC.
- The AT₁R antagonist E3174 displayed no cytotoxic effect in hVSMC at concentrations up to 10^{-4} mol/L.
- Taken together these data suggest that cultured hVSMC of saphenous vein origin constitute a suitable model to study the propensity for Ang II to induce senescence via AT₁R stimulation.

CHAPTER FOUR

Effect of Angiotensin II on Senescence in Cultures of Human Vascular Smooth Muscle Cells

Chapter 4.0 Effect of Angiotensin II on senescence in cultures of human vascular smooth muscle cells

Chapter 3.0 established a hVSMC culture as a model to study the ageing effects of Ang II. Irrespective of its growth effects, Ang II triggers a diverse array of cell signalling pathways (Touyz and Schiffrin, 2000), many of which could result in cellular activation or suppression (Wolf and Wenzel, 2004).

The normal age-related changes in arterial structure and function have been shown to accelerate in parallel with the presence of CVD. Arterial components of the Ang II-signalling cascade increase with age and are thought to play a major role in adjusting structural and functional responses in the vessel wall. These alterations can promote the development of CVD such as hypertension and atherosclerosis (Najjar *et al.*, 2005). Rodent models have shown that prolonged inhibition of Ang II with ARB and ACE inhibitors delay the development of many age-related changes in the blood vessel, heart and kidneys (Ferder *et al.*, 2002; de Cavanagh *et al.*, 2003; Basso *et al.*, 2007) that are associated with CVD. Similar observations from numerous human clinical trials also implicate this anti-ageing effect of RAS inhibition through observations made on reduced morbidity and mortality rates of CVD (Lithell *et al.*, 2003; Nickenig *et al.*, 2006).

4.1 Background

Senescent vascular cells have been characterised in atherosclerosis (Minamino *et al.*, 2003). Emerging evidence has revealed that elevated Ang II contributes to various age-related CVD; this suggests a possible role of Ang II in senescence. Therefore, Ang II may be implicated in the induction of vascular cell senescence and thereby enhance vascular ageing and disease development.

4.1.1 Cellular senescence

Cellular senescence is a mechanism that halts normal cell division in response to various types of stimuli or stresses that maybe potentially oncogenic. Senescence is initially characterized by the reduced growth rate of a population of cells in culture. Primary cells in culture do not grow indefinitely but display diminished PD with

sub-culturing after a prolonged period of time. This differs from tumour cells which continually divide irrespective of numbers of PD (Itahana *et al.*, 2001). In tissues, senescent cell lead to impaired homeostasis, and is characteristic of cells derived from aged and diseased tissue.

4.1.2 Characteristics of replicative cell senescence

The progressive loss in proliferative capacity due to continued cell division results in a state of permanent cell growth arrest with altered gene and protein expression, termed 'replicative senescence'. Mammalian cells *in vitro* display this finite replicative capacity that was originally described by Hayflick and Moorhead (1961). The limited number of cell divisions is deemed the 'biological clock', with signalling pathways causing cessation of cell division. It is therefore considered that cell intrinsic mechanisms initiate replicative senescence (Hayflick and Moorhead, 1961).

Although senescent cells remain viable and metabolically active, other specific phenotypes have also been determined in this cell state. Senescent cells remain arrested in the G₀/G₁-phase of the cell cycle and are unable to enter the S-phase in response to mitogenic stimuli. Coupled with this, is the acquired resistance to the induction of apoptosis and distinct morphological alterations, such as flattened and enlarged cells, loss of cell-cell contacts (Ben-Porath and Weinberg, 2005) and the increased expression of SA- β -gal at pH 6.0 (Dimri *et al.*, 1995). However, the senescent phenotype exhibited by cells is also dependent upon cell-type specific changes in gene and protein expressions (Erusalimsky and Kurz, 2005; Pascal *et al.*, 2005).

The intrinsic mechanisms which trigger replicative senescence apart from mitogenic or oncogenic activity include telomere shortening and DNA damage. The repetitive telomere DNA sequences (TTAGGG) found at the ends of chromosomes are preferentially lost, as telomeres progressively shorten with each round of cell division (Harley *et al.*, 1990). This protects sub-telomeric sequences from degradation (de Lange, 2005). Eventually telomeres reach a critically short length or altered structure that can no longer be protected and consequently this signals the onset of cell senescence (Masutomi *et al.*, 2003; Stewart *et al.*, 2003). Telomerase, a ribonucleoprotein which synthesises telomeric repeats, elongates telomeres in embryonic and stem cells. However, it is found at undetectable levels in adult tissues,

thereby leading to progressive telomere attrition (Harley *et al.*, 1990). Precisely how shortened telomeres signal their state to the cell is unclear, but it has been suggested to eventually lead to telomere ‘uncapping’. Uncapping refers to the disruption of the proper protective cap structure at the end of telomeres, thereby exposing the end of the DNA (Blackburn, 2001). Uncapped telomeres appear to be identified as DNA DSB which initiates a DNA damage response. This has been observed in senescent cells where loss of single-stranded telomere DNA results in a telomeric overhang (Stewart *et al.*, 2003). It is still not fully clarified how the uncapping event directly induces senescence; however common DNA damage protein foci have been determined in telomeres of senescent cells, such as γ -H2AX, 53BP1, MDC1 and NBS1 (d’Adda di Fagagna *et al.*, 2003; Herbig *et al.*, 2004).

Oxidative damage to DNA bases and DNA DSB also initiate a senescent phenotype similar to that caused by telomere attrition (Chen *et al.*, 1995). These forms of DNA damage occur following irradiation of cells or treatment with chemical DNA-damaging agents (Wahl and Carr, 2001). The DNA damage response triggers senescence through a signalling pathway that ultimately activates the tumour suppressor protein p53, which acts to block cell division. p53 has a major role in both senescence and apoptosis and the difference in the response induced is considered to be dependent upon the stimuli. Low levels of DNA damage are thought to favour senescence whereas higher levels are likely to cause apoptosis (Ben-Porath and Weinberg, 2005).

The induction of senescence is regarded as a foolproof mechanism that prevents the proliferation of cells at risk of tumorigenic transformation. Therefore, senescence is comparable in outcome to apoptosis, but also differs as apoptosis initiates the death of damaged or potentially oncogenic cells by completely eliminating them from tissues or organs (Itahana *et al.*, 2001).

4.1.3 Vascular cell senescence, ageing and disease

Senescent cells *in vivo* typically display alterations in function which can accumulatively lead to the loss of normal tissue or organ function and integrity (Campisi, 2005), or limit the regenerative capacity of stem cell pools (Chen, 2004). These features are characteristic of the ageing phenotype.

Age-related changes in blood vessel structure and function include a decrease in compliance and an increase in inflammation that promotes atherogenesis (Marin, 1995). These alterations are thought to attribute to age-related changes in vascular cell function. Vascular remodelling is one adaptive response to increased blood pressure and vessel wall tension; that is largely influenced by the RAS. Ang II has a major effect on the vasculature and has been shown to play a role in remodelling by activating cell signalling pathways that elevate cell growth, inflammation and fibrosis (Touyz *et al.*, 2003). Mitogens that stimulate cellular growth can also activate other cell signalling cascades and induce senescence and inflammation (Brasier *et al.*, 2002). Other changes include the endothelial-dependent reduction in the production of the vasodilators, ·NO and prostacyclin, which declines with age and causes impaired endothelial vasodilation. Ageing also causes diminished responsiveness of VSMC to these vasodilators (Brandes *et al.*, 2005). Increased proinflammatory and prothrombogenic molecules have been detected in aged arteries (Najjar *et al.*, 2005). These arterial alterations may themselves be risk factors in the manifestation and development of CVD.

The responses of senescent vascular cells are consistent with known changes expressed in various age-related vascular diseases, but have been extensively examined in the development of atherosclerosis (Samani *et al.*, 2001; Minamino *et al.*, 2002). Senescence in this case may arise from extensive cell replication due to ageing and/or from hemodynamic stress to the vascular wall bed. Senescent VSMC derived from atherosclerotic plaques exhibit a proinflammatory phenotype (Minamino *et al.*, 2003) and the accumulation of these cells in the fibrous cap is proposed to contribute to inefficient plaque repair and instability (Bennett *et al.*, 1998).

Vascular cell senescence has since been implicated in a wide range of human cardiovascular pathologies as summarised in **table 4.1**. This includes evidence of senescence in vascular regions prone to disease and during the initial and advanced stages of diseases.

Table 4.1 Evidence of human vascular ageing or senescence in cardiovascular pathologies/ risk factors

<i>Disease</i>	<i>Cell/ tissue</i>	<i>Observation</i>	<i>Reference</i>
Abdominal aortic aneurysms (AAA)	VSMC/ aneurysm wall	↓ CPD (<i>in vitro</i>)/ enlarged cell-shape	Liao <i>et al.</i> , 2000
AAA	WBC/ aortic wall	↓ tDNA content	Wilson <i>et al.</i> , 2008
Atherosclerosis	WBC	↓ TRF length	Samani <i>et al.</i> , 2001
Atherosclerosis	EC/ coronary artery	↑ SA-β-gal staining	Minamino <i>et al.</i> , 2002
Atherosclerosis	VSMC	↑ SA-β-gal staining/ ↓ TRF length/ ↑ DNA damage	Minamino <i>et al.</i> , 2003; Matthews <i>et al.</i> , 2006
Cardiovascular mortality	WBC	↓ TRF length	Cawthon <i>et al.</i> , 2003
Coronary artery disease	EC/ coronary artery	↓ telomere length	Ogami <i>et al.</i> , 2004
Coronary artery disease	EC/ mammary artery	↑ SA-β-gal staining/ ↓ TRF length	Voghel <i>et al.</i> , 2007
Heart disease	WBC	↓ telomere length	Starr <i>et al.</i> , 2007
Hemodynamic stress of vessels	EC/ iliac artery	↓ TRF length	Chang and Harley, 1995
Hypertension	WBC	↓ TRF length	Benetos <i>et al.</i> , 2001
Hypertension	EPC/ coronary artery	↑ SA-β-gal staining	Imanishi <i>et al.</i> , 2005b
Kawasaki disease coronary aneurysms	EC/ adventitia region of coronary artery	↑ SA-β-gal staining	Fukazawa <i>et al.</i> , 2007
Life stress	WBC	↓ telomere length	Epel <i>et al.</i> , 2004
Obesity/ smoking	WBC	↓ TRF length	Valdes <i>et al.</i> , 2005
Obesity	WBC	↓ TRF length	Zannolli <i>et al.</i> , 2008
Premature MI	WBC	↓ TRF length	Brouillette <i>et al.</i> , 2003
Type I diabetes	WBC	↓ TRF length	Jeanclous <i>et al.</i> , 1998
Type II diabetes	Monocytes	↓ telomere length	Sampson <i>et al.</i> , 2006
IGT/ type II diabetes	WBC	↓ TRF length/ >↓ TRF length in type II diabetics	Adaikalakoteswari <i>et al.</i> , 2007
Vascular dementia	WBC	↓ TRF length	von Zglinicki <i>et al.</i> , 2000

This table summarises the current evidence of vascular cell and tissue senescence based on biomarkers of cellular senescence in various cardiovascular pathologies. CPD, cumulative population doubling; EPC, endothelial progenitor cell; IGT, impaired glucose tolerance; MI, myocardial infarction; tDNA, telomere DNA; TRF, terminal restriction fragment; WBC, white blood cells.

Chapter 4:0 Effect of Ang II on hVSMC senescence

As common markers of altered cell morphology, telomere shortening and positive SA- β -gal staining have been used to investigate replicative senescence *in vitro*. These markers have also been determined in human cells or tissues from age-related CVD *in vivo*. This provides strong evidence that vascular cell senescence is correlated with vascular ageing and disease development.

The long-term cultivation of vascular cells *in vitro* results in the appearance of many of the previously mentioned biomarkers of replicative senescence. This has been described for human umbilical vein EC (hUVEC) (Carlisle *et al.*, 2002; Hastings *et al.*, 2004; Unterluggauer *et al.*, 2007) and VSMC (van der Loo *et al.*, 1998; Liao *et al.*, 2000). The senescent characteristics observed are thought to reflect what maybe happening *in vivo* with progressive age.

4.2 Aims

- The gradual shortening of telomere DNA with every round of cell division is regarded as a common molecular biomarker of *in vitro* replicative cell senescence and ageing. Ang II is a potent multifunctional hormone which elicits various cell signalling mechanisms in order to modulate cell function. It has however, also been associated with many age-related CVD. Therefore, to determine whether Ang II exposure affects the telomere attrition of hVSMC, TRF length was measured using the Southern blotting technique.
- To establish whether the length of telomere DNA is maintained within hVSMC by measuring telomerase activity levels.
- As a possible mechanism for triggering telomere attrition, DNA damage in hVSMC following Ang II exposure was assessed by the measurement of DNA strand breaks in single cells using the Comet assay.
- To ascertain whether prolonged Ang II exposure promotes cellular senescence in proliferating hVSMC.
- To establish whether chronic (over 30 days) Ang II exposure results in hVSMC apoptosis. Caspase-3/7 activity and nuclear fragmentation were used to assess apoptosis.

4.3 Experimental Approach

4.3.1 Cell culture

Early passage hVSMC were grown to near confluence in media containing 10% (v/v) FCS, at 37°C. In most experiments, cells were rendered quiescent for 24 hours prior to single Ang II treatments, as described in section 2.3.1.1. Treatment with H₂O₂ was performed on sub-confluent cells in media containing 10% (v/v) FCS. Cells that were continuously sub-cultured for 30 days were treated with Ang II on alternate days, and on the following days when cells were re-plated (see section 2.3.1.3).

Both hVSMC and HeLa cells were grown to confluence in T75cm² NuncTM flasks as described in 2.3.1.1, and harvested by trypsinization for Western blotting.

PD counts were performed to assess hVSMC proliferation and to correct for changes in the proliferation rate when assessing TRF length. Following Ang II treatment, cells were harvested by trypsinization, resuspended in 0.5ml of fresh media and counted using a haemocytometer. The total cell number and PD were calculated as described in 2.3.1.2.

4.3.2 Cell imaging

hVSMC growth, appearance and structural morphology were determined visually by microscopy. For comparison, late passage hVSMC (passage 21) were grown to ~70% confluence in T75cm² NuncTM flasks. Phase contrast micrographs were taken at ×40 and ×100 magnifications, using a colour camera attached to a Nikon inverted trinocular phase contrast light microscope.

Senescent hVSMC, determined by positive SA-β-gal staining after Ang II treatment for 30 days, were assessed visually by light microscopy. After the staining period, SA-β-gal solution was removed and cells were overlaid with 1ml of 70% (v/v) glycerol per well prior to taking images. Images were obtained at ×100 magnification.

4.3.3 SA- β -gal assay

The SA- β -gal stain was used to assess cellular senescence following Ang II treatment. hVSMC seeded at 1×10^5 cells per well in 6-well plates were treated with a range of Ang II concentrations (10^{-9} , 10^{-8} , 10^{-7} and 10^{-6} mol/L) in media containing 10% (v/v) FCS. Following 30 days of alternate Ang II treatment, cells were trypsinized, counted using a haemocytometer and re-seeded at 1×10^5 cells per well in 6-well plates, into media containing 10% (v/v) FCS. Cells were left to adhere for 24 hours at 37°C prior to fixation, then stained with SA- β -gal staining solution as described in 2.3.2.3. SA- β -gal staining was performed on non-confluent cells to avoid non-specific staining (Severino *et al.*, 2000). The number of positive (blue) and negative (transparent) stained cells was counted manually in five fields selected at random from each well using a Nikon inverted trinocular phase contrast microscope (under $\times 200$ magnification). The percentages of senescent cells following each treatment were calculated relative to the untreated cells.

4.3.4 Measurement of apoptosis

4.3.4.1 Caspase-3/7 activity

Caspase-3/7 activation in hVSMC was assessed to determine the induction of apoptosis signalling pathways following Ang II treatment, using the Caspase-Glo® 3/7 assay. Cells were seeded at 3×10^3 cells per well in sterilized white 96-well microplates. Near confluence was determined by viewing cells simultaneously grown in clear 96-well microplates. Prior to single Ang II treatments (10^{-8} , 10^{-7} and 10^{-6} mol/L) for 24 hours at 37°C, the FCS content in the cell media was changed to 0.5% (v/v). Following treatment, cells were lysed and caspase-3/7 activity was measured 1 hour after the addition of the caspase 3/7 reagent, as described in 2.3.3.1. Background luminescence measurements of cell media were subtracted from the measurements of Ang II-treated and untreated cells.

4.3.4.2 Detection of DNA fragmentation using Hoechst 33258 staining

Nuclear fluorescence staining with Hoechst 33258 solution was used to visually determine the morphology of apoptotic hVSMC, by the presence of condensed or fragmented nuclei following cell treatment. Cells were seeded at 1×10^5 cells per well on sterilized glass coverslips in 6-well plates. Near confluent cells were then rendered quiescent before single Ang II exposures at 10^{-9} or 10^{-8} mol/L for 4 and 24 hours. H₂O₂ exposure (10 and 25 μ mol/L) for 24 hours was performed on cells in media containing

10% (v/v) FCS. After treatment, cells were fixed then stained with Hoechst 33258 solution as described in section 2.3.3.2. The number of nuclei with intensely bright, fragmented or condensed DNA (positive) and those with uniform staining (negative) were counted in each field of view. Nuclei were assessed manually in four fields selected at random from each slide and images were taken using a Nikon inverted trinocular phase contrast fluorescent microscope (DAPI filter, ×400 magnification) using the Volocity Acquisition software. The percentage of apoptotic cells was calculated from the number of apoptotic cells divided by the total number of cells counted in each field.

4.3.5 Human telomerase (hTERT) protein expression by Western blotting

hTERT protein expression was determined in hVSMC and HeLa cells (positive control for telomerase expression) by Western blotting, as detailed in 2.3.6.1. Cell lysis buffer was used to extract whole cell proteins (2.3.5.6) from cells grown to confluence in media containing 10% (v/v) FCS. Protein samples (40µg protein per sample) were separated on 8% resolving gels under non-reduced and denaturing conditions. Membranes were blocked with 5% (w/v) milk/TBST for 1 hour at RT prior to antibody labelling (dilutions and incubation periods specified in **table 2.13**). Equal protein loading was confirmed by labelling for α-tubulin protein expression, using 10% (w/v) milk/TBST blocking solution (**table 2.14**).

4.3.6 Southern blotting

The median TRF length of treated hVSMC was measured by Southern blotting (section 2.3.6.2) to assess telomere length. Early passage cells were seeded at 1×10^5 cells per well in 6-well plates. Near confluent cells were exposed to a single dose of Ang II over a range of concentrations (10^{-9} , 10^{-8} , 10^{-7} and 10^{-6} mol/L) for 24 hours at 37°C. Following treatment, cells were harvested by trypsinization and counted using a haemocytometer in order to calculate PD (**4.3.1**). Cells were then collected by centrifugation and DNA was extracted and quantified (**2.3.5.1** and **2.3.5.2**). The change in mean (of the median) TRF length measurements of Ang II-treated and untreated cells was expressed per mean PD.

4.3.7 Comet assay

DNA damage in hVSMC was measured using the Comet assay by visually scoring DNA strand breaks in single cell nucleoids. Cells were seeded at 2×10^4 and 1×10^5 cells per well in 6-well plates for H_2O_2 and Ang II treatment respectively. Near confluent cells were rendered quiescent for 24 hours before treatment, as described in **2.3.1.1**. Exposure to H_2O_2 was conducted for 4 hours and to Ang II for 24 hours, at $37^\circ C$. After treatment, under minimal light, the 6-well plates were placed on ice and the cells were rinsed twice with 1ml of chilled DPBS. Cells were then scraped into chilled mincing solution, pipetted several times to ensure an individual-cell suspension and subjected to the Comet assay as detailed in **2.3.6.3**. The mean percentage tail DNA was used as the measure of DNA damage.

4.3.8 Telomerase activity detection

Telomerase activity was used to assess the maintenance of telomeric DNA in hVSMC using the TeloTAGGG Telomerase PCR ELISA kit. Early passage cells were seeded at 1×10^5 cells per well in 6-well plates and grown to confluence in media containing 10% (v/v) FCS. Cells were harvested by trypsinization and counted using a haemocytometer to determine the total number of cells (section **4.3.1**). Telomerase activity of 2×10^5 cells per sample was then measured as described in **2.3.6.4**. The positive control cell extract provided in the kit (293 cells), was simultaneously processed alongside hVSMC samples. Telomerase activity of cells was expressed as absorbance values at 450nm relative to the reference wavelength (690nm).

4.4 Results

4.4.1 Ang II accelerates telomere loss in hVSMC

To examine whether Ang II exposure had any effect on the gradual replicative senescence of hVSMC *in vitro*, Southern blotting analysis was used to measure the average median TRF length of cells exposed to Ang II. Measurement of PD was used to correct for differences in proliferation. This technique has been used extensively in the literature (Benetos *et al.*, 2001; Samani *et al.*, 2001; Duan *et al.*, 2005; Matthews *et al.*, 2006).

A single dose of Ang II markedly accelerated the rate of telomere loss in a dose-dependent manner (**figure 4.1A**). The rate of telomere loss per PD was substantial even with the lowest Ang II dose (10^{-9} mol/L) compared with control cells (**figure 4.1A**). The maximal rate of loss was observed following treatment with 10^{-7} mol/L Ang II. Although only small changes in TRF length were measured with Ang II at the different doses, it provides evidence that Ang II enhances the normal replicative senescence of hVSMC *in vitro*.

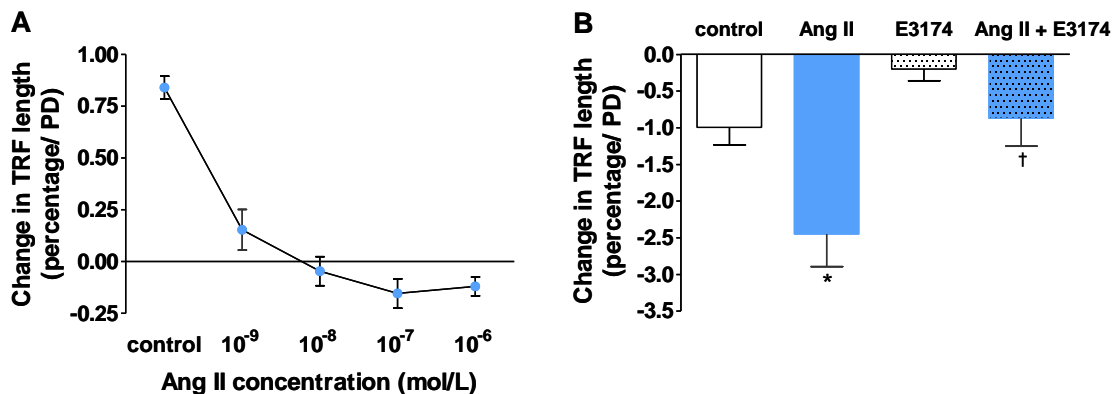


Figure 4.1 Ang II causes telomere attrition in hVSMC. **A**, Dose-dependent loss in TRF length with Ang II exposure. Near confluent cells grown in media containing 10% (v/v) FCS were treated with various Ang II concentrations for 24 hours. DNA was extracted from treated and untreated cells and telomere length was determined by Southern blotting analysis. Values represent the mean percentage change in the median TRF lengths per PD \pm SEM; n=5 ($p<0.001$ for all doses compared with control). **B**, Ang II accelerates the loss of TRF length via the AT₁R. Telomere length was measured in cells grown continuously in media containing 10% (v/v) FCS supplemented daily with Ang II (10^{-6} mol/L) for 7 days and for cells pre-incubated with E3174 (10^{-5} mol/L for 1 hour) prior to Ang II exposure (this work was conducted in collaboration with Dr R. A. Hastings, Department of Cardiovascular Sciences, University of Leicester). Bars represent mean \pm SEM; n=9 (E3174, n=3) (* $p<0.05$ compared with control and † $p<0.05$ compared with Ang II alone).

Co-incubation with the AT₁R antagonist E3174 over several days attenuated Ang II-induced telomere attrition (~1.5-fold), confirming that this effect was mediated via the AT₁R (**figure 4.1B**). The telomere loss observed in cells exposed to E3174 alone was less than that observed in untreated cells, but was not significant due to few replicates.

The ribonucleoprotein telomerase adds telomeric repeats to the ends of chromosomes, thereby maintaining telomere DNA length following cell division (Harley *et al.*, 1990). Human somatic cells exhibit undetectable levels of telomerase which is associated with shortening of telomeres and cell senescence (Masutomi *et al.*, 2003). To substantiate the telomere loss observed in hVSMC, telomerase levels were analysed using two different methods. Untreated hVSMC displayed virtually no expression of the hTERT (human catalytic subunit of telomerase reverse transcriptase) protein determined via Western blotting (**figure 4.2A**), whereas the HeLa cells displayed an intense band at 90kDa, indicating high levels of hTERT expression. The difference in expression levels was validated by confirming the uniform expression of α -tubulin, hence, equal protein loading.

The sensitive PCR ELISA was unable to detect telomerase activity in hVSMC (**figure 4.2B**), as the mean corrected absorbance was <0.1 AU, compared with the positive control sample (293 cells) which was 6-fold greater. The mean absorbance of the negative control (data not shown) was 0.062+ 0.005 (n=3), similar to that determined in hVSMC, suggesting these cells were essentially telomerase-negative.

These observations add support to the telomere attrition in hVSMC. Furthermore, this evidence discounts the modulation of telomerase activity as a primary mechanism for Ang II-induced telomere loss (**figure 4.1A**).

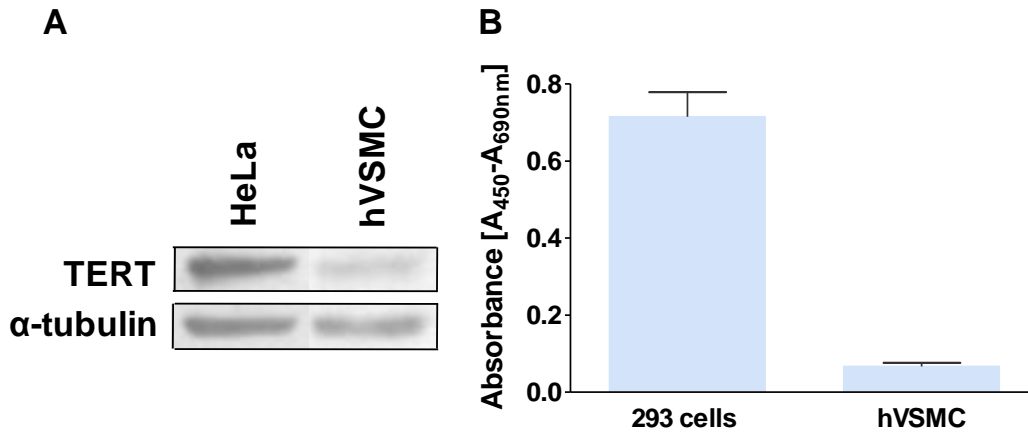


Figure 4.2 Telomerase levels in hVSMC. **A**, hTERT protein expression is relatively low in hVSMC. Representative blots show hTERT and α -tubulin (protein loading control) expression for 40 μ g of whole cell protein extract loaded per sample. A strong band, approximately 90kDa was determined in the telomerase-positive HeLa cells (positive control). **B**, hVSMC grown *in vitro* have undetectable levels of telomerase activity. Cells were grown to confluence in media containing 10% (v/v) FCS. Equal numbers (2×10^5) of both hVSMC and 293 cells were analysed to determine the level of telomerase activity using the TeloTAGGG telomerase PCR ELISA kit. The human telomerase-positive embryonic kidney cell line 293 (293 cells) was used as a positive control. Bars represent mean+SEM; n=3.

4.4.2 Ang II induces DNA damage in hVSMC

Cell senescence has been observed in response to DNA damage, damage to chromatin structure and oxidative stress (Serrano and Blasco, 2001). Growth arrest induced by DNA damage can occur after acute intense stress (Chen *et al.*, 2001a; Gorbunova *et al.*, 2002) or following successive treatments (Dumont *et al.*, 2000b; Duan *et al.*, 2005), which suggests that stress-induced senescence might also accelerate replicative senescence.

The ‘Comet assay’ was used in this study to evaluate Ang II-induced DNA damage in hVSMC. The alkaline Comet assay originally performed by Singh *et al* (1988) is a sensitive technique for measuring DNA strand breaks in single cells. During electrophoresis, damaged DNA migrates away from the undamaged DNA forming a comet-like appearance. The comet ‘head’ consists of the nucleoid body and intact DNA, whereas the ‘tail’ consists of damaged DNA. The quantity of DNA in the tail region is considered proportional to the level of damaged DNA in cells.

Measurements of DNA damage within the hVSMC model were validated by exposure to H₂O₂, a known precursor of other ROS and inducer of DNA damage. The percentage of DNA in the tail region (% tail DNA) was the parameter used to assess DNA damage as it correlates linearly to strand break frequency over a range of damage levels. H₂O₂ induced a dose-response in DNA damage (**figure 4.3A**) with increasing concentration. Exposure with the highest dose of H₂O₂ (100µmol/L) caused ~3-fold increase in % tail DNA compared with untreated cells. However, this data was not statistically significant as only a small number of replicates were performed.

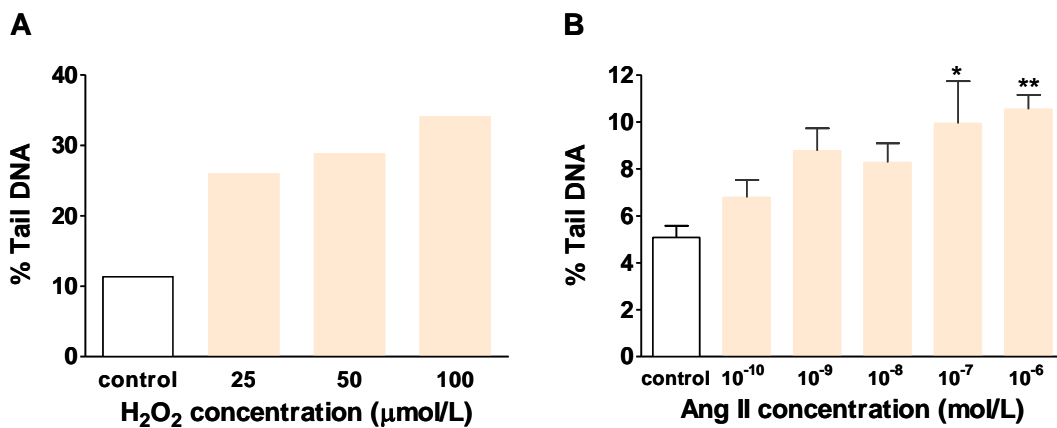


Figure 4.3 DNA damage in hVSMC measured using the Comet assay. Cells were rendered quiescent for 24 hours prior to treatment. **A**, H₂O₂ induces DNA damage. hVSMC were treated with various concentrations of H₂O₂ for 4 hours. Bars represent mean; n=2. **B**, Dose-dependent increase in DNA damage following Ang II exposure for 24 hours. Bars represent mean+SEM; n=4 (*p<0.05 and **p<0.01 compared with control).

Ang II exposure for 24 hours also induced a dose-dependent increase in DNA damage (**figure 4.3B**), with a 2-fold increase at the highest concentrations (10⁻⁷ and 10⁻⁶ mol/L). As predicted, the extent of DNA damage with Ang II was less than H₂O₂ treatment, suggesting Ang II to be a mild inducer of DNA damage. The maximal DNA damage was observed with the highest dose of Ang II (10⁻⁶ mol/L). Although this data does not directly link the induction of DNA damage with senescence, it does indicate low levels of DNA damage following Ang II exposure which might contribute to the induction of senescence (Ben-Porath and Weinberg, 2005). In contrast to this, H₂O₂-induced DNA damage was far greater due to a higher % tail DNA.

4.4.3 Ang II promotes senescence in cultured hVSMC

4.4.3.1 Morphological analysis of senescent hVSMC

The growth pattern and morphological appearance of normal hVSMC undergoing replicative senescence *in vitro* was analysed visually by microscopy, prior to Ang II treatment. This identified the typical characteristics exhibited by senescent hVSMC. Cells were continuously sub-cultured in media containing 10% (v/v) FCS up to passage 21, at which point the rate of cell proliferation declined (late passage cells displayed a mean PD of 0.44 ± 0.14 over 8 days, which was significantly lower than early passage cells (2.60 ± 0.15 over 4 days; $n=4$) following 30 days of cultivation). The population of cells as a whole displayed an irregular growth pattern and did not reach 100% confluence. Numerous cells appeared enlarged and irregular-shaped with a veil-like appearance, which are typical characteristics of senescent VSMC *in vitro* (van der Loo *et al.*, 1998; Matthews *et al.*, 2006), as identified by the white arrows in **figure 4.4A** and **B**; these were amongst some typical spindle-shaped cells. The cytoplasm of these large cells was also granular in distinct regions. Under higher magnification (**figure 4.4B**), no difference in nuclei was observed compared to early passage cells (**figure 3.1B**).

4.4.3.2 Optimisation of the SA- β -gal assay

The SA- β -gal cytochemical assay was developed by Dimri *et al.*, (1995), and is a commonly used marker of senescence and cellular ageing. The SA- β -gal activity is detected at pH 6.0, corresponding to lysosomal β -galactosidase enzyme activity expressed in senescent and pre-senescent cells with increased lysosomal content (Kurz *et al.*, 2000). In this assay, blue coloured cytoplasmic staining denotes a senescent cell, which can be enumerated as a percentage of the total cells present. However, the reliability and specificity of this assay has been queried, as SA- β -gal staining increases with cell age, as well as in confluent cells, those rendered quiescent and following treatment with H_2O_2 (Severino *et al.*, 2000; Yang and Hu, 2005). Therefore these interfering factors were addressed alongside optimisation of the SA- β -gal assay for the hVSMC model being studied.

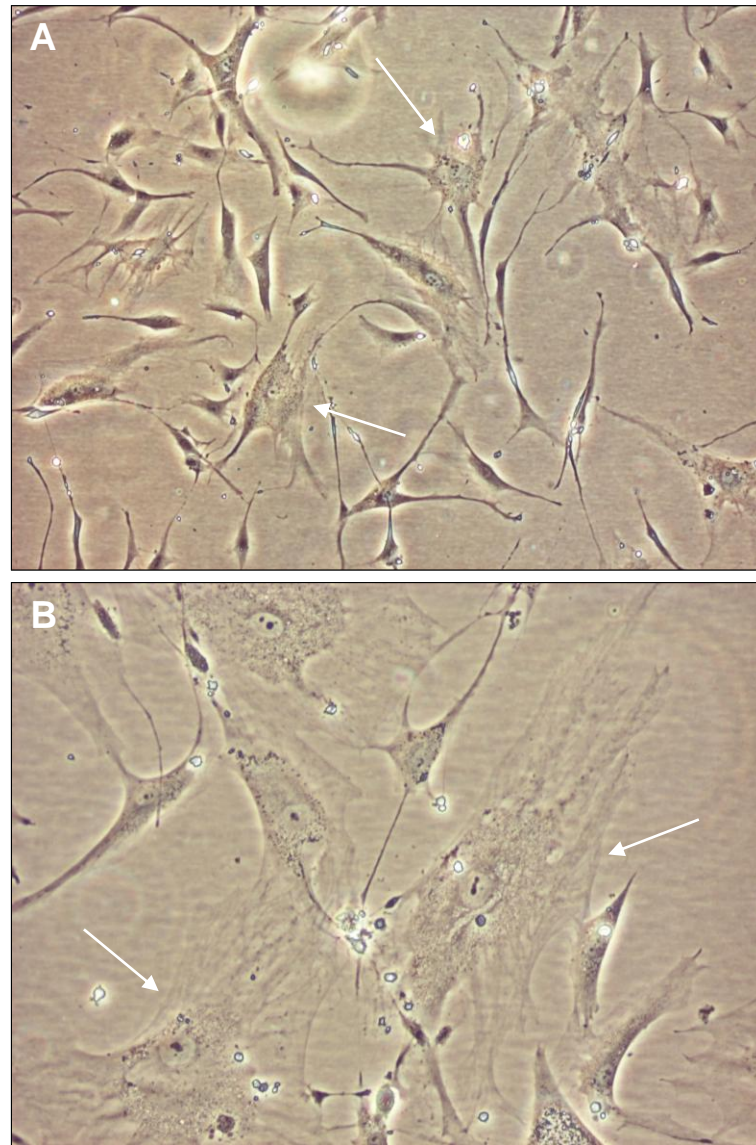


Figure 4.4 Late passage hVSMC (passage 21) exhibit enlarged and irregular-shaped cell morphology associated with cellular senescence. Phase contrast photomicrographs were taken at different magnifications, of hVSMC *in vitro* (grown in media containing 10% (v/v) FCS). **A**, $\times 40$ magnification **B**, $\times 100$ magnification; white arrows indicate individual senescent cells.

Initial experiments were conducted using early passage hVSMC to eliminate interfering factors and to optimise the assay (**figure 4.5**). Cells were stained for SA- β -gal activity 24 hours after seeding at different densities in 12-well plates. The highest cell density (5×10^5 cells per well) displayed 80% confluence and $>50\%$ SA- β -gal positive cells, which was relatively high compared to the lower cell densities (1×10^3 to 5×10^4) which displayed $<10\%$ SA- β -gal positive cells (**figure 4.5A**).

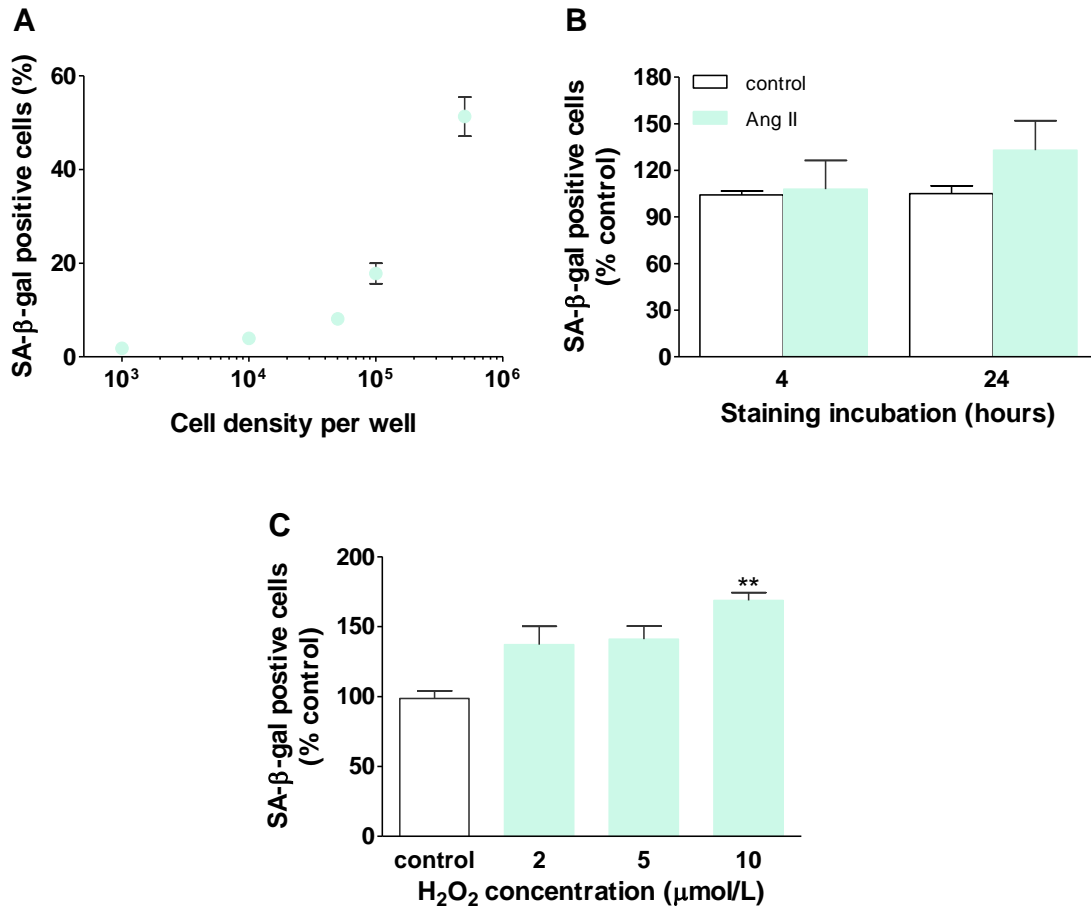


Figure 4.5 Optimisation of the detection of SA-β-gal activity in hVSMC. Cells were re-plated following treatment and left to adhere for 24 hours at 37°C. Cells were fixed and stained as described in section 2.3.2.3. **A**, Cell confluence affects SA-β-gal staining. Cells were seeded at different densities per well in 12-well plates prior to staining. Values represent mean±SEM; n=3. **B**, Effect of the staining period on SA-β-gal counts. Ang II treatment (10⁻⁸ mol/L) on alternate days and untreated cells cultured over 30 days were re-plated at 1×10⁵ cells per well in 6-well plates, prior to staining. Counts were performed after 4 and 24 hours SA-β-gal staining. Bars represent mean+SEM; n=3. White bars indicate untreated cells and light green bars indicate Ang II treated cells (data did not reach statistical significance). **C**, Dose-dependent increase in SA-β-gal activity following H₂O₂ treatment. A single dose of H₂O₂ was administered over a range of concentrations for 24 hours. Cells were re-plated at 5×10⁴ cells per well in 12-well plates, prior to staining. Bars represent mean+SEM; n=3 (**p<0.01 compared with control).

A cell density of 5×10⁴ cells per well displayed only 50% confluence and ~10% SA-β-gal positive cells. This was a reasonable seeding density to use to discount false staining that may arise from cell confluence. The duration of SA-β-gal staining was also crucial in eliminating false staining, as 4 hours incubation was not sufficient to differentiate between treated and untreated SA-β-gal stained cells (**figure 4.5B**), whereas 24-hours incubation was sufficient for the detection of SA-β-gal activity.

To measure senescence following stress treatment, cells were treated with low doses of H₂O₂, as chronic doses had previously shown to induce 100% SA-β-gal staining (Yang and Hu, 2005). **Figure 4.5C** displays a dose-dependent increase in senescence of cells re-plated 24 hours after a single H₂O₂ treatment (1.7-fold increase with 10 μmol/L H₂O₂).

Yang and Hu (2005) demonstrated that human fibroblasts released from serum deprivation by sub-culturing into media containing 10% (v/v) FCS, stained positively for SA-β-gal activity, which was reflective of the original cell passage number. Similarly, hVSMC were rendered quiescent for 24 hours before Ang II treatment, then re-plated in media containing 10% (v/v) FCS for 24 hours prior to SA-β-gal staining, at a density sufficient to microscopically view individual cells (1×10⁵/ 5×10⁴ cells per well in 6/ 12-well plates respectively) .

This assay has been criticised, as counting positive SA-β-gal stained cells can be subjective. Therefore, certain constraints were defined when using this assay to allow for a uniform measure of SA-β-gal stained cells following various cell treatments. Approximately the same five fields of view were counted in each well, excluding the outer edge and central regions of wells, from which a mean count was then calculated. Only ~80% positive SA-β-gal blue-staining of the cytoplasmic region of cells was classified as senescence; cells displaying faint or partial staining were discounted, and transparent cells were classified negative for SA-β-gal activity.

By optimising the assay for hVSMC and establishing specific cell counting parameters this allowed for a more reliable measure of SA-β-gal activity within a population of cells, and eliminated any major confounding factors of the assay.

Intra-assay variability was assessed for replicate counts of SA-β-gal stained blue (positive) and unstained (negative) cells. The mean coefficient of variation for the counts of senescent cells was 13% and for unstained cells was 8% (n=9), for cells from an untreated population.

4.4.3.3 Ang II induces senescence in hVSMC

SA- β -gal activity in hVSMC was determined following exposure to Ang II over a period of 30 days in continuous culture, with Ang II supplementation on alternate days. Representative photomicrograph images of SA- β -gal stained cells after Ang II exposure are shown in **figure 4.6A**. Only a small number of control cells displayed strong cytoplasmic blue-staining within a field of view. The majority of these cells appeared long and of the characteristic spindle-shape, whereas more of the Ang II treated cells (10^{-8} mol/L) that appeared enlarged, also expressed SA- β -gal activity. Senescent cells were always observed in control cultures of hVSMC and typically represented ~5 to 10% of the total cell population. However, Ang II induced a dose-dependent increase in cell senescence with a maximal effect at 10^{-8} mol/L (**figure 4.6B**) (>2-fold increase in senescence). A lower percentage of senescent cells was observed with Ang II exposure at 10^{-7} mol/L. In addition, the total number of cells counted in each view (i.e. senescent plus non-senescent) was decreased by the highest concentration of Ang II, suggesting the induction of apoptosis. To confirm whether more hVSMC were undergoing apoptosis at this Ang II dose, caspase-3/7 activity and DNA fragmentation were assessed as markers of apoptosis.

A

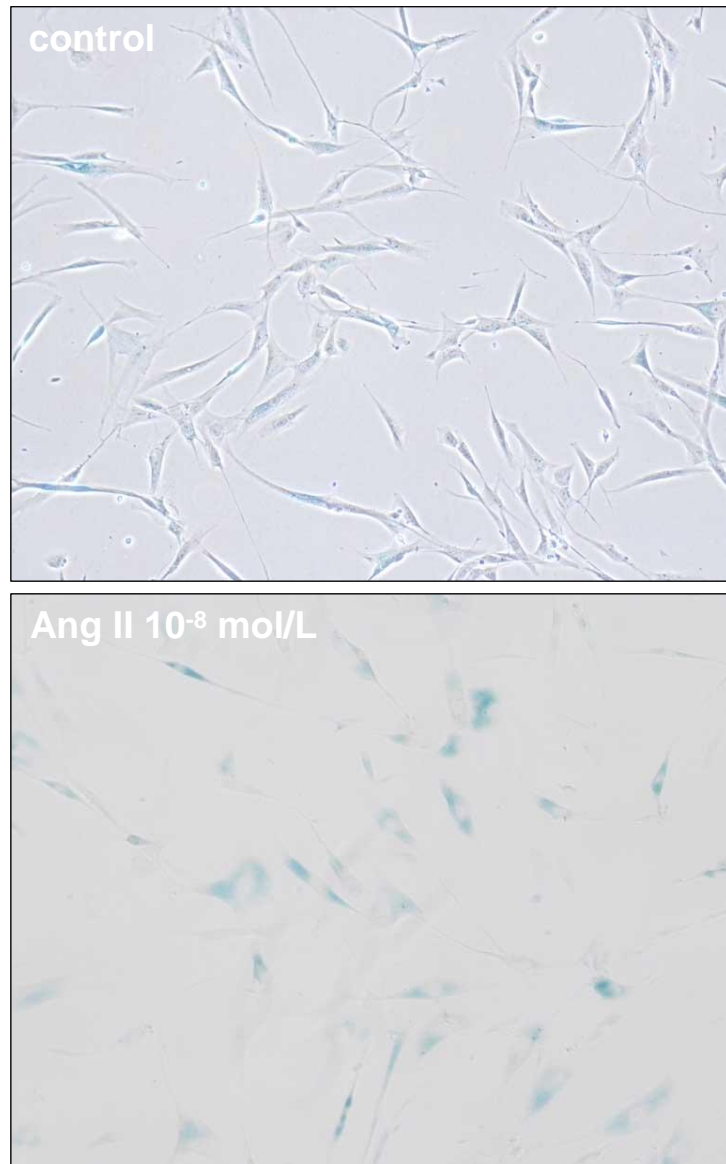


Figure 4.6A Ang II accelerates senescence in hVSMC. Cells were treated on alternate days for 30 days with Ang II, then re-plated at 1×10^5 cells per well in 6-well plates for 24 hours, then stained for SA- β -gal activity. Representative photomicrographs showing morphology and SA- β -gal staining changes of continuously cultured hVSMC with and without Ang II exposure. Wells were overlaid with 70% (v/v) glycerol solution following staining and images were taken at $\times 100$ magnification.

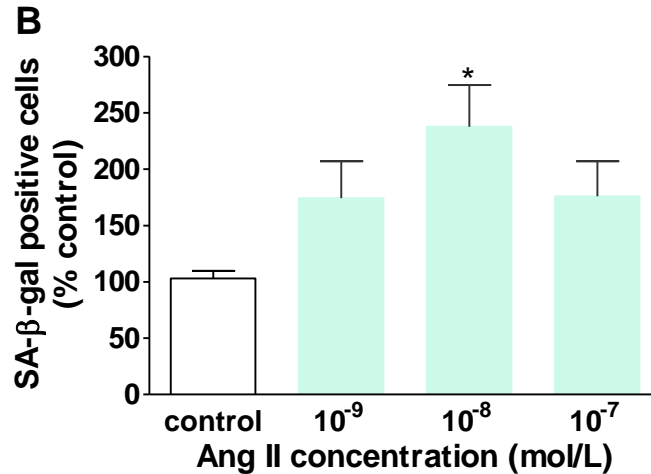


Figure 4.6B Dose-response of Ang II treated SA-β-gal positive cells, quantified at day 30. Bars represent mean+SEM; n=6 (*p<0.05 compared with control).

4.4.4 Ang II induces apoptosis in hVSMC

4.4.4.1 Effect of Ang II on caspase-3/7 activation

Apoptosis of VSMC has been observed in atherosclerosis and bypass graft disease, suggesting an important role of apoptosis in vascular diseases (Bauriedel *et al.*, 1999). In section 4.4.3.3, Ang II induced senescence of hVSMC in a dose-dependent manner, however at higher Ang II doses (10⁻⁷ mol/L) a lower percentage of senescent cells were observed. This suggested that a greater number of cells may have undergone apoptosis. This idea was investigated by analysing apoptosis of hVSMC. Cell death through apoptosis involves at least two stages, an early signal initiation stage involving death-receptor/mitochondria and caspase activation (Chen and Wang, 2002) and a later stage of final cell death characterised by changes in nuclear morphology (Earnshaw, 1995), DNA fragmentation and cell disintegration. Apoptosis can be initiated by various stimuli and can also induce an array of cellular effects. Therefore, no single experimental technique can conclusively measure apoptosis of cells due to the differing effects that can be induced. Therefore, two different measurements were taken following Ang II treatment. The initial signalling response was determined by measuring caspase-3/7 activity and nuclear morphology was assessed by Hoechst 33258 staining as an end-point effect.

The activation of caspase enzymes is central to the induction of apoptosis. The term caspase is derived from aspartate-specific proteases (Li *et al.*, 2007b). They can be activated in response to intrinsic and extrinsic pathways, mediated via death-receptor

activation or mitochondria (Mercer *et al.*, 2007). Caspase-3 is an effector enzyme which has a major role in apoptosis and is activated via both pathways; therefore caspase-3/7 activity was measured by chemiluminescence to assess apoptosis of hVSMC.

High Ang II concentrations (10^{-7} and 10^{-6} mol/L) caused an increase in caspase-3/7 activity compared to untreated cells (**figure 4.7**). The maximal activity after 24 hours exposure was for 10^{-6} mol/L Ang II of a ~1.4-fold increase. No change in caspase-3/7 activity was determined with the lowest Ang II dose (10^{-8} mol/L). This concentration corresponds to the maximum induction of SA- β -gal staining, suggesting senescence induction rather than apoptosis.

Caspase-8 activity was also measured in Ang II-treated hVSMC using a similar chemiluminescence-based assay (data not shown). This enzyme has an initiator role in the extrinsic or receptor-mediated induction of apoptosis, as suggested for hVSMC (Li *et al.*, 2006a). However, no significant difference in caspase-8 activity was determined with Ang II exposure over 24 hours, suggesting the activation of Ang II-induced apoptosis in these hVSMC may not be via this signalling mechanism.

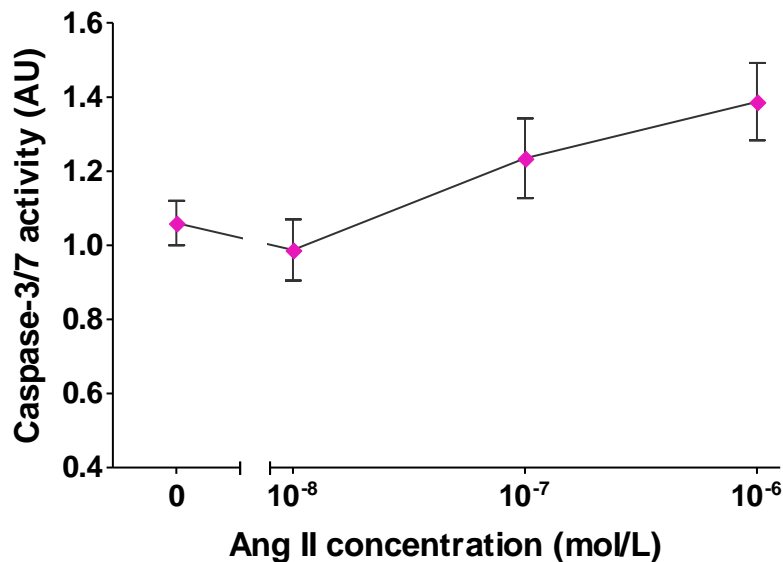


Figure 4.7 Caspase-3/7 activity in hVSMC. Cells were treated with a single dose of Ang II for 24 hours at the indicated concentrations. Near confluent cells were exposed to media containing 0.5% ($\%_v$) FCS just prior to Ang II treatment. Luminescence readings were recorded 1 hour following the addition of the caspase 3/7 reagent. Values represent mean \pm SEM; n=4 (data did not reach statistical significance). Results are expressed relative to control (mean control luminescent value for 24 hours= 1338 ALU (ALU, arbitrary light units; AU, arbitrary units)).

4.4.4.2 Effect of Ang II on the appearance of apoptotic nuclear morphology

Preliminary experiments were conducted to determine the appearance and staining of nuclei of apoptotic and control cells, prior to Ang II treatment. Sub-confluent adherent hVSMC were oxidatively damaged by H₂O₂ treatment at different concentrations to cause cell death. **Figure 4.8A, B and C** demonstrate the different nuclear staining observed. With Hoechst 33258 staining, the nuclei of healthy untreated cells appeared oval-shaped with uniform blue staining (**figure 4.8A**), whereas numerous nuclei of H₂O₂-treated cells appeared irregular-shaped with intensely blue stained, condensed and fragmented nuclear material (**figure 4.8B and C**). These morphological alterations were consistent with published observations in VSMC (Schaeffer *et al.*, 2003) and aortic SMC (Yang *et al.*, 2006).

H₂O₂ treatment for 24 hours caused a dose-dependent increase in apoptosis (**figure 4.8D**). A significant induction of apoptosis was observed with a ~2-fold increase at the highest concentration (p<0.001). These results were calculated with respect to the total number of nuclei counted in four fields selected on each coverslip.

Apoptosis was assessed to verify the senescence data determined following exposure to high Ang II concentrations, and was therefore analysed after a single treatment. Quiescent cells were treated with two different Ang II concentrations for 4 and 24 hours prior to fixing and staining with Hoechst 33258 solution. Ang II significantly induced apoptosis in a dose- and time-dependent manner (**figure 4.8E**). The highest percentage of apoptotic cells was observed at the highest Ang II concentration of 10⁻⁷ mol/L and this was statistically significant compared with the control (p<0.001), possibly accounting for the lower percentage of positive SA-β-gal stained cells observed at this dose. However, 10⁻⁸ mol/L Ang II also induced statistically significant apoptosis (p<0.01). The same trend of apoptosis was observed at both time points, with overall higher percentages of apoptotic cells determined after 24 hours. The percentage was double for Ang II exposure at 10⁻⁷ mol/L compared with control cells. Although these results were determined after a single exposure, they still provided evidence of increased apoptosis with Ang II exposure.

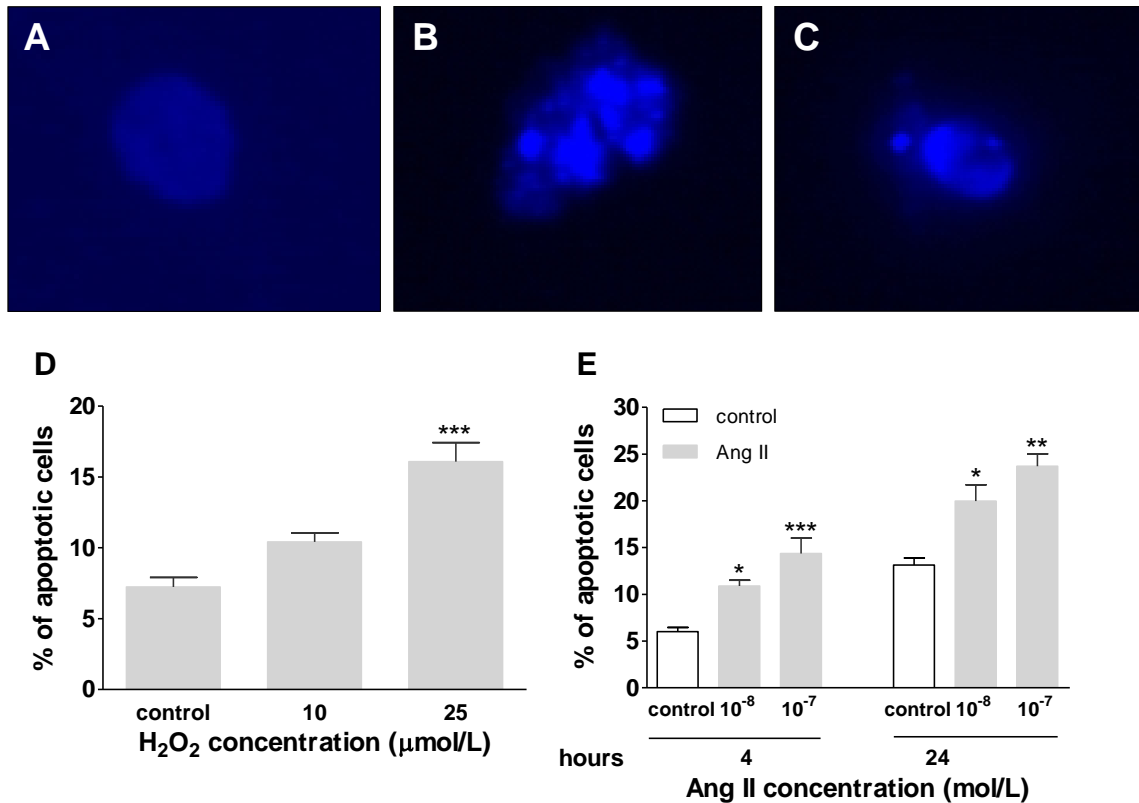


Figure 4.8 Nuclear staining of hVSMC with Hoechst 33258 to determine apoptosis. Fluorescent photomicrographs display the typical nuclei morphology of viable and apoptotic cells. **A**, Nucleus of a viable cell displaying uniform blue staining and regular oval shape. Nuclei of apoptotic cells appear **B**, fragmented, irregularly-shaped and intensely stained due to condensed chromatin or they appear as **C**, apoptotic bodies. Images were taken at $\times 400$ magnification. **D**, Dose-dependent increase in apoptosis with H₂O₂, after 24 hours exposure. Near confluent cells grown on coverslips in media containing 10% (v/v) FCS, were treated with a single dose of H₂O₂. Cells were then fixed and stained with Hoechst 33258 solution. Bars represent mean+SEM; n=4 (***)p<0.001 compared with control). **E**, Acute Ang II-induced apoptosis of hVSMC. Near confluent quiescent cells were treated with Ang II for 4 and 24 hours. The highest Ang II concentration (10⁻⁷ mol/L) induced the greatest amount of apoptosis at both time points. Bars represent mean+SEM; 4 hours, n=3 and 24 hours, n=4 (*p<0.05, **p<0.01 and ***p<0.001 compared with respective controls). Results are expressed as mean percentage of apoptotic cells relative to the total number of cells counted.

4.5 Discussion

The aim of this chapter was to investigate the effects of Ang II on the senescence of hVSMC and to establish whether this might be due to the induction of DNA damage and telomere attrition.

4.5.1 Ang II accelerated telomere attrition in hVSMC

Telomere length in cells is affected by genetic, environmental and replicative factors (Samani and van der Harst, 2008). Shortening in the average telomere length of cells and tissues has been used as a gold standard biological marker of ageing, replicative senescence and manifestation of age-related CVD (**table 4.1**). The gradual shortening in the average telomere length with each successive cell division is used as an indicator of progressive replicative senescence in cell cultures; whereas in pathological states, the presence of shortened telomeres is an indicator of increased senescence and ageing. Loss in telomere integrity is influenced by various factors such as advancing age and oxidative DNA damage (von Zglinicki, 2002). Loss of telomere structure and/or function is thus deemed a major trigger in the senescence mechanism. Exactly how truncated telomeres trigger senescence is still unclear, but it is thought that shortened telomeres are sensed in some way (possibly by DNA repair mechanisms in cells) which then activates a pathway leading to exit from the cell cycle (Minamino *et al.*, 2004). However, some evidence of loss of the single-stranded telomeric overhang, which is critical in the maintenance of the telomeric T-loop, is detected in senescent cells (Stewart *et al.*, 2003).

Telomere attrition with successive cell division has been confirmed in cultured VSMC and EC (Chang and Harley, 1995; Minamino *et al.*, 2002; Hastings *et al.*, 2004; Matthews *et al.*, 2006). The loss in TRF length has mainly been studied in EC, which line the inner wall of blood vessels and are in close proximity to the blood flow. Alterations in VSMC are far more difficult to assess, as these cells exhibit phenotypic modulation, initially expressing a contractile phenotype that is progressive lost *in vitro* and expressing a more synthetic phenotype (Owens *et al.*, 2004).

Chapter 4:0 Effect of Ang II on hVSMC senescence

There is a great variability in telomere length within individual cells and within the same population of dividing cells (Baird *et al.*, 2003), which has posed some difficulty in measuring changes in telomere length. Therefore the median TRF length measurement of a population of cells is commonly used to assess telomere length changes via Southern blotting. This approach was used in these experiments.

The average loss in TRF length of hVSMC was ~1.0% per PD, which was consistent with that observed in human EC (Hastings *et al.*, 2004). A single treatment with Ang II markedly accelerated this loss by 2.5-fold, correlating with accelerated senescence in these hVSMC. The Ang II dose-dependent loss in mean TRF length indicated a greater loss at high doses.

As yet, there is no direct evidence of the effects of Ang II on human telomere DNA, let alone its affect on telomeres in human saphenous vein derived SMC. However, hypertensive patients have been shown to have shorter telomere lengths in WBC than age-matched healthy patients (Benetos *et al.*, 2001; Demissie *et al.*, 2006), which is a major cardiovascular risk factor that is associated with high circulating levels of Ang II. In spontaneously hypertensive rats (SHR), shortened telomere fragments were determined in kidney cells, which maybe due to these cells being subjected to increased cell turnover and thereby leading to accelerated cell ageing (Hamet *et al.*, 2001). These studies strongly suggest that Ang II accelerates telomere attrition, due to its enhanced proliferative effects which eventually promote cell senescence (Fuster *et al.*, 2007). However, Ang II has also been shown to augment ROS production and induce DNA damage in vascular cells (Griendling *et al.*, 1994; Touyz *et al.*, 2002) which are cellular effects that can also trigger the induction of senescence, but also accelerate telomere shortening or dysfunction thereby increasing replicative senescence.

As the Southern blotting technique is time-consuming, TRF lengths were not continuously measured with Ang II treatment and sub-cultivation until senescence. Measurements were made following 3 days of treatment, where the same dose-dependent loss of the mean TRF length per PD was observed following Ang II treatment. A loss in TRF length was greater after 24-hour Ang II exposure determined with all doses, further supporting the idea that Ang II somehow alters telomeres and that this results in accelerated loss of telomere DNA with every round of division.

This effect on telomeres was completely prevented by pre-incubation of cells with E3174, suggesting Ang II mediates its effect through AT₁R activation and signalling. Although this has not been confirmed in other studies, many age-associated alterations in cells, that are typical of senescent cells, have been prevented in animal models with prolonged inhibition of the RAS (Ferder *et al.*, 2002; de Cavanagh *et al.*, 2003).

From these results it can be considered that Ang II triggers hVSMC senescence via a 'telomere-dependent' mechanism. However, during the period of this project, published data on Ang II treatment for 3 days revealed the induction of premature senescence of VSMC *in vitro* and *in vivo*, irrespective of telomere shortening (Kunieda *et al.*, 2006). The reasoning for this was that constitutive mitogenic stimuli or oxidative stress can induce senescence independent of replicative age and act before the replicative limit of cells (Serrano *et al.*, 1997), hence inducing 'telomere-independent' senescence, also known as 'premature senescence'. These characteristics resemble those induced by Ang II and therefore a telomere-independent induction of senescence cannot be entirely discounted in these cells.

Replicative senescence has extensively focussed on the loss of telomere integrity, but more recently this mechanism has been modified, suggesting an altered telomere state due to the related changes in telomere-binding proteins (de Lange, 2005). These identified proteins include telomeres-1 (Pot-1), Ku, telomere repeat-binding factor 1 (TRBF1) and 2 (TRBF2) (de Lange, 2005). Disruption of TRBF2 has been shown to cause telomere dysfunction and induce senescence (Smogorzewska and de Lange, 2002). Protein expression of both TRBF1 and TRBF2 were significantly reduced in EC isolated from atherosclerotic plaques of coronary artery disease patients, which rapidly underwent senescence *in vitro* (Voghel *et al.*, 2007). These observations support the idea that besides telomeres, proteins of the telomeric complex also participate in signalling the induction of senescence. However, these telomere-binding proteins were not assessed in the current hVSMC model.

Since senescent cells acquire characteristics that compromise normal tissue function, their accumulation is considered to contribute to the ageing process and development of many age-related diseases, e.g. atherosclerosis (Campisi, 2005). Accumulated evidence has demonstrated telomere shortening to occur in the human vasculature and WBC, in

various CVD states and in conditions which give rise to increased cardiovascular risk. These diseases are detailed in **table 4.1**. Telomere loss is therefore regarded as a typical senescent phenotype that maybe related to age-associated CVD. Endothelial telomeres have been shown to shorten with increasing age in iliac arteries and in the abdominal aorta (Chang and Harley, 1995; Okuda *et al.*, 2000) and this loss is more pronounced in areas prone to atheroma. It has been postulated that high levels of hemodynamic stress may enhance EC turnover and cause shortened telomeres in these vascular regions, compared to vessels subjected to low hemodynamic stress (Chang and Harley, 1995). Similarly, VSMC from the fibrous cap of atherosclerotic plaques displayed markedly shorter telomeres than medial VSMC from the same lesion. This reduction in telomere length was most likely due to additional cell replication initiated during lesion formation (Matthews *et al.*, 2006).

Vascular stem cells and progenitor cells have a major role in maintaining vascular integrity by replacing apoptotic and damaged vascular cells that occur in response to cardiovascular damage and disease. These cells exhibit increased replicative potential due to the presence of telomerase, which delays senescence compared to cells from the vessel wall. However, the age-related exhaustion of bone marrow vascular progenitor cells correlates with the development of atherosclerosis (Rauscher *et al.*, 2003). In coronary artery disease patients, significantly shorter telomeres and lower telomerase activity were determined in circulating endothelial progenitor cells (EPC) compared to aged-matched healthy cells (Sato *et al.*, 2008). These observations clearly indicate that telomere loss also occurs with ageing of vascular cell lineages and during the development of age-related CVD.

Human genetic disorders that are characterised by premature ageing have helped emphasise the link between telomere loss and ageing. Sufferers of progeroid syndromes such as Werner and Hutchinson-Gilford progeria syndrome, prematurely develop atherosclerosis. Cells derived from these patients undergo premature senescence *in vitro* (Allsopp *et al.*, 1992). Werner syndrome results from a genetic mutation in RecQ helicase, which is required in maintaining genome stability. Murine models of the condition exhibit similar cell ageing characteristics to that observed in humans, with telomere loss having a major role in the pathology of Werner syndrome (Chang *et al.*, 2004). Although the development of atherosclerosis has been described in these

conditions, it does not occur in other premature ageing syndromes associated with short telomeres, such as ataxia telangiectasia (Erusalimsky and Kurz, 2005), which implies that not all age-related phenotypes develop via a telomere-dependent mechanism.

To validate the telomere attrition observed in hVSMC, hTERT protein expression and telomerase activity were determined. The hVSMC model displayed undetectable levels of telomerase, as hTERT expression was undetectable in early passage hVSMC compared with HeLa cells which displayed high levels. The low levels of telomerase in hVSMC supports the replicative telomere loss observed. Nevertheless, it cannot be discounted that the observed effects on telomere length might be due to effects of low telomerase activity present within hVSMC. Human EC and VSMC have been shown to express telomerase following mitogenic stimuli (Minamino and Kourembanas, 2001), but a decline during *in vitro* ageing due to diminished TERT expression, leads to telomere shortening and senescence (Hsiao *et al.*, 1997). This suggests the loss in telomerase may arise from culturing conditions.

The results presented in this thesis demonstrate that Ang II enhances telomere shortening of hVSMC *in vitro*, thereby accelerating senescence. Since Ang II is implicated in many CVD, it suggests a possible source of telomere erosion in many of these age-related conditions. This is consistent with the undetectable levels of telomerase within these cells.

4.5.2 Ang II induced DNA damage

Cells undergo senescence following DNA damage that extensively affects normal cell function, is irreparable or threatens to overwhelm the DNA-repair machinery (Ben-Porath and Weinberg, 2005). Uncapped or dysfunctional telomeres maybe recognized as a form of DNA DSB, as various studies have revealed DNA damage foci at telomeres of senescent cells (d'Adda di Fagagna *et al.*, 2003; Herbig *et al.*, 2004). This indicates that DNA damage may contribute to replicative cell senescence and also induce premature senescence (Chen *et al.*, 2001a; Gorbunova *et al.*, 2002).

H₂O₂ was used to induce oxidative DNA damage in order to initially measure DNA strand breaks in hVSMC using the alkali Comet assay. The dose-dependent increase in % tail DNA observed signified increased DNA damage. This was consistent with observations in senescent human fibroblasts and young fibroblasts treated with H₂O₂ for

a short period (Duan, *et al.*, 2005), as well as in human spermatozoa treated with H₂O₂ (Li *et al.*, 2006b).

Ang II exposure for just 24 hours rapidly induced DNA damage in hVSMC, in a dose-dependent manner. This has not been reported previously in the literature. At high doses, the damage was greater indicating the potential to enhance replicative senescence at these doses. This data is consistent with the hypothesis that the fate of hVSMC exposed to Ang II is dependent upon the magnitude of the incurred DNA damage. Lower levels of damage are thought to induce senescence, whereas higher levels of damage may induce apoptosis (Ben-Porath and Weinberg, 2005). The latter has been observed previously with respect to Ang II exposure at a high concentration of 10⁻⁶ mol/L for 3 days in cultured VSMC (Bascands *et al.*, 2001).

Senescence triggered via DNA damage is mediated by p53 activation which is also the cell cycle regulator through which uncapped telomeres signal replicative senescence (Itahana *et al.*, 2001; Ben-Porath and Weinberg, 2005). p53 forms part of the DNA damage response mechanism, but was not assessed following prolonged Ang II exposure in hVSMC.

One study observing the same trend in DNA damage also used the Comet assay to measure Ang II induced DNA damage in epithelial porcine kidney cells. Low levels of DNA damage were observed and this was inhibited with NAC, implicating Ang II-induced ROS in the induction of DNA damage (Schupp *et al.*, 2007). Furthermore, pre-treatment with Candesartan (AT₁R antagonist) prevented this damage, which suggested Ang II mediated its effects via AT₁R. Similar experiments were performed in this laboratory (see **Appendix I**) demonstrating inhibition with E3174 (AT₁R antagonist). The accumulation of DNA damage has been proposed to contribute to replicative senescence, as senescent fibroblasts displayed higher 8-oxoG DNA base modifications, *in vitro* (Chen *et al.*, 1995).

Damage to DNA can occur in numerous ways, and is associated with many cardiovascular risk factors such as smoking (Fracasso *et al.*, 2006), obesity (de la Maza *et al.*, 2006) and diabetes mellitus (Sampson *et al.*, 2006). Many markers of DNA damage have been identified in various CVD. Indeed, significantly high levels of DNA

strand breaks, oxidized pyrimidines and altered purines have been revealed in coronary artery patients compared with healthy subjects (Botto *et al.*, 2002). High levels of 8-oxoG (oxidative modification of guanine residues in DNA) have been observed in macrophages and VSMC in human atherosclerotic plaques, which is consistent with increased oxidative stress in plaques and senescent VSMC (Matthews, *et al.*, 2006).

ROS are regarded as a major source of chronic persistent DNA damage in cells and are believed to contribute to ageing (Harman, 1972). One recent study using the Comet assay, demonstrated differences in the level of basal DNA damage in lymphocytes in an ageing population. The results showed increased DNA damage with age and reduced DNA repair capacity (Piperakis *et al.*, 2007). These observations suggest DNA damage increases with advancing age and may contribute to promoting replicative senescence, since DNA damage is a known trigger of cellular senescence. However, the link between increased ROS and increased DNA damage with age is not yet proven.

These results presented here demonstrate that Ang II induces DNA damage, in the form of strand breaks, in hVSMC *in vitro*, which may potentially enhance replicative senescence. Evidence of damaged DNA in CVD and with advancing age has further emphasised this link.

4.5.3 Assessment of hVSMC senescence, *in vitro*

4.5.3.1 Morphology of senescent hVSMC

VSMC are known to undergo phenotypic modulation in response to the required function and a more synthetic phenotype is exhibited with cultivation of these cells. The altered morphologic appearance of continuously cultured hVSMC thereby could be misinterpreted as senescence. The appearance of senescent hVSMC needed to be identified to eliminate any of these confounding factors. The appearance of late passage hVSMC displayed many spindle-shaped cells similar to early passage cells (**figure 3.1**). However, the later passage cells were amongst many enlarged and irregular-shaped cells. In addition these cells did not reach confluence which is also indicative of a senescent phenotype. None of these alterations in cellular appearance resembled a synthetic phenotype, as described by Matthews *et al.*, 2006.

Altered gene or protein expression in cells is often associated with the senescent state, but was not examined in this hVSMC model. These markers tend to be specific for the cell type under investigation, and only common senescent genes tend to be upregulated (Pascal *et al.*, 2005). Recently, the increase in cyclin D1 protein expression has been identified as a reproducible marker of replicative senescence of hVSMC, and is proposed a better senescent marker than SA- β -gal (Burton *et al.*, 2007). This is a possible avenue for future study with respect to Ang II-induced senescence.

The state of polyploidy whereby cells contain multiple copies of their genome has been suggested as a potential biomarker of senescence. Rodent models of hypertension and ageing have displayed increased polyploidy in VSMC (reviewed by McCrann *et al.*, 2008), even though this has not been confirmed in conjunction with SA- β -gal staining to establish it as a marker of senescent cells. Accumulating evidence suggests this is another potential morphological marker of senescence that could be associated with vascular disease and ageing. The appearance of senescent VSMC is of the typical senescent morphology, and is distinctly different from the appearance of early passage hVSMC *in vitro*.

4.5.3.2 Optimum parameters for SA- β -gal staining of hVSMC

A common senescent phenotype which is independent of the cell type is the positive staining for SA- β -gal activity (Dimri *et al.*, 1995). Presently, this is the most widely used biomarker for cellular senescence and has been successful in detecting senescent vascular cells *in vitro* (van der Loo *et al.*, 1998; Matthews *et al.*, 2006; Unterluggauer *et al.*, 2007) and within tissues *in situ* (Minamino *et al.*, 2002; Gorgoulis *et al.*, 2005). The cytochemical assay is based on the cleavage of the chromogenic X-gal substrate, which results in the production of a cytoplasmic blue precipitate. The staining reflects lysosomal β -galactosidase activity at the optimum pH 6.0, which is indicative of increased lysosomal content in senescent cells (Dimri *et al.*, 1995; Kurz *et al.*, 2000). Although the SA- β -gal marker is widely used, it has been demonstrated that false positives of cells in culture may occur as a result of stress-induced senescence and in tissue specimens where the presence of phagocytes, which are rich in lysosomes, may result in positive staining (Erusalimsky and Kurz, 2005). To overcome *in vitro* effects in hVSMC and other factors that influence SA- β -gal staining, various parameters were investigated to provide more optimal and reliable results with SA- β -gal staining.

hVSMC seeded at high densities presented 100% confluence and caused 100% SA- β -gal positive cells as similarly described in human fibroblasts (Yang and Hu, 2005); this maybe due to close cell-cell interactions and diminished growth. The optimum seeding density of 5×10^4 cells per well displayed evenly separately cells in 6-well plates, and consistently gave ~10% SA- β -gal positive cells. Complete confluence of early passage cells has been shown to have a confounding effect on SA- β -gal staining (Severino *et al.*, 2000), rendering this marker to be non-specific for measuring replicative senescence of confluent cells.

A 24-hour incubation period of staining was sufficient to detect SA- β -gal activity in hVSMC, as distinct cytoplasmic blue staining was determined in cells compared to just pale staining observed at 4 hours. This factor is important when counting positive and negative stained cells, to allow for the clear discrimination between senescent and non-senescent cells. Although this has not been highlighted by others, the majority of data published using this assay had incubated vascular cells with X-gal solution for 24 hours (van der Loo *et al.*, 1998; Matthews *et al.*, 2006; Unterluggauer *et al.*, 2007).

In response to stress induced by H₂O₂ treatment cells showed an increase in SA- β -gal staining with increasing time (Severino *et al.*, 2000). However the difference in percent senescent cells between doses was unclear. One study showed cells treated with a high concentration of H₂O₂, which were then sub-cultured to re-enter mitosis prior to SA- β -gal staining, showed no difference in the percentage of positive staining when compared to cells that were stained directly after treatment (Yang and Hu, 2005). These results differed to those presented here which examined hVSMC, and displayed differences in the percentage of SA- β -gal positive cells between doses of H₂O₂. Therefore, this may be due to differences in cell type.

The Ang II treatment of hVSMC required cells to be rendered quiescent prior to incubation with inhibitors and Ang II. However, the quiescence state has been shown to dramatically increase SA- β -gal positive cells, culminating in a false positive result. To overcome this effect hVSMC were sub-cultured into media containing 10% (v/v) FCS after treatment to re-enter mitosis before detecting SA- β -gal activity (as described by Yang and Hu, 2005). These authors postulated that senescence detected in quiescent cells is reversible by sub-culturing or placing cells in FCS-containing media.

Even after eliminating many of these assay interferences, the counting of senescent stained and non-senescent unstained cells has still been debated. Recent modifications to the SA- β -gal method have provided a more quantitative measure of senescent cells within a population of stained cells, which may help to rule out the human error incurred with counting senescent cells in randomly selected fields of view. A fluorimetric method using fluorescein di-beta-D-galactopyranoside as the substrate for SA- β -gal in place of X-gal, has demonstrated an increase in fluorescence with replicative senescence (Yang and Hu, 2004). However, the pH of the buffer was later found to be an interfering factor in the assay (Yang and Hu, 2005). This method was attempted within this project, in hVSMC, but gave very variable results. The “Galacton chemiluminescent assay” is reported to provide a more rapid and easy quantitative method for detecting β -galactosidase activity in senescent cells. This assay was found to be successful in detecting and quantifying β -galactosidase activity in replicative and SIPS cells (Bassaneze *et al.*, 2008).

4.5.3.3 Ang II accelerated senescence of hVSMC

Ang II has been widely implicated in normal vascular ageing and in the pathogenesis of CVD (Najjar *et al.*, 2005) such as hypertension and atherosclerosis. The effect of Ang II on vascular cells includes a diverse array of responses (Berk, 2001), extensively through the production of ROS (Touyz and Schiffrin, 2000). Ang II activates the Ras-signalling pathway, which in-turn has been shown to promote vascular cell senescence and inflammation (Minamino *et al.*, 2003). This early piece of evidence suggested a critical role of Ang II in triggering senescence. Rodent models have shown that prolonged inhibition of the RAS delays the development of many age-related changes in the blood vessel, heart and kidneys (Ferder *et al.*, 2002; de Cavanagh *et al.*, 2003; Basso *et al.*, 2007) that are characteristic of senescence *in vivo* and in CVD, which lends support to the idea that Ang II maybe a major factor in inducing these age effects.

SA- β -gal positive cells increased dose-dependently with Ang II exposure over a period of 30 days with continuous cultivation. This data clearly showed Ang II promotes the senescence of hVSMC *in vitro*, resulting in impaired proliferative activity. The representative photomicrographs visually clarified the presence of more enlarged cells expressing SA- β -gal activity following Ang II treatment compared with untreated cells, at the same passage. The maximal induction of Ang II induced senescence was at

10^{-8} mol/L and not after exposure with the highest dose (10^{-7} mol/L). Instead, a lower percentage of SA- β -gal positive cells was observed and this may have been due to a higher percentage of cells undergoing apoptosis than senescence at this dose. Induction of apoptosis was detected at 10^{-7} mol/L Ang II and is discussed in section 4.5.4.

At present no other data has been published showing that Ang II promotes senescence over this length of time and with sub-culturing. However, during the working of this thesis it was shown that Ang II exposure over 3 days increased SA- β -gal staining in cultured hVSMC and suggested Ang II induced premature senescence via a p53/p21-dependent pathway (Kunieda *et al.*, 2006). Another similar study in EPC observed an increase in SA- β -gal activity with Ang II exposure after 14 days, which was shown to be prevented when AT₁R were blocked prior to stimulation (Imanishi *et al.*, 2005a). Over the same period of exposure, rat VSMC underwent senescence in a time-dependent manner following exposure to just one treatment with Ang II (Min *et al.*, 2007). This suggested the Ang II induced senescent response was mediated in a similar manner and extent in other vascular cells grown *in vitro*. In addition to this, accelerated senescence of human EC following exposure to high concentrations of Ang II was demonstrated through the activation of MAPK (Shan *et al.*, 2008), however this was only determined after a single Ang II exposure.

No CVD or age-related vascular alteration can be solely attributed to the senescence inducing effects of Ang II. However, a recent study showed hypertension causes senescence in human kidneys and rat heart and kidneys via p16^{INK4a} induction (Westhoff *et al.*, 2008). Although SA- β -gal activity was not measured in these tissues, the increased expression of p16^{INK4a} did indicate a possible senescence signalling mechanism.

The increased senescent morphology and SA- β -gal activity data observed in hVSMC continuously exposed to Ang II, in addition to accelerated telomere loss and increased DNA damage, strongly suggests that Ang II promotes the normal replicative ageing of hVSMC. This effect may contribute to vascular disease development.

4.5.4 Ang II induced hVSMC apoptosis

The low level of SA- β -gal positive cells determined after continuous Ang II stimulation with 10^{-7} mol/L was an unexpected result. The presence of fewer cells that had adhered following sub-culturing in-conjunction with this observation indicated that exposure at this concentration of Ang II caused apoptosis of hVSMC. For this reason, apoptosis was assessed after Ang II treatment in hVSMC.

Ang II is pleiotropic and it can modulate various different cellular responses in VSMC (Touyz and Schiffrin, 1999). In this hVSMC model, it has already been shown to promote proliferation (**figure 3.5**) and induce senescence (**figure 4.6B**), therefore its role in initiating apoptosis could not be discounted. Ang II induced apoptosis in VSMC is considered to occur via AT₂R activation (Yamada *et al.*, 1998). The presence of these receptors at low levels was confirmed in these hVSMC (**figure 3.4B**).

VSMC apoptosis has been detected in numerous CVD. Atherosclerotic plaques have mainly exhibited increased levels of VSMC apoptosis (Bauriedel *et al.*, 1999), and the loss of medial VSMC results in vessel wall thinning, dilation and eventual rupture of aneurysms (Lopèz-Candales *et al.*, 1997). *In vitro* studies have also revealed that Ang II induces apoptosis of vascular cells (Ravassa *et al.*, 2000; Li *et al.*, 2006a; Ricci *et al.*, 2008).

The chemiluminescent measurement of caspase-3/7 activity revealed a dose-dependent increase with Ang II treatment. No significant change in caspase-3/7 activity was observed with Ang II at 10^{-8} mol/L, which suggested there was no induction of the apoptotic-response pathway following exposure at this dose. Increased caspase-3 activity following Ang II has also been confirmed in rat VSMC (Ruiz *et al.*, 2007).

No significant changes were observed in caspase-8 activity in this model, yet this had been described by Li *et al* (2006a). These authors demonstrated an increase in caspase-8 activity in hVSMC when exposed to Ang II (10^{-7} mol/L) for 24 hours using an absorbance-based assay. However, this increase was relatively small. Rendering these cells quiescent prior to Ang II treatment may have had an effect on caspase-8 activity; therefore even slight changes may have been undetectable. The visual analysis of fragmented and condensed nuclei with Hoechst 33258 staining revealed the greatest

Chapter 4:0 Effect of Ang II on hVSMC senescence

induction of apoptosis after a single treatment with 10^{-7} mol/L Ang II, which coincided with the observed effect of caspase-3/7 activity.

These results demonstrate that exposure to a relatively high concentration of Ang II (10^{-7} mol/L) caused increased apoptosis of hVSMC *in vitro*, which likely outweighed any senescence-induction. The lower concentration of Ang II (10^{-8} mol/L) primarily resulted in senescence rather than apoptosis. This suggests mild Ang II concentrations favour senescence whereas higher concentrations induce apoptosis.

Conclusions

- Ang II promotes telomere loss via AT₁R activation in hVSMC
- Undetectable hTERT protein expression and telomerase activity accounts for the progressive telomere attrition in proliferative hVSMC.
- Ang II causes DNA damage in hVSMC in a dose-dependent manner.
- Senescent hVSMC display the typical morphological characteristics of senescence in other primary human cells *in vitro*.
- Increased SA-β-gal activity and senescent morphology following continuous Ang II exposure accelerates hVSMC senescence.
- Maximum induction of senescence occurred at Ang II concentrations of 10⁻⁸ mol/L, with higher concentrations inducing relatively more apoptosis than senescence.
- Taken together, these data are consistent with the hypothesis that Ang II accelerates replicative senescence in hVSMC, via the induction of DNA damage and telomere attrition.

CHAPTER FIVE

The Induction of Stress-Induced Premature Senescence with Acute Angiotensin II Exposure

Chapter 5.0: The induction of stress-induced premature senescence with acute Angiotensin II exposure

Chapter 4.0 showed that continuous Ang II exposure accelerated the senescence of hVSMC in culture. The typical characteristics of replicative senescence were confirmed; growth arrest, senescent morphology, telomere loss, increased DNA damage and increased SA- β -gal activity. Enhanced telomere attrition and DNA damage were associated with increased senescence following just a single Ang II exposure. This raised the possibility of a much earlier induction of senescence perhaps independent of replication. Stress-induced premature senescence (SIPS) also known as stress aberrant signalling-inducing senescence (STASIS) is one such mechanism that may account for this premature growth arrest. Many human proliferative cells exposed to sub-lethal oxidative stresses or sub-optimal culturing conditions undergo SIPS *in vitro*, independent of telomere erosion and cell division. This has been extensively investigated by the Toussaint group (Chainiaux *et al.*, 2002; de Magalhães *et al.*, 2002; Fripiat *et al.*, 2003).

SIPS has not been investigated in vascular cells even though substantial evidence exists for replicative senescence of hVSMC and human EC *in vitro* (Liao *et al.*, 2000; Carlisle *et al.*, 2002) and *in vivo* (Minamino *et al.*, 2002; 2003). Therefore, since Ang II modulates various cell signalling mechanisms, enhances replicative senescence and is strongly implicated in CVD and vascular ageing, its potential to additionally trigger SIPS was investigated.

5.1 Background

5.1.1 Characteristics of SIPS

Cellular senescence can be triggered by various factors and ROS is a common mediator. Oxidative stress and ROS have been implicated in replicative senescence, but they are also strongly implicated in the induction of SIPS, by inducing a DNA damage-response or as a result of significant damage to cellular components which may trigger early growth arrest and ultimately lead to cell death. SIPS cells are commonly observed in cancer patients treated with radiotherapy (Quick and Gewirtz, 2006). Tissue localised

exposure to high doses of ionizing radiation has demonstrated the induction of SIPS in various cancers, rather than apoptosis (Chang *et al.*, 2002). This suggests that the onset of SIPS prevents cell death, at least initially, thereby resembling the behaviour of replicative senescent cells.

SIPS is defined as the rapid effect of subcytotoxic stresses on proliferating cells leading to premature senescence (Toussaint *et al.*, 2002). This induction of senescence is considered to be triggered by various extrinsic stresses (Ben-Porath and Weinberg, 2005). Subcytotoxic doses of cellular stresses (some experimental) such as ultra violet (UV) radiation, H₂O₂, t-BHP, ethanol, hypoxia, chemotherapeutic agents and ionizing radiation have been demonstrated to induce SIPS in cultured cells (Robles *et al.*, 1999, Dumont *et al.*, 2000b; Chainiaux *et al.*, 2002). However, the overexpression of oncogenes (Serrano *et al.*, 1997) and inadequate culture conditions (Parrinello *et al.*, 2003) can also trigger SIPS. These cells are considered to be resistant to apoptosis as healthy cells exposed to ionizing radiation mainly undergo SIPS instead of apoptosis (Suzuki *et al.*, 2001), suggesting that SIPS is also a tumour suppressor mechanism.

Cells which have undergone SIPS exhibit many of the cellular and molecular characteristics of replicative senescence. These common senescent characteristics have been determined from extensive studies using human fibroblasts and are summarized in **table 5.1**.

Although both forms of senescence exhibit similar phenotypes, the time at which these features are expressed differs. Replicative senescence is programmed at a specific time, i.e. when telomeres become critically short, whereas SIPS is not programmed but the response to a given stress is initiated rapidly when DNA is damaged (Suzuki and Boothman, 2008). Moreover, ROS are implicated in both mechanisms of senescence induction, by the immediate activation of the DNA damage response mechanism and DNA repair. Persistent damage to DNA can ultimately result in deterioration of cellular homeostasis and induce the onset of SIPS. Alternatively, progressive shortening of telomeres leading to dysfunctional telomeres can be recognized as DNA DSB thereby activating the DNA damage response pathway (d'Adda di Fagagna *et al.*, 2003) and resulting in replicative senescence. However, SIPS maybe more closely linked to replicative senescence than we think, as ROS-mediated DNA damage can affect

Table 5.1 Common characteristics determined in both replicative senescence and SIPS in human fibroblasts (*in vitro*)

<i>Common senescent features</i>	<i>Reference</i>
<i>Distinct cell morphology:</i> enlarged; flattened; accumulated granularity in the cytoplasm.	Naka <i>et al.</i> , 2004; Duan <i>et al.</i> , 2005; Straface <i>et al.</i> , 2007
↓ Proliferative capacity	Duan <i>et al.</i> , 2005; Stöckl <i>et al.</i> , 2006; 2007
↑ SA-β-gal activity	Dumont <i>et al.</i> , 2000b; Chainiaux <i>et al.</i> , 2002; Duan <i>et al.</i> , 2005; Straface <i>et al.</i> , 2007
<i>Overexpression of cell cycle regulators:</i> ↑p21 ^(WAF-1) , p16 ^(INK4a) , p53	de Magalhães <i>et al.</i> , 2004; Naka <i>et al.</i> , 2004; Duan <i>et al.</i> , 2005; Stöckl <i>et al.</i> , 2006
underphosphorylated Rb	Dumont <i>et al.</i> , 2000b
<i>Similarities in gene expressions:</i> ↑ apolipoprotein J, caveolin-1, collagenase, COX-2, fibronectin, IGFBP-3, MMP-1, osteonectin, SM22, transferrin receptor	Saretzki <i>et al.</i> , 1998; Dumont <i>et al.</i> , 2000b; Chainiaux <i>et al.</i> , 2002; Pascal <i>et al.</i> , 2005; Zdanov <i>et al.</i> , 2007a; Debacq-Chainiaux <i>et al.</i> , 2008
↓ <i>c-fos</i>	Dumont <i>et al.</i> , 2000a
Telomere attrition	Dumont <i>et al.</i> , 2001; Duan <i>et al.</i> , 2005
<i>Changes in mitochondria:</i> common 4977 bp mtDNA deletion; partial uncoupling of the mtRC	Dumont <i>et al.</i> , 2000b; Stöckl <i>et al.</i> , 2006; 2007

This table summarises the current senescent characteristics of cultured human fibroblasts observed in both replicative and SIPS. *c-fos*, proto-oncogene proteins; COX-2, cyclooxygenase-2; IGFBP-3, insulin-like growth factor-binding protein 3; MMP-1, matrix-metalloproteinase-1; mtDNA, mitochondrial DNA; mtRC, mitochondrial respiratory chain; Rb, retinoblastoma protein; SM22, calcium-binding protein.

telomerase activity and consequently affect the regulation of telomere length (Bertram and Hass, 2008), thereby identifying a molecular link between the two mechanisms. **Figure 5.1** displays the common intracellular downstream signals activated by both forms of senescence.

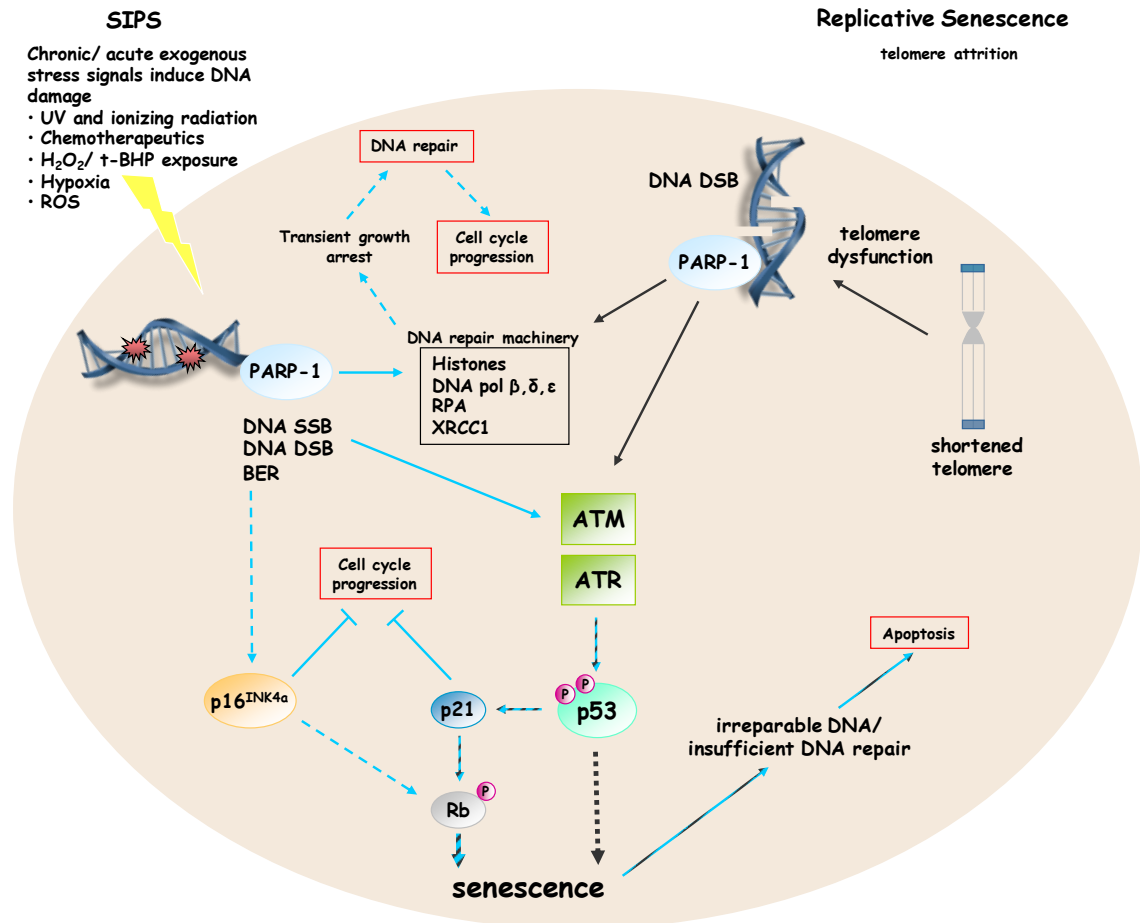


Figure 5.1 Common intracellular signalling mechanisms activated by SIPS and replicative senescence. Various extrinsic stresses that cause ROS generation can induce DNA damage, in the form of base damage, DNA SSB and DSB. Damaged DNA is detected by the nuclear enzyme poly-(ADP)-ribose polymerase-1 (PARP-1). An immediate cell cycle arrest can allow time for sufficient DNA repair (Abraham, 2001) before proceeding via the activation of DNA repair enzymes (e.g. histones, DNA polymerases (pol) β, δ, ε; replication protein A (RPA) and X-ray cross-complementing factor 1 (XRCC1)). Substantial damage triggers a cascade mechanism activating ataxia telangiectasia mutated (ATM) and ataxia telangiectasia and Rad-3-related (ATR), which leads to the phosphorylation of downstream cell cycle regulatory proteins and prevents cell mitosis and progression. The converging signal on p53 and/or pRb initiates cellular senescence. The insufficient repair of DNA or irreparable damage can eventually lead from a state of growth arrest to apoptosis. Replicative senescence similarly activates this DNA damage response, through truncated telomeres being detected as a DNA DSB (d’Adda di Fagagna *et al.*, 2003). Black arrows indicate pathways involved in the induction of the replicative senescence; blue arrows indicate SIPS induction and diagonal-coloured blue and black arrows show activation common to both mechanisms. (Adapted from Ben-Porath and Weinberg, 2005; Bertram and Hass, 2008)

5.1.2 Evidence of SIPS of vascular cells in vitro

Many studies have revealed that vascular cell models undergo replicative senescence *in vitro*, whereas the evidence of SIPS has only started emerging in the last few years. SIPS of VSMC and EC has been demonstrated by exposure to various oxidative stress-inducing agents and is correlated with an increase in inflammation, presenting the idea that premature senescence of these cells *in vivo* may contribute to phenotypic changes in aged vascular tissue and in the early development of CVD.

The constitutive activation of 'Ras', a promoter of cell proliferation and atherogenesis, induced premature senescence of hVSMC with the overexpression of p53 and p16^{INK4a} (Minamino *et al.*, 2003). Additionally, SIPS of human EC has also been observed. Proatherogenic and proinflammatory inducers such as oxidized low-density-lipoproteins, tumour necrosis factor- α and H₂O₂ have been shown to result in SIPS of EC accompanied by reduced telomerase activity, but without telomere loss (Breitschopf *et al.*, 2001). This has similarly been revealed in EC exposed to high concentrations of glucose (Deshpande *et al.*, 2003). However, accelerated telomere shortening has been observed in premature growth arrested cells following exposure to subcytotoxic doses of t-BHP (Kurz *et al.*, 2004), suggesting that it is not an exclusive marker of replicative senescence.

5.1.3 SIPS in age-related CVD

The accumulation of oxidative insults *in vivo* can bring about the induction of SIPS. Cells which have undergone SIPS are likely to participate in tissue alterations that resemble ageing, which may consequently lead to tissue or organ dysfunction (Toussaint *et al.*, 2002).

Alterations in cellular function and the accumulation of ROS-induced cellular damage may favour the onset of systemic disorders, including many CVD. Substantial evidence of replicative senescence in vascular cells with increased inflammation has been found in many age-related CVD (section 4.1.3). Furthermore, the presence of premature senescence has been detected following vascular injury and during disease development. For example, the repeated balloon catheter denudations of rabbit carotid arteries resulted in increased SA- β -gal activity in the injured arteries (Fenton *et al.*, 2001). Although this was suggested to occur from increased proliferation of vascular

cells, the stress mediated by denudations may have led to the onset of premature senescence. VSMC from the fibrous caps of human atheromas exhibit increased SA- β -gal activity, p16 and p21 expression, and telomere loss, but also increased oxidative DNA damage which is mimicked by oxidant exposure to VSMC *in vitro*, (Matthews *et al.*, 2006) suggesting the induction of premature senescence *in vivo*.

Moreover, immunohistochemical detection of insulin-like growth factor-binding protein-5 (IGFBP-5) revealed a high expression only in human atherosclerotic plaques and not in young and old healthy arteries (Kim *et al.*, 2007), which further indicates accelerated senescence in atherosclerosis. Increased levels of the senescent biomarker apolipoprotein J, has been determined in the serum of patients with type II diabetes developing coronary heart disease (Trogakos *et al.*, 2002). This protein has been associated with replicative senescence and SIPS and maybe indicative of the early onset of CVD.

More recently, a subpopulation of peripheral-blood mononuclear cells (PBMC) taken from sufferers of chronic kidney disease (CKD) revealed accelerated telomere attrition, increased p53 expression and overexpression of proinflammatory cytokines. These senescent characteristics were proposed to arise from repeated activation and accelerated proliferation of these cells (Ramirez *et al.*, 2005). CKD is characterized by increased oxidative stress, which is also strongly linked to the induction of SIPS in vascular cells and in atherosclerosis, suggesting that the premature senescence of PBMC may also play a role in other CVD (Tsirpanlis, 2008). Taken together these findings suggest that premature senescence might play a critical role in vascular ageing and throughout the development of vascular pathologies.

5.2 Aims

- Exposure of cells to sub-lethal stresses can initiate SIPS *in vitro*, as described by Toussaint's group (Chainiaux *et al.*, 2002; de Magalhães *et al.*, 2002; Fripiat *et al.*, 2003). To establish whether the hVSMC model undergoes SIPS, SA- β -gal activity was measured following sub-lethal t-BHP stresses.
- Ang II modulates a diverse array of cell signals in VSMC and initiates proliferation, accelerates replicative senescence, and after chronic exposure, induces apoptosis. In order to determine whether a single exposure or whether successive sub-lethal Ang II stresses causes SIPS in hVSMC, senescence was measured by SA- β -gal staining.
- To establish whether acute Ang II treatment promotes ROS production in hVSMC by specifically measuring NAD(P)H oxidase-derived $O_2^{\cdot-}$ generation using the lucigenin chemiluminescence assay.
- To investigate whether a single Ang II exposure affects the expression of cell cycle regulators involved in the induction of senescence. The protein expression of p21 and p53 were analysed via Western blotting.
- To establish whether Ang II-induced SIPS is telomere-independent by determining whether a single Ang II exposure induces premature senescence in hASMC-hTERT.
- To establish whether prolonged Ang II exposure on proliferating hASMC-hTERT promotes cellular senescence.

5.3 Experimental Approach

5.3.1 Cell culture

Early passage hVSMC were grown to near confluence in media containing 10% (v/v) FCS, at 37°C. In the single Ang II treatment protocol, cells were rendered quiescent in media containing 0.5% (v/v) FCS for 24 hours prior to treatment as described in section **2.3.1.1**. Pre-incubation with AT₁R and AT₂R antagonists, and ROS scavengers was performed prior to Ang II exposure.

hASMC-hTERT were grown to near confluence in media containing 20% (v/v) FCS, at 37°C. Cells were then rendered quiescent in media containing 1% (v/v) FCS for 24 hours prior to single Ang II treatments (section **2.3.1.1**). Pre-incubation with the AT₁R antagonist was performed prior to Ang II exposure. Cells continuously cultivated over 34 days were treated with Ang II on alternate days, and on the following days when cells were re-plated (section **2.3.1.3**).

HeLa and Hep G2 cells were grown to confluence in media containing 10% (v/v) FCS, in T75cm² NuncTM flasks (described in **2.3.1.1**), then harvested by trypsinization for Western blotting analysis.

PD were determined to assess hASMC-hTERT proliferation. Cells were seeded at 5×10⁴ cells per T25cm² NuncTM flask, until confluence was reached. Multiple Ang II exposures with 10⁻⁸ and 10⁻⁷ mol/L were conducted on alternate days and on the following days once cells were re-plated. Cells were harvested by trypsinization, resuspended in 0.5ml of fresh media and counted using a haemocytometer. PD and CPD were calculated as described in section **2.3.1.2**.

5.3.2 SIPS induction by t-BHP and Ang II treatments

hVSMC were seeded at 2×10⁴ cells per well in 6-well plates. After 48 hours, cells were rendered quiescent for 24 hours as described in **2.3.1.1**, and then incubated with Ang II (10⁻⁹ and 10⁻⁸ mol/L) for 2 hours. Ang II was removed afterwards by changing the culture media (containing 0.5% (v/v) FCS) to allow for cells to recover for 24 hours

prior to subsequent exposures. Treatment with 40 μ mol/L t-BHP was conducted in the same manner but in media containing 10% (v/v) FCS.

After 3 successive treatments with either Ang II or t-BHP and recovery periods, cells were trypsinized, counted, then re-plated into 6-well plates at 5 \times 10⁴ cells per well in media containing 10% (v/v) FCS. Cells were then analysed for SA- β -gal activity 48 hours after re-plating.

5.3.3 Cellular viability

hVSMC viability upon exposure to t-BHP was assessed using the trypan blue exclusion method (section 2.3.1.5). Cells were seeded at 1 \times 10⁴ cells per well in clear 6-well plates and incubated at 37°C to allow PD. Near confluent cells were treated for 2 hours with t-BHP (20, 40, 60, 80 and 100 μ mol/L) at 37°C. Culture media was then changed with fresh media (containing 10% (v/v) FCS) for 24 hours to allow cells to recover. Following this, cells were trypsinized, resuspended in 1ml of media and then an equal portion was further diluted 1:1 with 0.4% (w/v) trypan blue solution. Transparent and blue-stained cells were counted for each of the different doses using a haemocytometer.

5.3.4 SA- β -gal assay

The SA- β -gal biomarker stain was used to assess cellular senescence following single and successive stress treatments. hVSMC were seeded at 3 \times 10⁴ cells per well in 12-well plates and grown to near confluence for 48 hours, then rendered quiescent for 24 hours (section 2.3.1.1). Exposure to a single Ang II dose (10⁻⁹, 10⁻⁸ and 10⁻⁷ mol/L) was conducted for 24 hours, then cells were re-plated at 1 \times 10⁴/5 \times 10⁴ cells per well. Pre-incubation of cells with the AT₁R and AT₂R antagonists (E3174 (10⁻⁵ mol/L for 1 hour) and PD123319 (10⁻⁵ mol/L for 1 hour)), catalase (300 Units/ml for 3 hours), NAC (500 μ mol/L for 2 hours), SOD (50 Units/ml for 3 hours) and the NAD(P)H oxidase inhibitor apocynin (100 μ mol/L for 1 hour) were performed prior to Ang II exposure at 10⁻⁸ mol/L for 24 hours at 37°C. Following Ang II treatment, cells were trypsinized, counted using a haemocytometer and re-plated at 5 \times 10⁴ cells per well in 12-well plates, in media containing 10% (v/v) FCS. Cells were then left to adhere for 24 hours at 37°C prior to fixation and staining with SA- β -gal solution (section 2.3.2.3).

Chapter 5.0: Stress-induced premature senescence with Ang II

For successive t-BHP stresses, hVSMC were seeded at 2×10^4 cells per well in 6-well plates and left to adhere for 24 hours in media containing 10% (v/v) FCS. Successive 40 $\mu\text{mol/L}$ t-BHP stresses were performed for 2 hours each, followed by a media change (containing 10% (v/v) FCS) for 24 hours to allow cells to recover. This was repeated 3 times over 3 successive days, as described in 5.3.2. After the final recovery period, cells were trypsinized, counted using a haemocytometer and re-plated at 3×10^4 cells per well. SA- β -gal staining was performed on the second and fourth days after re-plating cells.

Successive Ang II (10^{-9} and 10^{-8} mol/L) stresses were performed in a similar manner as described for t-BHP (section 5.3.2), with the exception that cells were rendered quiescent prior to the first stress and during cell recovery following each treatment. These cells were then re-plated at 5×10^4 cells per well in media containing 10% (v/v) FCS for 48 hours before staining for SA- β -gal activity. Pre-incubation with E3174 (10^{-5} mol/L for 1 hour) was conducted prior to each 2-hour Ang II (10^{-8} mol/L) stress.

hASMC-hTERT were seeded at 4×10^4 cells per well in 12-well plates. Near-confluent cells were rendered quiescent in media containing 1% (v/v) FCS (section 2.3.1.1). Cells were treated with a single dose of Ang II (10^{-9} , 10^{-8} and 10^{-7} mol/L) for 24 hours. Following treatment, cells were trypsinized and re-plated at 5×10^4 cells per well in media containing 20% (v/v) FCS to adhere for 24 hours prior to staining. Pre-incubation of cells with E3174 (10^{-5} mol/L for 1 hour) was conducted prior to Ang II (10^{-7} mol/L) exposure for 24 hours.

For 34 days of continuous Ang II treatment, hASMC-hTERT were seeded at 5×10^4 cells per T25cm² NuncTM flask and treated with Ang II (10^{-8} and 10^{-7} mol/L) on alternate days, in media containing 20% (v/v) FCS and on the following days after sub-culturing. After the final treatment, cells were trypsinized, counted using a haemocytometer and re-plated at 5×10^4 cells per well in 12-well plates, prior to staining. SA- β -gal staining was performed on non-confluent cells to avoid non-specific staining. The number of senescent (blue) and non-senescent (transparent) cells were counted manually in five fields selected at random from each well, using a Nikon inverted trinocular phase contrast microscope (under $\times 200$ magnification). Percent senescent cells for each treatment were calculated.

5.3.5 ROS measurements

5.3.5.1 Measurement of Ang II generated intracellular ROS using CM-H₂DCFDA

hVSMC were seeded at 1×10^4 cells per well in clear 96-well microplates and grown to near confluence. Cellular ROS detection was optimized by investigating different concentrations of CM-H₂DCFDA (5, 8 and 10 $\mu\text{mol/L}$). Near-confluent cells were rendered quiescent as described in **2.3.1.1**, for 48 hours prior to Ang II treatment. Firstly, cells were labelled with the fluorescent probe CM-H₂DCFDA for 30 minutes as detailed in section **2.3.4.1**. Cells were either exposed to 20 $\mu\text{mol/L}$ H₂O₂ for 20 minutes or with Ang II for 4 hours at 37°C over a range of concentrations (10^{-10} , 10^{-9} , 10^{-8} and 10^{-7} mol/L). Fluorescence measurements were determined relative to untreated cells loaded with the probe.

5.3.5.2 Measurement of Ang II induced O₂⁻ using lucigenin chemiluminescence

Early passage hVSMC were grown to ~90% confluence in T175cm² NuncTM flasks then rendered quiescent for 24 hours. Cells were stimulated with 10^{-7} mol/L Ang II for 1 hour, with or without pre-incubation with E3174 (10^{-5} mol/L for 1 hour) or apocynin (3×10^{-5} mol/L for 30 minutes). Cells were trypsinized from then flasks, washed twice with cold DPBS, resuspended in ice-cold lysis buffer and sonicated as described in **2.3.4.2**. The protein content of cell lysates was determined using the Bradford protein assay (section **2.3.5.7**). The LCLA was used to measure NAD(P)H oxidase activity as detailed in **2.3.4.2**. The O₂⁻ generated over a range of Ang II incubation periods (1, 8, 12 and 24 hours) with 10^{-7} mol/L was measured, and the specificity of the assay for O₂⁻ generated in 1 hour Ang II-treated hVSMC was examined using AT₁R and ROS inhibitors. Ang II-treated and/or control cell lysates were pre-incubated for 5 minutes at 37°C with DPI, indomethacin, NAC or tiron prior to the addition of the NADPH substrate.

Luminescence was measured at each 40-second interval over 40 minutes in the luminometer. The total quantity of O₂⁻ generated was calculated from the area under the kinetic curve using the trapezoidal rule for each individual reaction.

5.3.6 Western blotting

hTERT, smooth muscle myosin, AT₁R, AT₂R, p21 and p53 protein expressions in hVSMC, hASMC-hTERT, HeLa and Hep G2 cells were determined by Western blotting (section 2.3.6.1).

5.3.6.1 hTERT protein expression

Expression of hTERT was determined in hASMC-hTERT using HeLa cells as a positive control. Cell lysis buffer was used to extract proteins (section 2.3.5.6) from cells grown to confluence in media containing 10% (v/v) FCS. Proteins (30µg protein per sample) were separated on 8% resolving gels under non-reduced and denaturing conditions. Membranes were blocked with 5% (w/v) milk/TBST for 1 hour at RT prior to antibody labelling (table 2.13). Equal protein loading was confirmed by labelling for α-tubulin expression, using 10% (w/v) milk/TBST blocking solution (table 2.12 and 2.14).

5.3.6.2 Human smooth muscle myosin protein expression

To assess whether hASMC-hTERT exhibited a contractile phenotype characteristic of SMC, the expression of smooth muscle myosin heavy chain (SM-MHC) protein was determined. RIPA buffer was used to extract proteins (section 2.3.5.6) from cells grown to confluence in media containing 20% (v/v) FCS and those rendered quiescent in media containing 1% (v/v) FCS. Proteins (30µg protein per sample) were separated on 7% resolving gels under reduced and denaturing conditions. Membranes were blocked with 5% (w/v) milk/TBST O/N at 4°C before antibody labelling (table 2.13). Equal protein loading was confirmed by labelling for α-tubulin expression, using 5% (w/v) milk/TBST blocking solution (table 2.12 and 2.14).

5.3.6.3 Human Ang II receptor subtype protein expression

Expression of human Ang II receptor subtypes (AT₁R and AT₂R) was analysed in hASMC-hTERT and Hep G2 cells. RIPA buffer was used to extract proteins (2.3.5.6) from hASMC-hTERT grown in media containing 20% (v/v) FCS and those rendered quiescent, and from Hep G2 cells grown in media containing 10% (v/v) FCS. Proteins (20/40µg protein per sample for AT₁R/AT₂R respectively) were separated on 8% resolving gels under non-reduced and denaturing conditions. Membranes were blocked with 5% (w/v) BSA/TBST overnight at 4°C prior to antibody labelling (table 2.13).

Equal protein loading was confirmed by labelling for α -tubulin expression for AT₁R labelled membranes, and β -actin for AT₂R labelled membranes, using 5% (^{w/v}) BSA/TBST as the blocking solution for both loading control antibodies (**table 2.12** and **2.14**).

5.3.6.4 Expression of cell cycle regulatory proteins

Expression of the CDKI p21, and the tumour suppressor protein p53, which are involved in regulating the cell cycle, was determined in hVSMC treated with a single concentration of Ang II (10^{-9} , 10^{-8} , and 10^{-7} mol/L) for 1, 4 and 24 hours at 37°C. Cell lysis buffer was used to extract proteins (section **2.3.5.6**) from quiescent cells treated with and without Ang II. Proteins (20 to 40 μ g protein per sample) were separated on 12% resolving gels under reduced and denaturing conditions. Membranes were blocked with 10% (^{w/v}) milk/TBST for 1 hour at RT prior to each antibody labelling, and following membrane stripping for subsequent antibody labelling (**table 2.13**). Equal protein loading was confirmed by labelling for β -actin or α -tubulin, using 10% (^{w/v}) milk/TBST blocking solution (**table 2.12** and **2.14**).

5.4 Results

5.4.1 Induction of SIPS in hVSMC by t-BHP

SIPS and replicative senescence can be triggered via similar intrinsic cell signalling mechanism (as represented in **figure 5.1**). Increased senescence determined in many age-related CVD, may have initially manifested from the induction of premature senescence during early disease development.

In order to study SIPS in cultured cells independent of other adaptive responses, cells were allowed to recover for several days following the last stress before measuring senescence-related biomarkers. This avoided interference from immediate growth arrest induced by the stress and the prolonged effects with continuous cell proliferation (Dumont *et al.*, 2000b). No experimental technique exclusively measures SIPS as yet. Since both forms of senescence display the same phenotypic changes, the commonly used SA- β -gal assay has also been used to detect SIPS. This has been well documented in numerous SIPS experiments (Dumont *et al.*, 2000b; Fenton *et al.*, 2001; Duan *et al.*, 2005).

The induction of SIPS in VSMC has not been previously studied. To establish whether hVSMC undergo SIPS in response to mild oxidative stress, exposure to sublethal t-BHP stresses was performed. t-BHP has been commonly used to induce SIPS in cultured cells (Dumont *et al.*, 2001; 2002).

Concentrations of t-BHP ranging from 0 to 10×10^{-5} mol/L were tested to determine a suitable dose at which sublethal stresses could be performed without inducing significant cell death. Cell viability was therefore measured by trypan blue exclusion after a single 2-hour stress and subsequent 24-hour recovery period. A high percentage of viable cells was maintained in untreated cells and those exposed to 20 μ mol/L t-BHP (~96 and 94% respectively) (**table 5.2**). Slight cytotoxicity was observed with higher concentrations of t-BHP and a significant reduction of ~13 and 16% viability was determined with 80 and 100 μ mol/L t-BHP. Both 40 and 60 μ mol/L t-BHP induced a ~10% reduction in viability. A t-BHP concentration of 40 μ mol/L was chosen to induce

successive stresses in hVSMC, which closely resembled the concentration used to induce SIPS in human fibroblasts (30 μ mol/L) (Dumont *et al.*, 2000b; 2001).

Table 5.2 Trypan blue exclusion of hVSMC exposed to t-BHP

<i>t-BHP concentration (μmol/L)</i>	<i>Trypan blue excluded cells (%)</i>
Control	96.3 \pm 0.8
20	93.9 \pm 0.4
40	88.8 \pm 1.1**
60	90.0 \pm 0.8*
80	87.7 \pm 2.6**
100	84.2 \pm 1.3***

Near confluent cells were exposed to a range of t-BHP concentrations for 2 hours. Following the stress period, cell media was changed with fresh media containing 10% (v/v) FCS to enable cells to recover for 24 hours. Cells were harvested by trypsinization, resuspended in fresh media, stained 1:1 with 0.4% (w/v) trypan blue solution and counted using a haemocytometer. Values are mean \pm SEM; n=3 (*p<0.05, **p<0.01 and ***p<0.001 compared with control).

The experimental protocol used to measure SIPS by SA- β -gal staining was performed after cells were given 24 hours of recovery time following a single or successive stresses. After the final recovery period, cells were re-plated and subsequently incubated with SA- β -gal solution for 24 hours, to reduce non-specific staining.

Sub-confluent hVSMC were submitted to 3 stresses for 2 hours each with 4 \times 10⁻⁵ mol/L t-BHP and allowed to recuperate for 24 hours in-between stresses by changing the culture media. At 3 days, after 3 stresses of t-BHP, the percentage of SA- β -gal positive cells was >2.5-fold greater than control cells (**figure 5.2**). After a further 2 days of recuperation, the percentage of senescence in the control cells was approximately the same as that determined after 3 days. However, t-BHP stressed cells displayed a 3.5-fold increase in positive SA- β -gal cells, which was higher than measured after just 3 days (**figure 5.2**). This indicated that the proportion of SIPS cells increased over time. Taken together these data indicate, for the first time, that hVSMC undergo SIPS in a manner similar to that described for human fibroblasts.

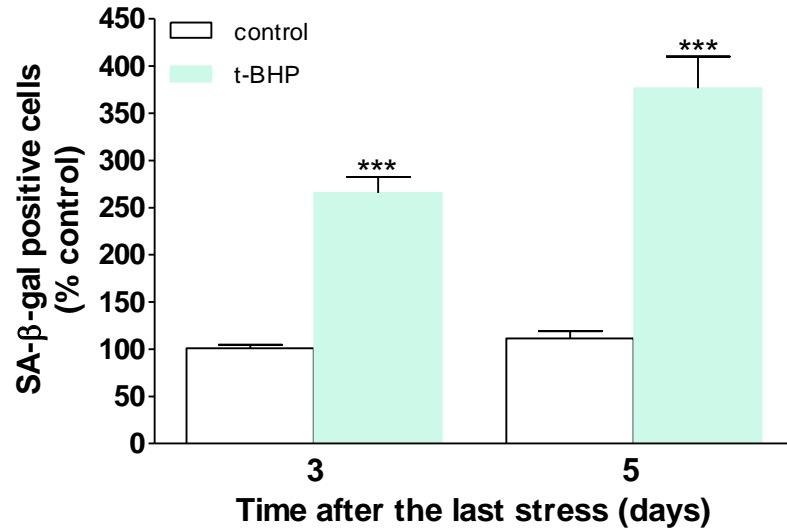


Figure 5.2 Effects of repeated t-BHP stresses on SA-β-gal activity in hVSMC. Early passage hVSMC were grown to ~60% confluence, and then submitted to 3 stresses for 2 hours with 4×10^{-5} mol/L t-BHP in media containing 10% (v/v) FCS. Media in each well was changed following each stress period, which allowed cells to recover for 24 hours prior to subsequent t-BHP stresses. After the last recovery period, cells were trypsinized, counted and re-plated at 3×10^4 cells per well in 12-well plates. Cells were then stained for SA-β-gal activity on the third and fifth days after the final recovery period. Bars represent mean+SEM; n=6 (***)p<0.001 compared with respective controls at each time point).

5.4.2 Premature induction of hVSMC senescence after a single Ang II exposure

SIPS was initially measured after a single exposure of Ang II, followed by sub-culture in media containing 10% (v/v) FCS for 24 hours to allow cells to resume proliferation. This treatment and recovery regime is considered important in the assessment of SIPS in cultured cells (Toussaint *et al.*, 2000).

Ang II induced a dose-dependent increase in cell senescence with a maximal effect at 10^{-8} mol/L (**figure 5.3**). This was a 3-fold increase in senescence compared with control cells. This result exactly coincided with the dose response determined for replicative senescent hVSMC continuously treated with Ang II for 30 days (**figure 4.6B**). Again, a lower percentage of senescent cells was observed with Ang II exposure at 10^{-7} mol/L, which suggests a greater proportion of cells may have undergone apoptosis at this dose.

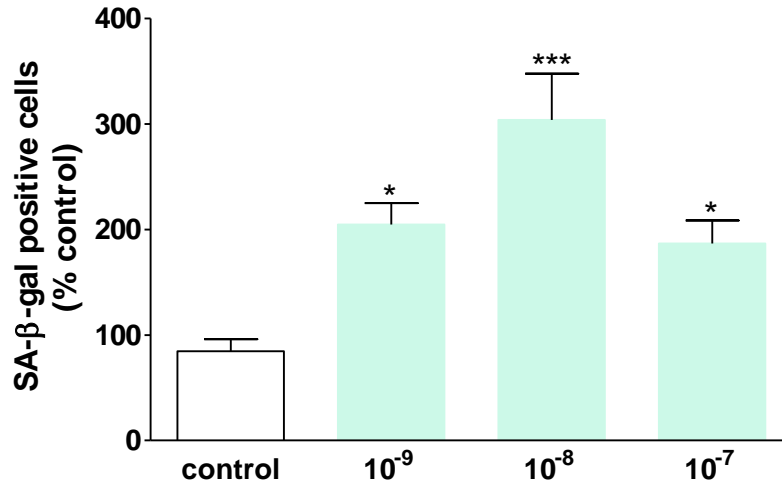


Figure 5.3 A single Ang II exposure induces premature senescence in hVSMC. Quiescent cells were treated with Ang II over a range of concentrations (10^{-9} , 10^{-8} and 10^{-7} mol/L) for 24 hours. Cells were then re-plated at 1×10^4 cells per well in 12-well plates in media containing 10% (v/v) FCS for 24 hours, before staining for SA-β-gal activity. Bars represent mean+SEM; n=5 (*p<0.05 and ***p<0.001 compared with control).

Further experiments were conducted to investigate the cause of this rapid induction of premature senescence by pre-incubating quiescent cells with Ang II receptor inhibitors, ROS scavengers and antioxidants, prior to Ang II exposure with 10^{-8} mol/L for 24 hours. Each individual experiment displayed ~150 to 250% induction of senescence with Ang II treatment. Co-incubation with E3174 (AT₁R inhibitor) completely prevented Ang II-induced SIPS (**figure 5.4A**) whereas PD123319 (AT₂R inhibitor) only marginally prevented this rapid onset of senescence (**figure 5.4B**). This suggested the induction of SIPS to be mainly AT₁R mediated. Unexpectedly, cells pre-incubated with PD123319 alone showed a slight increase in senescence, indicating that inhibiting AT₂R further enhances senescence in hVSMC; however this data was not statistically significant due to few replicates. Co-incubation with catalase or NAC effectively inhibited senescence, without affecting untreated cells (**figure 5.4C and D**). These data suggested increased ROS, specifically H₂O₂, were therefore involved in Ang II-induced SIPS.

Many studies have established Ang II stimulated O₂⁻ to be predominantly mediated via NAD(P)H oxidase activity (Griendling *et al.*, 1994; Touyz *et al.*, 2002; Kimura *et al.*, 2005b) and the expression of several NAD(P)H oxidase subunits to be upregulated following Ang II exposure (Touyz *et al.*, 2002; 2004).

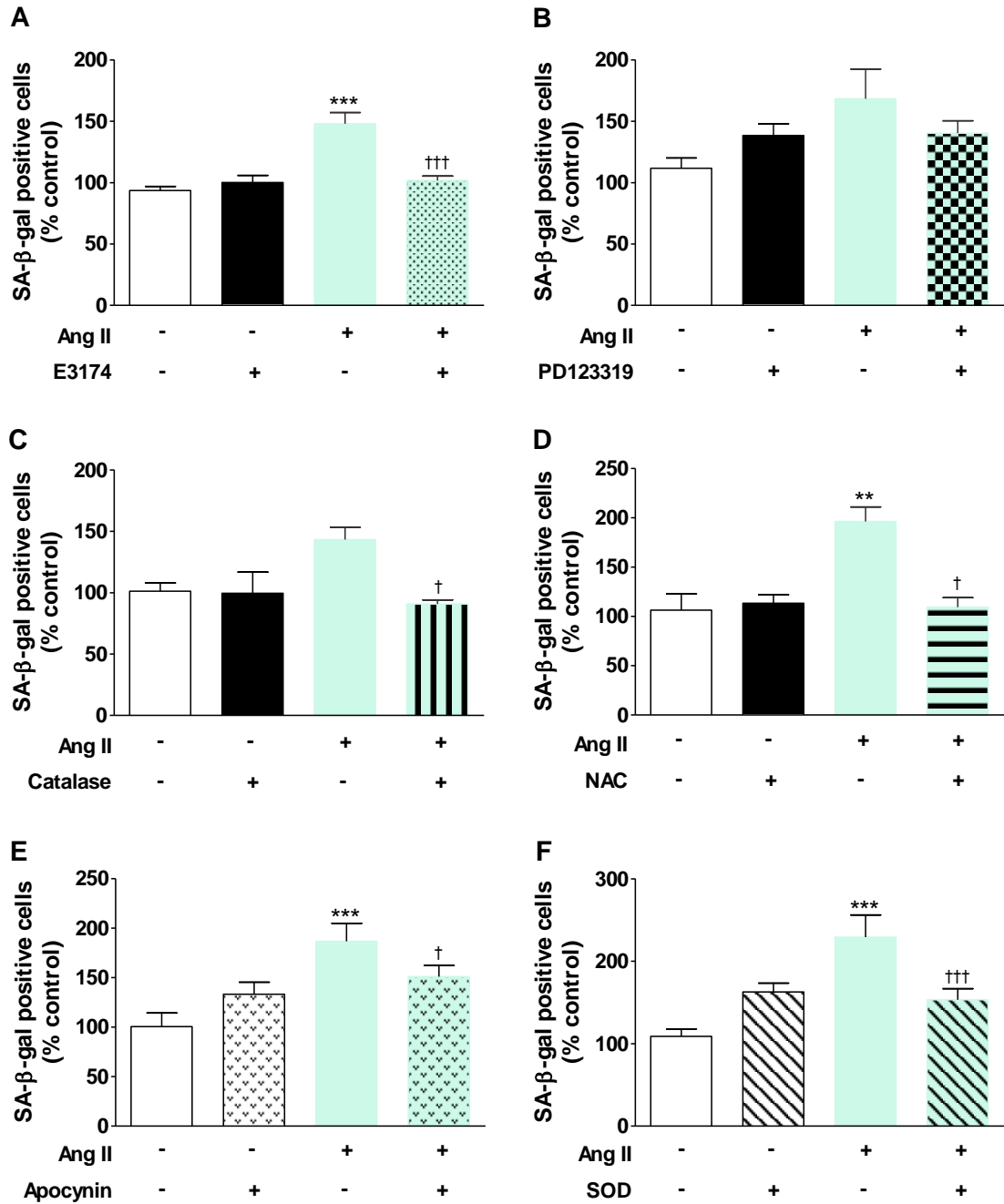


Figure 5.4 Ang II-induced premature senescence is mediated via AT₁R activation and ROS generation. Quiescent cells were pre-incubated with Ang II receptor inhibitors E3174 (AT₁R) or PD123319 (AT₂R), or ROS inhibitors, catalase (H₂O₂ scavenger), NAC (antioxidant), apocynin (inhibits association of NAD(P)H oxidase subunits) and SOD (O₂⁻ scavenger), before the induction of senescence with 10⁻⁸ mol/L Ang II for 24 hours. Each experiment revealed a ~1.5 to 2.5-fold increase in Ang II-induced senescence. **A**, Ang II-induced premature senescence is dependent upon AT₁R activity. Bars represent mean+SEM; n=5 (***)p<0.001 compared with control and †††p<0.001 compared with Ang II alone). **B**, AT₂R inhibition displayed no significant effect on the induction of senescence. Bars represent mean+SEM; n=3 (data was not significant). **C** to **F**, ROS inhibitors prevented the onset of Ang II-induced premature senescence. Bars represent mean+SEM; n=3 to 4 (**p<0.01 and ***p<0.001 compared with respective controls; †p<0.05 and †††p<0.001 compared with respective Ang II alone).

To determine whether the premature induction of senescence was mediated via NAD(P)H oxidase activity, cells were co-incubated with apocynin. Apocynin is a methoxy-substituted catechol that inhibits the association of p47phox and p67phox with gp91phox subunits, that form a functional NAD(P)H oxidase (**figure 1.6**). Over a half of Ang II-induced positive SA- β -gal staining was inhibited with apocynin (**figure 5.4E**), indicating that NAD(P)H oxidase activation is involved in SIPS, whereas pre-incubation with SOD completely prevented senescence induced by Ang II (**figure 5.4F**). Additionally, SOD caused a 0.5-fold increase in senescence in control cells indicating that scavenging basal levels of $O_2^{\cdot-}$ may promote the premature induction of senescence, although this was significant due to few replicates.

5.4.3 Ang II accelerates SIPS in hVSMC

Toussaint *et al* (2002) have suggested a definition of SIPS based upon repeated treatment of cells with suspected senescence inducing agents, such as H_2O_2 , t-BHP and UV radiation (Dumont *et al.*, 2000b; Chainiaux *et al.*, 2002). Ang II induced premature senescence in hVSMC after a single treatment, therefore the response after 3 stresses and 3 recovery periods was also assessed. Many of the stressed cells appeared enlarged in culture prior to staining for SA- β -gal activity, resembling replicative senescent cells. **Figure 5.5A** shows that Ang II induced SIPS with increasing concentration. This is the first direct evidence that Ang II induces SIPS in hVSMC. The maximal induction of senescence (200%) was observed following 10^{-8} mol/L Ang II. This pattern of response was similar to that determined after just a single Ang II exposure.

The cells in this experiment were retained in quiescence to ensure cells were synchronised during Ang II administered stresses and recovery periods. This allowed a more accurate measure of the proportion of cells that had undergone senescence in the population. Cells grown in media containing 10% (v/v) FCS were exposed to Ang II stresses in the same manner and the percentage of positive SA- β -gal cells was measured. Senescence was still induced by 10^{-8} mol/L Ang II and was 1.8-fold higher than the untreated cells (data not shown). This was slightly less than the SIPS induction determined in quiescent cells, as cells were not synchronised thereby Ang II may have initiated proliferation, hypertrophy or apoptosis within some of these cells. However, the growth factors present in FCS did not appear to affect the onset of Ang II-induced SIPS. The mechanism by which Ang II induces SIPS was investigated by co-incubation

with E3174. A partial but significant reduction in SA- β -gal activity revealed SIPS to be mediated via AT₁R (**figure 5.5B**), which was similar to the result determined following a single Ang II exposure.

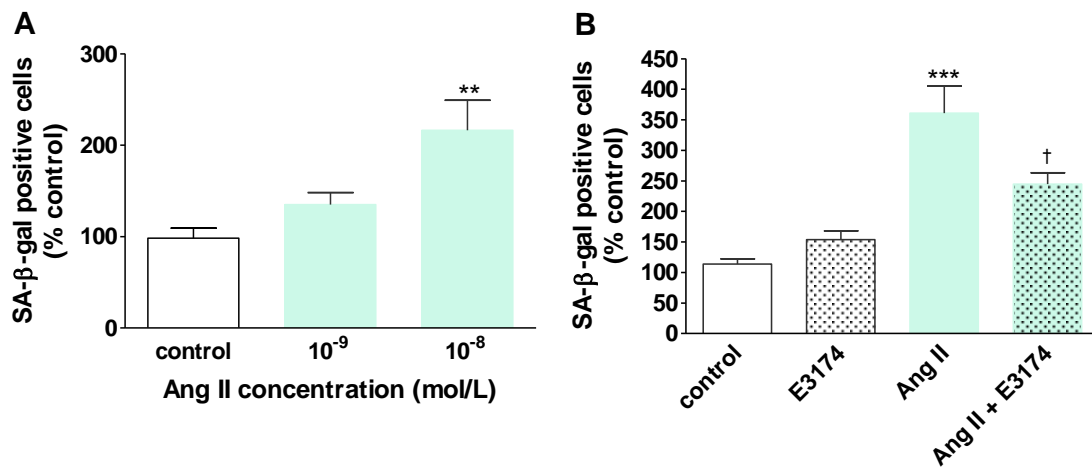


Figure 5.5 Effect of repeated Ang II stresses on SA- β -gal activity in hVSMC. Quiescent cells at ~50% confluence were submitted to 3 stresses with 10⁻⁹ or 10⁻⁸ mol/L Ang II for 2 hours at 37°C. After each stress, the media was changed (containing 0.5% (v/v) FCS) to allow cells to recover for 24 hours prior to subsequent Ang II stresses. After the final recovery period, cells were trypsinized, counted and re-plated at 5×10⁴ cells per well in 12-well plates for 48 hours in media containing 10% (v/v) FCS, before staining for SA- β -gal activity. **A**, Dose-dependent increase in Ang II initiated SIPS. Maximal induction of senescence was observed with 10⁻⁸ mol/L Ang II. Bars represent mean+SEM; n=6 to 9 (**p<0.01 compared with control). **B**, Ang II-induced SIPS is mediated via AT₁R activity. Quiescent cells were pre-incubated with E3174 for 1 hour prior to each Ang II stress. Bars represent mean+SEM; n=5 (***p<0.001 compared with control and †p<0.05 compared with Ang II alone).

5.4.4 Effect of acute Ang II on ROS generation in hVSMC

5.4.4.1 Fluorescent measurement of Ang II stimulated intracellular ROS

ROS are biologically important in vascular biology through their oxidation/reduction potential. ROS generated in a controlled manner at low concentrations act as signalling molecules to regulate VSMC growth and contraction-relaxation by inducing functional effects such as cell growth, apoptosis, migration, inflammation and ECM protein expressions (Griendling *et al.*, 1994; Han *et al.*, 1999; Wang *et al.*, 2001). An imbalance in this redox state where pro-oxidants overwhelm the antioxidant systems leads to oxidative stress. This can cause oxidative damage and cellular dysfunction. These mechanisms are hypothesised to play a role in mediating vascular injury and inflammation that are associated with many CVD (Touyz and Schiffrin, 2004).

$O_2^{\cdot-}$ and H_2O_2 production have been described in VSMC. These are mainly derived from the multi-subunit enzyme NAD(P)H oxidase, which is regulated by various humoral and physical factors. Ang II is one such stimulant that activates NAD(P)H oxidase by increasing the expression and assembly of its subunits, thereby increasing ROS production (Lassègue and Clempus, 2003). Cellular ROS generation, including that resulting from Ang II, is involved in numerous signalling pathways. By studying Ang II-induced ROS production in hVSMC we can decipher some of these pathways and perhaps determine the long-term effects ROS may have on disease development.

Various experimental methods have been developed to characterize and measure ROS production in cell culture models. In this study, the fluoroprobe CM- H_2 DCFDA was initially used to measure Ang II induced intracellular ROS in whole hVSMC. CM- H_2 DCFDA is a chloromethyl derivative of dichlorodihydrofluorescein diacetate (DCFDA) which exhibits better retention in viable cells than DCFDA (Touyz and Schiffrin, 2001). It remains non-fluorescent until the removal of acetate groups by intracellular esterases and subsequent oxidation to form fluorescein derivatives. The ROS generated within a cell can be observed by fluorescence microscopy or flow cytometry and quantified. In this thesis, ROS generation was measured with a fluorescent plate reader. This relatively simple method provides rapid, multiple well readings in a 96-well plate.

CM- H_2 DCFDA labelling of hVSMC was optimized before any cell treatment, to avoid cytotoxicity by the probe. Treatment with H_2O_2 to stimulate intracellular ROS production was used as a positive control. No change in fluorescence was measured over the range of CM- H_2 DCFDA concentrations in untreated cells (**figure 5.6A**), whereas a marginal increase in fluorescence was detected in H_2O_2 -treated cells labelled with $8\mu\text{mol/L}$ CM- H_2 DCFDA. Cells labelled with $10\mu\text{mol/L}$ CM- H_2 DCFDA showed a 2.5-fold increase in fluorescence following H_2O_2 treatment, which indicated that ROS production was being measured using the fluorescent probe at this concentration. This concentration of the fluorescent probe was sufficient in detecting changes in ROS generation in these cells and was used to measure Ang II stimulated ROS.

In order to solely measure the ROS generated upon Ang II stimulation, hVSMC were rendered quiescent then exposed to a range of Ang II concentrations for 4 hours. An increase in fluorescence was determined with 10^{-8} mol/L Ang II, indicating increased ROS generation (**figure 5.6B**). This suggested a greater stimulation of ROS with this Ang II dose than previously reported (Griendling *et al.*, 1994). The data shown in **figure 5.6B** is representative of two other experiments which all showed substantial variations in fluorescent measurements. Numerous experiments and replicates were conducted to measure Ang II mediated ROS and a large variation in results was observed due to differences in cell confluence, loss of cells with treatment and washes, possible leakage of the probe from cells and photo-bleaching of the probe. Measurements using this assay were therefore not considered to be very reliable and so a more sensitive measure of ROS was utilized. The lucigenin assay was used to measure real-time production of ROS, by specifically measuring $O_2^{\cdot -}$ generation.

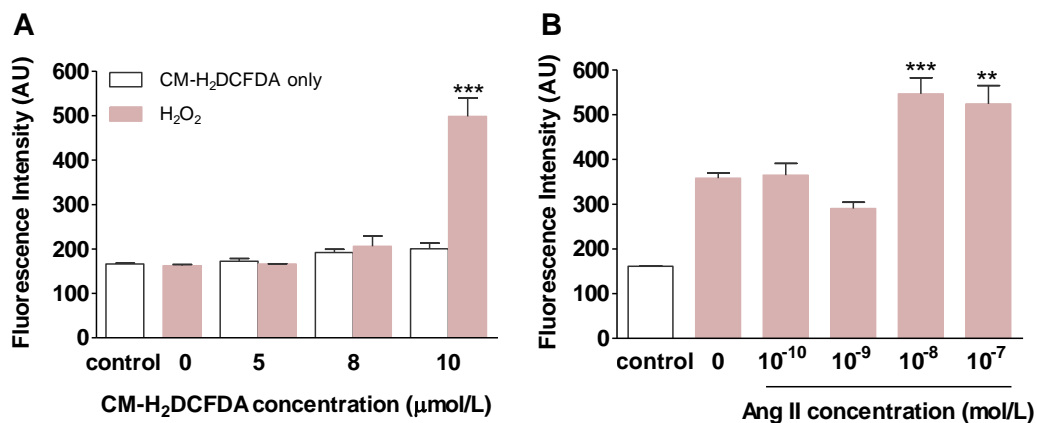


Figure 5.6 H₂O₂ and Ang II stimulate intracellular ROS generation in hVSMC. **A**, Acute H₂O₂ exposure increases intracellular ROS production. Confluent cells were labelled with different concentrations of the CM-H₂DCFDA probe for 30 minutes then treated with H₂O₂ (20μmol/L for 20 minutes) at 37°C. Fluorescence was measured after treatment. Bars represent mean+SEM; n=3 (**p<0.01 and ***p<0.001 compared with H₂O₂ treated cells that were not loaded with CM-H₂DCFDA). **B**, High Ang II concentrations induce increased levels of intracellular ROS generation in hVSMC. Cells were rendered quiescent for 48 hours then labelled with CM-H₂DCFDA (10μmol/L for 30 minutes) prior to Ang II exposure for 4 hours. Bars represent mean+SEM; n=6 to 12 (**p<0.01 and ***p<0.001 compared with untreated cells). (White bar is the fluorescence measurement of cells that were not loaded with CM-H₂DCFDA). AU indicates arbitrary units.

5.4.4.2 Optimization of the LCLA

Preliminary experiments were conducted to optimize conditions of the assay for specifically measuring $O_2^{\cdot-}$ production in hVSMC lysates. The mechanisms of ROS generation were determined by observing the effects of specific and non-specific stimulators and inhibitors of ROS. From these experiments it was found that NADPH mediated $O_2^{\cdot-}$ generation in untreated hVSMC lysates. There was no difference in $O_2^{\cdot-}$ production for cells grown in media containing 10% (v/v) FCS compared with 0.5% (v/v) FCS (figure 5.7A).

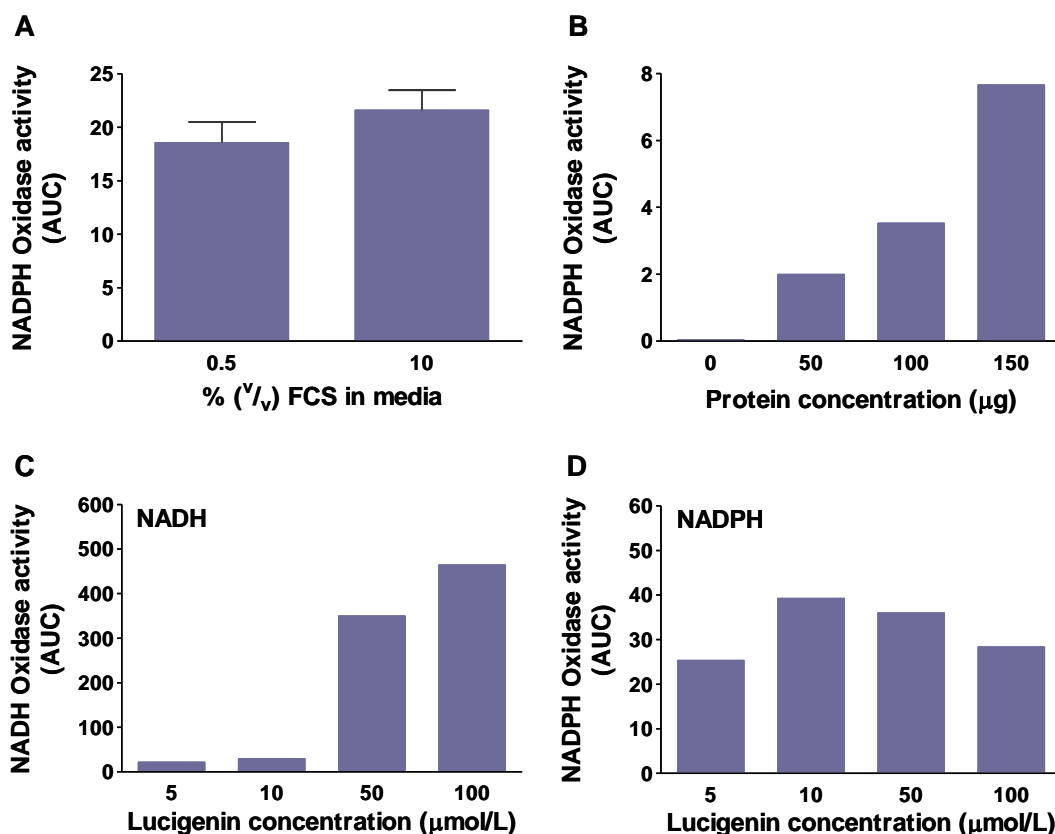


Figure 5.7 Lucigenin-derived chemiluminescence detection of $O_2^{\cdot-}$ generation in hVSMC lysates. **A**, $O_2^{\cdot-}$ generated in hVSMC does not differ between those rendered quiescent for 24 hours or those grown in media containing 10% (v/v) FCS. Chemiluminescence was determined in the presence of 10µmol/L lucigenin. Bars represent mean+SEM; n=6. **B**, NADPH oxidase activity increases in a protein concentration-dependent manner (0 to 150µg protein). Bars display the total amount of $O_2^{\cdot-}$ generated over 40 minutes in the presence of different protein concentrations, n=1. **C** and **D**, NADH-mediated $O_2^{\cdot-}$ generation increases with lucigenin concentration. A low concentration of lucigenin (10µmol/L) can be used to measure NADPH-mediated $O_2^{\cdot-}$ generation. Bars represent mean; n=2. NAD(P)H oxidase activity refers to the AUC, derived from the relative light units (RLU) per minute per 100µg protein (RLU/min/100µg protein), over 40 minutes (except for graph **B** where the amount of protein is different for each individual reaction). AUC indicates total area under the curve.

The same result was observed with NADH stimulated $O_2^{\cdot-}$, but a lower quantity of $O_2^{\cdot-}$ was generated (data not shown). This suggested that basal levels of ROS production were not affected by the withdrawal of serum and would therefore not likely affect measurements of Ang II induced $O_2^{\cdot-}$.

The total generation of NAD(P)H mediated $O_2^{\cdot-}$ from untreated hVSMC over a period of 40 minutes was determined to be relatively low compared with HEK293 cells and B-lymphocytes (data not shown). So to obtain a sufficient measurement of ROS the quantity of protein lysate needed per reaction had to be optimized. Generation of $O_2^{\cdot-}$ in hVSMC increased in a dose-dependent manner with amount of protein lysate, as demonstrated in **figure 5.7B**. One hundred micrograms protein was deduced as sufficient to use per reaction to measure $O_2^{\cdot-}$ over a 40-minute period.

The concentration of lucigenin is important in measuring $O_2^{\cdot-}$ production, as it has been suggested that at high concentrations redox-cycling occurs, which further generates $O_2^{\cdot-}$ (Skatchkov *et al.*, 1999) and therefore is not a true measure of the cellular $O_2^{\cdot-}$ generated. Increasing concentrations of lucigenin caused an increase in NADH-mediated $O_2^{\cdot-}$ (**figure 5.7C**), indicating redox-cycling. However, a 10 μ mol/L concentration of lucigenin was found to give an optimum measure of $O_2^{\cdot-}$ generation via NADPH oxidase activity (**figure 5.7D**) and furthermore the level of $O_2^{\cdot-}$ detected did not increase with lucigenin concentration, suggesting auto-oxidation was less of a problem with NADPH compared with NADH. This concentration of lucigenin was used in all $O_2^{\cdot-}$ measurements for hVSMC.

5.4.4.3 Ang II induces NADPH oxidase mediated $O_2^{\cdot-}$ production in hVSMC

Initial experiments were conducted to deduce the source of ROS generation in hVSMC, by measuring the effects of stimulators and inhibitors of ROS. NADPH induced a 3 to 4-fold increase in $O_2^{\cdot-}$ compared with control cells (**figure 5.8A**). In comparison to this NADH was relatively ineffective (~1.5-fold increase). Mitochondria and xanthine oxidoreductase appeared not to be significant sources of $O_2^{\cdot-}$ in these unstimulated cells, since neither antimycin A/succinate (donating electrons via the mtRC complex II) nor xanthine promoted lucigenin chemiluminescence (**figure 5.8A**).

The $O_2^{\cdot-}$ generated by NADPH was significantly inhibited when lysates were pre-incubated with DPI (flavoprotein inhibitor) and with tiron ($O_2^{\cdot-}$ scavenger) (**figure 5.8B**), suggesting the involvement of NADPH oxidase and that $O_2^{\cdot-}$ is specifically generated. The mechanism involving cyclooxygenase did not contribute to $O_2^{\cdot-}$ generation via NADPH, as indomethacin (20 μ mol/L) did not significantly decrease chemiluminescence.

Inhibition of the mtRC complex I with a low concentration of rotenone (10 μ mol/L) showed a 13 ± 2 (SEM) % inhibition of NADPH-mediated $O_2^{\cdot-}$ in hVSMC. This was statistically significant (n=4; p<0.05 compared with cells stimulated with NADPH alone), suggesting that further production of $O_2^{\cdot-}$ may occur via mitochondria (chapter 6.0). However, inhibition with a higher rotenone concentration of 50 μ mol/L showed a greater inhibition of $O_2^{\cdot-}$ of 28 ± 11 (SEM) % (n=4), however this was not significant due to the great variability in the percentage of inhibition determined for several repeat reactions. A possible reason for this is that high concentrations of rotenone may inhibit the chemiluminescence reaction. Taken together, these data show that $O_2^{\cdot-}$ production in hVSMC is predominantly mediated by NADPH oxidase activity.

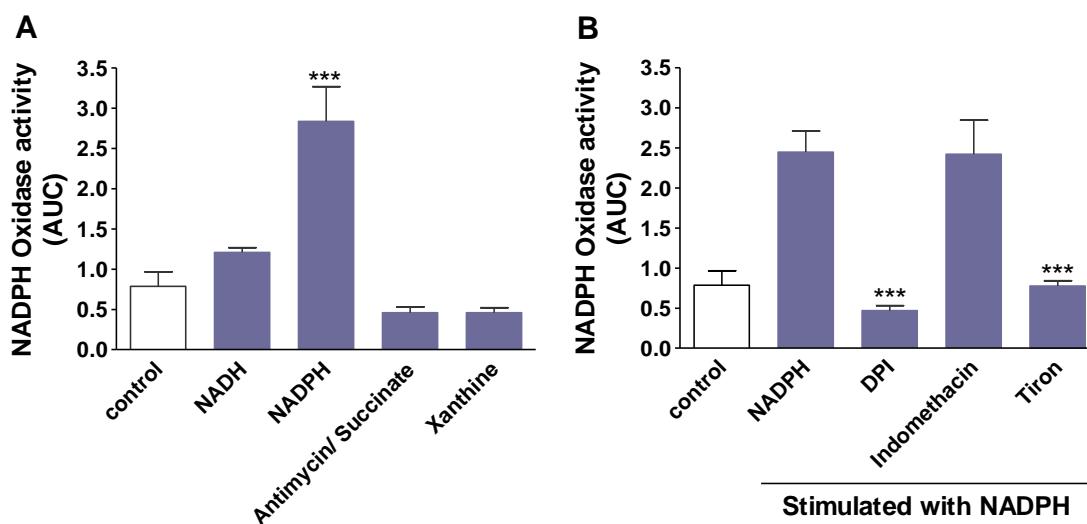


Figure 5.8 NADPH oxidase activity is the major source of $O_2^{\cdot-}$ production in untreated hVSMC. **A**, $O_2^{\cdot-}$ generation was predominantly stimulated by NADPH in cell lysates. Bars represent mean+SEM; n=4 (NADH, n=3) (***)p<0.001 compared with control). **B**, NADPH-mediated $O_2^{\cdot-}$ production was blocked by DPI and tiron. Cyclooxygenase (inhibited by indomethacin) and the mtRC (inhibited at complex I by rotenone) were not significant sources of $O_2^{\cdot-}$ induction in hVSMC. Bars represent mean+SEM; n=3 to 4 (***)p<0.001 compared with NADPH alone). Units are represented as RLU/min/100 μ g protein (AUC) over 40 minutes.

The $O_2^{\cdot-}$ generated via NADPH oxidase activity was significantly increased in cells stimulated with Ang II (10^{-7} mol/L for 1 hour) (**figure 5.9A**). Quantitation of the total AUC from the first 40 minute readings revealed that as little as 1 hour exposure of Ang II was sufficient to potentiate $O_2^{\cdot-}$ production in response to NADPH; this was consistent with reports in human arterial VSMC (Touyz *et al.*, 2002). However, the effect of Ang II in these cells was very rapid compared to the original description for rat aortic VSMC, which suggested 4 hours Ang II stimulation was required to elicit $O_2^{\cdot-}$ production (Griendling *et al.*, 1994). Moreover, Ang II induced $O_2^{\cdot-}$ in hVSMC in a time-dependent manner that persisted for up to 24 hours after the addition of Ang II (**figure 5.9B**).

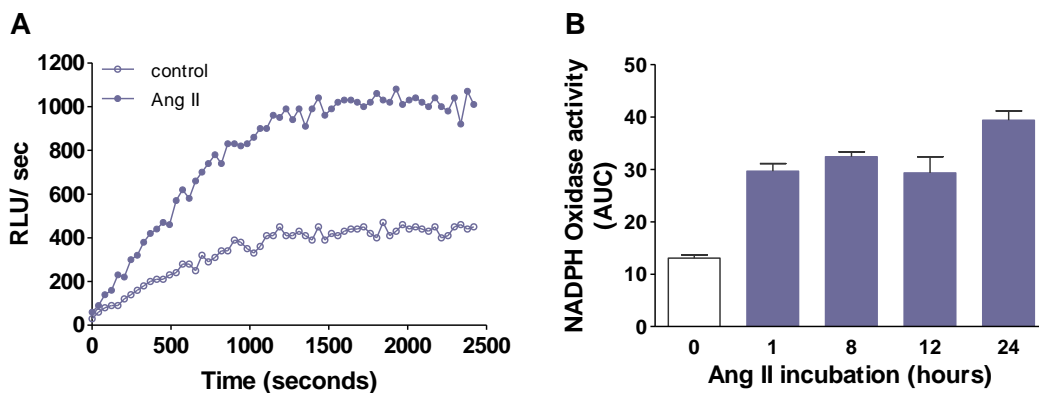


Figure 5.9 Ang II induces NADPH-mediated $O_2^{\cdot-}$ generation in hVSMC. Lucigenin chemiluminescence was used to detect NADPH oxidase derived $O_2^{\cdot-}$ generation from 100 μ g protein cell lysate. **A**, Real-time chemiluminescence measurements of hVSMC treated with acute Ang II (10^{-7} mol/L for 1 hour) relative to control cells. $O_2^{\cdot-}$ generation determined at 40-second intervals was plotted over a period of 40 minutes. Data is representative of 4 separate experiments. Empty circles represent RLU/sec of untreated cells and filled circles represent Ang II treated cells. **B**, Time-dependent increase in $O_2^{\cdot-}$ production with Ang II (10^{-7} mol/L) treatment. Quiescent cells were exposed to Ang II for the indicated time-points. Bars represent mean+SEM; n=5 ($p < 0.001$ for all time-points compared with untreated cells (0 hours)). RLU/sec refers to the relative light units per second.

Upon confirming that Ang II accentuates $O_2^{\cdot-}$ production, the sources and mechanisms involved in mediating ROS generation needed to be determined. Pre-incubation with either apocynin or DPI showed inhibition (48 and 30% respectively) of the Ang II-induced chemiluminescence, which indicated that $O_2^{\cdot-}$ was likely, derived from NADPH oxidase activity (**table 5.3**). Some inhibition was observed with pre-incubation of cells with the potent, selective AT₁R inhibitor E3174 for 1 hour, followed by 1-hour Ang II stimulation; however this did not reach statistical significance. A substantial inhibition of $O_2^{\cdot-}$ was expected with this inhibitor, however only a short Ang II

exposure was conducted in this experiment, which may explain the marginal inhibition. Pre-incubation with NAC caused an 82% inhibition of Ang II-stimulated $O_2^{\cdot-}$, which strongly showed that ROS production was elevated in response to acute Ang II, as NAC acts as an antioxidant by scavenging free radicals and increasing glutathione levels within cells. The addition of tiron, a relatively selective and non-toxic $O_2^{\cdot-}$ scavenger inhibited chemiluminescence, confirming $O_2^{\cdot-}$ was being detected.

Table 5.3 Inhibition of acute Ang II stimulated $O_2^{\cdot-}$ via antagonists of AT₁R, NAD(P)H oxidase and ROS, in hVSMC lysates

<i>Inhibitor</i>	<i>n</i>	<i>Inhibition of Ang II stimulated $O_2^{\cdot-}$ (%)</i>
Apocynin (100 μ mol/L)	3	48 \pm 2.7 ^{†††}
DPI (50 μ mol/L)	2	30
E3174 (10 μ mol/L)	4	20 \pm 14.8
NAC (10mmol/L)	4	82 \pm 1.9 ^{†††}
Tiron (10mmol/L)	4	36 \pm 10.2

Quiescent cells were pre-incubated with apocynin and E3174 for different periods of time (described in 5.3.5.2) prior to a single Ang II (10^{-7} mol/L) exposure for 1 hour. The final concentrations of inhibitors used are detailed in brackets. Ang II induced $O_2^{\cdot-}$ was ~1.6 to 2.6 RLU/min/100 μ g protein (AUC) in all experiments. Values are mean \pm SEM of percentage inhibition of chemiluminescence relative to Ang II alone (^{†††}p<0.001 compared with Ang II).

5.4.5 Effect of Ang II on cell cycle regulation in hVSMC

Cell cycle regulatory proteins have a critical role in the induction of cellular senescence. CDKI such as p16 and p21, act as brakes to stop cell cycle progression in response to cell signalling and stresses. The overexpression of tumour suppressor proteins p53 and pRb are also initiated in the DNA-damage response pathway (**figure 5.1**), and has also been shown to have a key role in triggering senescence (Itahana *et al.*, 2001). The different causes and severity of cellular stresses can determine the degree of p53 and pRb activation initiated, which also varies in different cell types. Replicative senescence is associated with p53 induction in response to telomere shortening, but is also similarly detected along with p21^{Cip1} in the acute onset of SIPS triggered by cellular stress such as oxidative stress (Chen *et al.*, 2000; Dumont *et al.*, 2000b).

The conclusive assessment of changes in protein expression between individual samples requires correction for protein loading. Equal protein loading of hVSMC protein lysates was initially assessed by labelling for β -actin expression. However, the β -actin protein

bands appeared heavily saturated, making it difficult to quantify proteins objectively. Therefore, different amounts of HeLa cell lysates were loaded and labelled for β -actin and α -tubulin (additionally used to determine equal protein loading) to distinguish differences in band intensities. Differences were observed with labelling for α -tubulin, with increased intensity observed with increasing protein concentration, particularly at 10 μ g and above. This was not true for β -actin (blots shown in **figure 5.10**). This showed that, under these conditions α -tubulin was more reliable as a protein loading control. The band intensities for β -actin were very intense and merged with the bands in the adjacent lanes, making it difficult to analyse via densitometry. In fact, in the dark, the ECL signal could be visualised by eye, with the signal being detected even after several hours. It is possible with further optimisation, for example more highly diluted primary antibody, for the detection of β -actin to be made more quantitative. This was not investigated further. Therefore, α -tubulin was used to ensure equal protein loading of Ang II treated hVSMC, and was used for Western blots performed to determine AT₁R, hTERT, p21, p53 and SM-MHC expression.

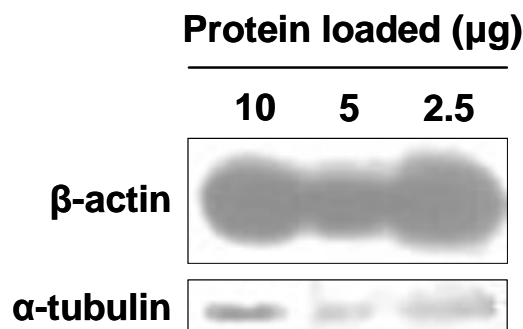


Figure 5.10 Differences in protein loading detected with α -tubulin for Western blot analysis. Different quantities of HeLa cell lysate were loaded then labelled with antibodies against β -actin (1:10,000) or α -tubulin (1:10,000) for various incubation periods, followed by detection with the secondary antibody (rabbit-anti-mouse IgG HRP, 1:10,000) for 1 hour at RT. Representative blots show the expression determined after primary antibodies had been incubated at RT for 15 minutes. Differences in the ECL signal (exposure of autoradiograph for 30 seconds) were determined for protein bands labelled with α -tubulin but not with β -actin.

Exposure of quiescent hVSMC to a range of Ang II concentrations for 4 or 24 hours induced no significant change in p16 protein expression (data not shown). Even though it has been associated with the induction of premature senescence, Ang II may not act via this mechanism. Ang II (10^{-7} mol/L) exposure over a range of times showed no substantial change in p21 (data not shown), however changes in p53 led to investigating whether Ang II induced changes at a later time-point (**figure 5.11A**).

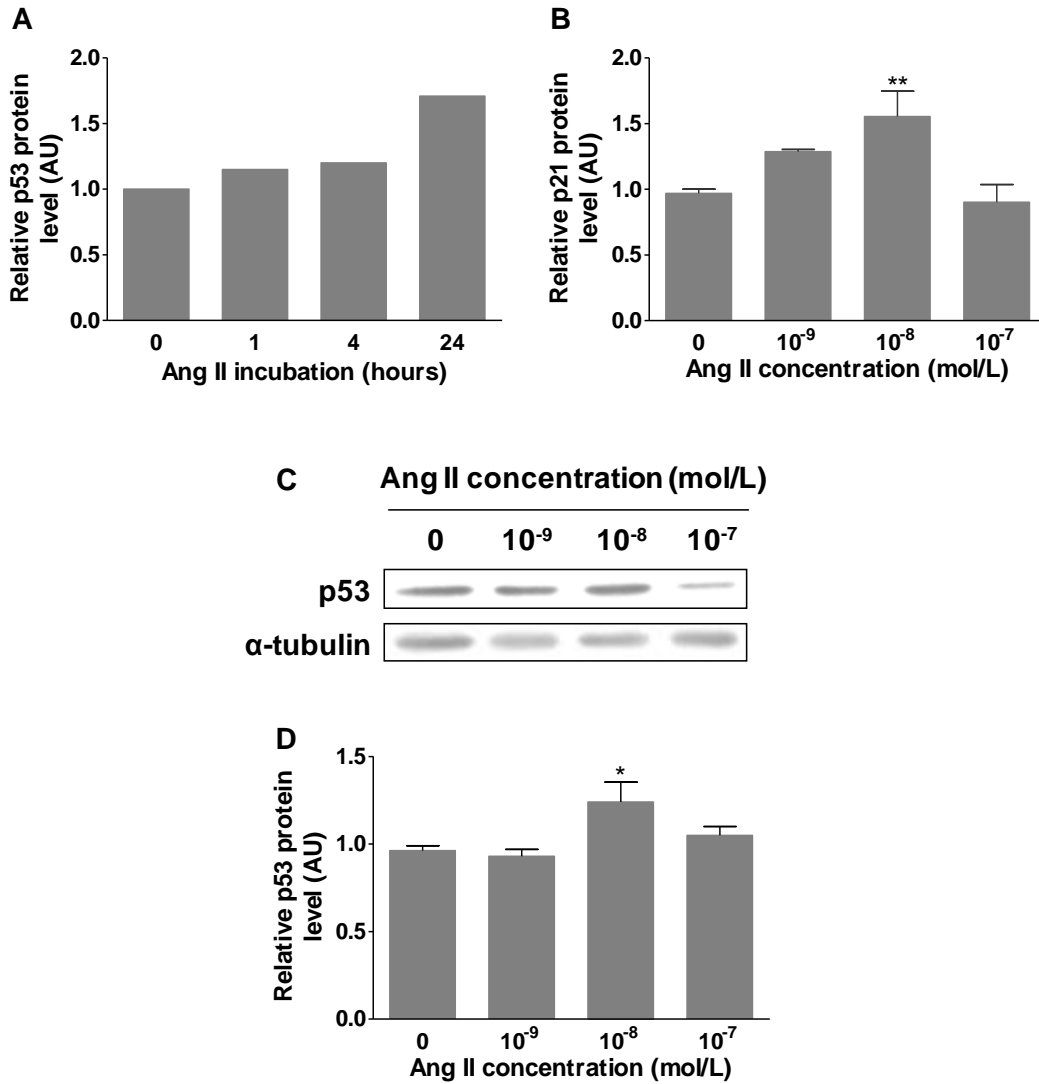


Figure 5.11 Western analyses of p21 and p53 protein expression levels in hVSMC treated with Ang II. Near-confluent cells were rendered quiescent prior to Ang II exposure. hVSMC were harvested by trypsinization, lysed in chilled cell lysis buffer, protein levels quantified and between 20-40 μ g loaded per sample. **A**, Time-dependent increase in p53 expression following Ang II induction. Quiescent cells were exposed to Ang II (10^{-7} mol/L) for 1, 4 and 24 hours. Bars represent p53 expression levels relative to a control at same time-points. **B**, p21 protein expression in Ang II treated hVSMC, over a range of concentrations (10^{-9} , 10^{-8} and 10^{-7} mol/L) for 24 hours. Bars represent mean+SEM, n=3 to 4 (**p<0.01 compared with untreated cells). **C**, Representative blots display the expression levels of p53 protein following 24 hours of Ang II exposure over a range of concentrations. **D**, p53 protein expression in Ang II treated hVSMC for 24 hours. Protein bands were quantified by densitometry, corrected for α -tubulin expression and the mean relative p53 protein expression was plotted. Bars represent mean+SEM; n=4 (*p<0.05 compared with untreated cells).

A time-dependent increase in p53 expression was determined when analysed by densitometry, with >1.5-fold increase determined after 24 hours (**figure 5.11A**). Ang II exposure for 24 hours induced an increase in p21 and p53 expression with maximal induction of both at 10^{-8} mol/L (**figure 5.11B, C and D**). These data support the increased percent premature senescence observed with SA- β -gal staining following Ang II treatment for 24 hours; particularly the maximal effect at 10^{-8} mol/L Ang II. This was assessed visually (representative p53 blots shown in **figure 5.11C**) and after densitometric analysis (**figure 5.11B and D**) which was corrected for α -tubulin expression.

5.4.6 Induction of premature senescence in hASMC-hTERT cells

5.4.6.1 Characterisation of hASMC-hTERT

The mechanism of Ang II induced senescence in the hVSMC model was investigated further by conducting experiments with hASMC-hTERT (kind gift from Professor Laura Niklason (Yale University, USA)).

To confirm that these cells were stably transfected with hTERT, the growth rate and the protein expression of hTERT was examined. hASMC-hTERT were continuously cultivated in media containing 20% (v/v) FCS for >20 days, and displayed an exponential growth curve (**figure 5.12A**), with no indication of a decline in PD. This verified published data on these cells of continuous growth *in vitro* for >365 days (Klinger *et al.*, 2006).

Western blotting showed hTERT protein was highly expressed in hASMC-hTERT. HeLa cells (positive control) also expressed hTERT but very little expression was detected in hVSMC (**figure 5.12B**). The intense bands detected in HeLa and hASMC-hTERT confirmed the expression of telomerase within these cells, although telomerase activity was not assessed directly.

To establish whether hASMC-hTERT were still phenotypically SMC, characteristics of morphology, growth and cytoskeletal protein expression of SM-MHC were investigated. Confluent, hASMC-hTERT appeared much smaller in size than hVSMC and epithelioid in shape. They grew as a monolayer with a cobblestone appearance at confluence, which is distinctive of a synthetic SMC phenotype (Rensen, *et al.*, 2007).

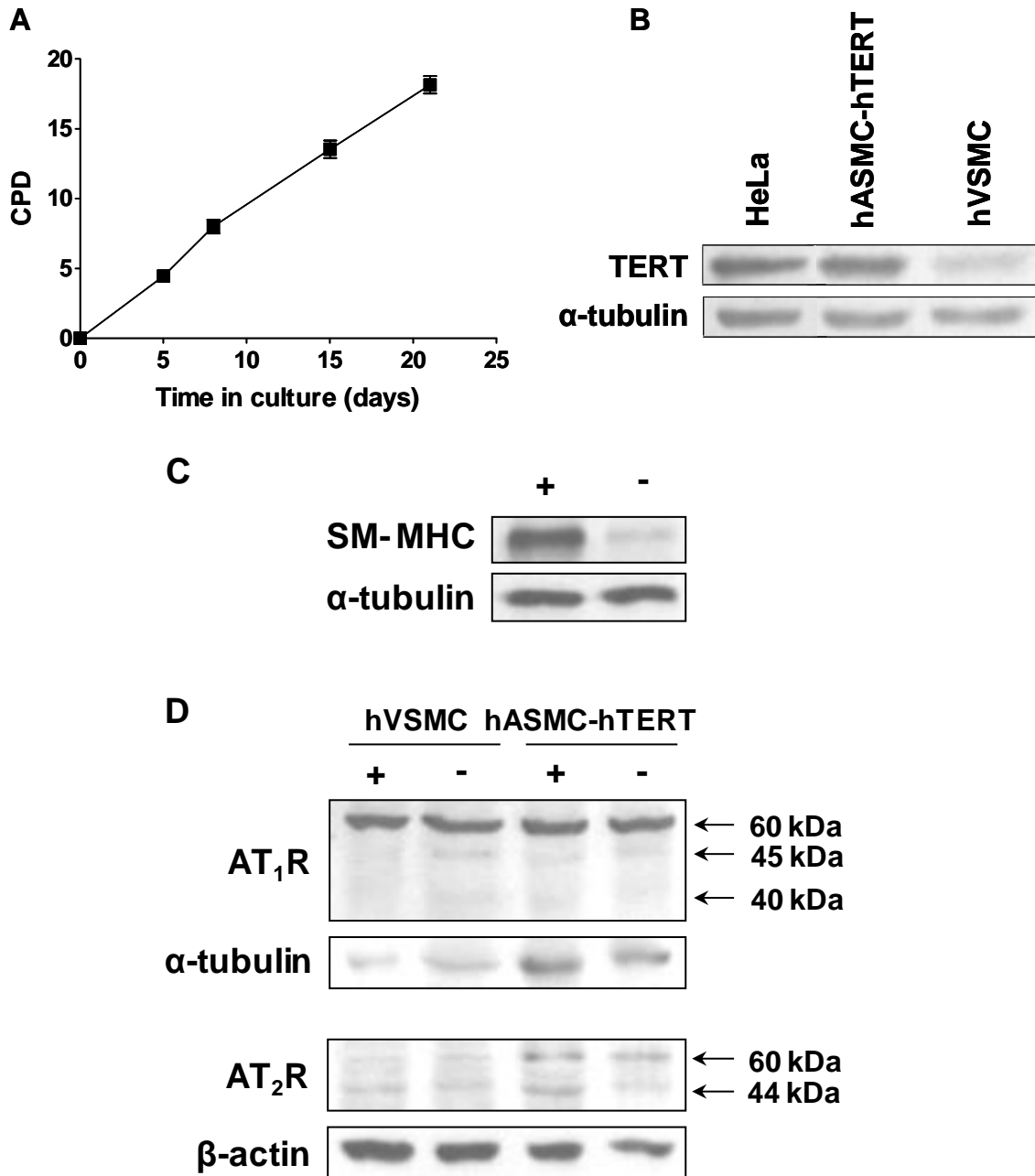


Figure 5.12 hASMC-hTERT exhibit many typical characteristics of SMC *in vitro*. **A**, Exponential growth curve of hASMC-hTERT. Values represent mean \pm SEM; n=3. **B**, Confirmation of hTERT protein expression in hASMC-hTERT. Representative blot shows hTERT expression determined in 40 μ g of whole cell protein loaded per sample (band approximately 90kDa). Equal protein loading was validated by α -tubulin expression. **C**, hASMC-hTERT display a contractile phenotype. Cells grown in media containing 20% (v/v) FCS (+) and those rendered quiescent in media containing 1% (v/v) FCS (-) are represented. Western blot shows SM-MHC and α -tubulin (loading control) protein expression in 30 μ g protein loaded per sample (intense band detected at ~200kDa). **D**, Ang II receptor subtype protein expression in hASMC-hTERT. Cells grown in media containing 20% (v/v) FCS (+) and those rendered quiescent in media containing 1% (v/v) FCS (-) are represented. Western blots show human AT₁R and α -tubulin (loading control) protein expression in 20 μ g protein loaded per sample, whereas 40 μ g protein was loaded per sample to determine human AT₂R and β -actin (loading control) expression.

Moreover, these cells exhibited a faster growth rate than hVSMC, of ~1.1 PD per day compared with typically 0.4 PD per day at the exponential stage of hVSMC cultures, which is characteristic of synthetic SMC *in vitro* (Hao *et al.*, 2003). However, the unexpected expression of SM-MHC protein implied a contractile phenotype in hASMC-hTERT. An intense band was observed in cells grown in media containing 20% (v/v) FCS which was absent when cells were grown in 1% (v/v) FCS (**figure 5.12C**). Overall, these data confirmed that hASMC-hTERT were SMC but that we were unable to definitely assign either a solely contractile or synthetic phenotype.

The protein expression of human AT₁R and AT₂R was determined in actively proliferating hASMC-hTERT and those rendered quiescent once confluence was reached. This was to establish whether hASMC-hTERT would respond to Ang II if they were either synchronized or non-synchronized. All hASMC-hTERT grown in either media containing 20% (v/v) FCS or rendered quiescent for 24 hours, expressed the AT₁R and AT₂R proteins (**figure 5.12D**). The most intense immunoreactive band observed for AT₁R was at 60 kDa which corresponds to the mature glycosylated form of the receptor (Desarnaud, *et al.*, 1993), and was similar to that expressed in hVSMC. This established the presence of the fully native form of the AT₁R in this model. Less intense bands at lower molecular masses of ~40 and 45 kDa were observed, irrespective of FCS content in culture media. This corresponds to the presence of unmodified AT₁R, indicating protein synthesis still occurs in the absence of growth factors.

This rapid protein turnover is characteristic of synthetic SMC as they exhibit more organelles that are involved in protein synthesis (Rensen *et al.*, 2007). These protein bands were not expressed in hVSMC grown in media containing 10% (v/v) FCS (**figure 3.5**).

The most intense band observed for AT₂R was at ~60 kDa, which corresponds to the glycosylated form of this receptor (**figure 5.12D**) (Servant *et al.*, 1994). The intensity of this band did not differ between proliferating and quiescent cells, but was greater than that detected in hVSMC. The non-glycosylated form of the AT₂R (44 kDa) was highly expressed in hASMC-hTERT grown in media containing 20% (v/v) FCS compared with quiescent cells. Cancerous cells have been shown to express high levels of AT₂R (De Paepe *et al.*, 2002) and since positive telomerase is a significant characteristic of cancer

cells, this may explain why hASMC-hTERT exhibited higher levels of AT₂R than hVSMC. As glycosylated forms of this receptor vary between cell types, the expression of AT₂R was confirmed by using Hep G2 cells as a positive control (see **figure 3.5**).

5.4.6.2 Induction of hASMC-hTERT premature senescence following a single Ang II exposure

Quiescent hASMC-hTERT were exposed to Ang II for 24 hours. A dose-dependent increase in the induction of premature senescence was detected, where the maximal effect (~1.8-fold increase over control) was observed with 10⁻⁷ mol/L (**figure 5.13A**). This observation differed from the Ang II-induction of premature senescence in telomerase-negative hVSMC (**figure 5.3**) where the highest concentration of Ang II (10⁻⁷ mol/L) resulted in less observable senescence. Co-incubation with E3174 completely prevented the induction of premature senescence initiated with 10⁻⁷ mol/L Ang II (**figure 5.13B**), indicating that premature senescence was mediated via AT₁R in hASMC-hTERT. This corresponded with observations made in hVSMC.

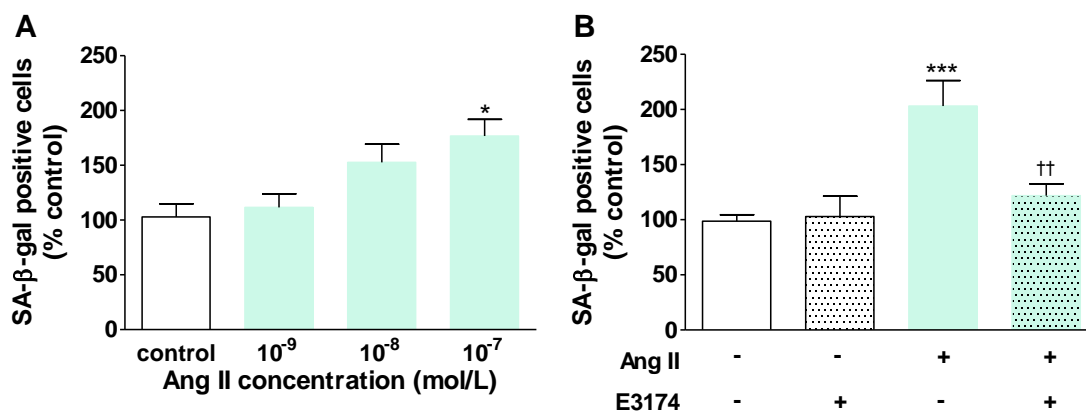


Figure 5.13 Ang II induces premature senescence in hASMC-hTERT. **A**, Dose-dependent increase in Ang II-induced premature senescence of hASMC-hTERT. Maximal induction of senescence was observed with 10⁻⁷ mol/L Ang II. Quiescent cells were treated with Ang II over a range of concentrations (10⁻⁹, 10⁻⁸ and 10⁻⁷ mol/L) for 24 hours. Cells were then re-plated at 5×10⁴ cells per well in 12-well plates in media containing 20% (v/v) FCS for 24 hours, before staining for SA-β-gal activity. Bars represent mean+SEM; n=3 (*p<0.05 compared with control). **B**, Ang II-induced premature senescence is mediated via AT₁R activation. Cells were pre-incubated with E3174 for 1 hour prior to Ang II (10⁻⁷ mol/L) stimulation for 24 hours. Bars represent mean+SEM; n=5 (***p<0.001 compared with control and ††p<0.01 compared with Ang II alone).

5.4.6.3 Ang II does not promote replicative senescence in hASMC-hTERT

Although hASMC-hTERT displayed premature senescence following a single acute Ang II exposure, the effect of continuous treatment with cultivation needed to be investigated. After 34 days of Ang II exposure on alternate days, only a 25% increase in senescence was determined with 10^{-8} mol/L Ang II exposures (**figure 5.14A**). This suggested that Ang II did not increase the normal replicative senescence of hASMC-hTERT, presumably due to maintained telomere length. The exponential growth rate of Ang II treated and untreated cells was maintained throughout this entire experiment (**figure 5.14B**) and did not show a decline in PD which is commonly associated with increased senescence. These data confirmed that acute Ang II induced premature senescence independent of telomere attrition.

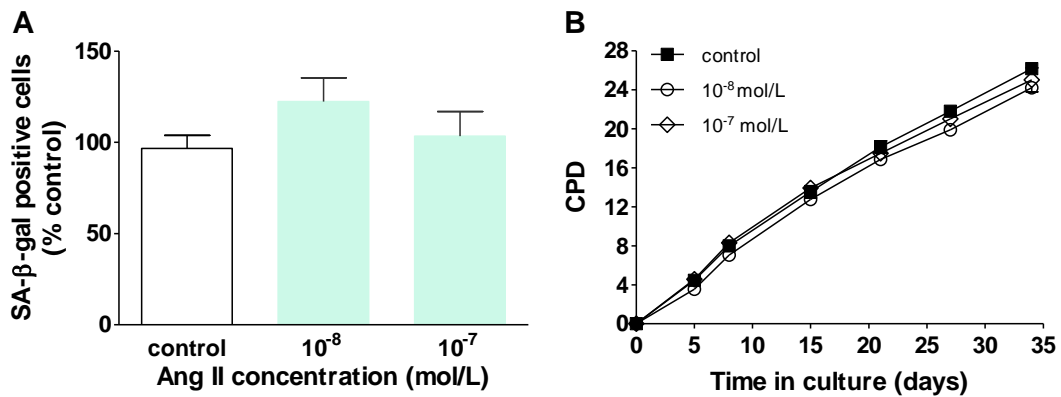


Figure 5.14 Successive Ang II exposure had no effect on the induction of replicative senescence and proliferation in hASMC-hTERT. **A**, Ang II did not augment replicative senescence. Cells were continuously grown in media containing 20% (v/v) FCS and were treated on alternate days for 34 days with Ang II at 10^{-8} or 10^{-7} mol/L. Once confluence was reached, cells were re-plated at 4×10^4 cells per T25cm² NuncTM flask. After the final Ang II treatment, cells were re-plated at 5×10^4 cells per well in 12-well plates then stained for SA-β-gal activity. Bars represent mean+SEM; n=3. No statistical difference was observed. **B**, Ang II had no effect on the rate of PD of hASMC-hTERT. Values represent the mean±SEM; n=3.

5.5 Discussion

The aim of this chapter was to investigate the effects of Ang II stresses on the induction of SIPS in hVSMC, and to establish whether premature senescence can be induced via a telomere-independent mechanism using the hASMC-hTERT model.

5.5.1 SIPS induction following t-BHP exposure in hVSMC

SIPS can be initiated by various extrinsic stresses (Ben-Porath and Weinberg, 2005), resulting in the rapid induction of cellular senescence. Although SIPS is classed as a separate form of senescence it shares many common cellular and molecular characteristics that are observed in replicative senescence (**figure 5.1**). The majority of these observations have been made in human fibroblasts (summarized in **table 5.1**). *In vitro* studies revealed cells to undergo SIPS following successive exposures to a range of agents at subcytotoxic doses (Robles *et al.*, 1999, Dumont *et al.*, 2000b; Chainiaux *et al.*, 2002); these studies demonstrated that oxidative stress was a major mediator in the induction of SIPS. Moreover, persistent stress can result in significant DNA damage and thereby trigger premature senescence (Duan *et al.*, 2005; Matthews *et al.*, 2006).

SIPS *in vivo*, may participate in the alterations of tissues or organs that are also observed in ageing (Toussaint *et al.*, 2002). This indicates that SIPS maybe initiated during the development of age-related diseases and possibly accelerate ageing of tissues.

The SA- β -gal assay is commonly employed to assess SIPS and replicative senescence. However, SIPS protocols differ from replicative senescence experiments, in the way in which cells are treated and allowed to recover for several days after the final stress, before measuring senescence (Dumont *et al.*, 2000b). The exact mechanism for the induction of SIPS is not known, but is thought to be triggered by the activation of various cell cycle regulatory proteins, similar to the induction of replicative senescence.

To initially assess whether hVSMC undergo SIPS *in vitro*, cells were exposed to short repeated sublethal oxidative stresses with t-BHP. t-BHP acts as a pro-oxidant, and has been shown to induce premature senescence in other cell types (Dumont *et al.*, 2000b; Kurz *et al.*, 2004; Glotin *et al.*, 2008), characterised by SA- β -gal activity and

other senescent biomarkers. In order to investigate the effects of t-BHP on hVSMC senescence, a suitably low concentration was required to increase mild oxidative stress without causing significant cell death. Trypan blue exclusion after a single t-BHP treatment over a range of concentrations for 2 hours followed by a 24-hour period of recovery, revealed 40 μ mol/L was a suitable dose to administer, as only a ~10% loss in viability was determined. This concentration was similar to that used successively on human fibroblasts (Dumont *et al.*, 2000b; 2001).

These results clearly demonstrated that hVSMC undergo SIPS. Early passage hVSMC submitted to successive stresses under t-BHP contained a significantly high proportion of positive SA- β -gal activity (2.5-fold increase) compared with untreated cells. A high proportion of senescent cells was maintained even after 5 days following the final stress. Chronic t-BHP treatment of hVSMC with sub-culturing has shown increased SA- β -gal activity, oxidative stress and telomere loss, suggesting repeated stresses causes a greater proportion of cells to undergo rapid growth arrest (Matthews *et al.*, 2006). A greater increase in SIPS following t-BHP stresses (4-fold increase) has been observed in human fibroblasts; however these cells were exposed to 5 stresses (Dumont *et al.*, 2000b), indicating the response to t-BHP-induced SIPS to vary between different cell types. These results established for the first time that hVSMC *in vitro* undergo SIPS in response to mild oxidative stress.

5.5.2 Ang II induced premature hVSMC senescence

A premature, rapid growth arrest with the characteristics of senescence has been described in the literature (Toussaint *et al.*, 2002) and is commonly referred to as premature senescence or SIPS. This form of senescence usually follows ROS-induced damage to cells. Therefore, in contrast to the prolonged effects of Ang II on normal replicative senescence, the response after a single exposure was investigated. Ang II has been widely implicated in normal vascular ageing and CVD development. The effect of Ang II on vascular cells can stimulate a diverse array of responses (Berk, 2001) through ROS generation and signalling (Touyz and Schiffrin, 2004). Ang II has been demonstrated to activate the Ras-signalling pathway, which in-turn has been shown to promote vascular cell senescence and inflammation (Minamino *et al.*, 2003). This early evidence suggested a critical role of Ang II in triggering senescence and contributing to vascular ageing and disease.

Since t-BHP stresses had demonstrated that hVSMC undergo SIPS, the effect of short Ang II stresses was investigated in a similar manner. A dose-dependent increase in SA- β -gal positive hVSMC was observed following a single Ang II treatment. Since the start of this thesis, other studies have also shown this premature induction of senescence following short-term Ang II exposure. A single Ang II exposure over 3 days displayed increased SA- β -gal staining and elevated p21 and p53 protein expressions in cultured hVSMC, and suggested that Ang II induced premature senescence via a p21/p53-dependent pathway (Kunieda *et al.*, 2006). EPC similarly displayed a dose-dependent increase in SA- β -gal activity with Ang II exposure over 14 days (Imanishi *et al.*, 2005a). Over the same duration of exposure, rat VSMC underwent senescence in a time-dependent manner following exposure to a single Ang II concentration (10^{-7} mol/L), which coincided with changes in p16, p21 and p53 protein expressions (Min *et al.*, 2007). An increase in p21 and p53 was also detected in this thesis after a single Ang II exposure (**figure 5.11**). This data along with accumulating evidence suggest that Ang II induced premature senescence is probably initiated via p21 and p53 activation. In addition to this, another study revealed activation of MAPK in Ang II-promoted EC senescence (Shan *et al.*, 2008), thereby identifying some of the mechanisms involved in initiating premature senescence signalled by acute Ang II. Moreover, exposure to UV radiation lead to a greater increase in premature senescence of male rat VSMC compared to female rat VSMC, presenting the novel idea of a gender difference with respect to senescence induction in these cells (Malorni *et al.*, 2008).

Experiments were conducted to establish the source of this premature senescence induction since ROS were thought to play a critical role. The highest senescence response to Ang II was inhibited with Ang II receptor subtype inhibitors, specific ROS scavengers and antioxidants. Premature senescence was predominantly mediated via AT₁R, since E3174 completely prevented the onset of senescence whereas PD123319 only showed a slight inhibition. This agreed with inhibition of Ang II-induced senescence with the AT₁R antagonist Valsartan, in EPC (Imanishi *et al.*, 2005a) and in rat VSMC (Min *et al.*, 2007), and suggests that rapid senescence is universally initiated via the AT₁R. Pre-incubation with catalase, NAC and SOD markedly inhibited the Ang II-stimulated premature SA- β -gal activity, indicating H₂O₂ and O₂⁻ were substantially generated in this acute response. The same effect was detected in hVSMC pre-incubated with NAC then treated for 3 days with Ang II (Kunieda *et al.*, 2006), and similarly by

pre-incubation with SOD in EPC (Imanishi *et al.*, 2005a). Ang II-stimulated ROS generation has been extensively attributed to NAD(P)H oxidase activation (Griendling *et al.*, 1994; Touyz *et al.*, 2002.). The effect of apocynin as a NADPH oxidase inhibitor in *in vitro* studies has recently been questioned, since it also acts as an antioxidant (Heumüller *et al.*, 2008). Nevertheless, the inhibition observed in this thesis further confirms that ROS are involved in this induction of senescence.

5.5.3 Ang II induced SIPS in hVSMC

Although Ang II displayed premature senescence after a single exposure, the classic induction of SIPS with successive stresses followed by recovery (Dumont *et al.*, 2000b) was also assessed. Quiescent cells successively stressed over a range of Ang II concentrations, again displayed a dose-dependent increase in SA- β -gal activity. However, the increase detected after 48-hours recovery was of a lesser magnitude compared to that determined after a single exposure. The senescent cells detected in these experiments would have been those terminally growth arrested, given that the recovery period would have potentially enabled some damaged cells to repair and eventually resume proliferation (outlined in **figure 5.1**). Therefore, the increased senescent cells detected after a single exposure probably represented both transient and terminally growth arrested cells. This stress protocol clearly showed Ang II induced SIPS in cultured hVSMC by discounting cell replication and immediate growth arrest. During the period of recovery many cells appeared enlarged which is characteristic of replicative senescent cells in culture. hVSMC grown in media containing 10% (v/v) FCS were also successively exposed to Ang II in the same manner, displaying a dose-dependent increase in positive SA- β -gal cells (data not shown). This demonstrated that the presence of growth factors in FCS had no effect on the induction of SIPS. Furthermore the successive inhibition of this stress response was found to be partially mediated via AT₁R. This is the first direct evidence that successive Ang II stresses induce SIPS and as yet has not been determined in other types of cells.

The sensitivity of cells to Ang II-induced stress and the magnitude of the exposure may even enhance replicative senescence, suggesting the idea that both forms of senescence maybe simultaneously present within the same population of cells.

Chapter 5.0: Stress-induced premature senescence with Ang II

Senescent vascular cells have been characterised in vascular ageing and in many age-related CVD. Elevated circulating Ang II has been implicated in CVD. The previous chapter utilized constant Ang II exposure to accelerate replicative senescence and this chapter demonstrated a rapid induction of senescence. It remains to be seen whether Ang II induces SIPS *in vivo*, in humans and if SIPS is detected in CVD.

No published data has looked at SIPS in response to Ang II exposure *in vivo*, however increased p16^{INK4a} expression in the human heart and kidney tissue was observed in hypertensive patients with CKD (Westhoff *et al.*, 2008), indicating increased cellular senescence. Hypertension is considered a major CVD that is characterised by high blood pressure and increased RAS. PBMC derived from CKD sufferers revealed accelerated telomere attrition, increased p53 expression and overexpression of proinflammatory cytokines, thereby presenting early senescent cells arising from oxidative stress and repeated cell activation (Ramirez *et al.*, 2005). This provided a link with the early onset of SIPS in vascular cells and the later development of chronic CVD such as atherosclerosis. Even though this evidence only correlates with the effects of Ang II, other *in vivo* factors may also have a considerable effect in these conditions. Additionally, the SA- β -gal biomarker was not used in any of these studies to determine senescence, and therefore the induction of SIPS cannot be confirmed.

5.5.4 Acute Ang II increased ROS generation in hVSMC

5.5.4.1 Ang II-stimulated intracellular ROS production

Fluorescent probes have been commonly used to measure Ang II-stimulated ROS in intact VSMC (Zafari *et al.*, 1998; Touyz *et al.*, 2002). In this thesis, CM-H₂DCFDA was used initially to detect ROS in treated hVSMC. Optimization of the assay for these cells revealed 10 μ mol/L CM-H₂DCFDA to be sufficient for labelling and for detecting changes in intracellular ROS. This ensured no induction of cytotoxicity by the probe.

Increased fluorescence was detected after 4 hours Ang II exposure at high concentrations, which was consistent with previous observations (Zafari *et al.*, 1998) but increases have also been detected after 30 minutes exposure (Touyz *et al.*, 2002). However, several repeat experiments displayed significant variation in the measured fluorescence. This was due to loss of cells during the labelling procedure and possible auto-oxidation of the probe, which consequently led to using a different assay to

measure Ang II-induced ROS. The use of CM-H₂DCFDA has been heavily scrutinised for the reasons outlined but additionally because it only measures generalized oxidative stress and not a specific ROS (Halliwell and Whiteman, 2004).

5.5.4.2 Measurement of NAD(P)H oxidase activity in hVSMC lysates using the LCLA

The sensitive LCLA was used to measure real-time production of ROS, by specifically measuring O₂^{•-} generation in cell lysates. Preliminary experiments were conducted to optimize conditions of the assay for hVSMC. No difference was observed in the NADPH-mediated O₂^{•-} production in either proliferating or quiescent hVSMC. This is important since continuous sub-culturing was thought to lead to considerable loss of AT₁R (Nickenig and Murphy, 1994). Therefore, by rendering cells quiescent, the optimum effects of Ang II could be assessed since the effects of other growth promoting factors that are present in FCS would be minimised.

The chemiluminescence signal increased in proportion with protein concentration of cell lysates, therefore 100µg of protein was considered sufficient to detect O₂^{•-} generation in all reactions. These cells were considered to generate modest amounts of O₂^{•-} as both HEK293 cells and B-lymphocytes exhibited greater levels of O₂^{•-} over the 40-minute period.

Use of the lucigenin probe for measuring O₂^{•-} production has been criticized due to its redox-cycling potential and artefactual O₂^{•-} generation at high concentrations of lucigenin (Li *et al.*, 1998). The optimum lucigenin concentration of 10µmol/L was determined with NADPH oxidase activity, with no indication of auto-oxidation at successively higher concentrations. However, increasing O₂^{•-} generation was detected with increasing lucigenin concentrations for NADH oxidase activity, which indicated redox-cycling by further generation of non-specific O₂^{•-} (Skatchkov *et al.*, 1999), and was therefore regarded as an artefact in measuring O₂^{•-}. This redox-cycling observed with NADH oxidase activity has similarly been identified when measuring O₂^{•-} production in vascular tissue homogenates and artery rings (Janiszewski *et al.*, 2002) further emphasising the potential effects of lucigenin. These data make assays of NADH oxidase activity difficult to interpret.

5.5.4.3 Source of O₂^{·-} generation in hVSMC

Experiments showed NADPH oxidase as the major source of O₂^{·-} production in human saphenous vein-derived VSMC, with only a small response detected via NADH. This was consistent with previously published data on VSMC derived from rodents (Griendling *et al.*, 1994; Ellmark *et al.*, 2005) and humans (Touyz *et al.*, 2002), but additionally in vascular EC derived from different species (Li and Shah, 2001). However, NADH was determined as the major source of O₂^{·-} in calf VSMC, but a high lucigenin concentration (50 μmol/L) was used in these experiments (Mohazzab and Wolin, 1994). This result must therefore be viewed with caution.

Significant inhibition of the NADPH-mediated response with DPI and tiron further confirmed O₂^{·-} was predominantly generated via NADPH oxidase activity, as DPI is a flavoprotein inhibitor. Moreover, the mtRC complex I inhibitor rotenone, displayed some inhibition indicating that NADPH-dependent O₂^{·-} may further stimulate ROS production via mitochondria. This concept was analysed in more depth with respect to Ang II and is discussed in chapter 6.0. These inhibitors also showed similar magnitudes of O₂^{·-} inhibition in murine VSMC (Ellmark *et al.*, 2005).

5.5.4.4 Ang II enhanced NADPH-dependent O₂^{·-} production in hVSMC

ROS scavengers and antioxidants almost completely prevented the senescence response to Ang II in hVSMC. ROS are regarded as mediators of cellular senescence and clearly appeared to be involved in Ang II-induced SIPS. Ang II-induced ROS generation via NADPH oxidase has already been reported in cultured VSMC (Griendling *et al.*, 1994; Zafari *et al.*, 1998; Touyz *et al.*, 2002) but there are no reports for SMC derived from human saphenous veins. NADPH-dependent O₂^{·-} was measured using a higher concentration of Ang II at 10⁻⁷ mol/L compared with that determined at the maximal induction of senescence (10⁻⁸ mol/L), as the extensive downstream processing of cells prior to measuring ROS resulted in lower levels of O₂^{·-} being detected with low Ang II concentrations. Therefore, a slightly higher concentration was used to measure O₂^{·-} production following short periods of exposure.

Acute Ang II exposure for 1 hour potentiated NADPH-dependent O₂^{·-} over the 40-minute measurement. This effect increased with exposure time of up to 24 hours. The effect of Ang II in these cells was very rapid compared to the original description

Chapter 5.0: Stress-induced premature senescence with Ang II

for rat aortic VSMC, which had suggested 4 hours stimulation with Ang II was required to elicit $O_2^{\cdot-}$ production (Griendling *et al.*, 1994). However, this Ang II concentration initiated a greater quantity of $O_2^{\cdot-}$ generation after just 15 minutes exposure in the same cell type (Touyz *et al.*, 2002). This data demonstrated that acute Ang II exposure stimulated NADPH-dependent $O_2^{\cdot-}$ and therefore might potentially contribute to the induction of SIPS in hVSMC.

Specific and non-specific ROS scavengers, antioxidants and the AT₁R antagonist were used to establish the extent of acute Ang II-stimulated $O_2^{\cdot-}$ via NADPH. NAC suppressed this response by almost 50%, confirming that Ang II stimulated ROS production. Apocynin induced a similar inhibition of $O_2^{\cdot-}$ production. Classically, this would be regarded as demonstrating the involvement of NADPH oxidase subunit associations. However, very recent studies suggest that apocynin primarily acts as an antioxidant (Heumüller *et al.*, 2008) and may therefore not be specific in blocking NAD(P)H oxidase subunit association. However, this cannot be entirely ruled out since NADPH oxidase is the main source of $O_2^{\cdot-}$ production detected in these cells. The same percentage inhibition by apocynin was observed in rat vascular tissue exposed to Ang II (Kimura *et al.*, 2005b). Inhibition of AT₁R only prevented 20% of the $O_2^{\cdot-}$ generated, which suggests that acute Ang II-induced ROS may not exclusively occur via this receptor activation, even though this was established as the main mechanism for the induction of senescence in hVSMC. However, AT₁R activation by Ang II has been proposed to primarily activate NAD(P)H oxidase (Seshiah *et al.*, 2002; Zuo *et al.*, 2005), and since this response was rapid this may account for the minor inhibition observed in these data. Moreover, a small AT₁R activation response maybe required to elicit a significant increase in $O_2^{\cdot-}$ production via NADPH oxidase.

The chemiluminescence signal was attributed to $O_2^{\cdot-}$ production as tiron substantially inhibited the Ang II-stimulated $O_2^{\cdot-}$ response. This has already been confirmed in hVSMC (Touyz *et al.*, 2002). Inhibition with DPI was less than with apocynin and NAC. Since this is a flavoprotein inhibitor, it indicated the source of $O_2^{\cdot-}$ was via NAD(P)H activation, which has long been the mechanism reported for Ang II-induced ROS in hVSMC (Touyz and Schiffrin, 2001; Touyz *et al.*, 2002), and VSMC derived from rat (Li *et al.*, 2007a). However, some evidence has shown DPI targets flavoproteins in mitochondria (Li and Trush., 1998) and therefore implies that

Ang II-mediated NADPH-dependent $O_2^{\cdot-}$ may further stimulate $O_2^{\cdot-}$ production via mitochondria.

Taken together these data confirm a rapid induction of NADPH-dependent $O_2^{\cdot-}$ by Ang II. Agents that inhibited $O_2^{\cdot-}$ production were also effective at inhibiting premature senescence in hVSMC. It is therefore concluded that ROS are central to the mechanism of Ang II-initiated premature senescence.

The association between the onset of senescence that is observed in aged vessels and in CVD, with Ang II-induced $O_2^{\cdot-}$ production is more difficult to study. Hypertension is characterised by structural changes in the vasculature that are promoted by Ang II. Increased $O_2^{\cdot-}$ via NADPH oxidase was detected in the aorta and mesenteric resistance arteries of Ang II-treated rats that developed hypertension. This indicated that Ang II-induced oxidative stress could cause vascular cell dysfunction and vascular remodelling (Zhou *et al.*, 2005), providing evidence for the potential involvement of oxidative stress in early senescence-related changes during vascular disease development.

5.5.5 Evidence for the role of p21 and p53 protein expression in hVSMC senescence

In conjunction with SA- β -gal staining, the expression of p21 and p53 was assessed to evaluate Ang II induced premature senescence. Increased $O_2^{\cdot-}$ production revealed Ang II to induce oxidative stress, which is a major mediator of senescence. The cell cycle regulators p21 and p53 have been characterised in the senescence-inducing mechanism (Ben-Porth and Weinberg, 2005; Bringold and Serrano, 2000), as outlined in **figure 5.1**, and are activated in both replicative and premature senescence.

No alterations in p16 protein expression were detected following Ang II exposure in hVSMC, which suggested senescence may not have been triggered via this signalling mechanism. No change in p53 protein expression was determined after 1 or 4 hours Ang II exposure. Therefore, exposure following 24 hours was examined, revealing an increase in p21 and p53 with a maximal induction at 10^{-8} mol/L. This data suggests a p21/p53-dependent mechanism of premature senescence in Ang II-treated hVSMC, since this concentration of Ang II also induced maximal SA- β -gal activity.

Chapter 5.0: Stress-induced premature senescence with Ang II

During work on this thesis, a similar observation was described in human aortic VSMC treated with Ang II for 3 days *in vitro* and the *apoE*-deficient mouse model treated with Ang II for 4 weeks *in vivo* (Kunieda *et al.*, 2006). However treatment of rat VSMC over several days showed increased p16^{INK4a} expression (Min *et al.*, 2007). These differences may be due to species differences.

Even though the expression of these cell cycle regulatory proteins was not analysed after successive Ang II stresses, they were highly expressed in human fibroblasts undergoing SIPS induced by t-BHP (Dumont *et al.*, 2000b), H₂O₂ (Duan *et al.*, 2005) and UV radiation exposure (Chen *et al.*, 2008). Therefore it is likely that a similar induction of these cell cycle regulatory proteins would be seen after successive Ang II treatments.

Increased CDKI expression has been detected in CVD, indicating increased senescence. For example, human atherosclerotic tissue exhibited increased p16 and p21 expression that coincided with positive SA- β -gal staining (Matthews *et al.*, 2006). Elevated p53 expression levels were determined in SMC of abdominal aortic aneurysms (López-Candales *et al.*, 1997) and the expression of p16^{INK4a} was augmented in human kidney biopsies derived from hypertensive patients compared with healthy biopsies, indicating cellular senescence may be mediated via this mechanism (Westhoff *et al.*, 2008).

5.5.6 Telomere-independent Ang II-induced premature senescence

Telomere shortening is regarded as the main trigger of replicative senescence. The data in this thesis demonstrated that Ang II accelerates replicative senescence via accelerated telomere attrition, and induces SIPS via oxidative stress. The telomere dependence of Ang II-induced senescence was assessed by using the hASMC-hTERT model.

Confirmation of continuous exponential growth *in vitro* and expression of hTERT protein showed these cells did not undergo telomere-dependent replicative senescence due to the ectopic expression of telomerase. In addition to this, since these cells had been modified by transfection, typical SMC characteristics were assessed to enable a fair comparison between this cell model and hVSMC. Essentially hASMC-hTERT exhibited a mixed SMC phenotype with some important contractile characteristics.

Chapter 5.0: Stress-induced premature senescence with Ang II

AT₁R and AT₂R protein expression was similar to that determined in primary hVSMC, indicating that these cells would likely respond to Ang II. The greater expression of AT₂R observed was unexpected but was indicative of rapid proliferating cells (De Paepe *et al.*, 2002).

The dose-dependent increase in SA- β -gal activity following a single Ang II exposure was similar to the observation in hVSMC, although the maximal induction of senescence was detected with a higher Ang II concentration. This indicated that hASMC-hTERT displayed a greater resistance to apoptosis. hVSMC showed increased apoptosis at this dose. The induction of premature senescence strongly indicated that Ang II can initiate this response irrespective of telomere length and the presence of telomerase. This response was prevented by pre-incubation with E3174, confirming that Ang II mediated this response via AT₁R activation.

One suggestion maybe that these hTERT expressing cells maybe resistant to apoptotic induction by Ang II, compared to the primary 'normal' pre-senescent VSMC. This effect on apoptosis has been described in hTERT expressing EC (Yang *et al.*, 2001), and human fibroblasts that underwent SIPS in response to H₂O₂ stresses (Gorbunova *et al.*, 2002). These data suggest that a DNA damage response maybe the more likely trigger of Ang II-stimulated premature senescence. Studies that support this idea compared the effects of H₂O₂-induced SIPS in human fibroblasts either expressing hTERT or not. Both cell types underwent SIPS and displayed elevated expressions of senescence-associated genes, including p21^{WAF-1} (de Magalhães *et al.*, 2004) and increased SA- β -gal activity (Zdanov *et al.*, 2007b). However, others still claim telomeres are involved in the induction of SIPS, whereby telomere shortening is not the actual trigger, but alterations in the structure of the T-loop and single-strand overhang maybe the inducing factors (Karlseder *et al.*, 2002).

Conclusions

- hVSMC undergo SIPS in response to successive sublethal t-BHP stresses.
- Ang II induces premature senescence in hVSMC via AT₁R activation and the induction of O₂^{·-} and H₂O₂.
- Ang II induces ‘true’ SIPS (i.e. via successive stimulation followed by a period of recovery) via AT₁R activation in hVSMC.
- Acute Ang II stimulates NADPH-dependent O₂^{·-} in hVSMC lysates.
- Elevated protein expressions of the CDKI p21 and tumour suppressor protein p53 are consistent with Ang II-increased SA-β-gal activity.
- A single Ang II exposure triggers premature senescence in hASMC-hTERT.
- Ectopic telomerase expression prevents the onset of senescence in cells continuously sub-cultured in the presence of exogenous Ang II.
- Taken together these data strongly suggest that Ang II induces SIPS. Moreover, SIPS is induced via NADPH oxidase mediated ROS generation.

CHAPTER SIX

Mitochondrial Alterations and Angiotensin II-Induced Premature Senescence

Chapter 6.0: Mitochondrial alterations and Angiotensin II-induced premature senescence

Data in chapter 5.0 strongly implicated ROS in the mechanism of premature senescence of hVSMC induced by Ang II. Ang II enhanced $O_2^{\cdot-}$ production via NADPH oxidase, which is the main source of $O_2^{\cdot-}$ generation in the vasculature (Berry *et al.*, 2000; Lassègue and Clempus, 2003). However, some studies have suggested that ROS generated via NAD(P)H oxidase may promote further ROS generation by other cellular sources (Landmesser *et al.*, 2003; Kimura *et al.*, 2005b). Mitochondria are a major source of ROS. In this chapter, the involvement of mitochondrial-derived ROS in Ang II-induced ROS and senescence in the hVSMC model was investigated.

6.1 Background

6.1.1 Evidence supporting the link between mitochondria and cellular senescence

At present there is only correlative data proposing the link between mitochondria and senescence. Many studies have demonstrated structural and functional alterations in mitochondria with increasing age which are associated with the accumulation of senescent cells (Lee and Wei, 2001; Yoon *et al.*, 2006; Preston *et al.*, 2008). This suggested the involvement of mitochondrial signalling or impaired mitochondria to contribute to the induction of senescence. The substantial ROS generated by mitochondria can result in dysfunctional mitochondria through macromolecular damage, giving rise to more ROS production. DNA damage resulting from ROS is thought to contribute to telomere shortening consequently accelerating the onset of replicative senescence.

Oxidative stress has been implicated in ageing and in the development and progression of various age-related diseases, which further indicates that mitochondria may have a significant role in senescence. This is supported by the proposed ‘Mitochondrial theory of ageing’, where the deleterious effects of ROS derived from the mtRC cause direct damage to mitochondrial components resulting in impaired mtRC function, culminating in further ROS generation (Harman, 1972).

Mitochondrial retrograde signalling is initiated in response to mitochondrial stress, where signalling from mitochondria to the nucleus causes cellular adaptations in order to maintain mitochondrial function. Alterations in mitochondrial membrane potential ($\Delta\Psi_M$), elevated levels of cytosolic Ca^{2+} , dysfunctional mitochondrial proteins and increased $\cdot\text{NO}$ production all elicit this signalling mechanism (Butow and Avadhani, 2004). Continuous alterations in the mitochondrial state resulting in retrograde signalling could eventually lead to impairment of this mechanism, potentially leading to cellular senescence.

Damaged and deficient mitochondria have been detected in various age-related CVD (Ramachandran *et al.*, 2002), but no direct evidence exists confirming impaired mitochondria within senescent tissue or cells. **Figure 6.1** summaries the mechanisms of damage to mitochondria in response to various cardiovascular risk factors and the proposed link to senescence induction, CVD and ageing arising from this.

6.1.2 Ang II mediated mitochondrial ROS generation

Since ROS are implicated in the induction of senescence and mitochondria are a major source of cellular ROS, a potential role of mitochondria in cell senescence is possible.

Ang II is a key mediator of ROS production in vascular cells and tissue (Griendling *et al.*, 1994; Zhang *et al.*, 1999; Miller *et al.*, 2005). The $\text{O}_2^{\cdot-}$ generated by Ang II in SMC is mainly via NAD(P)H oxidase activation (Griendling *et al.*, 1994; Touyz *et al.*, 2002) and as suggested in chapter 5.0. However ROS generated via NAD(P)H oxidase have been suggested to enhance further ROS production by other sources, such as mitochondria (Kimura *et al.*, 2005b; Rathore *et al.*, 2008).

Ang II has been shown to stimulate mitochondrial ROS production via NAD(P)H oxidase-derived ROS, through opening of the mitochondrial ATP-sensitive potassium channels (mitoK_{ATP}) by depolarizing the $\Delta\Psi_M$ in rat aorta and VSMC (Kimura *et al.*, 2005a). The ROS mediated preconditioning effect of Ang II in cardiac ischemic-reperfusion injury in rat hearts, was shown to be primarily caused by NAD(P)H oxidase. This was postulated to be essential in triggering mitochondrial ROS production involved in MAPK activation and preconditioning effects (Kimura *et al.*, 2005b).

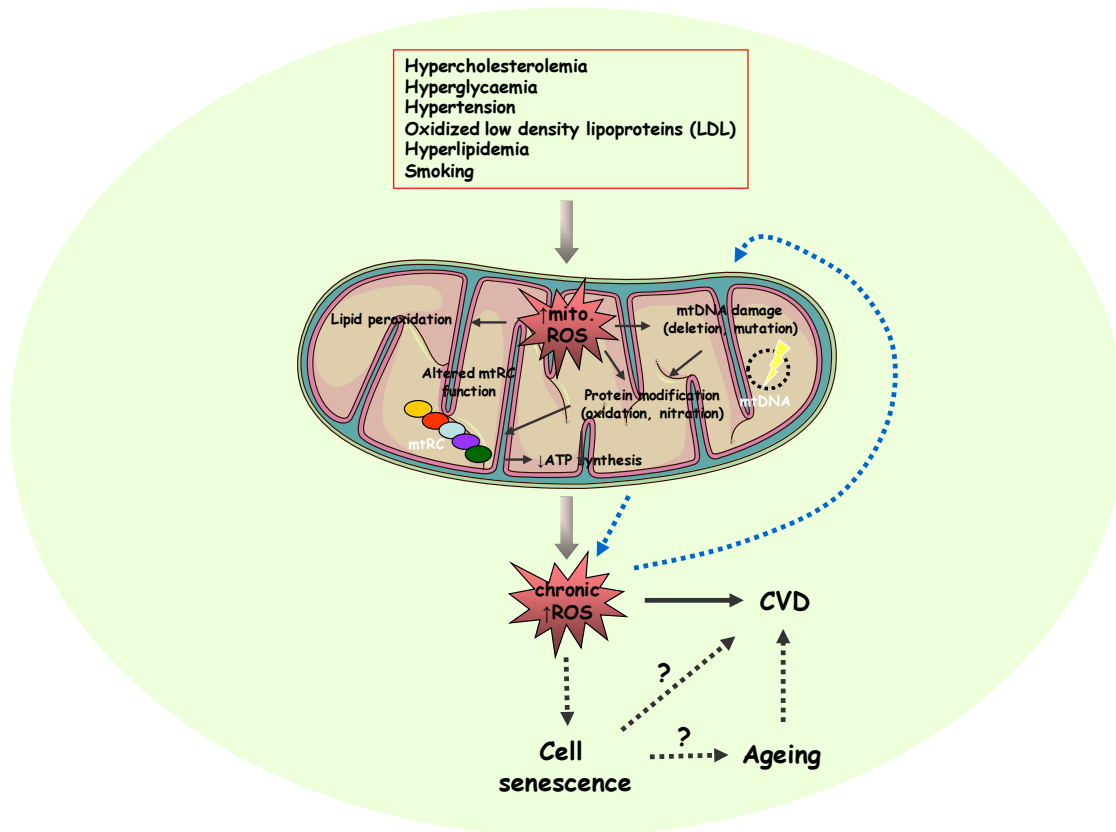


Figure 6.1 Proposed mechanisms of mitochondrial dysfunction in response to cardiovascular risk factors that may trigger cell senescence, or contribute to ageing and CVD development. Various factors influencing vascular pathology can cause sustained damage or dysfunction to mitochondria due to increased mitochondrial ROS production. Chronic ROS derived from mitochondria can initiate damage to cellular components and in theory induce premature senescence, potentially contributing to CVD. Mitochondrial DNA (mtDNA) damage promotes mitochondrial dysfunction causing increased ROS production which has been suggested to further instigate damage to mtDNA with proceeding age, creating a “vicious circle” (blue dotted line) (Harman, 1972). The accumulation of senescent cells can eventually result in tissue or organ dysfunction associated with ageing.

The mitochondrial ROS-induced ROS release (RIRR) is a plausible mechanism, as Ang II-induced ROS production by NAD(P)H oxidase can serve as a trigger for the opening of mitoK_{ATP} channels leading to a burst of mitochondrial ROS (Kimura *et al.*, 2005b). RIRR was demonstrated in cardiac myocyte mitochondria by Zorov *et al* (2000), where the accumulation of ROS can cause opening of mitochondrial channels accompanied by the collapse of the $\Delta\Psi_M$ and leads to a ROS burst via the mtRC. This can further trigger RIRR in nearby mitochondria resulting in enhanced mitochondrial and cellular damage.

The flavoprotein antagonist DPI has been previously shown to inhibit Ang II stimulated ROS by NAD(P)H oxidase, but has also been demonstrated to effectively inhibit mitochondrial-derived ROS (Li and Trush., 1998). Despite this lack of absolute specificity, DPI still provides further evidence that Ang II initiates ROS generation via mitochondria. Even though some studies have shown Ang II stimulates ROS generation via mitochondria, whether this has an important role in the induction of vascular cell senescence and ageing, is still to be determined.

6.1.3 Alterations in mitochondrial biogenesis and mitochondrial ATP generation in ageing and disease

mtDNA is prone to damage or modification by ROS as it is in close proximity to the site of ROS generation in mitochondria. Despite the existence of some repair mechanisms (Bohr and Dianov, 1999) the damage to mtDNA can be more extensive and persistent than nuclear DNA damage (Ballinger *et al.*, 2000; Van-Remmen and Richardson, 2001), subsequently leading to dysfunctional mitochondria. The integrity of mtDNA may therefore affect the maintenance of mtDNA in cells.

Virtually all of the mtDNA encodes for specific proteins of the mtRC, so any inherited defects in mtDNA, mutations or deletions could result in deficient energy production, which could lead to increased ROS, enhancing cell injury and disease development. The accumulation of damage to mtDNA has been found to be more prevalent in disease and aged tissues/cells, which may suggest a possible link with the onset of senescence.

The abundance of mitochondria in cells varies depending upon the energy requirements, as well as physiological and environmental effects. Increased mtDNA copy number has been observed in aged tissue in mice (Masuyama *et al.*, 2005) and humans (Barrientos A *et al.*, 1997; Pesce *et al.*, 2001), which has been postulated to reflect a feedback response compensating for the accumulation of damaged or defective mitochondria. However, a precise determination of mtDNA copy number using a PCR-based assay, showed no change in mtDNA content with age in human skeletal muscle and myocardial tissue (Miller *et al.*, 2003).

Chapter 6.0: Ang II-induced mitochondrial alterations

Exposure to sublethal oxidative stress has been shown to increase mtDNA content of growth arrested cells and is proposed to be an early molecular event in the induction of senescence (Lee *et al.*, 2000). Similarly, sustained hypoxia in neonatal rats also revealed increased mtDNA content within the brain, signifying mitochondrial adaptation to cellular energy demands in response to oxygen, which is required for growth and development (Lee *et al.*, 2008). Moreover mtDNA damage has been specifically detected in senescent cells (Passos *et al.*, 2007). These alterations in mtDNA content with increased oxidative stress may represent a potential role in senescence and disease.

Mitochondrial replication is orchestrated by the highly complex mechanism of mitochondrial biogenesis, involving thousands of nuclear and mitochondrial-encoded genes. This mechanism is initiated in response to the increased demand for cellular energy and following the release of hormones. However, recent work has shown alterations in this mechanism in pathological states (McLeod *et al.*, 2004; Xu *et al.*, 2007) and following cell injury (Lee *et al.*, 2002; Carraway *et al.*, 2008) in order to supply sufficient energy to the cell to maintain function and survival.

Correlative data has indicated mitochondrial biogenesis to have a role in replicative senescence, as expression of the master regulatory gene PGC1 α increased the rate of human fibroblast senescence (Xu and Finkel, 2002). Also high levels of expression of this gene are associated with increased mitochondrial mass in senescent fibroblasts (Lee *et al.*, 2002). However, the interaction of premature senescence and mitochondrial biogenesis has not yet been investigated.

ROS have been postulated to modulate the rate of mitochondrial biogenesis. This has been determined in cells exposed to oxidative stress. Exposure to t-BHP elevated PGC1 α levels which returned to basal levels after several days (Rasbach and Schnellmann, 2007). Increased PGC1 α and NRF-1 levels were determined following H₂O₂ treatment in human fibroblasts (Lee *et al.*, 2002). The continuous exposure to low ·NO concentration also caused an increase in mitochondrial biogenesis (Nisoli *et al.*, 2003). These observations indicated a compensatory increase in mitochondria as a result of increased ROS/RNS production and perhaps due to the presence of damaged mitochondria.

Chapter 6.0: Ang II-induced mitochondrial alterations

One of the primary functions of mitochondria is to conserve cellular energy in the form of ATP through the Krebs cycle and oxidative phosphorylation. Alterations in cellular energetics maintain cell function and survival, for example there is an increase in mitochondria to generate more ATP in response to physiological conditions such as fasting (Civitarese *et al.*, 2007), short-term exercise (Wright *et al.*, 2007) and cold exposure (Ricquier and Bouillaud, 2000).

Dysfunctional mitochondria can result in the defective capacity to generate sufficient ATP by oxidative phosphorylation and this is often accompanied by enhanced ROS production, resulting in cell death. These changes may also contribute to disease and ageing. One proposed compensatory mechanism for the insufficient supply of ATP is the increased rate of glycolysis to generate ATP. Glycolysis is used by cancer cell lines, which rapidly proliferate (Piechota *et al.*, 2006), however glycolysis alone does not produce adequate ATP for full cell functioning in all cells.

Reduced ATP levels have been detected in arterial hypertension accompanied by Ca^{2+} overload (Postnov, 2001), indicating a deficit in mitochondrial activity. A gradual decline in mitochondrial ATP production has been observed with advancing age in humans (Short *et al.*, 2005), although no change has been observed in some tissues. This correlates to the diminished levels of ATP determined in senescent fibroblasts (Zwerschke *et al.*, 2003), indicating that the regulation of mitochondrial energy metabolism may have a key role in cellular senescence and ageing.

6.2 Aims

- To determine whether mitochondria and mitochondrial-derived ROS participate in Ang II-induced hVSMC senescence.
- Extensive studies have shown NAD(P)H oxidase is the main source of Ang II-induced ROS generation in blood vessels. Data presented in chapter 5.0 showed Ang II enhanced $O_2^{\cdot-}$ production via NADPH oxidase activity in the hVSMC model. However, ROS generated via NAD(P)H oxidase could also serve to promote further ROS production via other sources. Mitochondria are the predominant source of cellular ROS in many cell types. To establish whether Ang II stimulates mitochondrial $O_2^{\cdot-}$ production in hVSMC, specific inhibitors of the mtRC were used to antagonise mitochondrial-ROS generation detected using the LCLA, by the MitoSOX assay to measure mitochondrial $O_2^{\cdot-}$ production.
- To investigate variations in mtDNA content in hVSMC following single and multiple Ang II exposures, as a measure of mtDNA quantity, integrity and dysfunction. Intact mtDNA relative to nDNA was determined via qPCR.
- To determine whether Ang II influences mitochondrial biogenesis, by measuring the mRNA levels of gene transcripts involved in modulating mtDNA transcription and replication by real-time RT-PCR.
- To assess the effects of Ang II on mitochondrial function in hVSMC, by assessing cellular ATP production following oxidative stress, Ang II and mtRC inhibition.

6.3 Experimental Approach

6.3.1 Cell culture

Early passage (2 to 9) hVSMC were grown to near confluence in media containing 10% (v/v) FCS, at 37°C. In the single Ang II treatment experiments, cells were rendered quiescent in media containing 0.5% (v/v) FCS for 24 hours prior to any treatment as described in section 2.3.1.1. Pre-incubation with an AT₁R antagonist, mitochondrial ROS scavengers and mtRC inhibitors were performed prior to Ang II exposure.

Successive Ang II treatment was performed on cells maintained in media containing 10% (v/v) FCS. Following each stress period, the cell media was replaced with fresh medium containing 10% (v/v) FCS for 24 hours before subsequent stress induction.

PD counts were performed to assess hVSMC proliferation. Cells were seeded at a density of 4×10^5 cells per T75cm² NuncTM flask, until confluence was reached. Multiple Ang II exposures with 10^{-7} mol/L were conducted on alternate days and on the days following counting and re-plating. Cells were harvested by trypsinization, resuspended in 1ml of fresh media and counted using a haemocytometer. PD and CPD were calculated as described in section 2.3.1.2.

6.3.2 Measurements of mitochondrial function

Intracellular ATP production was also used to assess mitochondrial function in hVSMC using the ApoGlow® adenylate nucleotide ratio assay, which is generally used to measure cell proliferation and viability. Cells were seeded at a density of 5×10^3 or 7×10^3 cells/well in sterilized white 96-well microplates within 100µl volumes of media containing 10% (v/v) FCS for 24 hours, prior to any treatment. Cells were simultaneously set up in clear, 96-well microplates to visually check cell adherence and confluence pre- and post-treatment. Ang II at 10^{-7} mol/L was administered over 0.5, 1, 4 and 24 hours. Cells were pre-treated with E3174 at 10^{-5} mol/L for 1 hour and rotenone at 2×10^{-6} mol/L for 3 hours, prior to Ang II treatment for 24 hours.

Chapter 6.0: Ang II-induced mitochondrial alterations

Cells were seeded at 5×10^3 cells per well for successive Ang II treatment at 10^{-8} and 10^{-7} mol/L. Cells were exposed to Ang II for 2 hours then the culture media was changed to remove any residual Ang II and to allow cells to recover for 24 hours. Three successive treatments and recovery periods were performed prior to measuring ATP levels, as described in **2.3.1.4**.

6.3.3 SA- β -gal assay

SA- β -gal staining was used to assess cellular senescence following treatment. hVSMC were seeded at 3×10^4 cells per well in 12-well plates and grown to near confluence for 48 hours, then rendered quiescent. Before exposure to Ang II at 10^{-8} mol/L for 24 hours, cells were pre-incubated with the mtRC complex inhibitors rotenone ($2 \mu\text{mol/L}$ for 3 hours) and TTFA ($1 \mu\text{mol/L}$ for 3 hours); the mitoK_{ATP} channel inhibitor 5-HD ($100 \mu\text{mol/L}$ for 2 hours); and the mitochondrial O₂^{•-} scavenger mito-TEMPO (25nmol/L for 4 hours). Following Ang II treatment, cells were harvested by trypsinization, counted using a haemocytometer and re-seeded at 5×10^4 cells per well in 12-well plates in media containing 10% (v/v) FCS. Cells were left to adhere for 24 hours at 37°C prior to fixation then staining for SA- β -gal as described in section **2.3.2.3**. The number of positive (blue) and negative (transparent) cells was counted manually in five fields selected at random from each well using a Nikon inverted trinocular phase contrast microscope (under $\times 200$ magnification). Percent senescent cells for each treatment were calculated from the number of SA- β -gal positive cells divided by the total counted cells.

6.3.4 Mitochondrial O₂^{•-} measurements

6.3.4.1 Measurement of NADPH-mediated O₂^{•-} via mitochondria

hVSMC were grown to ~90% confluence in T175cm² Nunclon flasks then rendered quiescent. Cells were stimulated with 10^{-7} mol/L Ang II for 1 hour, then trypsinized, washed twice with cold DPBS, resuspended in ice-cold lysis buffer and sonicated as described in **2.3.4.2**. The protein content of cell lysates was determined using the Bradford protein assay (**2.3.5.7**). The LCLA was used to measure NADPH-dependent O₂^{•-} production, as detailed in **2.3.4.2**. The specificity of the lucigenin assay for mitochondrial O₂^{•-} in hVSMC was examined by the effects of mitochondrial inhibitors on Ang II-stimulated O₂^{•-} production. Treated and untreated cell lysates were pre-incubated for 5 minutes at 37°C with rotenone ($10 \mu\text{mol/L}$), TTFA ($10 \mu\text{mol/L}$),

antimycin A (10 μ mol/L), DPI (50 μ mol/L) or 5-HD (100 μ mol/L) prior to the addition of NADPH and measuring O₂^{·-} production.

6.3.4.2 Fluorescent measurement of mitochondrial O₂^{·-}

hVSMC were seeded at 2 \times 10⁵ cells per well in 6-well plates and grown to ~80% confluence. Cells were then treated with 50 μ mol/L t-BHP for 2 hours or Ang II at 10⁻⁷ mol/L for 1 hour at 37°C. Following treatment, the media was discarded from wells and carefully rinsed twice with HBSS. Treated and untreated cells were then labelled in minimal light with the MitoSOXTM red fluorescent probe, as detailed in section **2.3.4.3**.

6.3.5 mtDNA content by quantitative PCR

hVSMC were seeded at 4 \times 10⁵ cells per T75cm² Nunclon flask for multiple Ang II treatments. Near confluent cells were treated with Ang II at 10⁻⁷ mol/L for 24 hours. Following treatment, cells were trypsinized, resuspended in fresh media, counted using a haemocytometer and re-seeded into T75cm² flasks at 4 \times 10⁵ cells. DNA was then extracted and quantified from the remaining subset of cells obtained at each passage. Untreated cells were seeded and re-seeded at confluence in the same manner as Ang II-treated cells. Cells were continuously cultured and treated with Ang II at confluence over 73 days. Single Ang II exposure was conducted in quiescent cells at the same dose, following short periods of incubation (0.25, 0.5, 1, 6 and 24 hours). DNA was then extracted from these cells once harvested by trypsinization.

The quantification of mtDNA was performed on the MX4000® spectrofluorometric thermal cycler. The PCR primers used to amplify specific human mtDNA and nDNA transcripts are detailed in **table 2.8**. PCR amplification was carried out using the Brilliant® SYBR® Green QPCR Core Reagent kit with 15ng or 250pg of total DNA template (for nDNA and mtDNA qPCR respectively) (section **2.3.6.6**). qPCR was performed in triplicate for each DNA sample. The relative initial template quantity of mtDNA and nDNA for each sample was determined from corresponding standard curves generated using a reference DNA stock. mtDNA content was then normalized to the amount of nDNA as a ratio for each cell sample.

Chapter 6.0: Ang II-induced mitochondrial alterations

Intra-assay variability was assessed for the replicate measurements of mtDNA and nDNA (6 replicates). The mean coefficient of variation for the measurement of mtDNA at 6 hours was 13.5% (untreated) and 14.8% (treated), while the variation of measurements of nDNA was 7.6% (untreated) and 9.5% (treated) based on ratio values.

6.3.6 RT-PCR analysis of PGC1 α and mtTFA mRNA

hVSMC were seeded at 3×10^6 cells per T175cm² Nunclon flask and left to adhere for 24 hours, then rendered quiescent. Single Ang II exposures at 10^{-7} mol/L were conducted over short periods of incubation (0.25, 0.5, 1, 4, and 24 hours). Following treatment, cells were harvested by trypsinization and each sample was resuspended in 200 μ l DPBS then stored on ice prior to RNA extraction. Total RNA was extracted, quantified and reverse transcribed to generate cDNA (sections **2.3.5.3**, **2.3.5.4** and **2.3.6.5**). RT-PCR was performed on the StepOneTM real-time PCR machine using SYBR[®] Green JumpStartTM Taq ReadyMixTM (**2.3.6.7**). The mitochondrial biogenesis gene transcripts amplified were PGC1 α and mtTFA (target genes). The HPRT1 gene was used as the endogenous control. The PCR primer sequences used to amplify these specific gene transcripts are detailed in **table 2.9**. PCR amplification was carried out on 16.7 and 33.3ng/ μ l of cDNA template. PCR was performed in triplicate for each cDNA sample, for each transcript analysed. The Ct values for each target gene were normalized against the endogenous control gene (HPRT1). The quantitative changes in gene expression were calculated using the 'Pfaffl method' (Pfaffl, 2001) (see **Appendix II**).

6.3.7 DNA Sequencing of PCR products

PCR products for each gene transcript were purified and quantified as described in section **2.3.6.8**, before BigDye DNA sequencing was carried out by PNAACL, Hodgkin Building, University of Leicester. Chromatograms were analysed using the Chromas software and sequence homology was assessed (**Appendix III**).

6.4 Results

6.4.1 Potential role of mitochondria in Ang II-induced premature senescence of hVSMC

Chapter 5.0 showed that Ang II promoted premature senescence of hVSMC, which could be prevented upon pre-treatment with various ROS scavengers and specific antioxidants. The elevated levels of $O_2^{\cdot-}$ generated following short periods of Ang II exposure suggested the involvement of ROS in this mechanism. As mitochondria generate the same cellular ROS and are increasingly recognised as signal transducers they may also contribute to the induction of SIPS. To determine whether mitochondria are involved in the mechanism of Ang II induced premature senescence of hVSMC, specific mitochondrial inhibitors targeting the mtRC, channels and the ROS produced, were investigated.

Ang II exposure for 24 hours consistently caused a ~1.5 to 2-fold increase in senescent cells (**figure 6.2**). Pre-incubation with rotenone caused complete inhibition of Ang II-induced senescence in hVSMC ($p < 0.001$) (**figure 6.2A**). TTFA also appeared to inhibit senescence but this data did not reach statistical significance (**figure 6.2B**). Since both inhibitors were dissolved in DMSO an equal volume of DMSO alone was used in the control cells for comparison.

To ascertain whether mitochondrial ROS stimulated by Ang II participates in the induction of senescence, a recently developed mitochondrial ROS scavenger, mito-TEMPO was used. TEMPO is a spin trap compound that specifically reacts with $O_2^{\cdot-}$. Mito-TEMPO is a derivative of this compound, conjugated to a lipophilic triphenylphosphonium cation. This enables it to be membrane permeable and highly accumulated within mitochondria where it scavenges $O_2^{\cdot-}$ and alkyl radicals specifically generated via mitochondria (Murphy and Smith., 2007).

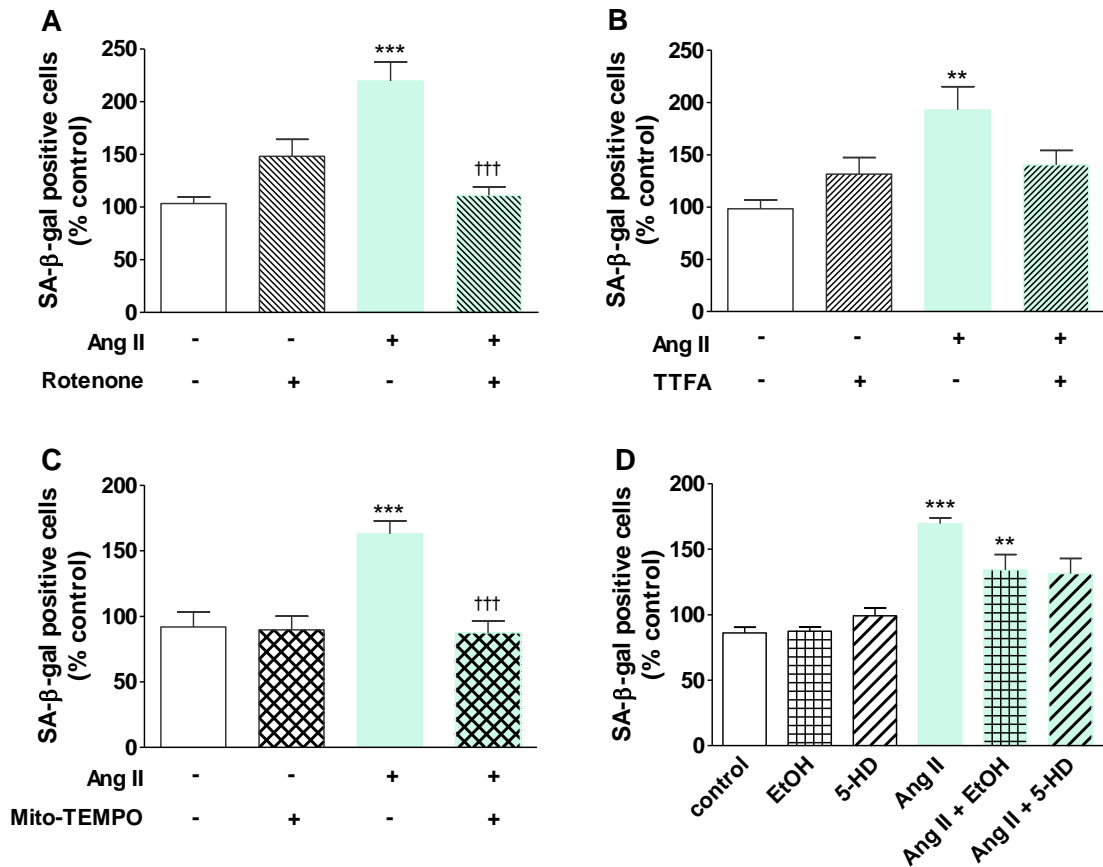


Figure 6.2 Effect of mitochondrial inhibitors and antioxidants on Ang II-induced premature senescence of hVSMC. Quiescent cells were pre-incubated with inhibitors of the mtRC (rotenone (complex I) or TTFA (complex II)), $\text{mitoK}_{\text{ATP}}$ channels (5-HD) or a scavenger of mitochondrial $\text{O}_2^{\cdot-}$ (mito-TEMPO) before the induction of senescence with 10^{-8} mol/L Ang II for 24 hours. Following treatment, cells were re-plated (5×10^4 cells per well) for 24 hours in media containing 10% (v/v) FCS before staining for SA- β -gal activity. **A** and **B**, Ang II-induced senescence is dependent upon the mtRC activity. Bars represent mean+SEM; $n=3$ to 5 (** $p<0.01$ and *** $p<0.001$ compared with control, ††† $p<0.001$ compared with Ang II alone). Controls received DMSO alone as vehicle. **C**, Mitochondrial $\text{O}_2^{\cdot-}$ contributes to Ang II-induced senescence. Bars represent mean+SEM; $n=6$ (*** $p<0.001$ compared with control and ††† $p<0.001$ compared with Ang II). **D**, Ang II-induced senescence is not mediated by the activation of $\text{mitoK}_{\text{ATP}}$ channels. Bars represent mean+SEM; $n=7$ (*** $p<0.001$ compared with control and ** $p<0.01$ compared with control cells treated with EtOH). Control cells consistently displayed $\leq 10\%$ senescent cells in individual experiments. EtOH refers to ethanol.

Figure 6.2C demonstrates pre-treatment with a low concentration of mito-TEMPO completely prevented Ang II-induced senescence. This strongly suggests mitochondrial ROS are involved in the rapid senescent response; on the other hand this conclusion is based upon the specificity of mito-TEMPO for mitochondrial $\text{O}_2^{\cdot-}$, therefore it may be possible that mito-TEMPO could also scavenge other sources of $\text{O}_2^{\cdot-}$. Both rotenone and mito-TEMPO displayed very similar results by completely preventing the onset of

senescence in the presence of Ang II ($p < 0.001$). This suggests $O_2^{\cdot-}$ is a major mediator in the senescence mechanism, since $O_2^{\cdot-}$ can be produced in mitochondria via complex I of the mtRC.

In addition to the mtRC, mitochondrial-derived ROS is also regulated by $\text{mitoK}_{\text{ATP}}$ channels. Inhibition of $\text{mitoK}_{\text{ATP}}$ channels with 5-HD showed no effect on Ang II-induced senescence of hVSMC (**figure 6.2D**), when compared to vehicle controls (ethanol (EtOH)). The same effect was determined in untreated cells and therefore limits the conclusions based on this data.

These experiments indicate for the first time that the induction of rapid senescence mediated by Ang II appears to involve mitochondrial $O_2^{\cdot-}$ and mtRC pathways. Chapter 5.0 provided substantial evidence that Ang II enhanced $O_2^{\cdot-}$ production via NADPH oxidase activation, in hVSMC. To investigate the relative contribution of mitochondrial $O_2^{\cdot-}$ from the total cell production of $O_2^{\cdot-}$ following acute Ang II, various inhibitors of mitochondrial components were used.

Quiescent hVSMC were incubated with a relatively high concentration of Ang II (10^{-7} mol/L) for 1 hour before the measurement of $O_2^{\cdot-}$ production. **Figure 6.3A** represents the real-time chemiluminescence measurements determined from cell lysates exposed to DPI. DPI is an effective, yet non-specific flavoprotein inhibitor that has been previously shown to inhibit NAD(P)H oxidase activity (Warnholtz, *et al.*, 1999; Griendling *et al.*, 1994), however, it has also been found to affect other sources of $O_2^{\cdot-}$ generation, including mitochondria (Li and Trush., 1998). DPI completely blocked the Ang II-dependent chemiluminescence, suggesting $O_2^{\cdot-}$ was not only derived from NADPH oxidase activation but also possibly from mitochondria.

In cell lysates derived from Ang II-treated cells, the addition of mtRC inhibitors rotenone and TTFA, specific inhibitors of complex I and II respectively, almost fully suppressed chemiluminescence suggesting the Ang II enhanced $O_2^{\cdot-}$ production was by the mtRC (**figure 6.3B and C**). No change in $O_2^{\cdot-}$ production was observed in Ang II-treated cells when complex III was inhibited with antimycin A, which indicated that $O_2^{\cdot-}$ was not generated via complex III (**figure 6.3D**), even though it is considered another major source of $O_2^{\cdot-}$ in mitochondria.

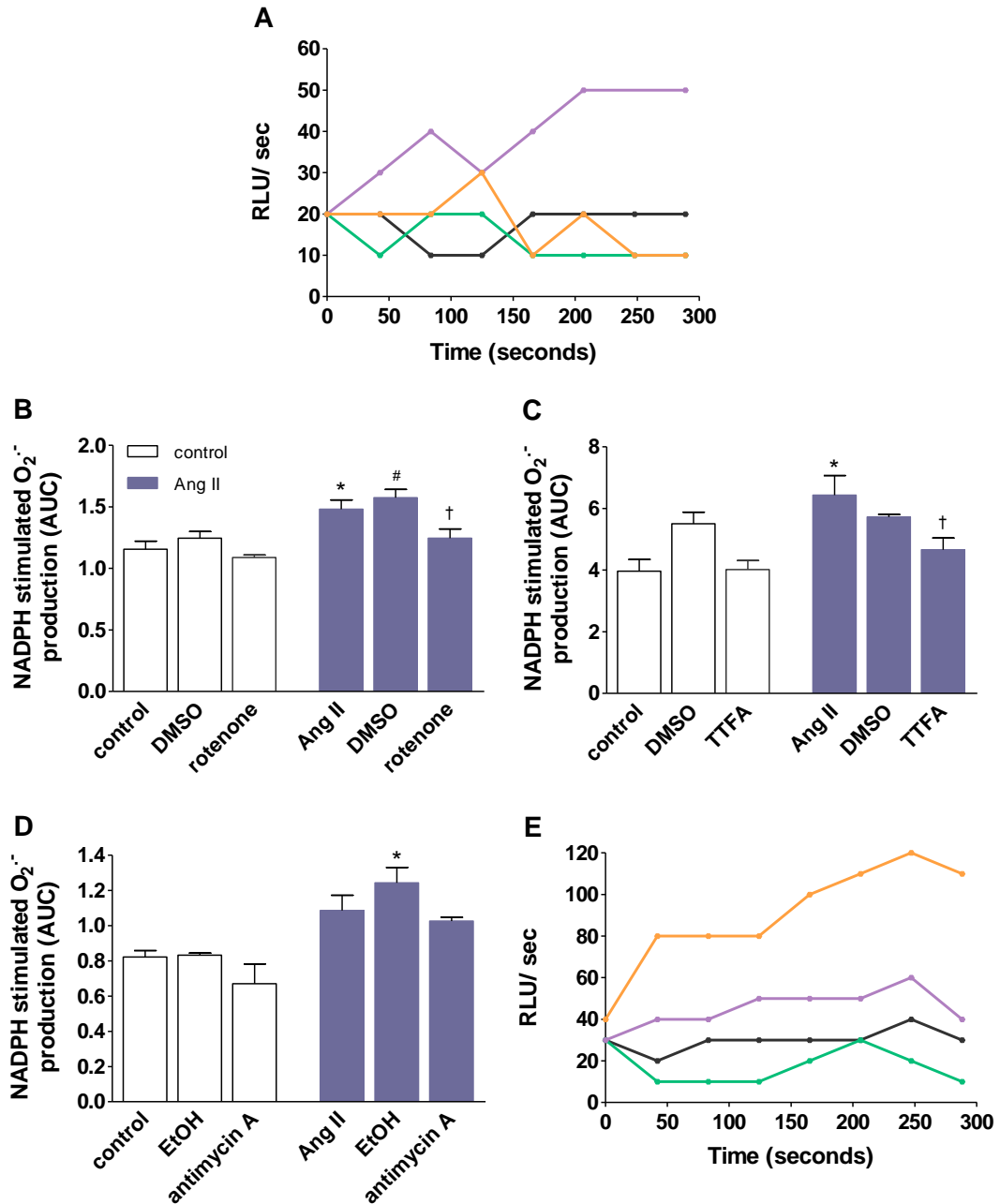


Figure 6.3 Ang II induces NADPH-mediated mitochondrial $O_2^{\cdot-}$ generation in hVSMC. Quiescent cells were pre-incubated with Ang II (10^{-7} mol/L) for 1 hour then lysates were exposed to mitochondrial inhibitors for 5 minutes prior to NADPH oxidase-derived $O_2^{\cdot-}$ measurements using the LCLA. **A**, Real-time chemiluminescence measurements of Ang II-induced $O_2^{\cdot-}$ production with the effect of DPI. **B** and **C**, Inhibition of complex I and II of the mtRC reduced the Ang II-induced $O_2^{\cdot-}$ production. Bars represent mean+SEM, $n=3$ to 4 (* $p<0.05$ compared with control; # $p<0.05$ compared with DMSO (vehicle) and † $p<0.05$ compared with Ang II and vehicle treated cells). **D**, Complex III inhibition did not significantly reduce Ang II-induced $O_2^{\cdot-}$ production. Bars represent mean+SEM, $n=3$ (* $p<0.05$ compared with control cells treated with EtOH). NADPH stimulated $O_2^{\cdot-}$ production is derived from the RLU/min/100 μ g of protein over 40 minutes. **E**, Real-time chemiluminescence measurements of Ang II-induced $O_2^{\cdot-}$ production in lysates exposed to 5-HD. Black indicates control; green, inhibitor alone; lilac, Ang II and orange, Ang II+inhibitor.

Although complex III inhibition displayed no contribution in acute Ang II stimulated $O_2^{\cdot-}$, some preliminary work was conducted with the complex IV inhibitor CCCP which also acts as an uncoupler of the mtRC (data not shown). CCCP completely blocked chemiluminescence in Ang II-treated and untreated cells, which confirms that a functional mtRC is required for ROS generation in these cells. The inhibition of Ang II stimulated NADPH-dependent $O_2^{\cdot-}$ with at least some mtRC inhibitors was necessary to ascertain the production of $O_2^{\cdot-}$ via mitochondria.

Figure 6.3E represents the real-time chemiluminescence measurements determined from cell lysates exposed to 5-HD. Inhibition of mitoK_{ATP} channels with 5-HD augmented the Ang II-stimulated $O_2^{\cdot-}$ response by ~2-fold (**figure 6.3E**), but had no effect in the untreated cell lysates. This elevated $O_2^{\cdot-}$ response and the senescence data suggests that Ang II does not mediate its effects via mitoK_{ATP} channel activation in hVSMC, but indicates that by blocking these channels $O_2^{\cdot-}$ is further generated via other enzymatic sources.

The chemiluminescence data revealed a proportion of Ang II induced NADPH-mediated $O_2^{\cdot-}$ to be derived via mitochondria. To further substantiate mitochondrial ROS production, MitoSOXTM red, a mitochondrial selective fluorescent probe for $O_2^{\cdot-}$ was used in intact hVSMC. Near confluent cells were treated with t-BHP to determine the level of mitochondrial $O_2^{\cdot-}$ following exposure to mild oxidative stress. t-BHP exposure for 2 hours caused a 1.8-fold increase in mitochondrial $O_2^{\cdot-}$ in hVSMC (**figure 6.4**). This response was only slightly greater than that determined after a single Ang II (10^{-7} mol/L) exposure for 1 hour, where a ~1.5-fold increase was detected. This data in conjunction with inhibitor studies on NADPH-dependent $O_2^{\cdot-}$ production lends support to the idea that Ang II stimulates mitochondrial $O_2^{\cdot-}$ in hVSMC. However, since the absolute specificity of these probes remains questionable it cannot be verified that MitoSOXTM red specifically detects mitochondrial-derived $O_2^{\cdot-}$.

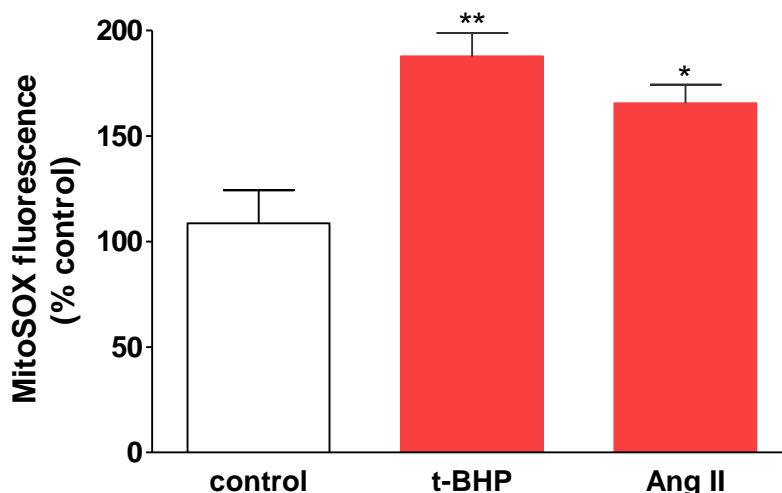


Figure 6.4 Detection of mitochondrial $O_2^{\cdot-}$ with MitoSOXTM red in live hVSMC. Near confluent cells were exposed to t-BHP (50 μ mol/L) for 2 hours or Ang II (10⁻⁷ mol/L) for 1 hour at 37°C. Following treatment, cells were loaded with 5 μ mol/L MitoSOXTM red in HBSS for 10 minutes at 37°C. Excess probe was rinsed from cells prior to measuring fluorescence. Bars represent mean+SEM; n=3 to 4 (**p<0.01 and *p<0.05 compared with control cells).

6.4.2 Effect of Ang II on mtDNA content

mtDNA is considered to be susceptible to oxidative damage due to close proximity to ROS generation and the limited presence of repair mechanisms. The amount of mtDNA can therefore be used to assess mtDNA integrity. In this thesis, mitochondrial-derived ROS and mtRC activity have been implicated in the mechanism of premature Ang II-induced hVSMC senescence (section 6.4.1). To further characterise the effect of Ang II on mitochondria, alterations in the content of intact mtDNA were investigated. The mtDNA content of hVSMC in response to Ang II was analysed using real-time qPCR, by determining the ratio of mtDNA (PCR product encodes partially for NADH dehydrogenase subunit 6, transfer-RNA glutamic acid, and partially cytochrome b) to nDNA (acidic ribosomal phosphoprotein PO gene) for each sample. The quantity of transcribed nDNA remained similar in all the DNA samples from Ang II-treated and untreated cells, over short and long-term treatments, indicating no significant damage or loss in intact nDNA with Ang II exposure. ‘Relative mtDNA content’ represents ratio values corrected against untreated, control cells.

Initial experiments showed a single Ang II (10^{-7} mol/L) exposure in quiescent hVSMC caused a significant but small increase in mtDNA content after only 24 hours, which was reduced back to baseline values at further time-points (**figure 6.5**). This has been observed previously within other cells exposed to oxidative stress (Lee *et al.*, 2000). The slight increase observed after 24 hours indicated that Ang II may have stimulated an increase in mtDNA at a much earlier time-point. In order to confirm this observation as a real effect the quantity of mtDNA was then measured over much shorter time periods.

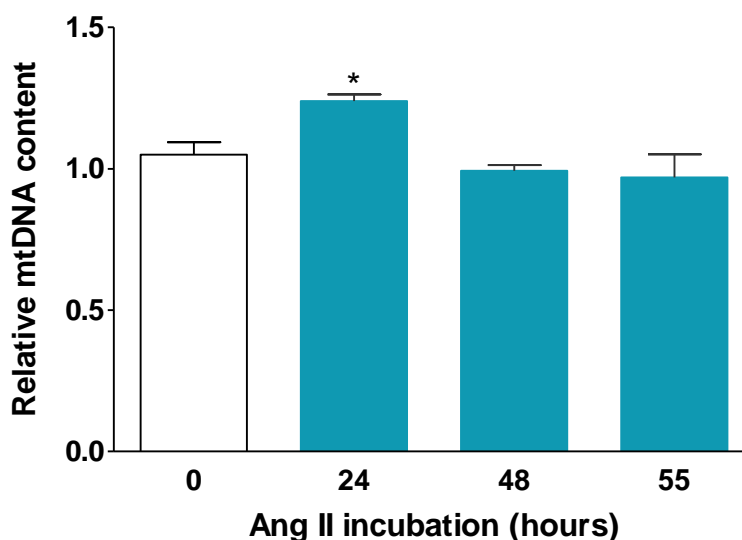


Figure 6.5 Ang II increases mtDNA content of hVSMC following a single exposure. Near confluent cells were rendered quiescent for 24 hours, followed by treatment with a single dose of Ang II at 10^{-7} mol/L for up to 55 hours. DNA was extracted from cells, quantified and analysed by qPCR for mtDNA and nDNA, as described in the methods, section 6.3.5. mtDNA content was elevated after Ang II exposure for 24 hours. mtDNA content returned to control levels at 48 and 55 hours. Relative mtDNA content = ratio of mtDNA normalized against the nDNA for each sample, corrected for the mtDNA content of untreated, control cells at each time-point. Bars represent mean+SEM; n=3 independent experiments (* $p < 0.05$ compared with control).

Table 6.1 shows the relative mtDNA content of Ang II-treated hVSMC compared to those untreated. Following a much shorter period of Ang II exposure (0 to 6 hours), a sharp increase in mtDNA content of >2.5-fold was determined after 0.5 hours which was maintained after 1 hour (~2-fold) and eventually returned to baseline levels after 6 hours. This rapid increase in mtDNA was consistent with the rapid elevated levels of $O_2^{\cdot -}$ generated within these cells following 1-hour Ang II treatment, as revealed by chemiluminescence measurements (see **figure 5.9A**). This indicates that Ang II induced oxidative stress may promote mtDNA replication.

This finding was unexpected since these experiments were initiated to determine whether mtDNA was lost following acute Ang II exposure perhaps due to enhanced mitochondrial O₂⁻ production and mtDNA damage.

Table 6.1 Alterations in mtDNA content of hVSMC following acute Ang II exposure

<i>Ang II incubation (hours)</i>	<i>Relative mtDNA content (AU)</i>
0	1.01 ± 0.07
0.25	0.96 ± 0.15
0.5	2.64 ± 0.37***
1	1.92 ± 0.19*
6	1.12 ± 0.03

Quiescent cells were treated with a single dose of Ang II at 10⁻⁷ mol/L over a relatively short period of time (up to 6 hours). The quantity of mtDNA following Ang II exposure was determined by qPCR. Relative mtDNA content refers to mtDNA:nDNA ratio corrected for values obtained from untreated cells. Values represent mean±SEM; n=5 (*p<0.05 and ***p<0.001 compared with untreated cells).

Although Ang II had been shown to modulate mtDNA content over a short period, successive exposure to Ang II was used in chapter 5.0 to induce SIPS. It was hypothesized that successive exposure of cells to Ang II may lead to mtDNA damage and eventually mtDNA loss. The continuous sub-culturing of hVSMC with Ang II treatment on alternate days, displayed higher mtDNA:nDNA ratio values compared with controls up to CPD ~9 (**figure 6.6A**). Beyond this CPD level, the ratio value was similar to that of control cells. This suggests that a greater amount of the damaged mtDNA transcript maybe present within these late passage cells that were exposed more to Ang II. Damaged DNA would not be amplified by PCR which is only able to generate full-length gene products. The high ratio values at early CPD are similar to the high relative mtDNA content determined over a short period, indicating increased mtDNA replication. Ang II-treated hVSMC showed a slower rate of proliferation beyond ~10 CPD, which indicated the presence of more growth arrested cells with lower levels of intact mtDNA. Little variation in the quantity of nDNA was detected with sub-culturing of hVSMC, with or without treatment. The greatest difference in ratio values between the two groups was observed after just two Ang II exposures, determined at CPD ~4.

Figure 6.6B shows no difference in CPD between Ang II-treated and untreated cells, confirming that changes in mtDNA:nDNA ratio, did not arise from changes in cell proliferation due to Ang II treatment. Therefore, the initial increase in mtDNA may be due to an increase in the number of mitochondria per cell, mtDNA per mitochondria or relative to mitochondrial mass. Electron microscopy would have to be conducted to visually determine the number of mitochondria; however this was not carried on these cells.

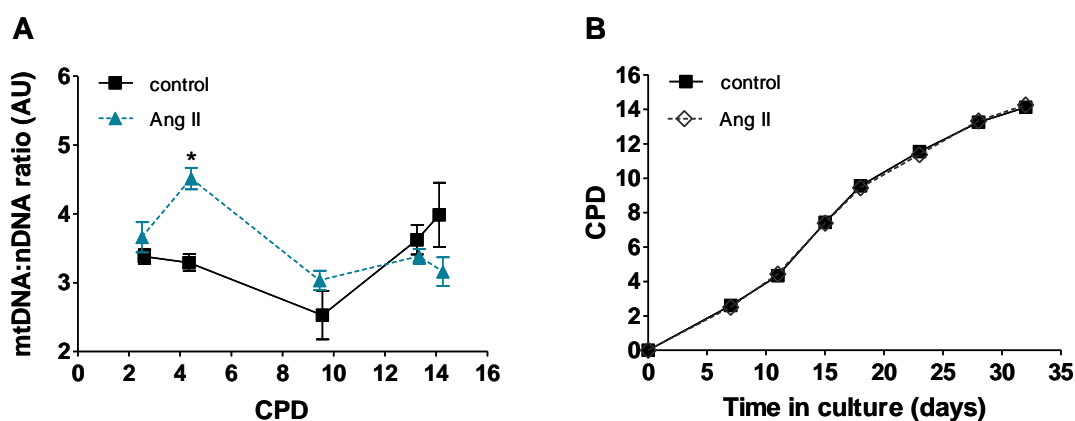


Figure 6.6 Successive Ang II exposure stimulates increased mtDNA content in hVSMC. **A**, Initial Ang II exposures induced a sustained increase in mtDNA content. A potential loss was observed following 13 CPD. Cells were continuously sub-cultured in media containing 10% (v/v) FCS with and without Ang II treatment (10^{-7} mol/L). When confluence was reached, cells were harvested, counted using a haemocytometer and re-seeded at 4×10^5 cells per flask. Ang II treatment was conducted on alternate days and on the following days after passage, over 32 days. Plotted data are arbitrary units for the mtDNA content of each sample, mean \pm SEM; $n=4$ (** $p < 0.01$ compared with the relative control value). **B**, Successive Ang II exposure had no significant effect on the PD of hVSMC. Changes in proliferation did not reflect the changes in mtDNA content which were observed following Ang II treatment. Data represents mean \pm SEM; $n=4$ (no statistical difference was determined).

6.4.3 Effect of Ang II on markers of mitochondrial biogenesis

To determine whether the rapid Ang II-stimulated increase in mtDNA was due to a signal to increase mitochondrial biogenesis, mRNA levels of regulatory genes PGC1 α and mtTFA that are involved in mtDNA replication were evaluated using quantitative RT-PCR. These genes signal for mtDNA transcription and replication (shown in **figure 1.9**). Following Ang II treatment for 0.25 hours, the messenger RNA (mRNA) levels of the master regulatory gene PGC1 α were sharply increased by ~ 2.5 -fold, although this did not reach statistical significance. Thereafter levels resumed to levels in untreated

cells (**figure 6.7A**). The expression of mtTFA increased to 1.6-fold after a 1 hour stimulation although again this was not statistically significant (**figure 6.7B**). As this was not a substantial change in mtTFA gene transcript levels, it was sustained up to 24 hours. This early elevation in PGC1 α followed by a later increase in mtTFA is the known response in mitochondrial biogenesis, and would therefore indicate that Ang II induces mtDNA transcription and replication. However, due to lack of statistical significance these experiments are equivocal and further experiments are required. The early trend of increased PGC1 α transcript (0.25 hours) coincides with the observed increase in relative mtDNA content after 0.5 hours following exposure with the same dose of Ang II (**table 6.1**). Even though changes in the transcript levels of mtTFA were not consistent with alterations in mtDNA content, the marginal increase detected was sustained for up to 24 hours.

Quality of the extracted RNA ranged between 2.0 and 1.6 prior to cDNA synthesis, which was within the acceptable range.

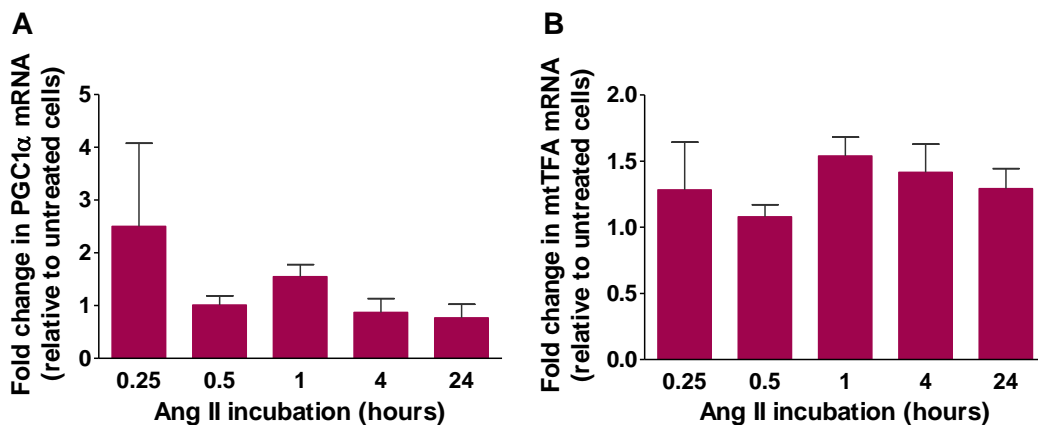


Figure 6.7 Effect of short-term Ang II exposure on the mRNA expression of genes involved in mitochondrial biogenesis. Quiescent cells were exposed to Ang II (10^{-7} mol/L) at the indicated time-points (0.25 to 24 hours) then harvested by trypsinization. RNA extracted from each sample was reverse-transcribed to generate cDNA. Expression was quantified using real-time RT-PCR as described in 6.3.6. Changes in the target gene were corrected versus the endogenous control, HPRT1. The relative quantification in gene expression of Ang II-treated hVSMC at each time-point compared against untreated cells (designated as 1-fold) was determined using the Pfaffl method (Pfaffl, 2001). Bars represent mean+SEM, n=3 (data did not reach statistical significance).

Sequencing of PCR products to verify specificity

Products generated from PCR were purified of residual dNTPs and enzymes, then quantified using the Quant-iT™ PicoGreen® dsDNA assay kit. Each sample was diluted to 3ng then sent to PNAAC (University of Leicester) for sequencing using ABI BigDye terminator sequencing processes. Following the removal of unincorporated BigDye, the products were analysed on an ABI 377 sequencer. Representative sequencing chromatograms for each gene are in **Appendix III**. Using the NCBI BLAST software, sense and anti-sense sequences of the PCR products were compared against the gene sequences for HPRT1, PGC1 α and mtTFA, and found to be between 100 and 82% homologous to published gene sequences.

6.4.4 Effect of Ang II on mitochondrial function

The rapid alterations in mtDNA content and O₂⁻ production via the mtRC indicated rapid changes in mitochondrial function, in response to Ang II. The effect of Ang II on mitochondrial function was examined by specifically measuring cellular ATP levels. The mtRC in mitochondria utilizes oxidative phosphorylation to generate ATP. The quantitation of ATP is commonly used as an index of cell proliferation and viability, but was used in this instance to assess the mitochondrial function of hVSMC. Both cellular ADP and ATP contents were analysed in these cells, however the measurements of ADP were below the limit of detection of the assay used. Initial experiments were conducted to assess the ATP content of hVSMC, whether levels differed between quiescent and proliferative cells and in response to mild oxidative stress. **Figure 6.8A** shows almost a 2-fold rise in ATP with t-BHP treatment for 1 hour of cells grown in media containing 10% (v/v) FCS. No change was observed within quiescent cells. AT₁R was shown to be highly expressed in both hVSMC rendered quiescent and in those grown in media containing 10% (v/v) FCS (**figure 3.5**). This indicated that Ang II would mediate its effect in both cellular conditions. ATP measurements were taken under both conditions following a short period of Ang II exposure (10⁻⁷ mol/L). Different responses were observed, as proliferating cells displayed a time-dependent increase in ATP content with a maximum generated after 4 hours (50% increase), whereas quiescent cells displayed a gradual reduction in ATP (**figure 6.8B**).

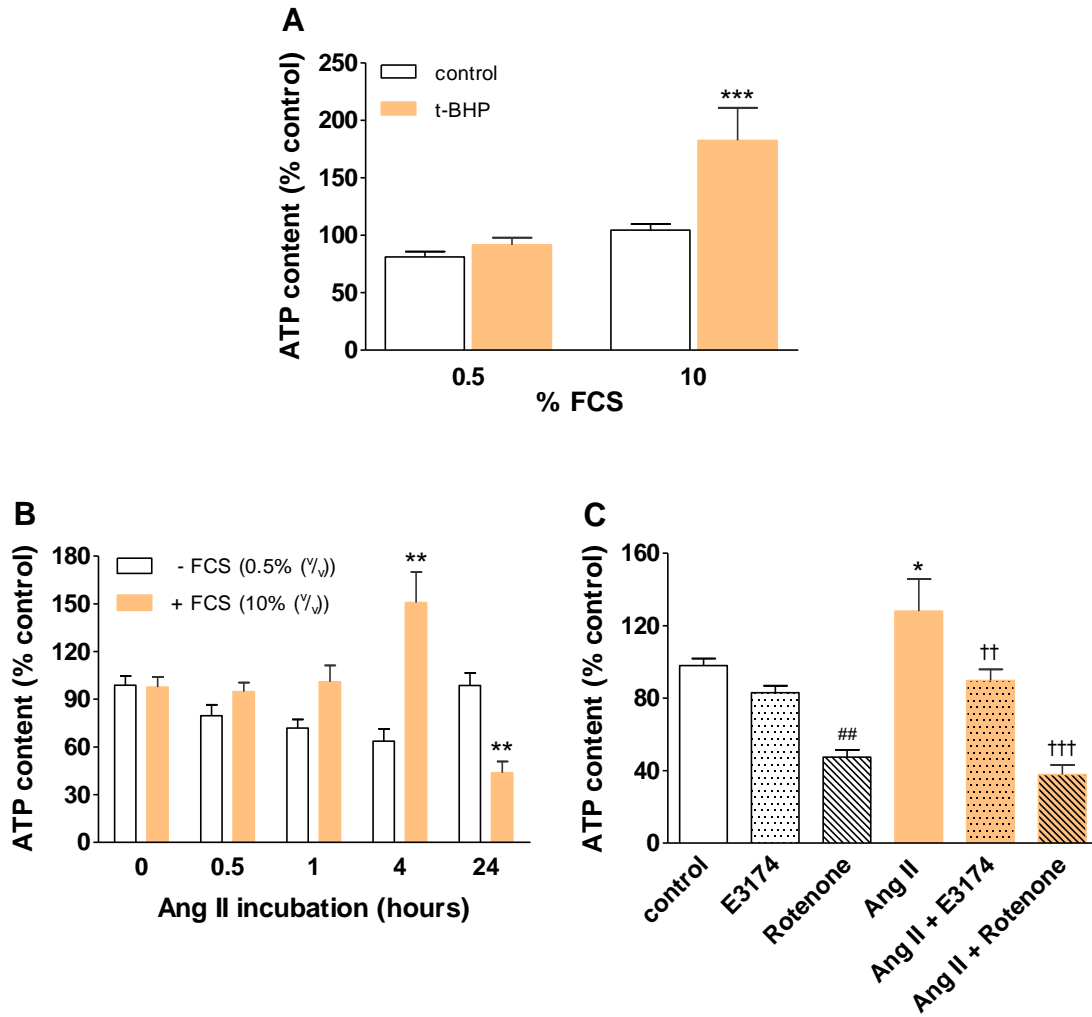


Figure 6.8 ATP production in hVSMC. **A**, Mild oxidative stress stimulates ATP production. Cells were seeded (5×10^3 cells per well) 24 hours prior to treatment in media containing 10% (v/v) FCS, and in those cells rendered quiescent. Treatment with t-BHP (40 μ mol/L) for 1 hour increased the ATP content in proliferating cells. The percent change following t-BHP treatment is relative to respective controls (control values are relative to 1 designated control value = 100%). Bars represent mean+SEM; n=4 to 5 (***)p<0.001 compared with respective control). **B**, Time-dependent increase in the ATP content of hVSMC. Cells were seeded at 7×10^3 cells per well for 24 hours prior to Ang II (10^{-7} mol/L) treatment. Maximum ATP content was observed after 4 hours. The percent change in ATP content following Ang II treatment is relative to respective controls at 0 hours (0.5/10% (v/v) FCS) for each time-point. Bars represent mean+SEM; n=7 to 8 (**p<0.01 compared with respective control). **C**, Inhibition of AT₁R activity and mtRC complex I reduces Ang II stimulated ATP. Cells in media containing 10% (v/v) FCS were pre-incubated with E3174 (10^{-5} mol/L for 1 hour) or rotenone (2 μ mol/L for 3 hours) prior to Ang II treatment for 4 hours. Ang II stimulated ATP was reduced to basal levels following pre-incubation with E3174. Rotenone substantially inhibited basal ATP content. The percent change in ATP content with pre-treatment and following Ang II exposure is relative to control (100%). Bars represent mean+SEM; n=6 (*p<0.05 and ##p<0.01 compared with control; ††p<0.01 and †††p<0.001 compared with Ang II alone).

Chapter 6.0: Ang II-induced mitochondrial alterations

The rapid increase in ATP suggests increased mtRC activity, which occurred approximately 3 hours after the observed increases in $O_2^{\cdot-}$ production (**figure 6.3**) and mtDNA content (**table 6.1**) suggesting changes in mitochondrial function follow these early responses. ATP content resumed to levels of untreated cells after 24 hours suggesting a compensatory mechanism whereby enhanced ROS elevates mitochondrial function in order to maintain cell survival.

To verify that Ang II initiated the rise in ATP observed after 4 hours, cells were pre-incubated with the AT_1R antagonist (E3174) and mtRC inhibitor rotenone. E3174 completely blocked the rise in ATP as the quantity of ATP measured was the same as untreated cells (**figure 6.8C**), demonstrating Ang II to mediate its effect via AT_1R . Rotenone substantially inhibited ATP content with Ang II exposure but also significantly reduced the levels present in untreated cells by 50% confirming ATP generation via the mtRC.

A single Ang II exposure had displayed a sharp increase in ATP levels over a short period before resuming to normal levels which is suggestive of a cell survival response. The effect of successive Ang II treatment on ATP content was therefore analysed. Cells were exposed to short stresses of Ang II for 2 hours each day, then exposed to fresh media for 24 hours in-between stresses, for 3 days. ATP measurements were taken after the final period of fresh media and were expressed per microgram of protein. Successive exposure with the lowest dose of Ang II (10^{-8} mol/L) stimulated a 2-fold increase in ATP ($p < 0.05$), whereas the highest dose (10^{-7} mol/L) reduced ATP levels by >0.5 -fold (**figure 6.9**). The dose at which the greatest amount of ATP was observed (10^{-8} mol/L) was consistent with the maximal induction of SIPS in hVSMC (**figure 5.5A**), suggesting high levels of ATP to be present in senescent cells, where altered mitochondrial function maybe required to maintain cell survival. Exposure with 10^{-7} mol/L Ang II diminished ATP levels indicating cell death and mitochondrial damage or dysfunction. Moreover, this dose was associated with the maximal Ang II-induced apoptosis of hVSMC (**figure 4.8E**).

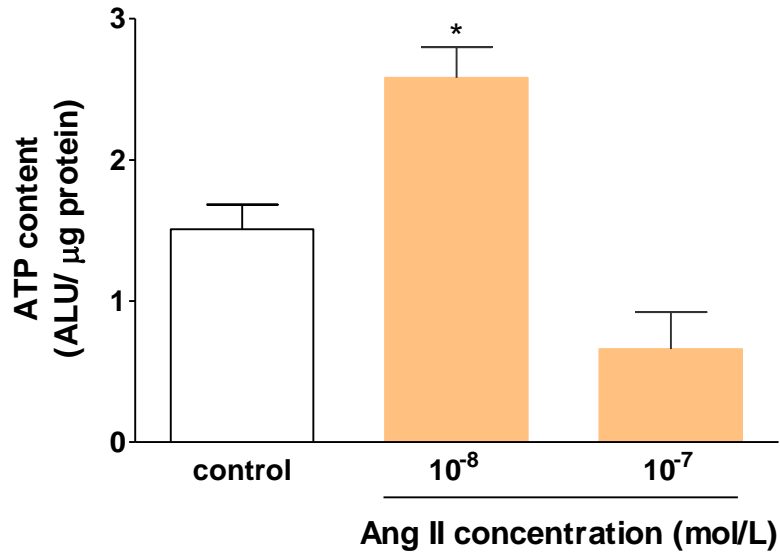


Figure 6.9 Effect of repeated Ang II stresses on the ATP content of hVSMC. Cells were seeded in media containing 10% (v/v) FCS (5×10^3 cells per well) for 48 hours prior to Ang II treatment for 2 hours per day for 3 days (10^{-8} and 10^{-7} mol/L). Media in each well was replaced following each treatment period. This allowed cells to recover for 24 hours prior to subsequent Ang II treatments. Repeated stresses of low Ang II concentration (10^{-8} mol/L) induced a higher production of ATP. Bars represent mean+SEM; n=4 (*p<0.05 compared with control).

6.5 Discussion

The aim of this chapter was to establish whether Ang II-induced premature senescence involved mitochondria and to study the effects of Ang II on mitochondrial structure and function in hVSMC.

6.5.1 Ang II stimulated mitochondrial $O_2^{\cdot-}$ in the induction of premature senescence

Investigations into the role of Ang II induced premature vascular cell senescence have implicated oxidative stress via AT₁R activation (chapter 5.0). The involvement of mitochondria in this mechanism has not been determined. As yet, only correlative data have supported the association between mitochondria and senescence. The data presented in this chapter contribute to this association.

Inhibition of the mtRC and mitochondrial $O_2^{\cdot-}$ was shown to significantly prevent senescence and NADPH-dependent $O_2^{\cdot-}$ production following Ang II administration. This indicated that enhanced mtRC activity increases ROS generation that maybe implicated in the induction of premature senescence.

SA- β -gal staining of hVSMC pre-incubated with rotenone and mito-TEMPO followed by Ang II treatment for 24 hours, revealed almost complete inhibition of Ang II-induced senescence. This indicated that Ang II-stimulated $O_2^{\cdot-}$ via mitochondria is primarily involved in accelerating the induction of senescence. Rotenone inhibits the first complex (I) of the mtRC through which $O_2^{\cdot-}$ is generated which may explain the substantial inhibition of senescence, and mito-TEMPO specifically scavenges mitochondrial generated $O_2^{\cdot-}$ and alkyl radicals (Murphy and Smith., 2007) preventing an increase in $O_2^{\cdot-}$. This data adds to but provides more detail than results with SOD (**figure 5.4F**) as SOD scavenges all sources of $O_2^{\cdot-}$.

Pre-incubation with the complex II inhibitor TTFA also showed some reduction of the induced senescence, which indicated that the activity of this complex contributes to senescence. A small increase in senescence of control cells was determined following incubation with mtRC inhibitors. SA- β -gal staining of colorectal cancer cells (HCT116) treated with rotenone and antimycin A displayed similar effects, proposing that the

Chapter 6.0: Ang II-induced mitochondrial alterations

reduction in $\Delta\Psi_M$ by blocking or uncoupling complexes causes premature, p53-dependent senescence (Behrend *et al.*, 2005).

Mito-TEMPO concentrations and pre-incubation periods were used as recommended by others (communication with S. Dikalov, Department of Medicine, Emory University School of Medicine, Atlanta, USA). However, a 2-fold increase in concentration also inhibited senescence to the same degree (data not shown), indicating no toxicity at the levels used. However, specificity and toxicity of mito-TEMPO were not determined in this hVSMC model, thus the inhibitory effect observed can not be entirely attributed with full certainty to scavenged mitochondrial $O_2^{\cdot-}$.

Senescence was not prevented upon blocking mitoK_{ATP} channels with 5-HD in both Ang II-treated and untreated cells, since the vehicle alone (EtOH) caused a reduction in senescence. Therefore further experiments are required to fully investigate of the role of mitoK_{ATP} channels in the induction of senescence by Ang II. The opening of these channels can cause depolarization of the $\Delta\Psi_M$ and stimulate mitochondrial ROS generation. So it is still possible that Ang II-stimulated senescence may be via opening of mitoK_{ATP} channels in mitochondria as has been described in rat VSMC (Kimura *et al.*, 2005a).

In VSMC, pre-treatment with 5-HD had been shown to reduce Ang II-stimulated ROS (Kimura *et al.*, 2005a) with the same effect determined in EC following post-treatment (Doughan *et al.*, 2008), providing evidence for Ang II-mediated effects on vascular mitochondria. However, the treatment regimes used greatly differed to those used in these studies, which may explain why a negative response was observed. Further experiments are required using different treatment regimes of 5-HD and lower concentrations of EtOH.

The flavoprotein inhibitor DPI was traditionally classed as an inhibitor of NAD(P)H oxidase, which was shown to significantly inhibit Ang II-stimulated ROS in VSMC (Touyz and Schiffrin, 2001; Touyz *et al.*, 2002). However, it was also demonstrated to potently block mitochondrial ROS (Li and Trush., 1998). The strength of $O_2^{\cdot-}$ inhibition in both Ang II-treated and untreated lysates revealed NAD(P)H oxidase and mitochondria to be involved in Ang II-stimulated $O_2^{\cdot-}$. Although DPI is not specific it

still supports the finding that a proportion of the $O_2^{\cdot-}$ generated can be attributed to mitochondrial ROS production within this model.

Rodent models have shown the chronic administration of Enalapril (ACE inhibitor) or Losartan (AT₁R inhibitor) to protect against age-related dysfunction and alteration in the ultrastructure of renal mitochondria (de Cavanagh, *et al.*, 2003), identifying the RAS to have a role in CVD development (de Cavanagh, *et al.*, 2008a) and age-accompanied damage or dysfunction to mitochondria. Although the morphology of hVSMC mitochondria was not analysed in response to acute or chronic Ang II treatment, the appearance of enlarged or giant mitochondria have been detected in aged tissue (Tandler *et al.*, 2002; Terman *et al.*, 2004). The accumulation of elongated giant mitochondria was identified as a possible mediator of SIPS and considered a potential phenotypic marker for this senescent state. Senescence models induced by treatment with desferoxamine and H₂O₂, as well as aged HDF had revealed this alteration in mitochondrial ultrastructure accompanied with elevated ROS levels (Yoon *et al.*, 2006). Sustained mitochondrial elongation was further supported by reduced expression of the human mitochondrial fission protein (hFis1) (Lee *et al.*, 2007) and mitochondrial specific changes in response to or as a consequence of growth arrest were identified. Age-related mitochondrial dysfunction in the myocardium has been associated with alterations in mitochondria resembling those of a senescent phenotype (Preston *et al.*, 2008). However, whether these alterations in mitochondria arise as a cause or consequence of senescence is yet to be determined.

6.5.2 Modulation of mtDNA content following Ang II exposure

Since mtDNA is reported to be prone to oxidative damage, the effects of acute and chronic Ang II treatment were assessed since Ang II-induced mitochondrial ROS have been implicated in this model. Increased mtDNA is thought to reflect enhanced biogenesis of new mitochondria. Mitochondrial biogenesis occurs to replace damaged mitochondria and to increase the number of mitochondria in response to cellular energy demands, to maintain cell survival. Moreover, diabetes is associated with oxidative stress and we have recently shown reduced mtDNA content in circulating leukocytes from patients with type II diabetes (unpublished observation).

Chapter 6.0: Ang II-induced mitochondrial alterations

The effect of Ang II on mtDNA content in human cells has not been previously reported. These results showed acute Ang II exposure in quiescent hVSMC to cause a rapid increase in mtDNA of ~2.5-fold after just 30 minutes which was maintained even after 1 hour. This was consistent with the increased $O_2^{\cdot-}$ levels determined after 1 hour, suggesting that increased ROS may have damaged mtDNA and triggered mtDNA replication to compensate for the decline in mitochondrial function. Levels eventually returned to basal levels after 6 hours, indicating that the effects of Ang II were not sustained. Equally, it could be argued that the mitochondrial biogenesis response is very rapid. These changes in mtDNA were not considered to reflect an increase in cell proliferation due to the presence of very little FCS in media and the short term measurements taken following Ang II treatment. Treatment with sublethal doses of H_2O_2 was demonstrated to cause a time-dependent (24 to 72 hours) increase in mtDNA content and mitochondrial mass of human lung fibroblasts, postulating mild oxidative stress to elicit this increase in mitochondria (Lee, *et al.*, 2000). However, over a similar time span Ang II induced a different response, as the relative mtDNA content was only marginally higher after 24 hours, with similar levels to untreated cells observed at 48 and 55 hours. This data indicated that alterations in mtDNA occurred much earlier than 24 hours.

To distinguish the effect observed with serum deprivation from that induced by Ang II, successive Ang II treatment was analysed over a longer period of time in media containing 10% (v/v) FCS. Using this approach, mtDNA was increased with Ang II treatment up to CPD 12. This suggested that the first few Ang II exposures may have induced a stress response by initiating mitochondrial replication or upregulation of mtDNA transcription. Due to limited mtDNA repair mechanisms, Ang II may have induced significant damage reflected by lowered intact mtDNA content values at the later passages compared with controls.

Increased mtDNA has been detected with progressive age in human (Barrientos A *et al.*, 1997; Pesce *et al.*, 2001) and murine tissues (Masuyama, *et al.*, 2005). The mtDNA:nDNA ratios varied over the first few passages of untreated hVSMC but did show an increase at the later passages, indicating the presence of more mtDNA or mitochondria with the accumulation of senescent cells, possibly due to increasing damage to mtDNA. A hUVEC model of replicative senescence also showed elevated

quantities of mtDNA up to CPD ~20 accompanied by increased oxygen consumption and ATP production which then substantially reduced at even higher CPD. This could be explained by increased replication of mitochondria, diminished mitochondrial turnover or defective mitochondria (Carlisle *et al.*, 2002).

Even though mtDNA content in VSMC has not been investigated previously, one other study has analysed mtDNA damage by PCR. H₂O₂ treated human aortic VSMC revealed significant mtDNA damage within 10 to 15 minutes compared to nuclear DNA damage (Ballinger *et al.*, 2000) suggesting ROS mediates rapid damage to mtDNA.

No difference in CPD was observed with successive Ang II treatments, indicating that the initial increases in mtDNA content were not a result of increased cell number and was not due to the induction of rapid mitosis and therefore an increased requirement for mitochondria, but due to increased number of mtDNA per unit mitochondria or mitochondrial numbers/ mass in the context of a similar cell turnover. Although the direct effect of Ang II on hyperplasia in these cells was not investigated, previous results suggest this is not occurring in this model.

Taken together these data suggest that initial adjustments in mtDNA content arise with acute Ang II in response to elevated ROS, in order to maintain adequate cell function and survival. With prolonged exposure a loss in intact mtDNA was ultimately observed. Damaged mtDNA was not determined in these samples, therefore the quantity of mtDNA only reflects the presence of intact mtDNA.

6.5.3 Increased mitochondrial biogenesis in response to Ang II

Oxidative stress has been shown to initiate mitochondrial biogenesis in order to maintain cell survival (Nisoli *et al.*, 2004; Rasbach and Schnellmann, 2007). Ang II increases ROS production which is implicated in physiological and pathological responses in vascular cells. However, there is no data at present showing the effect of Ang II on the expression of regulatory genes involved in mitochondrial biogenesis.

PGC1 α and mtTFA mRNA levels were analysed in hVSMC, as their expression influences mtDNA transcription and replication, signifying alterations in mitochondrial biogenesis. These genes were expressed relative to the expression of the endogenous

Chapter 6.0: Ang II-induced mitochondrial alterations

HPRT1 control gene. However, in order to validate the alterations in transcript levels, a comparison against more than one endogenous control is required (Vandesompele *et al.*, 2002). This is one aspect of further work required in this area.

The trend of a rapid elevation in PGC1 α shortly followed by an increase in mtTFA transcript levels suggests that Ang II initiates mitochondrial biogenesis as a compensatory response to damaged or defective mitochondria, as these levels eventually returned to near basal levels. The elevated O₂⁻ generated after a short Ang II exposure may have caused oxidative damage to mitochondria and its components and thereby triggered an increase in mitochondrial proliferation to provide sufficient energy for cells, in order to ensure cell survival. It has been proposed that changes in intracellular ROS/RNS may influence mitochondrial biogenesis, as H₂O₂ treatment augmented PGC1 α mRNA levels in human fibroblasts (Lee *et al.*, 2002) and the continuous exposure of low \cdot NO elevated the expression of PGC1 α , NRF-1 and mtTFA (Nisoli *et al.*, 2003).

A rapid increase in PGC1 α has similarly been observed in skeletal muscle following exercise. The increased expression of PGC1 α and its associated proteins indicated the initial response to be mediated by enhanced activation of PGC1 α present in the cytosol, which translocates to the nucleus after exercise and initiates the transcription of mitochondrial biogenesis genes (Wright *et al.*, 2007). This study identified a rapid change in mitochondrial biogenesis to be mediated by post-translational alterations in PGC1 α , and thereby suggests adaptations are not solely dependent upon changes in gene transcripts. Again this would be an area for an interesting future study, to investigate whether Ang II could rapidly result in PGC1 α translocation to the nucleus.

A decline in the rate of mitochondrial biogenesis with advancing age is proposed as a result of increased oxidative cell stress and mitochondrial dysfunction (Navarro and Boveris, 2007). In this thesis, the long-term effects of Ang II exposure on the expression of these genes were not examined. The prolonged inhibition of the RAS in old rats displayed enhancement of NRF-1 and PGC1 α mRNA in liver tissue consistent with mtRC activity, which improved mitochondrial function and extended the lifespan of rats (de Cavanagh *et al.*, 2008b). These observations indirectly show Ang II exposure to have a detrimental effect on mitochondrial biogenesis and cell ageing.

This data supports the observed increase in mtDNA content determined following a short Ang II exposure. The trends for early enhanced transcript levels of PGC1 α and mtTFA indicates further studies on the role of Ang II in mtDNA transcription and biogenesis are warranted.

6.5.4 Alterations in mitochondrial function following Ang II exposure

Mitochondria conserve energy for the cell. A defect in mitochondrial respiratory function arising from environmental stresses or during ageing can lead to a decline in ATP synthesis. Reduced levels of energy metabolism affect cellular function and survival, and therefore conceptually an increase in mitochondria is triggered to provide more energy to meet the cells requirements. Therefore, it can be postulated that alterations in mitochondrial respiratory function may arise as a cause or consequence of cellular senescence.

The response to mild oxidative stress following t-BHP treatment for 1 hour almost doubled the ATP levels of hVSMC in media containing 10% (v/v) FCS suggesting a stress response. This differed from the response observed with chronic ONOO⁻ treatment which caused a dramatic reduction in the ATP levels of VSMC (Ballinger, *et al.*, 2000). It is assumed that increased ATP levels means increased synthesis of ATP. However, it may be that oxidative stress causes decreased utilization of ATP. No effect on ATP was observed in quiescent cells suggesting that (1) these cells in the G₀-phase of the cell cycle did not respond to the short period of t-BHP exposure or that (2) the bioluminescent assay did not detect sufficient differences in ATP within this cell state or that (3) quiescent cells have reduced ATP levels. This was confirmed when cells were exposed to acute Ang II over time.

With acute Ang II exposure in proliferating cells, a maximal response in ATP was determined after 4 hours before levels resumed to untreated levels (after 24 hours). This compensatory response in ATP synthesis was similar to that observed in the short-term changes in mtDNA content. It can therefore be assumed that an increase in the number of mitochondria/ mitochondrial mass may have lead to increased mtRC function, hence ATP synthesis, following Ang II treatment. However, again decreased ATP utilization cannot be ruled out from this data alone.

Chapter 6.0: Ang II-induced mitochondrial alterations

Although this is the first evidence of Ang II-mediated alterations in ATP content within a cell model, changes have been determined in animal models. Chronic Ang II-infused rats for 14 days had higher renal interstitial fluid ATP levels than control rats and this was consistent with elevated blood pressure levels. This increase was associated with Ang II-dependent hypertension (Graciano, *et al.*, 2007)

Here, inhibition studies revealed the Ang II induction of ATP was mediated via AT₁R activation. The effect of Ang II was also blocked by rotenone confirming its response on the mtRC function. Substantial inhibition with the complex I inhibitor rotenone was also observed in untreated cells, further confirming the mtRC as a major source of cellular ATP.

Despite the short-term alterations in ATP that occurred in response to Ang II, the long-term effects were not determined. However the induction of SIPS over 3 days treatment at two different Ang II doses was analysed to determine effects on ATP levels. The highest ATP content was observed with 10^{-8} mol/L Ang II at which dose SIPS was maximal; suggesting successive exposure to mild oxidative stress increases mtRC function and also mediates SIPS of cells *in vitro*. The reduction in ATP with 10^{-7} mol/L Ang II may indicate damaged/reduced mtRC function as a single exposure at this dose had revealed short-term increases. Therefore continuous alterations in ATP mediated by Ang II may eventually cause a defect in the capacity of mitochondria to recover leading to mitochondrial dysfunction and reduced ATP. Alternatively, apoptosis which requires ATP was maximal at 10^{-7} mol/L Ang II, indicating apoptosis may result in a decline in ATP. Increased oxidative stress is thought to contribute to the decline in mtRC function with advancing age. Evidence for this has been demonstrated by a sharp reduction in mtRC function in cultured human cells treated with H₂O₂ (Yakes and van Houten, 1997) and in pulmonary arterial EC grown in hypoxic conditions (Xu *et al.*, 2007).

Hypertensive rodent models displayed a reduction in the rate of ATP synthesis accompanied by elevated blood pressure. This defective energy conversion in mitochondria was strongly associated with this cardiovascular risk factor (Budnikov, *et al.*, 2002). An opposite response to this was determined in the replicative senescent hUVEC model, whereby a progressive increase in ATP with CPD may have been due to

Chapter 6.0: Ang II-induced mitochondrial alterations

sustained energy production via glycolysis (Carlisle *et al.*, 2002), which makes it difficult to investigate cellular senescence with respect to mitochondrial function.

The progressive loss in mitochondrial function is strongly associated with increasing age. Ferder had shown significant improvements in mitochondrial function with prolonged inhibition of AT₁R in animal tissues (de Cavanagh, *et al.*, 2003; and 2008a), suggesting that Ang II may induce mitochondrial damage over time.

However, recent findings have revealed proteasomes to modulate mitochondrial function in senescent cells (Torres and Perez, 2008). Proteasomes undertake proteolytic activity which is essential for eliminating defective, oxidized and aged proteins that threaten cell survival (Grune *et al.*, 1997). They display an age-dependent decline in function and upon proteasome inhibition an increase in ROS and mitochondrial dysfunction has been determined in human senescent cells (Torres and Perez, 2008). The presence of damaged proteins, such as those that form the mtRC complex, leads to mitochondrial dysfunction and thereby contributes to the onset of senescence.

These results demonstrate alterations in the ATP content of hVSMC with oxidative stress and the induction of a compensatory response following short-term Ang II exposure, which are indicative of changes in mitochondrial function. Successive treatment appeared to cause diminished mtRC function.

Conclusions

- mtRC activity and mitochondrial-derived ROS are necessary for the induction of Ang II-induced premature senescence of hVSMC.
- Superoxide generation via the mtRC is initiated by Ang II-induced NADPH-dependent $O_2^{\cdot-}$.
- Short-term Ang II treatment caused an increase in mtDNA content of hVSMC.
- Continuous Ang II exposure caused a reduction in quantities of intact mtDNA to control levels.
- Ang II may stimulate a rapid increase in PGC1 α and mtTFA genes that regulate mitochondrial biogenesis.
- Short-term Ang II treatment caused an increase in ATP content of hVSMC.
- Ang II predominantly initiates mitochondrial-derived ATP in hVSMC.
- Ang II-induced SIPS resulted in diminished ATP content possibly due to depressed mitochondrial function.

CHAPTER SEVEN
General Discussion and Future Work

Chapter 7.0: General Discussion and Future Work

7.1 Discussion

The aim of this thesis was to study whether Ang II promoted VSMC senescence and then to investigate the mechanisms for this effect. The hVSMC model was established to measure cellular and biochemical changes associated with the onset of senescence. The effects on proliferation and apoptosis following exposure to Ang II, specific Ang II receptor inhibitors and ROS scavengers were also investigated. From this study, future work extends towards further investigation into the Ang II signalling of ROS generation by mitochondria and the emerging role of mitochondrial biogenesis on vascular cell function, in CVD and vascular ageing.

7.1.1 hVSMC as an *in vitro* model to study cellular effects of Ang II

Early passage hVSMC derived from adult saphenous veins exhibited typical morphological and growth characteristics associated with the contractile phenotype of SMC. This was supported by expression levels of the contractile proteins, α -smooth muscle actin and SM-MHC. Contractility is a major function of VSMC *in vivo* and the early passages of these cells reflected this phenotype *in vitro*.

High levels of protein expression of the fully native forms of both Ang II receptor subtypes, AT₁R and AT₂R, were determined in both proliferating and quiescent cells. This strongly suggested these hVSMC would respond to exogenous Ang II irrespective of the serum content in culture media.

The pleiotropic effects of Ang II can cause diverse responses in cells, especially at different phases of the cell cycle. To assess the growth effects of Ang II, hVSMC were rendered quiescent by placing into media containing 0.5% (^v/_v) FCS for 24 hours prior to treatment, without causing cell death. This eliminated the effects of other growth promoting factors that were present in culture media and enabled the effects of Ang II to be more accurately measured over short periods.

hVSMC proliferated in response to a single Ang II exposure and following treatment over several passages. This was determined by higher PD counts and MTT activity. Under these conditions these cells did not undergo hypertrophy as no change in protein content was detected after treatment. Although these short experiments were predominantly conducted on contractile hVSMC, phenotypic modulation in response to growth factors is known to occur *in vivo*. These changes lead to alterations in the physiological response of the cell and also play a role in pathological responses (Owens *et al.*, 2004). Moreover, it is not known whether phenotypic modulation occurs *in vitro*, and if it does, whether it is different to that *in vivo*, or if it is due to culturing parameters. Therefore one limitation of this study is that Ang II responses measured *in vitro* may not fully represent those observed *in vivo*.

7.1.2 Mechanisms of Ang II-induced VSMC senescence

Ang II stimulated an increase in ROS production, induced DNA damage and accelerated telomere attrition in hVSMC. These effects are all implicated in the induction of cellular senescence, as illustrated in **figure 1.7**. Increased senescence was determined following continuous Ang II exposure with sub-cultivation of cells over 30 days, and following short successive exposures and recovery periods over several days. As these different Ang II treatment regimes resulted in positive SA- β -gal staining of hVSMC it indicates that Ang II can initiate senescence by different mechanisms (replicative or SIPS). The common DNA-damage signalling pathways activated by these different senescence mechanisms (**figure 5.1**) and the pleiotropic effects of Ang II, postulate that both forms of senescence could be initiated within the same population of cells.

The maximum percent of SA- β -gal stained cells was observed with 10^{-8} mol/L Ang II with slightly fewer determined at 10^{-7} mol/L, suggesting the occurrence of cell death at this dose. These data were consistent with the elevated protein expressions of CDKI. Recent studies published during this thesis have supported the finding that short Ang II exposures accelerate the premature senescence of VSMC (Kunieda *et al.*, 2006; Min *et al.*, 2007) and EPC (Imanishi *et al.*, 2005a); but as yet there is no other evidence of the long-term effects of Ang II on senescence.

A major limitation to the interpretation of the senescent studies reported here is that telomere attrition, DNA damage and the expression of CDKI were not determined successively following continuous Ang II exposure on hVSMC. Therefore, it cannot be definitively confirmed from this model that Ang II induces replicative senescence. As there are no definitive markers for SIPS cells that are not also markers for replicative senescence, the interpretation of the data is solely based upon the length of treatment regime. This causes difficulty in deciphering the difference between SIPS and replicative senescence within the same population of cells.

Although the effect did not reach statistical significance, it was interesting to note that there was a trend towards inhibition of Ang II-induced premature senescence following AT₂R inhibition, suggesting AT₂R activation may also play a role in the induction of Ang II mediated senescence. However, further work is necessary to fully elucidate this effect.

The SA- β -gal assay does not differentiate between senescence-inducing factors. The cause of increased lysosomal content that contains SA- β -gal activity, has not been investigated in arterial wall and vessels, but has been hypothesised to reflect the accumulation of autophagic vacuoles in senescent cells which may contain damaged organelles (Erusalimsky and Kurz, 2005).

Ang II induced SIPS after a single treatment but also following short successive treatments. This mechanism of senescence can occur independent of telomere loss, as confirmed by the onset of senescence in hTERT-hASMC following Ang II exposure. This has been observed in fibroblasts expressing hTERT upon exposure to sublethal radiation or H₂O₂ (Gorbunova *et al.*, 2002). Although the mechanism of senescence was not investigated in this cell model, other models have demonstrated signalling of senescence to be mediated via oncogenic Ras activation (Takaoka *et al.*, 2004). The overexpression of Ras has been implicated in VSMC senescence (Minamino *et al.*, 2003) and Ras is activated upon Ang II signalling. This strongly suggests Ras activation maybe involved in the mechanism of premature senescence induction within these cells. However, this can only be speculated since Ras expression was not determined in these cells.

Recent evidence has indicated cellular senescence to be more than just a tumour suppressor mechanism. Growth arrest of hepatic cells *in vivo* has been shown to have a role in liver injury and subsequent repair (Green, 2008). This demonstrated the importance of this cellular mechanism and further verified the complexities in initiating this response. However, it does indicate that early age-related vascular alterations maybe due to injury.

Investigations into the effects of some pharmacological CVD treatments have provided links between the occurrence of vascular cell senescence, ageing and disease. Statin treatment for hypercholesterolemia/atherosclerosis using *in vivo* and *in vitro* models showed markedly accelerated DNA repair, thereby delaying the onset of VSMC senescence and subsequent disease. The novel mechanism involved the expression of Nijmegen breakage syndrome-1 and human double minute proteins (Hdm2) (Mahmoudi *et al.*, 2008).

7.1.3 Modulation of mitochondria in response to Ang II exposure

Mitochondria are a major source of cellular ROS and studies using a variety of inhibitors have identified that they contribute to increased ROS generation via Ang II signalling (Kimura *et al.*, 2005a; 2005b; Doughan *et al.*, 2008). Results from this thesis demonstrate that inhibition of the mtRC complexes causes lower levels of O₂^{·-} generation following NADPH stimulation and a reduction in Ang II-induced senescence. Since ROS are involved in the senescent mechanism, this data suggests that Ang II-stimulated ROS via mitochondria may accelerate the onset of premature senescence in hVSMC. Recently Doughan *et al* (2008) have suggested a similar mechanism for Ang II-stimulated EC. Although NADPH oxidase is upstream of mitochondrial ROS release, the latter further leads to enhanced NADPH oxidase activity via Rac (Doughan *et al.*, 2008). The data presented within this thesis show for the first time that mitochondrial ROS are necessary for Ang II-induced SIPS.

Evidence is beginning to emerge bridging the link between mitochondria and cellular senescence. However, the effects related to premature senescence are yet to be thoroughly investigated. For example, proteasomes potentially play a fundamental role in modulating mitochondrial function during senescence induction (Torres and Perez, 2008); mitochondrial impairment gives rise to ROS generation and DNA damage

thereby accelerating senescence (Ksiazek *et al.*, 2008); and partial uncoupling of the mtRC has been associated with the onset of premature senescence (Stöckl *et al.*, 2007).

Short Ang II exposures caused rapid increases in mitochondrial $O_2^{\cdot-}$ generation, ATP levels, mtDNA content and the transcription of mitochondrial biogenesis genes (**figure 7.1**). These eventually resumed to basal levels over time. These changes demonstrated alterations in mitochondrial components and function but did not confirm the involvement of mitochondria in Ang II-induced senescence. Further experimentation is required to establish whether this link is justified. Furthermore, the reduction in intact mtDNA content with continuous Ang II treatment implied the presence of more damaged mtDNA with continuous Ang II exposure.

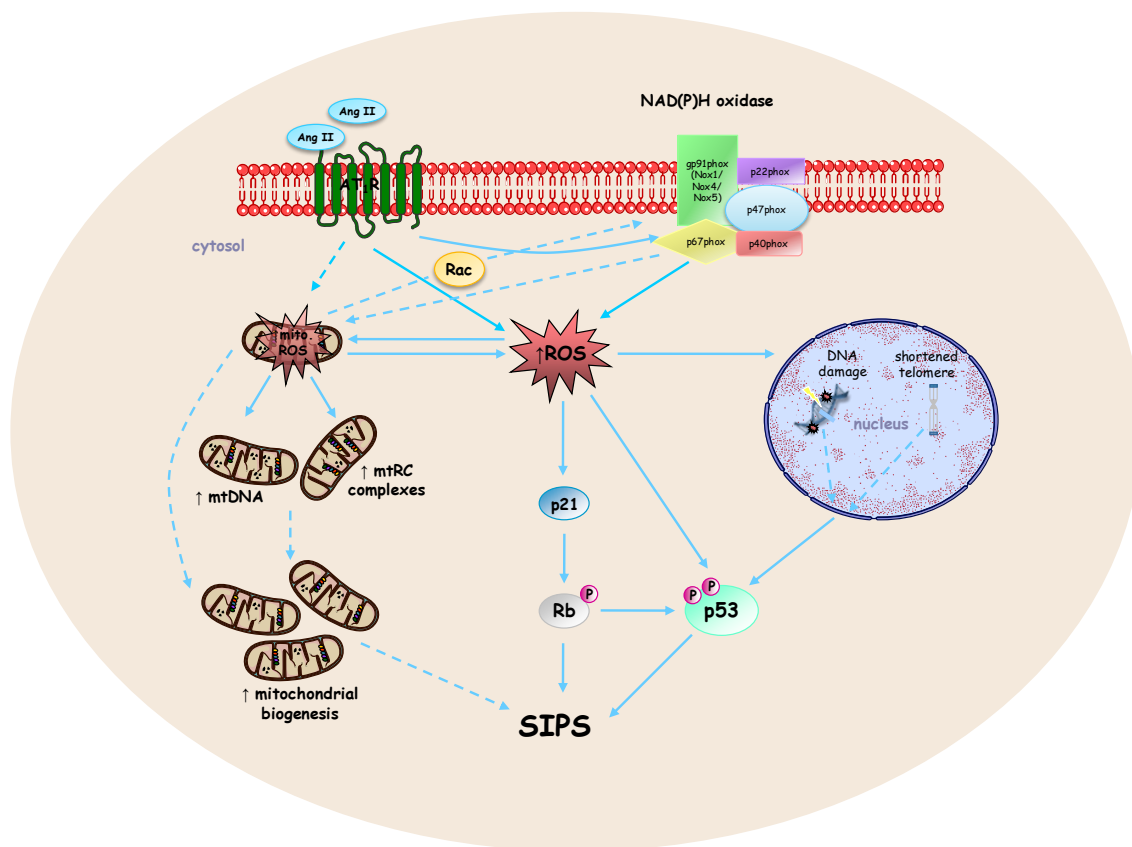


Figure 7.1 Proposed mechanisms of Ang II-mediated SIPS. Ang II binding to AT_1R stimulates intracellular responses by activating signalling cascades. Increased NADPH oxidase activation causes enhanced ROS generation. Oxidative damage to nDNA and/or shortening of telomeric DNA triggers the onset of senescence. Modulation of CDKI in response to oxidative stress can result in halting cell cycle progression and cause cells to undergo transient growth arrest. Enhanced NADPH oxidase may further activate other cellular sources of ROS, i.e. mitochondria. Short Ang II exposure increased mitochondrial $O_2^{\cdot-}$ production, upregulated mtRC activity, increased mtDNA content and the transcription of regulatory genes that coordinate and signal mitochondrial biogenesis. These rapid adaptations in mitochondria are further hypothesised to be involved in the induction of premature senescence.

Alterations in the gene expression of mitochondrial biogenesis regulators following Ang II exposure demonstrated changes similar to that determined in mtDNA content, indicating an effect on mitochondrial biogenesis. Whether or not these changes in mitochondrial biogenesis have an impact on the induction of senescence, is not clear.

7.1.4 Ang II and accelerated vascular ageing

Do these observations and mechanisms have any clinical relevance in man? The changes in morphology, gene expression and function of senescent cells are consistent with changes observed in many age-related vascular diseases, signifying a critical role in disease development. Ageing is a major risk factor in CVD, and is associated with changes in arterial structure and function. Observations in the arterial wall of healthy humans (≥ 65 years old) have shown increased arterial wall thickness, luminal diameter, wall stiffness due to the deposition of collagen, EC dysfunction, and increased pulse wave velocity (reviewed by Najjar *et al.*, 2005). These changes are also present in CVD and are considered a result of accelerated arterial ageing. Consistent with these alterations, patients with hypertension or atherosclerosis have increased wall thickness, arterial stiffness, central pressure augmentation, and EC dysfunction (Najjar *et al.*, 2005), indicating these effects are associated with the manifestation of CVD.

Studies using rodent models have shown the prolonged inhibition of the RAS to prevent many age-related vascular changes (Basso *et al.*, 2007) and those associated with mitochondrial dysfunction (de Cavanagh *et al.*, 2003; 2008b) and result in extended lifespan. This indicated that Ang II responses contribute to age-associated changes within animals.

SA- β -gal positive cells have been observed in rabbit carotid arteries subjected to vascular injury, which was strikingly enhanced upon repeated denudation (Fenton *et al.*, 2001). This implies that extensive damage to the vascular wall may trigger premature senescence. Many senescent characteristics have been identified in advanced atherosclerotic plaques; SA- β -gal positive VSMC in the intimal region were identified and exhibited increased p16 and p53 protein expression (Minamino *et al.*, 2003; Matthews *et al.*, 2006). Senescent EC showed decreased eNOS activity and increased generation of proinflammatory molecules suggesting impairment of endothelial-dependent vasodilation and enhanced recruitment of inflammatory cells to the site of atherogenesis (Minamino *et al.*, 2003).

Telomere attrition is strongly correlated with the induction of replicative senescence in vascular cells. Aged vessels displayed a greater loss in telomere length as a result of continuous exposure to hemodynamic stress (Chang and Harley, 1995). Evidence of telomere shortening has been determined in many clinical studies with respect to age-related CVD (Samani *et al.*, 2001; Benetos *et al.*, 2004; Demissie *et al.*, 2006). Many of these pathologies are associated with Ang II, thereby indicating a correlation between senescence, ageing and disease development.

Ang II initiates many cell signalling mechanisms, and is highly expressed in thickened intimal regions of arteries (Wang *et al.*, 2003), and is implicated in hypertension. Many of the stimulatory responses invoked by Ang II may contribute to its age-associated effects, as Ang II signalling causes an increase in collagen, upregulates NAD(P)H oxidase activity and increases VSMC migration (Najjar *et al.*, 2005). Exogenous Ang II has also been shown to induce premature cell senescence *in vitro* and *in vivo* (Imanishi *et al.*, 2005a; Kunieda *et al.*, 2006; this thesis). These observations suggest that Ang II signalling plays an important role in arterial ageing and CVD development.

As mitochondria are regarded as the main source of cellular ROS, at least in “non-professional” phagocytes, this may explain why they have been implicated in the free radical theory of ageing. Diseases such as atherosclerosis may involve enhanced ROS signalling. This has been demonstrated to cause mitochondrial dysfunction and damage to mtDNA in vascular cells *in vitro* (Ballinger *et al.*, 2000). Alterations in other mitochondrial components and function have been determined in aged vessels and in the development of CVD (Xu *et al.*, 2007; Preston *et al.*, 2008). More recently, the impairment of mitochondrial biogenesis has been associated with a decline in mitochondrial mass, mtRC components and increased mitochondrial ROS in EC of healthy aged vessels (Ungvari *et al.*, 2008). However, the effect of Ang II on mitochondria with respect to vascular cell ageing had not been investigated until this thesis.

7.2 Future Work

Future work that could complement the studies in this thesis are:

7.2.1 Ang II induced ROS mediated via NAD(P)H oxidase and mitochondria

A continuation of the work on Ang II stimulated ROS production via NAD(P)H oxidase and via mitochondrial activation could be conducted by eliminating whole subunits and components of these sources of cellular ROS, using small interference RNA (siRNA) techniques (Cucoranu *et al.*, 2005; Kuroda *et al.*, 2005). This would identify which components are enhanced and/or involved in Ang II-induced ROS signalling via this mechanism in hVSMC.

The lack of specificity and the toxicity of fluorescent ROS reporting probes have led to difficulty in accurately measuring mitochondrial ROS. The need for reliable markers of mitochondrial-derived ROS and the use of specific mitochondrial ROS scavengers in intact cells would enable a more concise measure of the ROS generated via this organelle in response to Ang II.

7.2.2 Modulation of mitochondrial biogenesis in vascular ageing

Rapid changes in the mRNA transcript levels of the master gene regulators of mitochondrial biogenesis were suggested following short Ang II exposures, by real-time qPCR. However, it would be interesting to see what effects short successive and prolonged Ang II exposures had on the levels of these gene transcripts in hVSMC, with continuous cultivation and upon approaching senescence. Additionally, protein expression levels would further confirm any changes in gene transcripts.

Inhibition with specific siRNA that would prevent the transcription of mitochondrial biogenesis genes could be utilized to determine those genes that are directly initiated upon Ang II stimulation.

At present, it is only speculated that the mitochondrial biogenesis mechanism deteriorates or is dysfunctional with increasing age, which may be due to damaged or reduced mitochondrial components determined in aged tissue (Preston *et al.*, 2008).

Alterations in the various signalling responses involved in this mechanism have been detected in aged animals, displaying a decline in biogenesis (Navarro and Boveris, 2007). In humans, many age-related cardiovascular risk factors such as insulin resistance, obesity and type II diabetes have revealed reduced numbers of mitochondria, indicating a decline in mitochondrial biogenesis. However, this mechanism has not been fully investigated in the vasculature of healthy aged individuals. The levels of these master regulatory genes would need to be determined in different tissues of the body in order to assess whether ageing in general affects this process or whether there are changes associated with particular tissues.

7.2.3 New biomarkers for vascular cell senescence

The identification of biomarkers specific for senescent vascular cells would allow for the detection of early senescence in humans presenting with cardiovascular risk factors such as hypertension, hypercholesterolemia, insulin resistance and obesity. As all of these can contribute to the manifestation of adverse CVD the detection of senescence could help in early diagnosis and prevention.

At present, the rapid expression of specific proteins in certain cell types has been associated with the state of SIPS. The development of an exclusive marker or more likely a panel of biomarkers for measuring SIPS *in vivo*, would aid investigations into accelerated ageing and disease, both in terms of investigating pathology and the effects of therapeutic regimes.

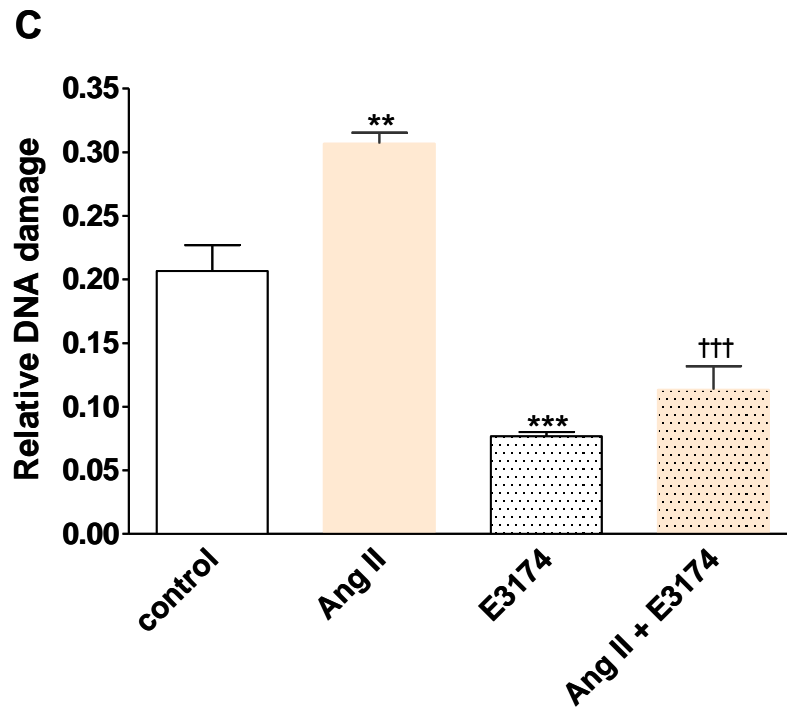
APPENDIX I *Inhibition of Ang II induced DNA damage by E3174*

Figure 4.3C, Ang II induces DNA damage in hVSMC via the AT₁R. DNA damage was measured using the Comet assay in cells treated with Ang II (10^{-6} mol/L) \pm E3174 (10^{-5} mol/L) for 20 hours. Bars represent mean \pm SEM. (** $p < 0.01$ and *** $p < 0.001$ compared with control; ††† $p < 0.001$ compared with Ang II alone; $n = 3$). This work was carried out by Dr. R. A Hastings, Department of Cardiovascular Sciences, University of Leicester. (Relative DNA damage refers to the fold change in Olive Tail moment measurements).

APPENDIX II *Raw data and calculations for relative quantification of mitochondrial biogenesis gene expressions*

Changes in PGC1 α and mtTFA gene transcripts following Ang II exposure using the ‘Pfaffl’ formula (Pfaffl, 2001):

$$\text{Relative change in gene expression} = \frac{\text{Efficiency}^{\text{TARGET(untreated-treated)}}}{\text{Efficiency}^{\text{CONTROL(untreated-treated)}}$$

1. Untreated= HPRT1, 29.35; PGC1 α , 28.60

<i>Ang II (hours)</i>	<i>HPRT1 expression</i>	<i>HPRT1 (control-Ang II)</i>	<i>Efficiency^(HPRT1)</i>	<i>PGC1α expression</i>	<i>PGC1α (control-Ang II)</i>	<i>Efficiency^(PGC1α)</i>	<i>Relative change in PGC1α</i>
0.25	29.38	-0.03	0.98	25.45	3.15	5.52	5.63
0.5	29.76	-0.41	0.79	28.48	0.12	1.07	1.35
1	29.56	-0.21	0.89	28.19	0.41	1.25	1.40
4	28.96	0.39	1.25	28.90	-0.30	0.85	0.68
24	28.98	0.37	1.24	29.93	-1.33	0.49	0.40

2. Untreated= HPRT1, 29.45; PGC1 α , 28.91

0.25	29.62	-0.17	0.91	28.70	0.21	1.12	1.23
0.5	28.77	0.68	1.48	28.63	0.28	1.16	0.78
1	29.16	0.29	1.18	28.19	0.72	1.48	1.25
4	28.95	0.50	1.33	28.36	0.55	1.35	1.39
24	28.66	0.79	1.58	28.88	0.03	1.02	0.65

3. Untreated= HPRT1, 29.86, PGC1 α , 28.85

0.25	29.43	0.43	1.28	29.11	-0.26	0.87	0.65
0.5	29.31	0.55	1.37	28.47	0.38	1.23	0.90
1	30.16	-0.30	0.84	27.89	0.96	1.68	2.00
4	29.10	0.46	1.55	29.16	-0.31	0.85	0.55
24	28.80	1.06	1.84	27.30	1.55	2.32	1.26

PCR efficiency for HPRT1 = 78% (1.78) and PGC1 α = 72% (1.72).

1. Untreated= HPRT1,29.35; mtTFA,27.68

<i>Ang II</i> (hours)	<i>HPRT1</i> expression	<i>HPRT1</i> (control-Ang II)	<i>Efficiency</i> ^(<i>HPRT1</i>)	<i>mtTFA</i> expression	<i>mtTFA</i> (control-Ang II)	<i>Efficiency</i> ^(<i>mtTFA</i>)	<i>Relative change in</i> <i>mtTFA</i>
0.25	29.38	-0.03	0.98	27.73	-0.05	0.97	0.99
0.5	29.76	-0.41	0.79	27.70	-0.02	0.99	1.25
1	29.56	-0.21	0.89	27.05	0.63	1.47	1.65
4	28.96	0.39	1.25	26.90	0.78	1.62	1.30
24	28.98	0.37	1.24	26.99	0.69	1.53	1.23
2. Untreated= HPRT1,29.45; mtTFA,28.32							
0.25	29.62	-0.17	0.91	27.35	0.97	1.82	2.00
0.5	28.77	0.68	1.48	27.60	0.72	1.56	1.05
1	29.16	0.29	1.18	27.18	1.14	2.02	1.71
4	28.95	0.50	1.33	26.88	1.44	2.43	1.83
24	28.66	0.79	1.58	26.83	1.49	2.50	1.58
3. Untreated= HPRT1,29.86; mtTFA,27.95							
0.25	29.43	0.43	1.28	27.79	0.16	1.10	0.86
0.5	29.31	0.55	1.37	27.54	0.41	1.29	0.94
1	30.16	-0.30	0.84	27.85	0.10	1.06	1.26
4	29.10	0.46	1.55	27.05	0.90	1.74	1.12
24	28.80	1.06	1.84	26.85	1.10	1.97	1.07

PCR efficiency for mtTFA = 85% (1.85)

The amplification efficiency for each PCR reaction was calculated from the slope of the regression line in the standard curve by the StepOne™ software.

APPENDIX III

PCR product sequencing data of mitochondrial biogenesis genes and the endogenous control gene

A, Comparison of complementary and non-complementary base sequences of the human PGC1 α gene

PGC1 α sequence exported from chromatogram file

NNNNNNNNNNNNNNNNNNNGACCCCAAGGGTTCCCCATTTGAGAACAAGAC
TATTGAACGCACCTTAAGTGTGAGNCNAGACTANNNNNNGCACCTTNGTN
TNNATAAATGTGCCATATCTTCCAG**TGACCCCAAGGGTTCCCCATTTGAGAA**
CAAGACTATTGAACGCACCTTAAGTGTG

PGC1 α sense sequence

CCAAACCAACAACCTTTATCTCTTCCTCTGACCCAGAGTCACCAAATGAC
CCCAAGGGTTCCCCATTTGAGAACAAGACTATTGAACGCACCTTAAGTGT
G

Matched 54/54 nucleotide bases

100% homology

B, Comparison of complementary and non-complementary base sequences of the human mtTFA gene

mtTFA sequence exported from chromatogram file

NNNNNNNNNNNNNNCGTTGGAGGGACTTCCTGATTCAAGAAAAAATATATC
AAGATGCTTATAGGGCGGA AANNNNCCNNNTTTNNNNGGNNNTCNNNNNN
TGGNNNNNNNNNNNGNNNNNNNNNNNNNNNNNNNNNNNNNNNNNNNNNNNN
NNNNNNNNNNNNANNNGNNNNNNCCCNCTNCNCTTANNNN

mtTFA sense sequence

CCCAGATGCAAAAACCTACAGAACTAATTAGAAGAATTGCCAGCGTTGGA
GGGA ACTTCCTGATTCAAAGAAAAAATATATCAAGATGCTTATAGGGCG
GA

Matched 57/59 nucleotide bases

97% homology

C, Comparison of complementary and non-complementary base sequences of the HPRT1 housekeeper gene

HPRT1 sequence exported from chromatogram file

NNNNNNNCNANNNGGTCA NGTCNNNNCTTGCTGGTGAAAGGACCCACGA
AGTGTGGATATAANCCNNACA

HPRT1 sense sequence

GCAGACTTTGCTTTCCTTGGTCAGGCAGTATAATCCAAAGATGGTCAAGG
TCGCAAGCTTGCTGGTGAAAAGGACCCACGAAGTGTGGATATAAGCCA
GAC

Matched 50/61 nucleotide bases

82% homology

APPENDIX IV *Communications arising from this thesis*

Abstracts

Herbert, K. E., **Mistry, Y** and Williams, B. (2008). Mitochondria and premature senescence of vascular smooth muscle cells. *Free Radic Biol Med.* **45** (Suppl 1) S145

Mistry, Y., Poolman, T., Hastings, R., Niklason, L., Williams, B and Herbert, K. E. (2007). Reactive oxygen species generation in human vascular smooth muscle cells: a trigger for stress-induced premature senescence. *Free Radic Biol Med.* **43** (Suppl.1), S97

Herbert, K. E., **Mistry, Y.**, Hastings, R., Poolman, T., Williams, B. (2006). Reactive oxygen species as mediators of human vascular smooth muscle cell senescence induced by Angiotensin II. *Free Radic Res* **40**: (Suppl.1), S84

Herbert, K. E., **Mistry, Y.**, Stanley, A.G., Hastings, R.A., Williams, B. (2005). Angiotensin II induces human vascular smooth muscle cell senescence via reactive oxygen species generation. *Free Radic Biol Med* **39** (Suppl.1), S512

Paper

Herbert, K. E., **Mistry, Y.**, Hastings, R., Poolman, T., Niklason, L and Williams, B (2008). Angiotensin II-mediated oxidative DNA damage accelerates cellular senescence in cultured human vascular smooth muscle cells via telomere-dependent and independent pathways. *Circ Res* **102**, 201-8

Paper in preparation

Mistry, Y., Williams, B and Herbert K. E. (in preparation). Modulation of mitochondria in response to Angiotensin II-induced stress-induced premature senescence in human vascular smooth muscle cells.

References

- Abraham, R. T. (2001). Cell cycle checkpoint signaling through the ATM and ATR kinases. *Genes Dev* **15**, 2177-96.
- Adaikalakoteswari, A., Balasubramanyam, M., Ravikumar, R., Deepa, R., and Mohan, V. (2007). Association of telomere shortening with impaired glucose tolerance and diabetic macroangiopathy. *Atherosclerosis* **195**, 83-9.
- Aguilar, D., Solomon, S. D., Kober, L., Rouleau, J. L., Skali, H., McMurray, J. J., Francis, G. S., Henis, M., O'Connor, C. M., Diaz, R., Belenkov, Y. N., Varshavsky, S., Leimberger, J. D., Velazquez, E. J., Califf, R. M., and Pfeffer, M. A. (2004). Newly diagnosed and previously known diabetes mellitus and 1-year outcomes of acute myocardial infarction: the VALsartan In Acute myocardial iNfarcTion (VALIANT) trial. *Circulation* **110**, 1572-8.
- Allsopp, R. C., Vaziri, H., Patterson, C., Goldstein, S., Younglai, E. V., Futcher, A. B., Greider, C. W., and Harley, C. B. (1992). Telomere length predicts replicative capacity of human fibroblasts. *Proc Natl Acad Sci U S A* **89**, 10114-8.
- Babior, B. M., Lambeth, J. D., and Nauseef, W. (2002). The neutrophil NADPH oxidase. *Arch Biochem Biophys* **397**, 342-4.
- Baird, D. M., Rowson, J., Wynford-Thomas, D., and Kipling, D. (2003). Extensive allelic variation and ultrashort telomeres in senescent human cells. *Nat Genet* **33**, 203-7.
- Ballinger, S. W., Patterson, C., Knight-Lozano, C. A., Burow, D. L., Conklin, C. A., Hu, Z., Reuf, J., Horaist, C., Lebovitz, R., Hunter, G. C., McIntyre, K., and Runge, M. S. (2002). Mitochondrial integrity and function in atherogenesis. *Circulation* **106**, 544-9.
- Ballinger, S. W., Patterson, C., Yan, C. N., Doan, R., Burow, D. L., Young, C. G., Yakes, F. M., Van Houten, B., Ballinger, C. A., Freeman, B. A., and Runge, M. S. (2000). Hydrogen peroxide- and peroxynitrite-induced mitochondrial DNA damage and dysfunction in vascular endothelial and smooth muscle cells. *Circ Res* **86**, 960-6.
- Barker, S., Marchant, W., Ho, M. M., Puddefoot, J. R., Hinson, J. P., Clark, A. J., and Vinson, G. P. (1993). A monoclonal antibody to a conserved sequence in the extracellular domain recognizes the angiotensin II AT1 receptor in mammalian target tissues. *J Mol Endocrinol* **11**, 241-5.
- Barrientos, A., Casademont, J., Cardellach, F., Ardite, E., Estivill, X., Urbano-Marquez, A., Fernandez-Checa, J. C., and Nunes, V. (1997). Qualitative and quantitative changes in skeletal muscle mtDNA and expression of mitochondrial-encoded genes in the human aging process. *Biochem Mol Med* **62**, 165-71.

- Bascands, J. L., Girolami, J. P., Troly, M., Escargueil-Blanc, I., Nazzal, D., Salvayre, R., and Blaes, N. (2001). Angiotensin II induces phenotype-dependent apoptosis in vascular smooth muscle cells. *Hypertension* **38**, 1294-9.
- Bassaneze, V., Miyakawa, A. A., and Krieger, J. E. (2008). A quantitative chemiluminescent method for studying replicative and stress-induced premature senescence in cell cultures. *Anal Biochem* **372**, 198-203.
- Basso, N., Cini, R., Pietrelli, A., Ferder, L., Terragno, N. A., and Inserra, F. (2007). Protective effect of long-term angiotensin II inhibition. *Am J Physiol Heart Circ Physiol* **293**, H1351-8.
- Bauriedel, G., Hutter, R., Welsch, U., Bach, R., Sievert, H., and Luderitz, B. (1999). Role of smooth muscle cell death in advanced coronary primary lesions: implications for plaque instability. *Cardiovasc Res* **41**, 480-8.
- Beckmann, J. S., Ye, Y. Z., Anderson, P. G., Chen, J., Accavitti, M. A., Tarpey, M. M., and White, C. R. (1994). Extensive nitration of protein tyrosines in human atherosclerosis detected by immunohistochemistry. *Biol Chem Hoppe Seyler* **375**, 81-8.
- Beer, M., Seyfarth, T., Sandstede, J., Landschutz, W., Lipke, C., Kostler, H., von Kienlin, M., Harre, K., Hahn, D., and Neubauer, S. (2002). Absolute concentrations of high-energy phosphate metabolites in normal, hypertrophied, and failing human myocardium measured noninvasively with (31)P-SLOOP magnetic resonance spectroscopy. *J Am Coll Cardiol* **40**, 1267-74.
- Behrend, L., Mohr, A., Dick, T., and Zwacka, R. M. (2005). Manganese superoxide dismutase induces p53-dependent senescence in colorectal cancer cells. *Mol Cell Biol* **25**, 7758-69.
- Benetos, A., Gardner, J. P., Zureik, M., Labat, C., Xiaobin, L., Adamopoulos, C., Temmar, M., Bean, K. E., Thomas, F., and Aviv, A. (2004). Short telomeres are associated with increased carotid atherosclerosis in hypertensive subjects. *Hypertension* **43**, 182-5.
- Benetos, A., Okuda, K., Lajemi, M., Kimura, M., Thomas, F., Skurnick, J., Labat, C., Bean, K., and Aviv, A. (2001). Telomere length as an indicator of biological aging: the gender effect and relation with pulse pressure and pulse wave velocity. *Hypertension* **37**, 381-5.
- Bennett, M. R., Macdonald, K., Chan, S. W., Boyle, J. J., and Weissberg, P. L. (1998). Cooperative interactions between RB and p53 regulate cell proliferation, cell senescence, and apoptosis in human vascular smooth muscle cells from atherosclerotic plaques. *Circ Res* **82**, 704-12.
- Ben-Porath, I., and Weinberg, R. A. (2005). The signals and pathways activating cellular senescence. *Int J Biochem Cell Biol* **37**, 961-76.

- Berk, B. C. (2001). Vascular smooth muscle growth: autocrine growth mechanisms. *Physiol Rev* **81**, 999-1030.
- Berry, C., Hamilton, C. A., Brosnan, M. J., Magill, F. G., Berg, G. A., McMurray, J. J., and Dominiczak, A. F. (2000). Investigation into the sources of superoxide in human blood vessels: angiotensin II increases superoxide production in human internal mammary arteries. *Circulation* **101**, 2206-12.
- Bertram, C., and Hass, R. (2008). Cellular responses to reactive oxygen species-induced DNA damage and aging. *Biol Chem* **389**, 211-20.
- Blackburn, E. H. (2001). Switching and signaling at the telomere. *Cell* **106**, 661-73.
- Bohr, V. A., and Dianov, G. L. (1999). Oxidative DNA damage processing in nuclear and mitochondrial DNA. *Biochimie* **81**, 155-60.
- Botto, N., Masetti, S., Petrozzi, L., Vassalle, C., Manfredi, S., Biagini, A., and Andreassi, M. G. (2002). Elevated levels of oxidative DNA damage in patients with coronary artery disease. *Coron Artery Dis* **13**, 269-74.
- Bradbury, D. A., Simmons, T. D., Slater, K. J., and Crouch, S. P. (2000). Measurement of the ADP:ATP ratio in human leukaemic cell lines can be used as an indicator of cell viability, necrosis and apoptosis. *J Immunol Methods* **240**, 79-92.
- Bradford, M. M. (1976). A rapid and sensitive method for the quantitation of microgram quantities of protein utilizing the principle of protein-dye binding. *Anal Biochem* **72**, 248-54.
- Brandes, R. P., Fleming, I., and Busse, R. (2005). Endothelial aging. *Cardiovasc Res* **66**, 286-94.
- Brasier, A. R., Recinos, A., 3rd, and Eledrisi, M. S. (2002). Vascular inflammation and the renin-angiotensin system. *Arterioscler Thromb Vasc Biol* **22**, 1257-66.
- Breitschopf, K., Zeiher, A. M., and Dimmeler, S. (2001). Pro-atherogenic factors induce telomerase inactivation in endothelial cells through an Akt-dependent mechanism. *FEBS Lett* **493**, 21-5.
- Bringold, F., and Serrano, M. (2000). Tumor suppressors and oncogenes in cellular senescence. *Exp Gerontol* **35**, 317-29.
- Brouillette, S., Singh, R. K., Thompson, J. R., Goodall, A. H., and Samani, N. J. (2003). White cell telomere length and risk of premature myocardial infarction. *Arterioscler Thromb Vasc Biol* **23**, 842-6.
- Brouillette, S. W., Moore, J. S., McMahon, A. D., Thompson, J. R., Ford, I., Shepherd, J., Packard, C. J., Samani, N. J., and West of Scotland Coronary Prevention Study Group (2007). Telomere length, risk of coronary heart disease, and statin treatment in the West of Scotland Primary Prevention Study: a nested case-control study. *Lancet* **369**, 107-14.

- Budnikov, E. I., Postnov, A. I., Doroshchuk, A. D., Afanasjeva, G. V., and Postnov, I. (2002). Decreased ATP-synthesis ability of liver mitochondria in spontaneously hypertensive rats (SHR): role of calcium overload of the mitochondria. *Kardiologiia* **42**, 47-50.
- Burnier, M., and Brunner, H. R. (2000). Angiotensin II receptor antagonists. *Lancet* **355**, 637-45.
- Burrig, K. F. (1991). The endothelium of advanced arteriosclerotic plaques in humans. *Arterioscler Thromb* **11**, 1678-89.
- Burton, D. G., Sheerin, A. N., Ostler, E. L., Smith, K., Giles, P. J., Lowe, J., Rhys-Williams, W., Kipling, D. G., and Faragher, R. G. (2007). Cyclin D1 overexpression permits the reproducible detection of senescent human vascular smooth muscle cells. *Ann N Y Acad Sci* **1119**, 20-31.
- Butow, R. A., and Avadhani, N. G. (2004). Mitochondrial signaling: the retrograde response. *Mol Cell* **14**, 1-15.
- Campisi, J. (2001). Cellular senescence as a tumor-suppressor mechanism. *Trends Cell Biol* **11**, S27-31.
- Campisi, J. (2005). Senescent cells, tumor suppression, and organismal aging: good citizens, bad neighbors. *Cell* **120**, 513-22.
- Capell, B. C., Collins, F. S., and Nabel, E. G. (2007). Mechanisms of cardiovascular disease in accelerated aging syndromes. *Circ Res* **101**, 13-26.
- Carlisle, R., Rhoads, C. A., Aw, T. Y., and Harrison, L. (2002). Endothelial cells maintain a reduced redox environment even as mitochondrial function declines. *Am J Physiol Cell Physiol* **283**, C1675-86.
- Carraway, M. S., Suliman, H. B., Kliment, C., Welty-Wolf, K. E., Oury, T. D., and Piantadosi, C. A. (2008). Mitochondrial biogenesis in the pulmonary vasculature during inhalational lung injury and fibrosis. *Antioxid Redox Signal* **10**, 269-75.
- Cassis, L. A., Rateri, D. L., Lu, H., and Daugherty, A. (2007). Bone marrow transplantation reveals that recipient AT1a receptors are required to initiate angiotensin II-induced atherosclerosis and aneurysms. *Arterioscler Thromb Vasc Biol* **27**, 380-6.
- Cawthon, R. M., Smith, K. R., O'Brien, E., Sivatchenko, A., and Kerber, R. A. (2003). Association between telomere length in blood and mortality in people aged 60 years or older. *Lancet* **361**, 393-5.
- Chainiaux, F., Magalhaes, J. P., Eliaers, F., Remacle, J., and Toussaint, O. (2002). UVB-induced premature senescence of human diploid skin fibroblasts. *Int J Biochem Cell Biol* **34**, 1331-9.

- Chamley-Campbell, J., Campbell, G. R., and Ross, R. (1979). The smooth muscle cell in culture. *Physiol Rev* **59**, 1-61.
- Chang, B. D., Swift, M. E., Shen, M., Fang, J., Broude, E. V., and Roninson, I. B. (2002). Molecular determinants of terminal growth arrest induced in tumor cells by a chemotherapeutic agent. *Proc Natl Acad Sci U S A* **99**, 389-94.
- Chang, E., and Harley, C. B. (1995). Telomere length and replicative aging in human vascular tissues. *Proc Natl Acad Sci U S A* **92**, 11190-4.
- Chang, S. (2005). A mouse model of Werner Syndrome: what can it tell us about aging and cancer? *Int J Biochem Cell Biol* **37**, 991-9.
- Chang, S., Multani, A. S., Cabrera, N. G., Naylor, M. L., Laud, P., Lombard, D., Pathak, S., Guarente, L., and DePinho, R. A. (2004). Essential role of limiting telomeres in the pathogenesis of Werner syndrome. *Nat Genet* **36**, 877-82.
- Chen, J. (2004). Senescence and functional failure in hematopoietic stem cells. *Exp Hematol* **32**, 1025-32.
- Chen, M., and Wang, J. (2002). Initiator caspases in apoptosis signaling pathways. *Apoptosis* **7**, 313-9.
- Chen, Q., Fischer, A., Reagan, J. D., Yan, L. J., and Ames, B. N. (1995). Oxidative DNA damage and senescence of human diploid fibroblast cells. *Proc Natl Acad Sci U S A* **92**, 4337-41.
- Chen, Q. M., Bartholomew, J. C., Campisi, J., Acosta, M., Reagan, J. D., and Ames, B. N. (1998). Molecular analysis of H₂O₂-induced senescent-like growth arrest in normal human fibroblasts: p53 and Rb control G1 arrest but not cell replication. *Biochem J* **332** (Pt 1), 43-50.
- Chen, Q. M., Liu, J., and Merrett, J. B. (2000). Apoptosis or senescence-like growth arrest: influence of cell-cycle position, p53, p21 and bax in H₂O₂ response of normal human fibroblasts. *Biochem J* **347**, 543-51.
- Chen, Q. M., Prowse, K. R., Tu, V. C., Purdom, S., and Linskens, M. H. (2001a). Uncoupling the senescent phenotype from telomere shortening in hydrogen peroxide-treated fibroblasts. *Exp Cell Res* **265**, 294-303.
- Chen, W., Kang, J., Xia, J., Li, Y., Yang, B., Chen, B., Sun, W., Song, X., Xiang, W., Wang, X., Wang, F., Wan, Y., and Bi, Z. (2008). p53-related apoptosis resistance and tumor suppression activity in UVB-induced premature senescent human skin fibroblasts. *Int J Mol Med* **21**, 645-53.
- Chen, X., Touyz, R. M., Park, J. B., and Schiffrin, E. L. (2001b). Antioxidant effects of vitamins C and E are associated with altered activation of vascular NADPH oxidase and superoxide dismutase in stroke-prone SHR. *Hypertension* **38**, 606-11.

- Christen, T., Bochaton-Piallat, M. L., Neuville, P., Rensen, S., Redard, M., van Eys, G., and Gabbiani, G. (1999). Cultured porcine coronary artery smooth muscle cells. A new model with advanced differentiation. *Circ Res* **85**, 99-107.
- Civitaresse, A. E., Carling, S., Heilbronn, L. K., Hulver, M. H., Ukropcova, B., Deutsch, W. A., Smith, S. R., Ravussin, E., and CALERIE Pennington Team (2007). Calorie restriction increases muscle mitochondrial biogenesis in healthy humans. *PLoS Med* **4**, e76.
- Colavitti, R., and Finkel, T. (2005). Reactive oxygen species as mediators of cellular senescence. *IUBMB Life* **57**, 277-81.
- Crass, M. F., 3rd, Borst, S. E., and Scarpace, P. J. (1992). Beta-adrenergic responsiveness in cultured aorta smooth muscle cells. Effects of subculture and aging. *Biochem Pharmacol* **43**, 1811-5.
- Cucoranu, I., Clempus, R., Dikalova, A., Phelan, P. J., Ariyan, S., Dikalov, S., and Sorescu, D. (2005). NAD(P)H oxidase 4 mediates transforming growth factor-beta1-induced differentiation of cardiac fibroblasts into myofibroblasts. *Circ Res* **97**, 900-7.
- d'Adda di Fagagna, F., Reaper, P. M., Clay-Farrace, L., Fiegler, H., Carr, P., Von Zglinicki, T., Saretzki, G., Carter, N. P., and Jackson, S. P. (2003). A DNA damage checkpoint response in telomere-initiated senescence. *Nature* **426**, 194-8.
- Dahlof, B., Devereux, R. B., Kjeldsen, S. E., Julius, S., Beevers, G., de Faire, U., Fyhrquist, F., Ibsen, H., Kristiansson, K., Lederballe-Pedersen, O., Lindholm, L. H., Nieminen, M. S., Omvik, P., Oparil, S., Wedel, H., and LIFE Study Group (2002). Cardiovascular morbidity and mortality in the Losartan Intervention For Endpoint reduction in hypertension study (LIFE): a randomised trial against atenolol. *Lancet* **359**, 995-1003.
- de Cavanagh, E. M., Ferder, L., Toblli, J. E., Piotrkowski, B., Stella, I., Fraga, C. G., and Inserra, F. (2008a). Renal mitochondrial impairment is attenuated by AT1 blockade in experimental Type I diabetes. *Am J Physiol Heart Circ Physiol* **294**, H456-65.
- de Cavanagh, E. M., Flores, I., Ferder, M., Inserra, F., and Ferder, L. (2008b). Renin-angiotensin system inhibitors protect against age-related changes in rat liver mitochondrial DNA content and gene expression. *Exp Gerontol* **43**, 919-28.
- de Cavanagh, E. M., Piotrkowski, B., Basso, N., Stella, I., Inserra, F., Ferder, L., and Fraga, C. G. (2003). Enalapril and losartan attenuate mitochondrial dysfunction in aged rats. *FASEB J* **17**, 1096-8.
- de Gasparo, M., Catt, K. J., Inagami, T., Wright, J. W., and Unger, T. (2000). International union of pharmacology. XXIII. The angiotensin II receptors. *Pharmacol Rev* **52**, 415-72.

- de la Maza, M. P., Olivares, D., Hirsch, S., Sierralta, W., Gattas, V., Barrera, G., Bunout, D., Leiva, L., and Fernandez, M. (2006). Weight increase and overweight are associated with DNA oxidative damage in skeletal muscle. *Clin Nutr* **25**, 968-76.
- de la Monte, S. M., Luong, T., Neely, T. R., Robinson, D., and Wands, J. R. (2000). Mitochondrial DNA damage as a mechanism of cell loss in Alzheimer's disease. *Lab Invest* **80**, 1323-35.
- de Lange, T. (2005). Shelterin: the protein complex that shapes and safeguards human telomeres. *Genes Dev* **19**, 2100-10.
- de Magalhaes, J. P., Chainiaux, F., de Longueville, F., Mainfroid, V., Migeot, V., Marcq, L., Remacle, J., Salmon, M., and Toussaint, O. (2004). Gene expression and regulation in H₂O₂-induced premature senescence of human foreskin fibroblasts expressing or not telomerase. *Exp Gerontol* **39**, 1379-89.
- de Magalhaes, J. P., Chainiaux, F., Remacle, J., and Toussaint, O. (2002). Stress-induced premature senescence in BJ and hTERT-BJ1 human foreskin fibroblasts. *FEBS Lett* **523**, 157-62.
- De Paepe, B., Verstraeten, V. M., De Potter, C. R., and Bullock, G. R. (2002). Increased angiotensin II type-2 receptor density in hyperplasia, DCIS and invasive carcinoma of the breast is paralleled with increased iNOS expression. *Histochem Cell Biol* **117**, 13-9.
- Debacq-Chainiaux, F., Borlon, C., Pascal, T., Royer, V., Eliaers, F., Ninane, N., Carrard, G., Friguet, B., de Longueville, F., Boffe, S., Remacle, J., and Toussaint, O. (2005). Repeated exposure of human skin fibroblasts to UVB at subcytotoxic level triggers premature senescence through the TGF-beta1 signaling pathway. *J Cell Sci* **118**, 743-58.
- Debacq-Chainiaux, F., Pascal, T., Boilan, E., Bastin, C., Bauwens, E., and Toussaint, O. (2008). Screening of senescence-associated genes with specific DNA array reveals the role of IGFBP-3 in premature senescence of human diploid fibroblasts. *Free Radic Biol Med* **44**, 1817-32.
- Demissie, S., Levy, D., Benjamin, E. J., Cupples, L. A., Gardner, J. P., Herbert, A., Kimura, M., Larson, M. G., Meigs, J. B., Keaney, J. F., and Aviv, A. (2006). Insulin resistance, oxidative stress, hypertension, and leukocyte telomere length in men from the Framingham Heart Study. *Aging Cell* **5**, 325-30.
- Denizot, F., and Lang, R. (1986). Rapid colorimetric assay for cell growth and survival. Modifications to the tetrazolium dye procedure giving improved sensitivity and reliability. *J Immunol Methods* **89**, 271-7.
- Desarnaud, F., Marie, J., Lombard, C., Larguier, R., Seyer, R., Lorca, T., Jard, S., and Bonnafous, J. C. (1993). Deglycosylation and fragmentation of purified rat liver angiotensin II receptor: application to the mapping of hormone-binding domains. *Biochem J* **289** (Pt 1), 289-97.

- Deshpande, S. S., Qi, B., Park, Y. C., and Irani, K. (2003). Constitutive activation of rac1 results in mitochondrial oxidative stress and induces premature endothelial cell senescence. *Arterioscler Thromb Vasc Biol* **23**, e1-6.
- Di Micco, R., Fumagalli, M., Cicalese, A., Piccinin, S., Gasparini, P., Luise, C., Schurra, C., Garre', M., Nuciforo, P. G., Bensimon, A., Maestro, R., Pelicci, P. G., and d'Adda di Fagagna, F. (2006). Oncogene-induced senescence is a DNA damage response triggered by DNA hyper-replication. *Nature* **444**, 638-42.
- Dickinson, D. A., and Forman, H. J. (2002). Cellular glutathione and thiols metabolism. *Biochem Pharmacol* **64**, 1019-26.
- Dimri, G. P., Lee, X., Basile, G., Acosta, M., Scott, G., Roskelley, C., Medrano, E. E., Linskens, M., Rubelj, I., and Pereira-Smith, O. (1995). A biomarker that identifies senescent human cells in culture and in aging skin *in vivo*. *Proc Natl Acad Sci U S A* **92**, 9363-7.
- Dinh, D. T., Frauman, A. G., Johnston, C. I., and Fabiani, M. E. (2001). Angiotensin receptors: distribution, signalling and function. *Clin Sci (Lond)* **100**, 481-92.
- Doughan, A. K., Harrison, D. G., and Dikalov, S. I. (2008). Molecular mechanisms of angiotensin II-mediated mitochondrial dysfunction: linking mitochondrial oxidative damage and vascular endothelial dysfunction. *Circ Res* **102**, 488-96.
- Duan, J., Duan, J., Zhang, Z., and Tong, T. (2005). Irreversible cellular senescence induced by prolonged exposure to H₂O₂ involves DNA-damage-and-repair genes and telomere shortening. *Int J Biochem Cell Biol* **37**, 1407-20.
- Dumont, P., Burton, M., Chen, Q. M., Fripiat, C., Pascal, T., Dierick, J. F., Eliaers, F., Chainiaux, F., Remacle, J., and Toussaint, O. (2000a). Human diploid fibroblasts display a decreased level of c-fos mRNA at 72 hours after exposure to sublethal H₂O₂ stress. *Ann N Y Acad Sci* **908**, 306-9.
- Dumont, P., Burton, M., Chen, Q. M., Gonos, E. S., Fripiat, C., Mazarati, J. B., Eliaers, F., Remacle, J., and Toussaint, O. (2000b). Induction of replicative senescence biomarkers by sublethal oxidative stresses in normal human fibroblast. *Free Radic Biol Med* **28**, 361-73.
- Dumont, P., Chainiaux, F., Eliaers, F., Petropoulou, C., Remacle, J., Koch-Brandt, C., Gonos, E. S., and Toussaint, O. (2002). Overexpression of apolipoprotein J in human fibroblasts protects against cytotoxicity and premature senescence induced by ethanol and *tert*-butylhydroperoxide. *Cell Stress Chaperones* **7**, 23-35.
- Dumont, P., Royer, V., Pascal, T., Dierick, J. F., Chainiaux, F., Fripiat, C., de Magalhaes, J. P., Eliaers, F., Remacle, J., and Toussaint, O. (2001). Growth kinetics rather than stress accelerate telomere shortening in cultures of human diploid fibroblasts in oxidative stress-induced premature senescence. *FEBS Lett* **502**, 109-12.

- Duprez, D. A. (2006). Role of the renin-angiotensin-aldosterone system in vascular remodeling and inflammation: a clinical review. *J Hypertens* **24**, 983-91.
- Earnshaw, W. C. (1995). Nuclear changes in apoptosis. *Curr Opin Cell Biol* **7**, 337-43.
- Ellmark, S. H., Dusting, G. J., Fui, M. N., Guzzo-Pernell, N., and Drummond, G. R. (2005). The contribution of Nox4 to NADPH oxidase activity in mouse vascular smooth muscle. *Cardiovasc Res* **65**, 495-504.
- Epel, E. S., Blackburn, E. H., Lin, J., Dhabhar, F. S., Adler, N. E., Morrow, J. D., and Cawthon, R. M. (2004). Accelerated telomere shortening in response to life stress. *Proc Natl Acad Sci U S A* **101**, 17312-5.
- Erusalimsky, J. D., and Kurz, D. J. (2005). Cellular senescence *in vivo*: its relevance in ageing and cardiovascular disease. *Exp Gerontol* **40**, 634-42.
- Esther, C. R., Jr, Howard, T. E., Marino, E. M., Goddard, J. M., Capecchi, M. R., and Bernstein, K. E. (1996). Mice lacking angiotensin-converting enzyme have low blood pressure, renal pathology, and reduced male fertility. *Lab Invest* **74**, 953-65.
- Faragher, R. G., Kill, I. R., Hunter, J. A., Pope, F. M., Tannock, C., and Shall, S. (1993). The gene responsible for Werner syndrome may be a cell division "counting" gene. *Proc Natl Acad Sci U S A* **90**, 12030-4.
- Fenton, M., Barker, S., Kurz, D. J., and Erusalimsky, J. D. (2001). Cellular senescence after single and repeated balloon catheter denudations of rabbit carotid arteries. *Arterioscler Thromb Vasc Biol* **21**, 220-6.
- Ferbeyre, G., de Stanchina, E., Lin, A. W., Querido, E., McCurrach, M. E., Hannon, G. J., and Lowe, S. W. (2002). Oncogenic ras and p53 cooperate to induce cellular senescence. *Mol Cell Biol* **22**, 3497-508.
- Ferder, L. F., Inserra, F., and Basso, N. (2002). Advances in our understanding of aging: role of the renin-angiotensin system. *Curr Opin Pharmacol* **2**, 189-94.
- Foreman, K. E., and Tang, J. (2003). Molecular mechanisms of replicative senescence in endothelial cells. *Exp Gerontol* **38**, 1251-7.
- Fortuno, A., Oliván, S., Beloqui, O., San Jose, G., Moreno, M. U., Diez, J., and Zalba, G. (2004). Association of increased phagocytic NADPH oxidase-dependent superoxide production with diminished nitric oxide generation in essential hypertension. *J Hypertens* **22**, 2169-75.
- Fracasso, M. E., Doria, D., Franceschetti, P., Perbellini, L., and Romeo, L. (2006). DNA damage and repair capacity by comet assay in lymphocytes of white-collar active smokers and passive smokers (non- and ex-smokers) at workplace. *Toxicol Lett* **167**, 131-41.

- Frid, M. G., Dempsey, E. C., Durmowicz, A. G., and Stenmark, K. R. (1997). Smooth muscle cell heterogeneity in pulmonary and systemic vessels. Importance in vascular disease. *Arterioscler Thromb Vasc Biol* **17**, 1203-9.
- Fridovich, I. (1997). Superoxide anion radical ($O_2\cdot^-$), superoxide dismutases, and related matters. *J Biol Chem* **272**, 18515-7.
- Frippiat, C., Remacle, J., and Toussaint, O. (2003). Down-regulation and decreased activity of cyclin-dependent kinase 2 in H_2O_2 -induced premature senescence. *Int J Biochem Cell Biol* **35**, 246-54.
- Fukazawa, R., Ikegam, E., Watanabe, M., Hajikano, M., Kamisago, M., Katsube, Y., Yamauchi, H., Ochi, M., and Ogawa, S. (2007). Coronary artery aneurysm induced by Kawasaki disease in children show features typical senescence. *Circ J* **71**, 709-15.
- Furman, C., Rundlof, A. K., Larigauderie, G., Jaye, M., Bricca, G., Copin, C., Kandoussi, A. M., Fruchart, J. C., Arner, E. S., and Rouis, M. (2004). Thioredoxin reductase 1 is upregulated in atherosclerotic plaques: specific induction of the promoter in human macrophages by oxidized low-density lipoproteins. *Free Radic Biol Med* **37**, 71-85.
- Fuster, J. J., Diez, J., and Andres, V. (2007). Telomere dysfunction in hypertension. *J Hypertens* **25**, 2185-92.
- Gabbiani, G., Kocher, O., Bloom, W. S., Vandekerckhove, J., and Weber, K. (1984). Actin expression in smooth muscle cells of rat aortic intimal thickening, human atheromatous plaque, and cultured rat aortic media. *J Clin Invest* **73**, 148-52.
- Galindo, M., Santiago, B., Palao, G., Gutierrez-Canas, I., Ramirez, J. C., and Pablos, J. L. (2005). Coexpression of AT1 and AT2 receptors by human fibroblasts is associated with resistance to angiotensin II. *Peptides* **26**, 1647-53.
- Garnier, A., Fortin, D., Delomenie, C., Momken, I., Veksler, V., and Ventura-Clapier, R. (2003). Depressed mitochondrial transcription factors and oxidative capacity in rat failing cardiac and skeletal muscles. *J Physiol* **551**, 491-501.
- Glotin, A. L., Debaq-Chainiaux, F., Brossas, J. Y., Faussat, A. M., Treton, J., Zubielewicz, A., Toussaint, O., and Mascarelli, F. (2008). Prematurely senescent ARPE-19 cells display features of age-related macular degeneration. *Free Radic Biol Med* **44**, 1348-61.
- Goldstein, S. (1990). Replicative senescence: the human fibroblast comes of age. *Science* **249**, 1129-33.
- Gonzalez Bosc, L. V., Kurnjek, M. L., Muller, A., Terragno, N. A., and Basso, N. (2001). Effect of chronic angiotensin II inhibition on the nitric oxide synthase in the normal rat during aging. *J Hypertens* **19**, 1403-9.

- Gorbunova, V., Seluanov, A., and Pereira-Smith, O. M. (2002). Expression of human telomerase (hTERT) does not prevent stress-induced senescence in normal human fibroblasts but protects the cells from stress-induced apoptosis and necrosis. *J Biol Chem* **277**, 38540-9.
- Gorenne, I., Kavurma, M., Scott, S., and Bennett, M. (2006). Vascular smooth muscle cell senescence in atherosclerosis. *Cardiovasc Res* **72**, 9-17.
- Gorgoulis, V. G., Pratsinis, H., Zacharatos, P., Demoliou, C., Sigala, F., Asimacopoulos, P. J., Papavassiliou, A. G., and Kletsas, D. (2005). p53-dependent ICAM-1 overexpression in senescent human cells identified in atherosclerotic lesions. *Lab Invest* **85**, 502-11.
- Graciano, M. L., Nishiyama, A., Jackson, K., Seth, D. M., Ortiz, R. M., Prieto-Carrasquero, M. C., Kobori, H., and Navar, L. G. (2008). Purinergic receptors contribute to early mesangial cell transformation and renal vessel hypertrophy during angiotensin II-induced hypertension. *Am J Physiol Renal Physiol* **294**, F161-9.
- Gray, M. D., Wang, L., Youssoufian, H., Martin, G. M., and Oshima, J. (1998). Werner helicase is localized to transcriptionally active nucleoli of cycling cells. *Exp Cell Res* **242**, 487-94.
- Green, M. R. (2008). Senescence: not just for tumor suppression. *Cell* **134**, 562-4.
- Griendling, K. K., Minieri, C. A., Ollerenshaw, J. D., and Alexander, R. W. (1994). Angiotensin II stimulates NADH and NADPH oxidase activity in cultured vascular smooth muscle cells. *Circ Res* **74**, 1141-8.
- Grune, T., Reinheckel, T., and Davies, K. J. (1997). Degradation of oxidized proteins in mammalian cells. *FASEB J* **11**, 526-34.
- Guzik, T. J., Chen, W., Gongora, M. C., Guzik, B., Lob, H. E., Mangalat, D., Hoch, N., Dikalov, S., Rudzinski, P., Kapelak, B., Sadowski, J., and Harrison, D. G. (2008). Calcium-dependent NOX5 nicotinamide adenine dinucleotide phosphate oxidase contributes to vascular oxidative stress in human coronary artery disease. *J Am Coll Cardiol* **52**, 1803-9.
- Hafizi, S., Chester, A. H., Allen, S. P., Morgan, K., and Yacoub, M. H. (1998). Growth response of human coronary smooth muscle cells to angiotensin II and influence of angiotensin AT1 receptor blockade. *Coron Artery Dis* **9**, 167-75.
- Halliwell, B., and Whiteman, M. (2004). Measuring reactive species and oxidative damage *in vivo* and in cell culture: how should you do it and what do the results mean? *Br J Pharmacol* **142**, 231-55.
- Hamet, P., Thorin-Trescases, N., Moreau, P., Dumas, P., Tea, B. S., deBlois, D., Kren, V., Pravenec, M., Kunes, J., Sun, Y., and Tremblay, J. (2001). Workshop: excess growth and apoptosis: is hypertension a case of accelerated aging of cardiovascular cells? *Hypertension* **37**, 760-6.

- Han, D., Antunes, F., Canali, R., Rettori, D., and Cadenas, E. (2003). Voltage-dependent anion channels control the release of the superoxide anion from mitochondria to cytosol. *J Biol Chem* **278**, 5557-63.
- Han, J., and Sun, P. (2007). The pathways to tumor suppression via route p38. *Trends Biochem Sci* **32**, 364-71.
- Han, Y., Runge, M. S., and Brasier, A. R. (1999). Angiotensin II induces interleukin-6 transcription in vascular smooth muscle cells through pleiotropic activation of nuclear factor-kappa B transcription factors. *Circ Res* **84**, 695-703.
- Hao, H., Gabbiani, G., and Bochaton-Piallat, M. L. (2003). Arterial smooth muscle cell heterogeneity: implications for atherosclerosis and restenosis development. *Arterioscler Thromb Vasc Biol* **23**, 1510-20.
- Harley, C. B., Futcher, A. B., and Greider, C. W. (1990). Telomeres shorten during ageing of human fibroblasts. *Nature* **345**, 458-60.
- Harman, D. (1956). Aging: a theory based on free radical and radiation chemistry. *J Gerontol* **11**, 298-300.
- Harman, D. (1972). The biologic clock: the mitochondria? *J Am Geriatr Soc* **20**, 145-7.
- Hastings, R., Qureshi, M., Verma, R., Lacy, P. S., and Williams, B. (2004). Telomere attrition and accumulation of senescent cells in cultured human endothelial cells. *Cell Prolif* **37**, 317-24.
- Hatefi, Y. (1985). The mitochondrial electron transport and oxidative phosphorylation system. *Annu Rev Biochem* **54**, 1015-69.
- Hayflick, L., and Moorhead, P. S. (1961). The serial cultivation of human diploid cell strains. *Exp Cell Res* **25**, 585-621.
- Herbig, U., Jobling, W. A., Chen, B. P., Chen, D. J., and Sedivy, J. M. (2004). Telomere shortening triggers senescence of human cells through a pathway involving ATM, p53, and p21^(CIP1), but not p16^(INK4a). *Mol Cell* **14**, 501-13.
- Heumuller, S., Wind, S., Barbosa-Sicard, E., Schmidt, H. H., Busse, R., Schroder, K., and Brandes, R. P. (2008). Apocynin is not an inhibitor of vascular NADPH oxidases but an antioxidant. *Hypertension* **51**, 211-7.
- Hsiao, R., Sharma, H. W., Ramakrishnan, S., Keith, E., and Narayanan, R. (1997). Telomerase activity in normal human endothelial cells. *Anticancer Res* **17**, 827-32.
- Imanishi, T., Hano, T., and Nishio, I. (2005a). Angiotensin II accelerates endothelial progenitor cell senescence through induction of oxidative stress. *J Hypertens* **23**, 97-104.

- Imanishi, T., Moriwaki, C., Hano, T., and Nishio, I. (2005b). Endothelial progenitor cell senescence is accelerated in both experimental hypertensive rats and patients with essential hypertension. *J Hypertens* **23**, 1831-7.
- Inoguchi, T., Li, P., Umeda, F., Yu, H. Y., Kakimoto, M., Imamura, M., Aoki, T., Etoh, T., Hashimoto, T., Naruse, M., Sano, H., Utsumi, H., and Nawata, H. (2000). High glucose level and free fatty acid stimulate reactive oxygen species production through protein kinase C-dependent activation of NAD(P)H oxidase in cultured vascular cells. *Diabetes* **49**, 1939-45.
- Intengan, H. D., and Schiffrin, E. L. (2000). Structure and mechanical properties of resistance arteries in hypertension: role of adhesion molecules and extracellular matrix determinants. *Hypertension* **36**, 312-8.
- Itahana, K., Dimri, G., and Campisi, J. (2001). Regulation of cellular senescence by p53. *Eur J Biochem* **268**, 2784-91.
- Itazaki, K., Shigeri, Y., and Fujimoto, M. (1993). Molecular cloning and characterization of the angiotensin receptor subtype in porcine aortic smooth muscle. *Eur J Pharmacol* **245**, 147-56.
- Ito, M., Oliverio, M. I., Mannon, P. J., Best, C. F., Maeda, N., Smithies, O., and Coffman, T. M. (1995). Regulation of blood pressure by the type 1A angiotensin II receptor gene. *Proc Natl Acad Sci U S A* **92**, 3521-5.
- Iwai, M., Chen, R., Li, Z., Shiuchi, T., Suzuki, J., Ide, A., Tsuda, M., Okumura, M., Min, L. J., Mogi, M., and Horiuchi, M. (2005). Deletion of angiotensin II type 2 receptor exaggerated atherosclerosis in apolipoprotein E-null mice. *Circulation* **112**, 1636-43.
- Janiszewski, M., Souza, H. P., Liu, X., Pedro, M. A., Zweier, J. L., and Laurindo, F. R. (2002). Overestimation of NADH-driven vascular oxidase activity due to lucigenin artifacts. *Free Radic Biol Med* **32**, 446-53.
- Jeanclous, E., Krolewski, A., Skurnick, J., Kimura, M., Aviv, H., Warram, J. H., and Aviv, A. (1998). Shortened telomere length in white blood cells of patients with IDDM. *Diabetes* **47**, 482-6.
- Karlseder, J., Smogorzewska, A., and de Lange, T. (2002). Senescence induced by altered telomere state, not telomere loss. *Science* **295**, 2446-9.
- Khaliulin, I., Schwalb, H., Wang, P., Houminer, E., Grinberg, L., Katzeff, H., Borman, J. B., and Powell, S. R. (2004). Preconditioning improves postischemic mitochondrial function and diminishes oxidation of mitochondrial proteins. *Free Radic Biol Med* **37**, 1-9.
- Kim, K. S., Seu, Y. B., Baek, S. H., Kim, M. J., Kim, K. J., Kim, J. H., and Kim, J. R. (2007). Induction of cellular senescence by insulin-like growth factor binding protein-5 through a p53-dependent mechanism. *Mol Biol Cell* **18**, 4543-52.

- Kimura, S., Zhang, G. X., Nishiyama, A., Shokoji, T., Yao, L., Fan, Y. Y., Rahman, M., and Abe, Y. (2005a). Mitochondria-derived reactive oxygen species and vascular MAP kinases: comparison of angiotensin II and diazoxide. *Hypertension* **45**, 438-44.
- Kimura, S., Zhang, G. X., Nishiyama, A., Shokoji, T., Yao, L., Fan, Y. Y., Rahman, M., Suzuki, T., Maeta, H., and Abe, Y. (2005b). Role of NAD(P)H oxidase- and mitochondria-derived reactive oxygen species in cardioprotection of ischemic reperfusion injury by angiotensin II. *Hypertension* **45**, 860-6.
- Klinger, R. Y., Blum, J. L., Hearn, B., Lebow, B., and Niklason, L. E. (2006). Relevance and safety of telomerase for human tissue engineering. *Proc Natl Acad Sci U S A* **103**, 2500-5.
- Kohno, M., Ohmori, K., Nozaki, S., Mizushige, K., Yasunari, K., Kano, H., Minami, M., and Yoshikawa, J. (2000). Effects of valsartan on angiotensin II-induced migration of human coronary artery smooth muscle cells. *Hypertens Res* **23**, 677-81.
- Krege, J. H., John, S. W., Langenbach, L. L., Hodgin, J. B., Hagaman, J. R., Bachman, E. S., Jennette, J. C., O'Brien, D. A., and Smithies, O. (1995). Male-female differences in fertility and blood pressure in ACE-deficient mice. *Nature* **375**, 146-8.
- Ksiazek, K., Passos, J. F., Olijslagers, S., and von Zglinicki, T. (2008). Mitochondrial dysfunction is a possible cause of accelerated senescence of mesothelial cells exposed to high glucose. *Biochem Biophys Res Commun* **366**, 793-9.
- Kuma, S., Oki, E., Onohara, T., Komori, K., and Maehara, Y. (2007). Angiotensin II-induced growth of vascular smooth muscle cells is associated with modulation of cell surface area and platelet-derived growth factor receptor expression. *Clin Exp Pharmacol Physiol* **34**, 153-60.
- Kunieda, T., Minamino, T., Nishi, J., Tateno, K., Oyama, T., Katsuno, T., Miyauchi, H., Orimo, M., Okada, S., Takamura, M., Nagai, T., Kaneko, S., and Komuro, I. (2006). Angiotensin II induces premature senescence of vascular smooth muscle cells and accelerates the development of atherosclerosis via a p21-dependent pathway. *Circulation* **114**, 953-60.
- Kuroda, J., Nakagawa, K., Yamasaki, T., Nakamura, K., Takeya, R., Kuribayashi, F., Imajoh-Ohmi, S., Igarashi, K., Shibata, Y., Sueishi, K., and Sumimoto, H. (2005). The superoxide-producing NAD(P)H oxidase Nox4 in the nucleus of human vascular endothelial cells. *Genes Cells* **10**, 1139-51.
- Kurz, D. J., Decary, S., Hong, Y., and Erusalimsky, J. D. (2000). Senescence-associated β -galactosidase reflects an increase in lysosomal mass during replicative ageing of human endothelial cells. *J Cell Sci* **113** (Pt 20), 3613-22.

- Kurz, D. J., Decary, S., Hong, Y., Trivier, E., Akhmedov, A., and Erusalimsky, J. D. (2004). Chronic oxidative stress compromises telomere integrity and accelerates the onset of senescence in human endothelial cells. *J Cell Sci* **117**, 2417-26.
- Laderman, K. A., Penny, J. R., Mazzucchelli, F., Bresolin, N., Scarlato, G., and Attardi, G. (1996). Aging-dependent functional alterations of mitochondrial DNA (mtDNA) from human fibroblasts transferred into mtDNA-less cells. *J Biol Chem* **271**, 15891-7.
- Lakatta, E. G., and Levy, D. (2003). Arterial and cardiac aging: major shareholders in cardiovascular disease enterprises: Part I: aging arteries: a "set up" for vascular disease. *Circulation* **107**, 139-46.
- Landmesser, U., Dikalov, S., Price, S. R., McCann, L., Fukai, T., Holland, S. M., Mitch, W. E., and Harrison, D. G. (2003). Oxidation of tetrahydrobiopterin leads to uncoupling of endothelial cell nitric oxide synthase in hypertension. *J Clin Invest* **111**, 1201-9.
- Landmesser, U., and Harrison, D. G. (2001). Oxidative stress and vascular damage in hypertension. *Coron Artery Dis* **12**, 455-61.
- Landmesser, U., Spiekermann, S., Dikalov, S., Tatge, H., Wilke, R., Kohler, C., Harrison, D. G., Hornig, B., and Drexler, H. (2002). Vascular oxidative stress and endothelial dysfunction in patients with chronic heart failure: role of xanthine-oxidase and extracellular superoxide dismutase. *Circulation* **106**, 3073-8.
- Lassegue, B., Alexander, R. W., Nickenig, G., Clark, M., Murphy, T. J., and Griendling, K. K. (1995). Angiotensin II down-regulates the vascular smooth muscle AT1 receptor by transcriptional and post-transcriptional mechanisms: evidence for homologous and heterologous regulation. *Mol Pharmacol* **48**, 601-9.
- Lassegue, B., and Clempus, R. E. (2003). Vascular NAD(P)H oxidases: specific features, expression, and regulation. *Am J Physiol Regul Integr Comp Physiol* **285**, R277-97.
- Le Floch, J. P., Escuyer, P., Baudin, E., Baudon, D., and Perlemuter, L. (1990). Blood glucose area under the curve. Methodological aspects. *Diabetes Care* **13**, 172-5.
- Lee, A. C., Fenster, B. E., Ito, H., Takeda, K., Bae, N. S., Hirai, T., Yu, Z. X., Ferrans, V. J., Howard, B. H., and Finkel, T. (1999). Ras proteins induce senescence by altering the intracellular levels of reactive oxygen species. *J Biol Chem* **274**, 7936-40.
- Lee, H. C., and Wei, Y. H. (2001). Mitochondrial alterations, cellular response to oxidative stress and defective degradation of proteins in aging. *Biogerontology* **2**, 231-44.
- Lee, H. C., Yin, P. H., Chi, C. W., and Wei, Y. H. (2002). Increase in mitochondrial mass in human fibroblasts under oxidative stress and during replicative cell senescence. *J Biomed Sci* **9**, 517-26.

- Lee, H. C., Yin, P. H., Lu, C. Y., Chi, C. W., and Wei, Y. H. (2000). Increase of mitochondria and mitochondrial DNA in response to oxidative stress in human cells. *Biochem J* **348 Pt 2**, 425-32.
- Lee, H. M., Greeley, G. H., Jr, and Englander, E. W. (2008). Sustained hypoxia modulates mitochondrial DNA content in the neonatal rat brain. *Free Radic Biol Med* **44**, 807-14.
- Lee, S., Jeong, S. Y., Lim, W. C., Kim, S., Park, Y. Y., Sun, X., Youle, R. J., and Cho, H. (2007). Mitochondrial fission and fusion mediators, hFis1 and OPA1, modulate cellular senescence. *J Biol Chem* **282**, 22977-83.
- Lenaz, G. (1998). Role of mitochondria in oxidative stress and ageing. *Biochim Biophys Acta* **1366**, 53-67.
- Levy, B. I. (2005). How to explain the differences between renin angiotensin system modulators. *Am J Hypertens* **18**, 134S-41S.
- Li, J. M., and Shah, A. M. (2001). Differential NADPH- versus NADH-dependent superoxide production by phagocyte-type endothelial cell NADPH oxidase. *Cardiovasc Res* **52**, 477-86.
- Li, P., Ferrario, C. M., and Brosnihan, K. B. (1997). Nonpeptide angiotensin II antagonist Losartan inhibits thromboxane A₂-induced contractions in canine coronary arteries. *J Pharmacol Exp Ther* **281**, 1065-70.
- Li, Y., Lappas, G., and Anand-Srivastava, M. B. (2007a). Role of oxidative stress in angiotensin II-induced enhanced expression of Gi- α proteins and adenylyl cyclase signaling in A10 vascular smooth muscle cells. *Am J Physiol Heart Circ Physiol* **292**, H1922-30.
- Li, Y., Song, Y. H., Mohler, J., and Delafontaine, P. (2006a). ANG II induces apoptosis of human vascular smooth muscle via extrinsic pathway involving inhibition of Akt phosphorylation and increased FasL expression. *Am J Physiol Heart Circ Physiol* **290**, H2116-23.
- Li, Y., and Trush, M. A. (1998). Diphenyleneiodonium, an NAD(P)H oxidase inhibitor, also potently inhibits mitochondrial reactive oxygen species production. *Biochem Biophys Res Commun* **253**, 295-9.
- Li, Y., Wang, B., Zhou, C., and Bi, Y. (2007b). Matrine induces apoptosis in angiotensin II-stimulated hyperplasia of cardiac fibroblasts: effects on Bcl-2/Bax expression and caspase-3 activation. *Basic Clin Pharmacol Toxicol* **101**, 1-8.
- Li, Y., Zhu, H., Kuppasamy, P., Roubaud, V., Zweier, J. L., and Trush, M. A. (1998). Validation of lucigenin (bis-N-methylacridinium) as a chemilumigenic probe for detecting superoxide anion radical production by enzymatic and cellular systems. *J Biol Chem* **273**, 2015-23.

- Li, Y., Zhu, H., and Trush, M. A. (1999). Detection of mitochondria-derived reactive oxygen species production by the chemilumigenic probes lucigenin and luminol. *Biochim Biophys Acta* **1428**, 1-12.
- Li, Z., Yang, J., and Huang, H. (2006b). Oxidative stress induces H2AX phosphorylation in human spermatozoa. *FEBS Lett* **580**, 6161-8.
- Liao, S., Curci, J. A., Kelley, B. J., Sicard, G. A., and Thompson, R. W. (2000). Accelerated replicative senescence of medial smooth muscle cells derived from abdominal aortic aneurysms compared to the adjacent inferior mesenteric artery. *J Surg Res* **92**, 85-95.
- Lithell, H., Hansson, L., Skoog, I., Elmfeldt, D., Hofman, A., Olofsson, B., Trenkwalder, P., Zanchetti, A., and SCOPE Study Group (2003). The Study on Cognition and Prognosis in the Elderly (SCOPE): principal results of a randomized double-blind intervention trial. *J Hypertens* **21**, 875-86.
- Lopez-Candales, A., Holmes, D. R., Liao, S., Scott, M. J., Wickline, S. A., and Thompson, R. W. (1997). Decreased vascular smooth muscle cell density in medial degeneration of human abdominal aortic aneurysms. *Am J Pathol* **150**, 993-1007.
- Loscalzo, J. (2003). Oxidant stress: a key determinant of atherothrombosis. *Biochem Soc Trans* **31**, 1059-61.
- Luoma, J. S., Stralin, P., Marklund, S. L., Hiltunen, T. P., Sarkioja, T., and Yla-Herttuala, S. (1998). Expression of extracellular SOD and iNOS in macrophages and smooth muscle cells in human and rabbit atherosclerotic lesions: colocalization with epitopes characteristic of oxidized LDL and peroxynitrite-modified proteins. *Arterioscler Thromb Vasc Biol* **18**, 157-67.
- Mahmoudi, M., Gorenne, I., Mercer, J., Figg, N., Littlewood, T., and Bennett, M. (2008). Statins use a novel Nijmegen breakage syndrome-1-dependent pathway to accelerate DNA repair in vascular smooth muscle cells. *Circ Res* **103**, 717-25.
- Malorni, W., Straface, E., Matarrese, P., Ascione, B., Coinu, R., Canu, S., Galluzzo, P., Marino, M., and Franconi, F. (2008). Redox state and gender differences in vascular smooth muscle cells. *FEBS Lett* **582**, 635-42.
- Marin, J. (1995). Age-related changes in vascular responses: a review. *Mech Ageing Dev* **79**, 71-114.
- Martin, J. A., Brown, T. D., Heiner, A. D., and Buckwalter, J. A. (2004). Chondrocyte senescence, joint loading and osteoarthritis. *Clin Orthop Relat Res* (**427 Suppl**), S96-103.
- Masutomi, K., Yu, E. Y., Khurts, S., Ben-Porath, I., Currier, J. L., Metz, G. B., Brooks, M. W., Kaneko, S., Murakami, S., DeCaprio, J. A., Weinberg, R. A., Stewart, S. A., and Hahn, W. C. (2003). Telomerase maintains telomere structure in normal human cells. *Cell* **114**, 241-53.

- Masuyama, M., Iida, R., Takatsuka, H., Yasuda, T., and Matsuki, T. (2005). Quantitative change in mitochondrial DNA content in various mouse tissues during aging. *Biochim Biophys Acta* **1723**, 302-8.
- Matesanz, N., Lafuente, N., Azcutia, V., Martin, D., Cuadrado, A., Nevado, J., Rodriguez-Manas, L., Sanchez-Ferrer, C. F., and Peiro, C. (2007). Xanthine oxidase-derived extracellular superoxide anions stimulate activator protein 1 activity and hypertrophy in human vascular smooth muscle via c-Jun N-terminal kinase and p38 mitogen-activated protein kinases. *J Hypertens* **25**, 609-18.
- Matsubara, H., Sugaya, T., Murasawa, S., Nozawa, Y., Mori, Y., Masaki, H., Maruyama, K., Tsutumi, Y., Shibasaki, Y., Moriguchi, Y., Tanaka, Y., Iwasaka, T., and Inada, M. (1998). Tissue-specific expression of human angiotensin II AT1 and AT2 receptors and cellular localization of subtype mRNAs in adult human renal cortex using in situ hybridization. *Nephron* **80**, 25-34.
- Matthews, C., Gorenne, I., Scott, S., Figg, N., Kirkpatrick, P., Ritchie, A., Goddard, M., and Bennett, M. (2006). Vascular smooth muscle cells undergo telomere-based senescence in human atherosclerosis: effects of telomerase and oxidative stress. *Circ Res* **99**, 156-64.
- McCrann, D. J., Nguyen, H. G., Jones, M. R., and Ravid, K. (2008). Vascular smooth muscle cell polyploidy: an adaptive or maladaptive response? *J Cell Physiol* **215**, 588-92.
- McLeod, C. J., Jeyabalan, A. P., Minners, J. O., Clevenger, R., Hoyt, R. F., Jr, and Sack, M. N. (2004). Delayed ischemic preconditioning activates nuclear-encoded electron-transfer-chain gene expression in parallel with enhanced postanoxic mitochondrial respiratory recovery. *Circulation* **110**, 534-9.
- McMurray, J. J., Ostergren, J., Swedberg, K., Granger, C. B., Held, P., Michelson, E. L., Olofsson, B., Yusuf, S., Pfeffer, M. A., and CHARM Investigators and Committees (2003). Effects of candesartan in patients with chronic heart failure and reduced left-ventricular systolic function taking angiotensin-converting-enzyme inhibitors: the CHARM-Added trial. *Lancet* **362**, 767-71.
- Mehta, P. K., and Griendling, K. K. (2007). Angiotensin II cell signaling: physiological and pathological effects in the cardiovascular system. *Am J Physiol Cell Physiol* **292**, C82-97.
- Mercer, J., Mahmoudi, M., and Bennett, M. (2007). DNA damage, p53, apoptosis and vascular disease. *Mutat Res* **621**, 75-86.
- Miller, A. A., Drummond, G. R., Schmidt, H. H., and Sobey, C. G. (2005). NADPH oxidase activity and function are profoundly greater in cerebral versus systemic arteries. *Circ Res* **97**, 1055-62.

- Miller, F. J., Rosenfeldt, F. L., Zhang, C., Linnane, A. W., and Nagley, P. (2003). Precise determination of mitochondrial DNA copy number in human skeletal and cardiac muscle by a PCR-based assay: lack of change of copy number with age. *Nucleic Acids Res* **31**, e61.
- Min, L. J., Mogi, M., Iwanami, J., Li, J. M., Sakata, A., Fujita, T., Tsukuda, K., Iwai, M., and Horiuchi, M. (2007). Cross-talk between aldosterone and angiotensin II in vascular smooth muscle cell senescence. *Cardiovasc Res* **76**, 506-16.
- Minamino, T., and Kourembanas, S. (2001). Mechanisms of telomerase induction during vascular smooth muscle cell proliferation. *Circ Res* **89**, 237-43.
- Minamino, T., Mitsialis, S. A., and Kourembanas, S. (2001). Hypoxia extends the life span of vascular smooth muscle cells through telomerase activation. *Mol Cell Biol* **21**, 3336-42.
- Minamino, T., Miyauchi, H., Yoshida, T., Ishida, Y., Yoshida, H., and Komuro, I. (2002). Endothelial cell senescence in human atherosclerosis: role of telomere in endothelial dysfunction. *Circulation* **105**, 1541-4.
- Minamino, T., Miyauchi, H., Yoshida, T., Tateno, K., Kunieda, T., and Komuro, I. (2004). Vascular cell senescence and vascular aging. *J Mol Cell Cardiol* **36**, 175-83.
- Minamino, T., Yoshida, T., Tateno, K., Miyauchi, H., Zou, Y., Toko, H., and Komuro, I. (2003). Ras induces vascular smooth muscle cell senescence and inflammation in human atherosclerosis. *Circulation* **108**, 2264-9.
- Miura, H., Bosnjak, J. J., Ning, G., Saito, T., Miura, M., and Gutterman, D. D. (2003). Role for hydrogen peroxide in flow-induced dilation of human coronary arterioles. *Circ Res* **92**, e31-40.
- Miyauchi, H., Minamino, T., Tateno, K., Kunieda, T., Toko, H., and Komuro, I. (2004). Akt negatively regulates the *in vitro* lifespan of human endothelial cells via a p53/p21-dependent pathway. *EMBO J* **23**, 212-20.
- Mohazzab, K. M., and Wolin, M. S. (1994). Sites of superoxide anion production detected by lucigenin in calf pulmonary artery smooth muscle. *Am J Physiol* **267**, L815-22.
- Morishita, R., Gibbons, G. H., Ellison, K. E., Lee, W., Zhang, L., Yu, H., Kaneda, Y., Ogihara, T., and Dzau, V. J. (1994). Evidence for direct local effect of angiotensin in vascular hypertrophy. *In vivo* gene transfer of angiotensin converting enzyme. *J Clin Invest* **94**, 978-84.
- Mosmann, T. (1983). Rapid colorimetric assay for cellular growth and survival: application to proliferation and cytotoxicity assays. *J Immunol Methods* **65**, 55-63.
- Murphy, M. P., and Smith, R. A. (2007). Targeting antioxidants to mitochondria by conjugation to lipophilic cations. *Annu Rev Pharmacol Toxicol* **47**, 629-56.

- Najjar, S. S., Scuteri, A., and Lakatta, E. G. (2005). Arterial aging: is it an immutable cardiovascular risk factor? *Hypertension* **46**, 454-62.
- Naka, K., Tachibana, A., Ikeda, K., and Motoyama, N. (2004). Stress-induced premature senescence in hTERT-expressing ataxia telangiectasia fibroblasts. *J Biol Chem* **279**, 2030-7.
- Nakamura, A., Isoyama, S., Watanabe, T., Katoh, M., and Sawai, T. (1998). Heterogeneous smooth muscle cell population derived from small and larger arteries. *Microvasc Res* **55**, 14-28.
- Naseem, K. M. (2005). The role of nitric oxide in cardiovascular diseases. *Mol Aspects Med* **26**, 33-65.
- Navalkar, S., Parthasarathy, S., Santanam, N., and Khan, B. V. (2001). Irbesartan, an angiotensin type 1 receptor inhibitor, regulates markers of inflammation in patients with premature atherosclerosis. *J Am Coll Cardiol* **37**, 440-4.
- Navarro, A., and Boveris, A. (2007). The mitochondrial energy transduction system and the aging process. *Am J Physiol Cell Physiol* **292**, C670-86.
- Nawrot, T. S., Staessen, J. A., Gardner, J. P., and Aviv, A. (2004). Telomere length and possible link to X chromosome. *Lancet* **363**, 507-10.
- Negishi, H., Ikeda, K., Nara, Y., and Yamori, Y. (2001). Increased hydroxyl radicals in the hippocampus of stroke-prone spontaneously hypertensive rats during transient ischemia and recirculation. *Neurosci Lett* **306**, 206-8.
- Neumeister, P., Albanese, C., Balent, B., Grealley, J., and Pestell, R. G. (2002). Senescence and epigenetic dysregulation in cancer. *Int J Biochem Cell Biol* **34**, 1475-90.
- Nickenig, G., and Murphy, T. J. (1994). Down-regulation by growth factors of vascular smooth muscle angiotensin receptor gene expression. *Mol Pharmacol* **46**, 653-9.
- Nickenig, G., Ostergren, J., and Struijker-Boudier, H. (2006). Clinical evidence for the cardiovascular benefits of angiotensin receptor blockers. *J Renin Angiotensin Aldosterone Syst* **7 Suppl 1**, S1-7.
- Nishiyama, A., Seth, D. M., and Navar, L. G. (2002). Renal interstitial fluid concentrations of angiotensins I and II in anesthetized rats. *Hypertension* **39**, 129-34.
- Nisoli, E., Clementi, E., Paolucci, C., Cozzi, V., Tonello, C., Sciorati, C., Bracale, R., Valerio, A., Francolini, M., Moncada, S., and Carruba, M. O. (2003). Mitochondrial biogenesis in mammals: the role of endogenous nitric oxide. *Science* **299**, 896-9.

- Nisoli, E., Falcone, S., Tonello, C., Cozzi, V., Palomba, L., Fiorani, M., Pisconti, A., Brunelli, S., Cardile, A., Francolini, M., Cantoni, O., Carruba, M. O., Moncada, S., and Clementi, E. (2004). Mitochondrial biogenesis by ·NO yields functionally active mitochondria in mammals. *Proc Natl Acad Sci U S A* **101**, 16507-12.
- Norrbom, J., Sundberg, C. J., Ameln, H., Kraus, W. E., Jansson, E., and Gustafsson, T. (2004). PGC-1 α mRNA expression is influenced by metabolic perturbation in exercising human skeletal muscle. *J Appl Physiol* **96**, 189-94.
- O'Callaghan, C. J., and Williams, B. (2000). Mechanical strain-induced extracellular matrix production by human vascular smooth muscle cells: role of TGF-beta(1). *Hypertension* **36**, 319-24.
- Ogami, M., Ikura, Y., Ohsawa, M., Matsuo, T., Kayo, S., Yoshimi, N., Hai, E., Shirai, N., Ehara, S., Komatsu, R., Naruko, T., and Ueda, M. (2004). Telomere shortening in human coronary artery diseases. *Arterioscler Thromb Vasc Biol* **24**, 546-50.
- Okuda, K., Khan, M. Y., Skurnick, J., Kimura, M., Aviv, H., and Aviv, A. (2000). Telomere attrition of the human abdominal aorta: relationships with age and atherosclerosis. *Atherosclerosis* **152**, 391-8.
- Oliverio, M. I., Best, C. F., Kim, H. S., Arendshorst, W. J., Smithies, O., and Coffman, T. M. (1997). Angiotensin II responses in AT1A receptor-deficient mice: a role for AT1B receptors in blood pressure regulation. *Am J Physiol* **272**, F515-20.
- Oliverio, M. I., Kim, H. S., Ito, M., Le, T., Audoly, L., Best, C. F., Hiller, S., Kluckman, K., Maeda, N., Smithies, O., and Coffman, T. M. (1998). Reduced growth, abnormal kidney structure, and type 2 (AT2) angiotensin receptor-mediated blood pressure regulation in mice lacking both AT1A and AT1B receptors for angiotensin II. *Proc Natl Acad Sci U S A* **95**, 15496-501.
- Owens, G. K., Kumar, M. S., and Wamhoff, B. R. (2004). Molecular regulation of vascular smooth muscle cell differentiation in development and disease. *Physiol Rev* **84**, 767-801.
- Parrinello, S., Samper, E., Krtolica, A., Goldstein, J., Melov, S., and Campisi, J. (2003). Oxygen sensitivity severely limits the replicative lifespan of murine fibroblasts. *Nat Cell Biol* **5**, 741-7.
- Pascal, T., Debacq-Chainiaux, F., Chretien, A., Bastin, C., Dabee, A. F., Bertholet, V., Remale, J., and Toussaint, O. (2005). Comparison of replicative senescence and stress-induced premature senescence combining differential display and low-density DNA arrays. *FEBS Lett* **579**, 3651-9.
- Passos, J. F., Saretzki, G., Ahmed, S., Nelson, G., Richter, T., Peters, H., Wappler, I., Birket, M. J., Harold, G., Schaeuble, K., Birch-Machin, M. A., Kirkwood, T. B., and von Zglinicki, T. (2007). Mitochondrial dysfunction accounts for the stochastic heterogeneity in telomere-dependent senescence. *PLoS Biol* **5**, e110.

- Passos, J. F., and von Zglinicki, T. (2005). Mitochondria, telomeres and cell senescence. *Exp Gerontol* **40**, 466-72.
- Patel, R. P., Moellering, D., Murphy-Ullrich, J., Jo, H., Beckman, J. S., and Darley-Usmar, V. M. (2000). Cell signaling by reactive nitrogen and oxygen species in atherosclerosis. *Free Radic Biol Med* **28**, 1780-94.
- Patti, M. E., Butte, A. J., Crunkhorn, S., Cusi, K., Berria, R., Kashyap, S., Miyazaki, Y., Kohane, I., Costello, M., Saccone, R., Landaker, E. J., Goldfine, A. B., Mun, E., DeFronzo, R., Finlayson, J., Kahn, C. R., and Mandarino, L. J. (2003). Coordinated reduction of genes of oxidative metabolism in humans with insulin resistance and diabetes: Potential role of PGC1 and NRF1. *Proc Natl Acad Sci U S A* **100**, 8466-71.
- Pawlikowski, M. (2006). Immunohistochemical detection of angiotensin receptors AT1 and AT2 in normal rat pituitary gland, estrogen-induced rat pituitary tumor and human pituitary adenomas. *Folia Histochem Cytobiol* **44**, 173-7.
- Pesce, V., Cormio, A., Fracasso, F., Vecchiet, J., Felzani, G., Lezza, A. M., Cantatore, P., and Gadaleta, M. N. (2001). Age-related mitochondrial genotypic and phenotypic alterations in human skeletal muscle. *Free Radic Biol Med* **30**, 1223-33.
- Pfaffl, M. W. (2001). A new mathematical model for relative quantification in real-time RT-PCR. *Nucleic Acids Res* **29**, e45.
- Phillips, M. I., Speakman, E. A., and Kimura, B. (1993). Levels of angiotensin and molecular biology of the tissue renin angiotensin systems. *Regul Pept* **43**, 1-20.
- Piechota, J., Szczesny, R., Wolanin, K., Chlebowski, A., and Bartnik, E. (2006). Nuclear and mitochondrial genome responses in HeLa cells treated with inhibitors of mitochondrial DNA expression. *Acta Biochim Pol* **53**, 485-95.
- Piperakis, S. M., Kontogianni, K., Karanastasi, G., Iakovidou-Kritsi, Z., and Piperakis, M. M. (2007). The use of comet assay in measuring DNA damage and repair efficiency in child, adult, and old age populations. *Cell Biol Toxicol* **25**, 65-71.
- Postnov, I. (2001). The role of mitochondrial calcium overload and energy deficiency in pathogenesis of arterial hypertension. *Arkh Patol* **63**, 3-10.
- Preston, C. C., Oberlin, A. S., Holmuhamedov, E. L., Gupta, A., Sagar, S., Syed, R. H., Siddiqui, S. A., Raghavakaimal, S., Terzic, A., and Jahangir, A. (2008). Aging-induced alterations in gene transcripts and functional activity of mitochondrial oxidative phosphorylation complexes in the heart. *Mech Ageing Dev* **129**, 304-12.
- Quick, Q. A., and Gewirtz, D. A. (2006). An accelerated senescence response to radiation in wild-type p53 glioblastoma multiforme cells. *J Neurosurg* **105**, 111-8.
- Ramachandran, A., Levonen, A. L., Brookes, P. S., Ceaser, E., Shiva, S., Barone, M. C., and Darley-Usmar, V. (2002). Mitochondria, nitric oxide, and cardiovascular dysfunction. *Free Radic Biol Med* **33**, 1465-74.

- Ramirez, R., Carracedo, J., Soriano, S., Jimenez, R., Martin-Malo, A., Rodriguez, M., Blasco, M., and Aljama, P. (2005). Stress-induced premature senescence in mononuclear cells from patients on long-term hemodialysis. *Am J Kidney Dis* **45**, 353-9.
- Ramirez, R. D., Morales, C. P., Herbert, B. S., Rohde, J. M., Passons, C., Shay, J. W., and Wright, W. E. (2001). Putative telomere-independent mechanisms of replicative aging reflect inadequate growth conditions. *Genes Dev* **15**, 398-403.
- Rasbach, K. A., and Schnellmann, R. G. (2007). Signaling of mitochondrial biogenesis following oxidant injury. *J Biol Chem* **282**, 2355-62.
- Rathore, R., Zheng, Y. M., Niu, C. F., Liu, Q. H., Korde, A., Ho, Y. S., and Wang, Y. X. (2008). Hypoxia activates NADPH oxidase to increase [ROS]_i and [Ca²⁺]_i through the mitochondrial ROS-PKCepsilon signaling axis in pulmonary artery smooth muscle cells. *Free Radic Biol Med* **45**, 1223-31.
- Rauscher, F. M., Goldschmidt-Clermont, P. J., Davis, B. H., Wang, T., Gregg, D., Ramaswami, P., Pippen, A. M., Annex, B. H., Dong, C., and Taylor, D. A. (2003). Aging, progenitor cell exhaustion, and atherosclerosis. *Circulation* **108**, 457-63.
- Ravassa, S., Fortuno, M. A., Gonzalez, A., Lopez, B., Zalba, G., Fortuno, A., and Diez, J. (2000). Mechanisms of increased susceptibility to angiotensin II-induced apoptosis in ventricular cardiomyocytes of spontaneously hypertensive rats. *Hypertension* **36**, 1065-71.
- Rensen, S. S., Doevendans, P. A., and van Eys, G. J. (2007). Regulation and characteristics of vascular smooth muscle cell phenotypic diversity. *Neth Heart J* **15**, 100-8.
- Rheinwald, J. G., Hahn, W. C., Ramsey, M. R., Wu, J. Y., Guo, Z., Tsao, H., De Luca, M., Catricala, C., and O'Toole, K. M. (2002). A two-stage, p16^(INK4A)- and p53-dependent keratinocyte senescence mechanism that limits replicative potential independent of telomere status. *Mol Cell Biol* **22**, 5157-72.
- Ricci, C., Pastukh, V., Leonard, J., Turrens, J., Wilson, G., Schaffer, D., and Schaffer, S. W. (2008). Mitochondrial DNA damage triggers mitochondrial-superoxide generation and apoptosis. *Am J Physiol Cell Physiol* **294**, C413-22.
- Ricquier, D., and Bouillaud, F. (2000). Mitochondrial uncoupling proteins: from mitochondria to the regulation of energy balance. *J Physiol* **529 Pt 1**, 3-10.
- Robles, S. J., Buehler, P. W., Negrusz, A., and Adami, G. R. (1999). Permanent cell cycle arrest in asynchronously proliferating normal human fibroblasts treated with doxorubicin or etoposide but not camptothecin. *Biochem Pharmacol* **58**, 675-85.
- Ruilope, L. M., Rosei, E. A., Bakris, G. L., Mancia, G., Poulter, N. R., Taddei, S., Unger, T., Volpe, M., Waeber, B., and Zannad, F. (2005). Angiotensin receptor blockers: therapeutic targets and cardiovascular protection. *Blood Press* **14**, 196-209.

- Ruiz, E., Redondo, S., Padilla, E., Gordillo-Moscoso, A., Salices, M., Balfagon, G., and Tejerina, T. (2007). Importance of intracellular angiotensin II in vascular smooth muscle cell apoptosis: inhibition by the angiotensin AT1 receptor antagonist Irbesartan. *Eur J Pharmacol* **567**, 231-9.
- Ryan, M. T., and Hoogenraad, N. J. (2007). Mitochondrial-nuclear communications. *Annu Rev Biochem* **76**, 701-22.
- Sachinidis, A., Ko, Y., Weisser, P., Meyer zu Brickwedde, M. K., Dusing, R., Christian, R., Wieczorek, A. J., and Vetter, H. (1993). EXP3174, a metabolite of losartan (MK 954, DuP 753) is more potent than losartan in blocking the angiotensin II-induced responses in vascular smooth muscle cells. *J Hypertens* **11**, 155-62.
- Sales, V. L., Sukhova, G. K., Lopez-Illasaca, M. A., Libby, P., Dzau, V. J., and Pratt, R. E. (2005). Angiotensin type 2 receptor is expressed in murine atherosclerotic lesions and modulates lesion evolution. *Circulation* **112**, 3328-36.
- Samani, N. J., Boulton, R., Butler, R., Thompson, J. R., and Goodall, A. H. (2001). Telomere shortening in atherosclerosis. *Lancet* **358**, 472-3.
- Samani, N. J., and van der Harst, P. (2008). Biological ageing and cardiovascular disease. *Heart* **94**, 537-9.
- Sampson, M. J., Gopaul, N., Davies, I. R., Hughes, D. A., and Carrier, M. J. (2002). Plasma F2 isoprostanes: direct evidence of increased free radical damage during acute hyperglycemia in type 2 diabetes. *Diabetes Care* **25**, 537-41.
- Sampson, M. J., Winterbone, M. S., Hughes, J. C., Dozio, N., and Hughes, D. A. (2006). Monocyte telomere shortening and oxidative DNA damage in type 2 diabetes. *Diabetes Care* **29**, 283-9.
- Saretzki, G., Feng, J., von Zglinicki, T., and Villeponteau, B. (1998). Similar gene expression pattern in senescent and hyperoxic-treated fibroblasts. *J Gerontol A Biol Sci Med Sci* **53**, B438-42.
- Satoh, M., Ishikawa, Y., Takahashi, Y., Itoh, T., Minami, Y., and Nakamura, M. (2008). Association between oxidative DNA damage and telomere shortening in circulating endothelial progenitor cells obtained from metabolic syndrome patients with coronary artery disease. *Atherosclerosis* **198**, 347-53.
- Scarpulla, R. C. (2008). Transcriptional paradigms in mammalian mitochondrial biogenesis and function. *Physiol Rev* **88**, 611-38.
- Schaeffer, C., Vandroux, D., Thomassin, L., Athias, P., Rochette, L., and Connat, J. L. (2003). Calcitonin gene-related peptide partly protects cultured smooth muscle cells from apoptosis induced by an oxidative stress via activation of ERK1/2 MAPK. *Biochim Biophys Acta* **1643**, 65-73.

References

- Schafer, F. Q., and Buettner, G. R. (2001). Redox environment of the cell as viewed through the redox state of the glutathione disulfide/glutathione couple. *Free Radic Biol Med* **30**, 1191-212.
- Schupp, N., Schmid, U., Rutkowski, P., Lakner, U., Kanase, N., Heidland, A., and Stopper, H. (2007). Angiotensin II-induced genomic damage in renal cells can be prevented by angiotensin II type 1 receptor blockage or radical scavenging. *Am J Physiol Renal Physiol* .
- Serrano, M., and Blasco, M. A. (2001). Putting the stress on senescence. *Curr Opin Cell Biol* **13**, 748-53.
- Serrano, M., Lin, A. W., McCurrach, M. E., Beach, D., and Lowe, S. W. (1997). Oncogenic ras provokes premature cell senescence associated with accumulation of p53 and p16^{INK4a}. *Cell* **88**, 593-602.
- Servant, G., Dudley, D. T., Escher, E., and Guillemette, G. (1994). The marked disparity between the sizes of angiotensin type 2 receptors from different tissues is related to different degrees of N-glycosylation. *Mol Pharmacol* **45**, 1112-8.
- Seshiah, P. N., Weber, D. S., Rocic, P., Valppu, L., Taniyama, Y., and Griendling, K. K. (2002). Angiotensin II stimulation of NAD(P)H oxidase activity: upstream mediators. *Circ Res* **91**, 406-13.
- Severino, J., Allen, R. G., Balin, S., Balin, A., and Cristofalo, V. J. (2000). Is beta-galactosidase staining a marker of senescence *in vitro* and *in vivo*? *Exp Cell Res* **257**, 162-71.
- Shan, H., Bai, X., and Chen, X. (2008). Angiotensin II induces endothelial cell senescence via the activation of mitogen-activated protein kinases. *Cell Biochem Funct* **26**, 459-66.
- Shargorodsky, M., Leibovitz, E., Lubimov, L., Gavish, D., and Zimlichman, R. (2002). Prolonged treatment with the AT1 receptor blocker, Valsartan, increases small and large artery compliance in uncomplicated essential hypertension. *Am J Hypertens* **15**, 1087-91.
- Shay, J. W., and Wright, W. E. (2000). Hayflick, his limit, and cellular ageing. *Nat Rev Mol Cell Biol* **1**, 72-6.
- Shiloh, Y. (2003). ATM and related protein kinases: safeguarding genome integrity. *Nat Rev Cancer* **3**, 155-68.
- Shiomi, T., Tsutsui, H., Matsusaka, H., Murakami, K., Hayashidani, S., Ikeuchi, M., Wen, J., Kubota, T., Utsumi, H., and Takeshita, A. (2004). Overexpression of glutathione peroxidase prevents left ventricular remodeling and failure after myocardial infarction in mice. *Circulation* **109**, 544-9.

- Short, K. R., Bigelow, M. L., Kahl, J., Singh, R., Coenen-Schimke, J., Raghavakaimal, S., and Nair, K. S. (2005). Decline in skeletal muscle mitochondrial function with aging in humans. *Proc Natl Acad Sci U S A* **102**, 5618-23.
- Singh, N. P., McCoy, M. T., Tice, R. R., and Schneider, E. L. (1988). A simple technique for quantitation of low levels of DNA damage in individual cells. *Exp Cell Res* **175**, 184-91.
- Siragy, H. M., Inagami, T., Ichiki, T., and Carey, R. M. (1999). Sustained hypersensitivity to angiotensin II and its mechanism in mice lacking the subtype-2 (AT₂) angiotensin receptor. *Proc Natl Acad Sci U S A* **96**, 6506-10.
- Sitte, N., Merker, K., Grune, T., and von Zglinicki, T. (2001). Lipofuscin accumulation in proliferating fibroblasts *in vitro*: an indicator of oxidative stress. *Exp Gerontol* **36**, 475-86.
- Skatchkov, M. P., Sperling, D., Hink, U., Mulsch, A., Harrison, D. G., Sindermann, I., Meinertz, T., and Munzel, T. (1999). Validation of lucigenin as a chemiluminescent probe to monitor vascular superoxide as well as basal vascular nitric oxide production. *Biochem Biophys Res Commun* **254**, 319-24.
- Smogorzewska, A., and de Lange, T. (2002). Different telomere damage signaling pathways in human and mouse cells. *EMBO J* **21**, 4338-48.
- Southern, E. M. (1975). Long range periodicities in mouse satellite DNA. *J Mol Biol* **94**, 51-69.
- Spiekermann, S., Landmesser, U., Dikalov, S., Brecht, M., Gamez, G., Tatge, H., Reepschlager, N., Hornig, B., Drexler, H., and Harrison, D. G. (2003). Electron spin resonance characterization of vascular xanthine and NAD(P)H oxidase activity in patients with coronary artery disease: relation to endothelium-dependent vasodilation. *Circulation* **107**, 1383-9.
- Stanley, A. G., Patel, H., Knight, A. L., and Williams, B. (2000). Mechanical strain-induced human vascular matrix synthesis: the role of angiotensin II. *J Renin Angiotensin Aldosterone Syst* **1**, 32-5.
- Starr, J. M., McGurn, B., Harris, S. E., Whalley, L. J., Deary, I. J., and Shiels, P. G. (2007). Association between telomere length and heart disease in a narrow age cohort of older people. *Exp Gerontol* **42**, 571-3.
- Stewart, S. A., Ben-Porath, I., Carey, V. J., O'Connor, B. F., Hahn, W. C., and Weinberg, R. A. (2003). Erosion of the telomeric single-strand overhang at replicative senescence. *Nat Genet* **33**, 492-6.
- Stockl, P., Hutter, E., Zwerschke, W., and Jansen-Durr, P. (2006). Sustained inhibition of oxidative phosphorylation impairs cell proliferation and induces premature senescence in human fibroblasts. *Exp Gerontol* **41**, 674-82.

- Stockl, P., Zankl, C., Hutter, E., Unterluggauer, H., Laun, P., Heeren, G., Bogengruber, E., Herndler-Brandstetter, D., Breitenbach, M., and Jansen-Durr, P. (2007). Partial uncoupling of oxidative phosphorylation induces premature senescence in human fibroblasts and yeast mother cells. *Free Radic Biol Med* **43**, 947-58.
- Straface, E., Vona, R., Ascione, B., Matarrese, P., Strudthoff, T., Franconi, F., and Malorni, W. (2007). Single exposure of human fibroblasts (WI-38) to a sub-cytotoxic dose of UVB induces premature senescence. *FEBS Lett* **581**, 4342-8.
- Stralin, P., Karlsson, K., Johansson, B. O., and Marklund, S. L. (1995). The interstitium of the human arterial wall contains very large amounts of extracellular superoxide dismutase. *Arterioscler Thromb Vasc Biol* **15**, 2032-6.
- Sullivan, J. A., Rupnow, H. L., Cale, J. M., Magness, R. R., and Bird, I. M. (2005). Pregnancy and ovarian steroid regulation of angiotensin II type 1 and type 2 receptor expression in ovine uterine artery endothelium and vascular smooth muscle. *Endothelium* **12**, 41-56.
- Suzuki, K., Mori, I., Nakayama, Y., Miyakoda, M., Kodama, S., and Watanabe, M. (2001). Radiation-induced senescence-like growth arrest requires TP53 function but not telomere shortening. *Radiat Res* **155**, 248-53.
- Suzuki, M., and Boothman, D. A. (2008). Stress-induced premature senescence (SIPS)-influence of SIPS on radiotherapy. *J Radiat Res (Tokyo)* **49**, 105-12.
- Takaoka, M., Harada, H., Deramandt, T. B., Oyama, K., Andl, C. D., Johnstone, C. N., Rhoades, B., Enders, G. H., Opitz, O. G., and Nakagawa, H. (2004). Ha-Ras(G12V) induces senescence in primary and immortalized human esophageal keratinocytes with p53 dysfunction. *Oncogene* **23**, 6760-8.
- Tandler, B., Dunlap, M., Hoppel, C. L., and Hassan, M. (2002). Giant mitochondria in a cardiomyopathic heart. *Ultrastruct Pathol* **26**, 177-83.
- Tanimoto, K., Sugiyama, F., Goto, Y., Ishida, J., Takimoto, E., Yagami, K., Fukamizu, A., and Murakami, K. (1994). Angiotensinogen-deficient mice with hypotension. *J Biol Chem* **269**, 31334-7.
- Taniyama, Y., and Griendling, K. K. (2003). Reactive oxygen species in the vasculature: molecular and cellular mechanisms. *Hypertension* **42**, 1075-81.
- Taubman, M. B. (2003). Angiotensin II: a vasoactive hormone with ever-increasing biological roles. *Circ Res* **92**, 9-11.
- Terman, A., Dalen, H., Eaton, J. W., Neuzil, J., and Brunk, U. T. (2004). Aging of cardiac myocytes in culture: oxidative stress, lipofuscin accumulation, and mitochondrial turnover. *Ann N Y Acad Sci* **1019**, 70-7.
- Torres, C. A., and Perez, V. I. (2008). Proteasome modulates mitochondrial function during cellular senescence. *Free Radic Biol Med* **44**, 403-14.

- Toussaint, O., Medrano, E. E., and von Zglinicki, T. (2000). Cellular and molecular mechanisms of stress-induced premature senescence (SIPS) of human diploid fibroblasts and melanocytes. *Exp Gerontol* **35**, 927-45.
- Toussaint, O., Remacle, J., Dierick, J. F., Pascal, T., Frippiat, C., Zdanov, S., Magalhaes, J. P., Royer, V., and Chainiaux, F. (2002). From the Hayflick mosaic to the mosaics of ageing. Role of stress-induced premature senescence in human ageing. *Int J Biochem Cell Biol* **34**, 1415-29.
- Touyz, R. M. (2005). Intracellular mechanisms involved in vascular remodelling of resistance arteries in hypertension: role of angiotensin II. *Exp Physiol* **90**, 449-55.
- Touyz, R. M., Chen, X., Tabet, F., Yao, G., He, G., Quinn, M. T., Pagano, P. J., and Schiffrin, E. L. (2002). Expression of a functionally active gp91phox-containing neutrophil-type NAD(P)H oxidase in smooth muscle cells from human resistance arteries: regulation by angiotensin II. *Circ Res* **90**, 1205-13.
- Touyz, R. M., He, G., Wu, X. H., Park, J. B., Mabrouk, M. E., and Schiffrin, E. L. (2001). Src is an important mediator of extracellular signal-regulated kinase 1/2-dependent growth signaling by angiotensin II in smooth muscle cells from resistance arteries of hypertensive patients. *Hypertension* **38**, 56-64.
- Touyz, R. M., and Schiffrin, E. L. (1999). Ang II-stimulated superoxide production is mediated via phospholipase D in human vascular smooth muscle cells. *Hypertension* **34**, 976-82.
- Touyz, R. M., and Schiffrin, E. L. (2001). Increased generation of superoxide by angiotensin II in smooth muscle cells from resistance arteries of hypertensive patients: role of phospholipase D-dependent NAD(P)H oxidase-sensitive pathways. *J Hypertens* **19**, 1245-54.
- Touyz, R. M., and Schiffrin, E. L. (2004). Reactive oxygen species in vascular biology: implications in hypertension. *Histochem Cell Biol* **122**, 339-52.
- Touyz, R. M., and Schiffrin, E. L. (2000). Signal transduction mechanisms mediating the physiological and pathophysiological actions of angiotensin II in vascular smooth muscle cells. *Pharmacol Rev* **52**, 639-72.
- Touyz, R. M., Tabet, F., and Schiffrin, E. L. (2003). Redox-dependent signalling by angiotensin II and vascular remodelling in hypertension. *Clin Exp Pharmacol Physiol* **30**, 860-6.
- Touyz, R. M., Yao, G., Viel, E., Amiri, F., and Schiffrin, E. L. (2004). Angiotensin II and endothelin-1 regulate MAP kinases through different redox-dependent mechanisms in human vascular smooth muscle cells. *J Hypertens* **22**, 1141-9.
- Trifunovic, A., Wredenberg, A., Falkenberg, M., Spelbrink, J. N., Rovio, A. T., Bruder, C. E., Bohlooly-Y, M., Gidlof, S., Oldfors, A., Wibom, R., Tornell, J., Jacobs, H. T., and Larsson, N. G. (2004). Premature ageing in mice expressing defective mitochondrial DNA polymerase. *Nature* **429**, 417-23.

References

- Triggle, D. J. (1995). Angiotensin II receptor antagonism: Losartan - sites and mechanisms of action. *Clin Ther* **17**, 1005-30.
- Trougakos, I. P., Poulakou, M., Stathatos, M., Chalikia, A., Melidonis, A., and Gonos, E. S. (2002). Serum levels of the senescence biomarker clusterin/apolipoprotein J increase significantly in diabetes type II and during development of coronary heart disease or at myocardial infarction. *Exp Gerontol* **37**, 1175-87.
- Tsirpanlis, G. (2008). Cellular senescence, cardiovascular risk, and CKD: a review of established and hypothetical interconnections. *Am J Kidney Dis* **51**, 131-44.
- Ungvari, Z., Labinsky, N., Gupte, S., Chander, P. N., Edwards, J. G., and Csiszar, A. (2008). Dysregulation of mitochondrial biogenesis in vascular endothelial and smooth muscle cells of aged rats. *Am J Physiol Heart Circ Physiol* **294**, H2121-8.
- Unterluggauer, H., Hutter, E., Voglauer, R., Grillari, J., Voth, M., Bereiter-Hahn, J., Jansen-Durr, P., and Jendrach, M. (2007). Identification of cultivation-independent markers of human endothelial cell senescence *in vitro*. *Biogerontology* **8**, 383-97.
- Urata, H., Nishimura, H., Ganten, D., and Arakawa, K. (1996). Angiotensin-converting enzyme-independent pathways of angiotensin II formation in human tissues and cardiovascular diseases. *Blood Press Suppl* **2**, 22-8.
- Valdes, A. M., Andrew, T., Gardner, J. P., Kimura, M., Oelsner, E., Cherkas, L. F., Aviv, A., and Spector, T. D. (2005). Obesity, cigarette smoking, and telomere length in women. *Lancet* **366**, 662-4.
- Vallance, P., and Leiper, J. (2004). Cardiovascular biology of the asymmetric dimethylarginine:dimethylarginine dimethylaminohydrolase pathway. *Arterioscler Thromb Vasc Biol* **24**, 1023-30.
- van der Loo, B., Fenton, M. J., and Erusalimsky, J. D. (1998). Cytochemical detection of a senescence-associated beta-galactosidase in endothelial and smooth muscle cells from human and rabbit blood vessels. *Exp Cell Res* **241**, 309-15.
- Van Remmen, H., and Richardson, A. (2001). Oxidative damage to mitochondria and aging. *Exp Gerontol* **36**, 957-68.
- Vanderheyden, P. M., Fierens, F. L., De Backer, J. P., Fraeyman, N., and Vauquelin, G. (1999). Distinction between surmountable and insurmountable selective AT1 receptor antagonists by use of CHO-K1 cells expressing human angiotensin II AT1 receptors. *Br J Pharmacol* **126**, 1057-65.
- Vandesompele, J., De Preter, K., Pattyn, F., Poppe, B., Van Roy, N., De Paepe, A., and Speleman, F. (2002). Accurate normalization of real-time quantitative RT-PCR data by geometric averaging of multiple internal control genes. *Genome Biol* **3**, RESEARCH0034.

- Vasquez-Vivar, J., Kalyanaraman, B., and Martasek, P. (2003). The role of tetrahydrobiopterin in superoxide generation from eNOS: enzymology and physiological implications. *Free Radic Res* **37**, 121-7.
- Villacorta, L., Azzi, A., and Zingg, J. M. (2007). Regulatory role of vitamins E and C on extracellular matrix components of the vascular system. *Mol Aspects Med* **28**, 507-37.
- Viswanathan, M., and Saavedra, J. M. (1992). Expression of angiotensin II AT2 receptors in the rat skin during experimental wound healing. *Peptides* **13**, 783-6.
- Voghel, G., Thorin-Trescases, N., Farhat, N., Nguyen, A., Villeneuve, L., Mamarbachi, A. M., Fortier, A., Perrault, L. P., Carrier, M., and Thorin, E. (2007). Cellular senescence in endothelial cells from atherosclerotic patients is accelerated by oxidative stress associated with cardiovascular risk factors. *Mech Ageing Dev* **128**, 662-71.
- Von Thun, A. M., Vari, R. C., el-Dahr, S. S., and Navar, L. G. (1994). Augmentation of intrarenal angiotensin II levels by chronic angiotensin II infusion. *Am J Physiol* **266**, F120-8.
- von Zglinicki, T. (2002). Oxidative stress shortens telomeres. *Trends Biochem Sci* **27**, 339-44.
- von Zglinicki, T. (2001). Telomeres and replicative senescence: Is it only length that counts? *Cancer Lett* **168**, 111-6.
- von Zglinicki, T., Saretzki, G., Docke, W., and Lotze, C. (1995). Mild hyperoxia shortens telomeres and inhibits proliferation of fibroblasts: a model for senescence? *Exp Cell Res* **220**, 186-93.
- von Zglinicki, T., Saretzki, G., Ladhoff, J., d'Adda di Fagagna, F., and Jackson, S. P. (2005). Human cell senescence as a DNA damage response. *Mech Ageing Dev* **126**, 111-7.
- von Zglinicki, T., Serra, V., Lorenz, M., Saretzki, G., Lenzen-Grossimlighaus, R., Gessner, R., Risch, A., and Steinhagen-Thiessen, E. (2000). Short telomeres in patients with vascular dementia: an indicator of low antioxidative capacity and a possible risk factor? *Lab Invest* **80**, 1739-47.
- Wahl, G. M., and Carr, A. M. (2001). The evolution of diverse biological responses to DNA damage: insights from yeast and p53. *Nat Cell Biol* **3**, E277-86.
- Wang, E. (1995). Senescent human fibroblasts resist programmed cell death, and failure to suppress bcl2 is involved. *Cancer Res* **55**, 2284-92.
- Wang, M., Takagi, G., Asai, K., Resuello, R. G., Natividad, F. F., Vatner, D. E., Vatner, S. F., and Lakatta, E. G. (2003). Aging increases aortic MMP-2 activity and angiotensin II in nonhuman primates. *Hypertension* **41**, 1308-16.

- Wang, Z., Castresana, M. R., and Newman, W. H. (2001). Reactive oxygen and NF-kappaB in VEGF-induced migration of human vascular smooth muscle cells. *Biochem Biophys Res Commun* **285**, 669-74.
- Wang, Z., Rao, P. J., Shillcutt, S. D., and Newman, W. H. (2005). Angiotensin II induces proliferation of human cerebral artery smooth muscle cells through a basic fibroblast growth factor (bFGF) dependent mechanism. *Neurosci Lett* **373**, 38-41.
- Warnholtz, A., Nickenig, G., Schulz, E., Macharzina, R., Brasen, J. H., Skatchkov, M., Heitzer, T., Stasch, J. P., Griendling, K. K., Harrison, D. G., Bohm, M., Meinertz, T., and Munzel, T. (1999). Increased NADH-oxidase-mediated superoxide production in the early stages of atherosclerosis: evidence for involvement of the renin-angiotensin system. *Circulation* **99**, 2027-33.
- Wassmann, S., Wassmann, K., and Nickenig, G. (2004). Modulation of oxidant and antioxidant enzyme expression and function in vascular cells. *Hypertension* **44**, 381-6.
- Watanabe, T., Barker, T. A., and Berk, B. C. (2005). Angiotensin II and the endothelium: diverse signals and effects. *Hypertension* **45**, 163-9.
- Webley, K., Bond, J. A., Jones, C. J., Blaydes, J. P., Craig, A., Hupp, T., and Wynford-Thomas, D. (2000). Posttranslational modifications of p53 in replicative senescence overlapping but distinct from those induced by DNA damage. *Mol Cell Biol* **20**, 2803-8.
- Weiss, D., Kools, J. J., and Taylor, W. R. (2001). Angiotensin II-induced hypertension accelerates the development of atherosclerosis in apoE-deficient mice. *Circulation* **103**, 448-54.
- Westhoff, J. H., Hilgers, K. F., Steinbach, M. P., Hartner, A., Klanke, B., Amann, K., and Melk, A. (2008). Hypertension induces somatic cellular senescence in rats and humans by induction of cell cycle inhibitor p16INK4a. *Hypertension* **52**, 123-9.
- Wilson, W. R., Herbert, K. E., Mistry, Y., Stevens, S. E., Patel, H. R., Hastings, R. A., Thompson, M. M., and Williams, B. (2008). Blood leucocyte telomere DNA content predicts vascular telomere DNA content in humans with and without vascular disease. *Eur Heart J* **29**, 2689-94.
- Winterbourn, C. C., Vissers, M. C., and Kettle, A. J. (2000). Myeloperoxidase. *Curr Opin Hematol* **7**, 53-8.
- Wolf, G., and Wenzel, U. O. (2004). Angiotensin II and cell cycle regulation. *Hypertension* **43**, 693-8.
- Wong, J., Patel, R. A., and Kowey, P. R. (2004). The clinical use of angiotensin-converting enzyme inhibitors. *Prog Cardiovasc Dis* **47**, 116-30.

- Wong, P. C., Price, W. A., Jr, Chiu, A. T., Duncia, J. V., Carini, D. J., Wexler, R. R., Johnson, A. L., and Timmermans, P. B. (1990). Nonpeptide angiotensin II receptor antagonists. XI. Pharmacology of EXP3174: an active metabolite of DuP 753, an orally active antihypertensive agent. *J Pharmacol Exp Ther* **255**, 211-7.
- Wright, D. C., Han, D. H., Garcia-Roves, P. M., Geiger, P. C., Jones, T. E., and Holloszy, J. O. (2007). Exercise-induced mitochondrial biogenesis begins before the increase in muscle PGC-1 α expression. *J Biol Chem* **282**, 194-9.
- Wright, J. W., and Harding, J. W. (1997). Important role for angiotensin III and IV in the brain renin-angiotensin system. *Brain Res Brain Res Rev* **25**, 96-124.
- Wu, H., Kanatous, S. B., Thurmond, F. A., Gallardo, T., Isotani, E., Bassel-Duby, R., and Williams, R. S. (2002). Regulation of mitochondrial biogenesis in skeletal muscle by CaMK. *Science* **296**, 349-52.
- Xu, D., and Finkel, T. (2002). A role for mitochondria as potential regulators of cellular life span. *Biochem Biophys Res Commun* **294**, 245-8.
- Xu, W., Koeck, T., Lara, A. R., Neumann, D., DiFilippo, F. P., Koo, M., Janocha, A. J., Masri, F. A., Arroliga, A. C., Jennings, C., Dweik, R. A., Tuder, R. M., Stuehr, D. J., and Erzurum, S. C. (2007). Alterations of cellular bioenergetics in pulmonary artery endothelial cells. *Proc Natl Acad Sci U S A* **104**, 1342-7.
- Yakes, F. M., and Van Houten, B. (1997). Mitochondrial DNA damage is more extensive and persists longer than nuclear DNA damage in human cells following oxidative stress. *Proc Natl Acad Sci U S A* **94**, 514-9.
- Yamada, T., Akishita, M., Pollman, M. J., Gibbons, G. H., Dzau, V. J., and Horiuchi, M. (1998). Angiotensin II type 2 receptor mediates vascular smooth muscle cell apoptosis and antagonizes angiotensin II type 1 receptor action: an *in vitro* gene transfer study. *Life Sci* **63**, PL289-95.
- Yamawaki, H., Haendeler, J., and Berk, B. C. (2003). Thioredoxin: a key regulator of cardiovascular homeostasis. *Circ Res* **93**, 1029-33.
- Yanai, K., Saito, T., Kakinuma, Y., Kon, Y., Hirota, K., Taniguchi-Yanai, K., Nishijo, N., Shigematsu, Y., Horiguchi, H., Kasuya, Y., Sugiyama, F., Yagami, K., Murakami, K., and Fukamizu, A. (2000). Renin-dependent cardiovascular functions and renin-independent blood-brain barrier functions revealed by renin-deficient mice. *J Biol Chem* **275**, 5-8.
- Yang, G., Wu, L., and Wang, R. (2006). Pro-apoptotic effect of endogenous H₂S on human aorta smooth muscle cells. *FASEB J* **20**, 553-5.
- Yang, J., Nagavarapu, U., Relloma, K., Sjaastad, M. D., Moss, W. C., Passaniti, A., and Herron, G. S. (2001). Telomerized human microvasculature is functional *in vivo*. *Nat Biotechnol* **19**, 219-24.

- Yang, N. C., and Hu, M. L. (2004). A fluorimetric method using fluorescein di-beta-D-galactopyranoside for quantifying the senescence-associated beta-galactosidase activity in human foreskin fibroblast Hs68 cells. *Anal Biochem* **325**, 337-43.
- Yang, N. C., and Hu, M. L. (2005). The limitations and validities of senescence associated-beta-galactosidase activity as an aging marker for human foreskin fibroblast Hs68 cells. *Exp Gerontol* **40**, 813-9.
- Yoon, Y. S., Yoon, D. S., Lim, I. K., Yoon, S. H., Chung, H. Y., Rojo, M., Malka, F., Jou, M. J., Martinou, J. C., and Yoon, G. (2006). Formation of elongated giant mitochondria in DFO-induced cellular senescence: involvement of enhanced fusion process through modulation of Fis1. *J Cell Physiol* **209**, 468-80.
- Zafari, A. M., Ushio-Fukai, M., Akers, M., Yin, Q., Shah, A., Harrison, D. G., Taylor, W. R., and Griendling, K. K. (1998). Role of NADH/NADPH oxidase-derived H₂O₂ in angiotensin II-induced vascular hypertrophy. *Hypertension* **32**, 488-95.
- Zahradka, P., Yau, L., Lalonde, C., Buchko, J., Thomas, S., Werner, J., Nguyen, M., and Saward, L. (1998). Modulation of the vascular smooth muscle angiotensin subtype 2 (AT2) receptor by angiotensin II. *Biochem Biophys Res Commun* **252**, 476-80.
- Zannolli, R., Mohn, A., Buoni, S., Pietrobelli, A., Messina, M., Chiarelli, F., and Miracco, C. (2008). Telomere length and obesity. *Acta Paediatr* **97**, 952-4.
- Zdanov, S., Bernard, D., Debacq-Chainiaux, F., Martien, S., Gosselin, K., Vercamer, C., Chelli, F., Toussaint, O., and Abbadie, C. (2007a). Normal or stress-induced fibroblast senescence involves COX-2 activity. *Exp Cell Res* **313**, 3046-56.
- Zdanov, S., Debacq-Chainiaux, F., and Toussaint, O. (2007b). Knocking down p53 with siRNA does not affect the overexpression of p21^{WAF-1} after exposure of IMR-90 hTERT fibroblasts to a sublethal concentration of H₂O₂ leading to premature senescence. *Ann N Y Acad Sci* **1100**, 316-22.
- Zhang, H., Schmeisser, A., Garlichs, C. D., Plotze, K., Damme, U., Mugge, A., and Daniel, W. G. (1999). Angiotensin II-induced superoxide anion generation in human vascular endothelial cells: role of membrane-bound NADH/NADPH-oxidases. *Cardiovasc Res* **44**, 215-22.
- Zhang, Y., Griendling, K. K., Dikalova, A., Owens, G. K., and Taylor, W. R. (2005). Vascular hypertrophy in angiotensin II-induced hypertension is mediated by vascular smooth muscle cell-derived H₂O₂. *Hypertension* **46**, 732-7.
- Zhou, C. H., Qian, Z. Y., Zheng, S. G., and Xiang, M. (2006). ERK1/2 pathway is involved in the inhibitory effect of crocetin on angiotensin II-induced vascular smooth muscle cell proliferation. *Eur J Pharmacol* **535**, 61-8.
- Zhou, M. S., Jaimes, E. A., and Raij, L. (2005). Vascular but not cardiac remodeling is associated with superoxide production in angiotensin II hypertension. *J Hypertens* **23**, 1737-43.

References

- Zhu, J., Woods, D., McMahon, M., and Bishop, J. M. (1998). Senescence of human fibroblasts induced by oncogenic Raf. *Genes Dev* **12**, 2997-3007.
- Zorov, D. B., Filburn, C. R., Klotz, L. O., Zweier, J. L., and Sollott, S. J. (2000). Reactive oxygen species (ROS)-induced ROS release: a new phenomenon accompanying induction of the mitochondrial permeability transition in cardiac myocytes. *J Exp Med* **192**, 1001-14.
- Zuo, L., Ushio-Fukai, M., Ikeda, S., Hilenski, L., Patrushev, N., and Alexander, R. W. (2005). Caveolin-1 is essential for activation of Rac1 and NAD(P)H oxidase after angiotensin II type 1 receptor stimulation in vascular smooth muscle cells: role in redox signaling and vascular hypertrophy. *Arterioscler Thromb Vasc Biol* **25**, 1824-30.
- Zwerschke, W., Mazurek, S., Stockl, P., Hutter, E., Eigenbrodt, E., and Jansen-Durr, P. (2003). Metabolic analysis of senescent human fibroblasts reveals a role for AMP in cellular senescence. *Biochem J* **376**, 403-11.